# Distal radioulnar joint kinematics assessed by dynamic radiostereometry

PhD thesis

**Janni Kjærgaard Thillemann**

Faculty of Health Sciences
University of Aarhus

&

University Clinic for Hand, Hip and Knee Surgery
Department of Orthopaedic Surgery
Gødstrup Hospital

# Supervisors

**Maiken Stilling**, Professor, MD, PhD (*Main supervisor)*
Sector of Hand Surgery, Department of Orthopaedics
Aarhus University Hospital, Denmark

**Torben Bæk Hansen**, Professor, MD, PhD *(Co-supervisor)*
Department of Orthopaedics
University Clinic for Hand, Hip and Knee Surgery
Gødstrup Hospital, Denmark

**Sepp de Raedt**, Senior Researcher, MSc, PhD *(Co-supervisor)*
Institute for Cancer Genetics and Informatics
Oslo University Hospital, Norway

# Evaluation committee

**Kresten Krarup Keller,** Associate Professor, MD, PhD *(Chairman)*
Department of Rheumatology, Aarhus University Hospital, Denmark

**Niels Thomsen**, Associate Professor, MD, PhD
Department of Hand Surgery, Skåne University Hospital, Sweden

**Stephan Maximillian Röhrl,** Associate Professor, MD, PhD
Division of Orthopaedic Surgery, Oslo University Hospital, Department Ullevål, Norway

# Funding

The work presented in this thesis was generously supported by financial grants gratefully received from the Faculty of Health at Aarhus University, the Health Research Fund of Central Denmark Region, Aase and Ejnar Danielsens Fundation, The Danish Rheumatism Association, Midwest Orthopaedic Research Foundation, and the Innovation Fund Grant 69-2013-1: “Transforming radiological technology for assessment of implant fixation from research tool to clinical application”.

# Acknowledgements

The studies presented in this thesis were conducted from October 2016 to October 2021, during my enrolment as a PhD student at the Faculty of Health at Aarhus University.

Many supportive colleagues need mentioning for the help they have provided and thereby allowing me to conclude the dissertation.

All patient inclusion and radiostereometric examinations were performed at the University Clinic for Hand, Hip and Knee Surgery at Holstebro Regional Hospital and Aarhus University Hospital. Thanks to Torben Bæk Hansen and Sten Larsen, Head of Departments, for making this possible. Especially, I would like to thank Torben for giving me the chance to be enrolled as a PhD student and to perform the work with support from Holstebro Regional Hospital. Thank you for believing in such an *'aged surgeon'* being able to learn and conduct research. Thank you for your sharp clinical perspectives and final refinements of the manuscripts as my co-supervisor.

I would like to thank my main supervisor Maiken Stilling for believing in me, as we met in Aarhus, at the department of Hand Surgery. Maiken introduced me to radiostereometry studies. Thereafter many days and nights have been spent in company with Maiken – but also together with a '*stacks of arms'* who '*gave a hand'* to the project. Together we have lifted our research devotedness to higher levels, thanks to increasingly more expensive champagne and growing friendship.

Thank you Maiken for being an extremely dedicated supervisor, thank you for your endless time spent making red correction marks in my manuscripts, conjuring my gnarled sentences into the most elegant precise formulations I have ever dreamt of.

I highly appreciate your dedication and hope I have learned at least some of your *refinement* skills.

I would also like to thank Sepp de Raedt who has been an invaluable co-supervisor, contributing with his expertise in dynamic radiostereometry analysis and continued development of the AutoRSA software, even though you and the family moved up north, you devotedly kept developing and supporting me and the project.

Behind the final data an enormous load of work has been done. Thank you, Lars Lindgren, Michael Frosted Mathiasen, Lone Rømer, Katriina Bøcker Puhakka, Bo

Munk, Peter Bo Jørgensen and Emil Toft Petersen – for always saying 'yes' and willingly helping me with each of your expertise's.
It has been a pleasure joining the RSA research group and I appreciate the time we spend in the office, your company and willingness to mutually help each other.

Fellow ships aboard at the Pulvertaft Hand Center in England, at Prince of Wales Hospital in Hong Kong and visits at Shalgrenska University Hospital in Gothenburg has given me great inspiration. Thank you, Tommy Lindau, Pak-Cheong Ho, Allan Ibsen and Peter Axelson, for your kindness and gracious reception of me at your institutions.
Let's all go having even more fun in the time coming. Let's keep on puzzling with my field of research and clinical interest: ulnar sided wrist pain and injuries to the triangular fibrocartilage complex (TFCC) - the 'Black box of the wrist'!

Finally, I thank my family and friends for your support and encouragement. Thank you, Helle and Mikkel, for your patience during the final refinement of the thesis in Trysil. Thank you, Theis, my amazing husband, for taking care of our wonderful boys, Storm and Theo, when I fly away to Australia, Hong Kong, Paris, Milano, Santander…. Thank you for putting up with me and '*my precious Mac*' and not attacking it during my productive COVID-19 pandemic. Most of all, thank you Theis, Storm and Theo for your love and support. You all mean the world to me.

Janni Kjærgaard Thillemann
December 30, 2021

# List of Studies

I: **Thillemann JK**, de Raedt S, Jorgensen PB, Romer L, Hansen TB, Stilling M. Distal radioulnar joint stability measured with radiostereometry during the piano key test. *Journal of Hand Surgery European Volume. 2020 Nov;45(9):923-930.* DOI: 10.1177/1753193420934689.

II: **Thillemann JK**, de Raedt S, Hansen TB, Munk B, Stilling M. Distal radioulnar joint stabilization with open foveal reinsertion versus tendon graft reconstruction: an experimental study using radiostereometry. *Journal of Experimental Orthopaedics. 2021, 8: 10.* DOI: 10.1186/s40634-021-00329-y

III: **Thillemann JK**, de Raedt S, Petersen ET, Puhakka KB, Hansen TB, Stilling M. Normal values of distal radioulnar joint kinematics during a dynamic press test. *Journal of Wrist Surgery, e-publication December 2021.* DOI: 10.1055/s-0041-1740486

IV: **Thillemann JK**, de Raedt S, Petersen ET, Puhakka KB, Hansen TB, Stilling M. Kinematics of the distal radioulnar joint before and after open reinsertion of the foveal triangular fibrocartilage complex in comparison to normal joints performing the hand press test. *Manuscript submitted to Acta Orthopaedica, December 2021.*

The papers of this thesis will be referred to in the text by Roman numerals (I-IV).

# Abbreviations

| | |
|---|---|
| ANOVA | Analysis of Variance |
| AROM | Active Range of Motion |
| AutoRSA | Automated Radiostereometric Analysis |
| CI | Confidence Interval |
| $C_{prox}$ | Proximal rotation center point of the radial head |
| $C_{dist}$ | Ulnar head center point |
| CT | Computed Tomography |
| dc | Distal component (of the ulnar TFCC insertion on styloid) |
| DRR | Digitally Reconstructed Radiographs |
| dRSA | Dynamic Radiostereometric Analysis |
| DRUJ | Distal Radioulnar Joint |
| DRUL | Dorsal Radioulnar ligament |
| ICC | Intraclass Correlation Coefficient |
| IQR | Interquartile Range |
| MRI | Magnetic Resonance Imaging |
| MCID | Minimal Clinically Important Difference. |
| NRS | Numeric Rating Scale |
| pc | Proximal component (of the TFCC foveal insertion) |
| PROM | Patient Reported Outcome Measure |
| PRUL | Palmar Radioulnar ligament |
| PRWE | Patient-Rated Wrist Evaluation |
| RSA | Radiostereometric Analysis |
| RUL | Radioulnar Ligament |
| SD | Standard Deviation |
| SID | Source to Images Distance |
| SN | Sigmoid Notch |
| SPM | Statistical Parametric Mapping |
| SSD | Source Skin Distance |
| TFCC | Triangular Fibrocartilage Complex |
| VAS | Visual Analog Scale |

# Definitions

| | |
|---|---|
| **Accuracy** | The closeness of agreement between a test result and an accepted reference value or the true value |
| **Hook test** | Arthroscopic evaluation of the foveal insertion of the triangular fibrocartilage complex (TFCC) that can be performed from the radiocarpal joint. The test confirms foveal TFCC lesion when the ulnar edge can be dragged radially and distal by the hook of a probe. |
| **Intraclass Correlation** | A statistical method that analyzes the agreement of data structured as groups. The strength of correlations is computed as intraclass correlation coefficients, ICC. |
| **Inter-rater agreement** | Variation between observers |
| **Intra-rater agreement** | Variation between observations for the same observer |
| **NRS** | Numeric Rating Scale. A segmented numeric instrument to quantify the intensity or frequency of subjective characteristics. NRS is frequently used to assess pain. |
| **QDASH** | Quick Disabilities of the Arm, Shoulder and Hand |
| **NVP** | Negative Predictive Value |
| **PPV** | Positive Predictive Value |
| **MDC** | Minimal Detectable Change |

| | |
|---|---|
| **MCID** | Minimal Clinically Important Difference. The minimal amount of change that is perceived as important or meaning full to the patient. |
| **Precision** | The closeness of agreement between repeated measures with unchanged conditions |
| **PROM** | Patient Reported Outcome Measure. An instrument used in a clinical setting for evaluation of outcome, where the responses are collected directly from the patient and without interference from the clinician, or others. |
| **PRWE** | Patient-Rated Wrist Evaluation. A wrist specific outcome instrument that quantifies pain and disability. |
| **Reliability** | The degree to which an assessment tool produces stable and consistent results |
| **Repeatability** | The variation in repeated measurements made on the same subject under identical conditions. The variation can be ascribed to the measuring method. |
| **Reproducibility** | The variation in measurements made on the same subject under changing conditions, i.e., different raters. |
| **Validity** | The extent to which an instrument/method measures what it is intended to measure and is free from bias. |
| **VAS** | Visual Analog Scale. An instrument to quantify the intensity or frequency of subjective characteristics believed to range over a continuum of values. |

# Contents

# 1 English summary

# 1

# English summary

Ulnar sided wrist pain after falling on the extended wrist or torque loading in work injuries is common and often related to lesion of the triangular fibrocartilage complex (TFCC). Traumatic lesions of the radioulnar ligaments of the TFCC can lead to distal radioulnar joint (DRUJ) instability as these structures are the main contributors to DRUJ stability. In clinical examination of DRUJ instability the observer manually feels and subjectively quantify the anterior posterior translation of the DRUJ, and the method has limited reproducibility. Likewise, imaging methods such as computer tomography scans and magnetic resonance scans have inadequate specificity and sensitivity for TFCC injuries. Therefore, the gold standard diagnostic method of TFCC injuries is arthroscopic evaluation. However, it is not feasible to operate patients to get a diagnosis. Thus, a valid objective tool to diagnose TFCC injuries and grade DRUJ instability before and after surgical treatment is warranted. Radiostereometry (RSA) is a very precise and accurate method, which has been used for decades to evaluate hip and knee implant migration with repeated imaging over time in a static setting. Dynamic RSA has been used for experimental as well as clinical evaluation of joint kinematics with high precision, but never before for evaluation of the DRUJ.

The focus of this PhD thesis was TFCC injuries and application of static and dynamic RSA as an objective measure of DRUJ stability.

*In Study I*, the feasibility and precision of AutoRSA for analysis of RSA imaging of DRUJ translation was demonstrated experimentally. Lesion of the distal and proximal insertion of the TFCC to the ulna styloid and ulna fovea, led to increasing DRUJ translation during Static RSA examination during a Piano key test.

*In Study II*, a surgical treatment with foveal reinsertion of the TFCC or Adams TFCC reconstruction was compared in a randomizes experimental study. The Piano key test was used to apply DRUJ translation, which was recorded by static RSA at end-points. A stabilizing effect was demonstrated by foveal TFCC reinsertion, whereas the variation in the stabilizing effect of Adams TFCC reconstruction was large and did not prove a statistically significant reduction of DRUJ translation.

*In Study III*, the feasibility and precision of a AutoRSA for analysis of dynamic RSA imaging during a Press test was demonstrated in a clinical study. DRUJ kinematics during an active Press test was recorded in participants with asymptomatic clinical stable non-injured DRUJs and classified as "normal DRUJ kinematics". Using a DRUJ position ratio was recommended to take individual sigmoid notch size into account.

*In Study IV*, DRUJ kinematics during a patient active Press test was recorded with dynamic RSA and a paired comparison was done between the patients asymptomatic non-injured DRUJ and the symptomatic DRUJ with an arthroscopically verified foveal TFCC lesion. A statistically significant difference of the DRUJ position ratio in foveal TFCC injured DRUJs compared to the asymptomatic side was demonstrated as the ulnar head center translated 10 percent points more volar in the sigmoid notch with foveal TFCC injury. Surgical treatment with open foveal TFCC reinsertion was performed and postoperative clinical and dynamic RSA imaging showed a stabilizing effect on the DRUJ stability towards normal values at 6-month and 1-year follow-up. Surgery did not normalize grip strength and AROM to the level of the non-injured contralateral side, but PROMs (QDASH, PRWE, and pain during activity) were improved to the level of the minimal clinically important difference (MCID).

In conclusion, this thesis documented static and dynamic RSA imaging and AutoRSA analysis to be a feasible and precise method for evaluation of DRUJ kinematics and stability. The studies contributed with precise estimates of DRUJ kinematics and improved the understanding of normative DRUJ kinematics, and the kinematic impact of TFCC injuries. This inspires to further explore the DRUJ kinematic patterns using clinically relevant and more complex DRUJ exercises that mimic the situations in which patient's report symptoms and DRUJ instability. Furthermore, dynamic RSA imaging and AutoRSA analysis of the DRUJ now makes it possible to evaluate the stabilizing effect of existing and new surgical treatments for DRUJ instability.

# 2 Danish summary

# 2

# Danish summary

Fald på strakt håndled eller kraftfuld rotation af underarmen kan medføre skade på det ’triangulære fibrocartilaginøse kompleks’ (TFCC), der kan betegnes som håndleddets menisk. Skader på TFCC kan resultere i ulnare håndledssmerter, samt instabilitet i underarmens nedre drejeled (DRUJ).
Ved klinisk undersøgelse af DRUJ mærker undersøgeren efter, om det passive bevægeudslag er øget, når albuebenets ledhoved skubbes frem og tilbage i forhold til spolebenet. Resultatet afhænger meget af lægen der undersøger og derfor har metoden begrænset reproducerbarhed. Ligeledes har billeddannende metoder såsom computer tomografi (CT) scanning og magnetisk resonans (MR) scanning utilstrækkelig specificitet og sensitivitet til sikkert at diagnosticere TFCC skader. Den diagnostiske ’guldstandard’ er en kikkertundersøgelse af håndleddet, hvor tilstanden af TFCC vurderes ved en såkaldt krog-test. Det er problematisk at diagnostik af TFCC skader afhænger af en operation, set i forhold til patientens risiko for komplikationer og sundhedsøkonomien. Derfor er udvikling af en præcis og objektiv metode til at diagnosticere TFCC-skader og til at gradere instabilitet i DRUJ før og efter kirurgisk behandling efterspurgt. Stereorøntgen (RSA) er en reproducerbar og nøjagtig billeddannende metode, som har været brugt i årtier til at evaluere mikrobevægelser af hofte- og knæimplantater over tid i et statisk RSA set-up. Dynamisk RSA er blevet brugt både eksperimentelt såvel som klinisk til evaluering af kinematik med høj præcision, men aldrig før til undersøgelse af kinematik i underarmens DRUJ.

Fokus for denne ph.d.-afhandling er TFCC skader og anvendelse af statisk og dynamisk RSA som objektiv målemetode til evaluering af stabilitet og kinematik i DRUJ.

*I studie I*, blev anvendeligheden og reproducerbarheden af statisk RSA-analyse med en automatiseret metode (AutoRSA) til vurdering af DRUJ-translation demonstreret eksperimentelt. Læsion af TFCC resulterede i øget instabilitet i DRUJ ved undersøgelse med 'Piano key testen' under optagelse af statisk RSA.

*I studie II*, blev kirurgisk behandling med 'åben fiksation af TFCC' til den ulnare fovea eller 'Adams rekonstruktion' med sene-transplantat sammenlignet i et eksperimentelt randomiseret studie. 'Piano key testen' blev anvendt til at demonstrere DRUJ translation undersøgt med statisk RSA. 'åben fiksation af TFCC' demonstrerede en statistisk signifikant stabiliserende effekt, hvilket ikke kunne påvises efter 'Adams rekonstruktion', som havde stor variation i den stabiliserende effekt af DRUJ.

*I studie III*, blev anvendelighed og reproducerbarhed af AutoRSA til vurdering af dynamisk RSA ved en aktiv patientudført 'Pres test' demonstreret i et klinisk studie. Kinematik i DRUJ blev målt hos deltagere med klinisk stabile, ikke-skadede DRUJ og klassificeret som 'normal DRUJ kinematik' ved 'Pres testen'. Undersøgelsen viste desuden, at man kan tage højde for individuelle forskelle i størrelse af den ledfladen på radius ved at rapportere en ratio som udtryk for knoglernes indbyrdes translation of position (DRUJ-position ratio).

*I studie IV*, blev DRUJ kinematik undersøgt med dynamisk RSA ved en aktiv patient-udført 'Pres test'. Patienternes DRUJ med TFCC-skade blev sammenlignet med det modsidige, klinisk stabile og ikke-skadede DRUJ i en parret undersøgelse, som påviste en betydende forskel i DRUJ-positions ratio. Kirurgisk behandling med 'åben fiksation af TFCC' blev gennemført og dynamisk RSA dokumenterede en bedring af DRUJ-stabiliteten mod det normale ved 6- og 12-måneders opfølgning. Kirurgisk behandling normaliserede ikke patienternes grebsstyrke og bevægelighed i den opererede hånd. Patientrapporterede mål i form af spørgeskemaet 'Handicaps i arm, skulder og hånd' (QDASH), 'Spørgeskema om smerter og bevægelser i håndled' (PRWE) og smerte-score under aktivitet blev derimod forbedret svarende til den minimale kliniske relevante forskel.

Overordnet viste denne ph.d.-afhandling, at statisk og dynamisk stereorøntgen kombineret med AutoRSA analyse er en anvendelig og reproducerbar metode til evaluering af kinematik og stabilitet i DRUJ. Undersøgelserne bidrog med præcise estimater af DRUJ kinematik og forbedrede forståelsen af den 'den normale DRUJ kinematik' og den kinematiske effekt af TFCC skader.

Resultaterne og erfaringerne fra ph.d.-afhandlingen inspirerer til at måle DRUJ kinematik ved mere komplekse og symptomprovokerende belastninger af DRUJ, hvor patienterne oplever en fornemmelse af instabilitet. Ydermere gør dynamiske RSA og AutoRSA-analyse af DRUJ det nu muligt at evaluere den stabiliserende effekt af eksisterende og nye kirurgiske metoder til at behandling af DRUJ instabilitet.

# 3 Introduction

# 3

# Introduction

The mammal species have developed highly mobile limbs, but in most the radius and ulna of the upper extremity do not articulate. Through primate evolution the human's ability to rotate the forearm has been of immense value, as forearm rotation is essential for positioning the hand when using tools, and have given primates superiority to other species (Linscheid, 1992). Consequently, injuries affecting the forearm function may lead to notable dysfunction.

The focus of this PhD thesis is triangular fibrocartilaginous complex (TFCC) injuries and objectively measured instability in the distal radioulnar joint (DRUJ) in an experimental ex vivo setting, and functional instability and objectively measured instability in an in vivo setting.

## 3.1 Anatomy and stabilizers of the DRUJ

In clinical practice, detailed knowledge of the complex anatomy and function of the DRUJ and the soft tissue stabilizers of the DRUJ may increase the quality of the clinical examination.

The bones of the human forearm include the radius and ulna, which are linked together by the interosseous membrane (IOM), the proximal the radioulnar joint (PRUJ) and the DRUJ as a complex diarthrodial joint, which enables rotation and can be regarded functionally as a single 'forearm joint' rotating about a common longitudinal radioulnar joint (RUJ) axis.

Any interruption to these anatomical structures may have impact on the joint stability, rotation of the forearm about the RUJ axis, and consequently on the forearm function (Andersson et al., 2016). Thus, the DRUJ cannot be assessed as a solitary joint.

### 3.1.1 The proximal radioulnar joint

Proximally, the radial head both articulate with the capitellum of the humerus in the radiocapitellar joint and with the radial notch of the ulna, in the PRUJ. The PRUJ is firmly stabilized by the annular ligament that courses around the symmetrical radial head (Fliegel et al., 2021).

### 3.1.2 The distal radioulnar joint

Distally, the DRUJ articulation of the ulnar head and the radial sigmoid notch (SN) is on a small area of approximately 10% of the joint surface (Gammon et al., 2018). This is due to the disproportion between the radii of articulating SN curvature and the radii of the articulating ulnar head (af Ekenstam and Hagert, 1985; Stuart et al., 2000; Szabo, 2006). Thus, the DRUJ articulation is incongruent and inherently unstable (Figure 3.1).

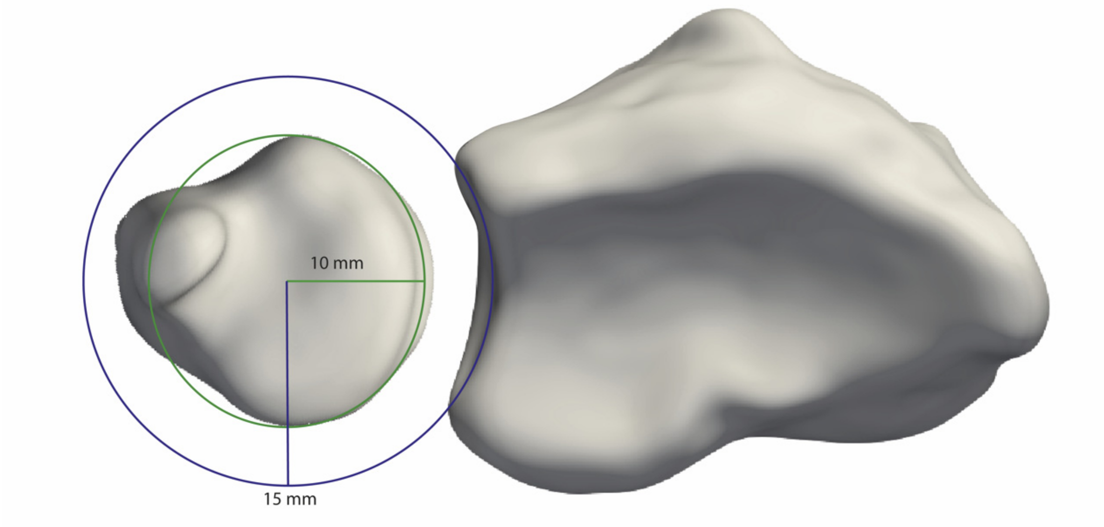


**Figure 3.1.** Axial view of the DRUJ. The radius of a circle fitted to the radius sigmoid notch curvature is lager compared to the ulnar head radius.

This incongruency of the DRUJ allows a wide range of motion and combined joint kinematics; forearm rotation about the radioulnar joint (RUJ) axis, longitudinal pistoning as the radius rotate around the fixed ulna, and anteroposterior translation of the point of articulation (af Ekenstam, 1992; Palmer and Werner, 1984; Tolat et al., 1996), but gapping is not expected in the stable DRUJ as the TFCC, provide a compressive force perpendicular to the articular surface (Hagert and Hagert, 2010).
Individual morphology of the SN influence the congruency but the bony contribution to DRUJ stability is limited (Tolat et al., 1996) as the joint is inherently unstable due to bony and articular incongruency between the smaller ulnar head and the greater sigmoid notch concavity (Stuart et al., 2000; Szabo, 2006) (Figure 3.2).
Thus, the soft-tissue restraints including ligaments and dynamic muscular stabilizers are the major contributors to DRUJ stability and of utmost importance (Linscheid, 1992).

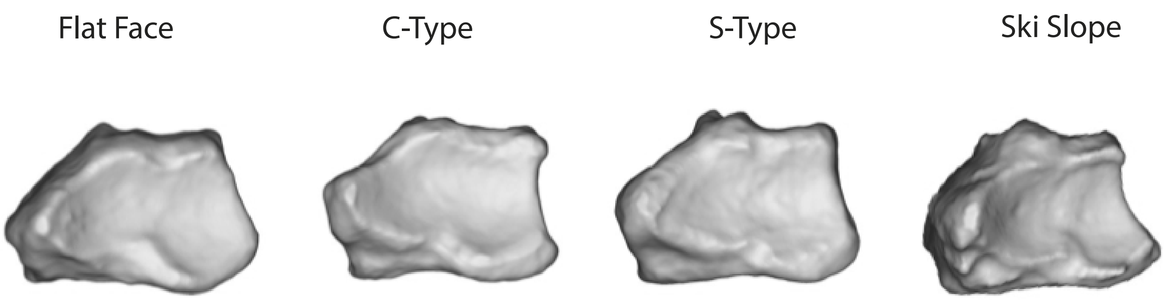


**Figure 3.2.** The four types of sagittal plane DRUJ morphology as described by Tolat et al. (1996).

### 3.1.3 Stabilizing soft tissues of the DRUJ

Stability of the DRUJ is a necessity for facilitating force transmission and load bearing. The soft-tissue structures providing DRUJ stability include (Figure 3.3):

- *Passive stabilizers*
  - The DRUJ capsule (Kleinman and Graham, 1998)
  - The ulnocarpal ligaments (UCL)
  - The dorsal radioulnar ligaments (DRULs) and palmar radioulnar ligaments and (PRULs) of the TFCC (Nakamura et al., 1996; Schuind et al., 1991; Stuart et al., 2000)
  - The IOM (Pfaeffle et al., 2000)
  - The extensor carpi ulnaris (ECU) subsheath (Spinner and Kaplan, 1970; Tang et al., 1998)
- *Active stabilizers*
  - The ECU tendon and muscle (Spinner and Kaplan, 1970; Tang et al., 1998)
  - The pronator quadratus (PQ) (Stuart, 1996).

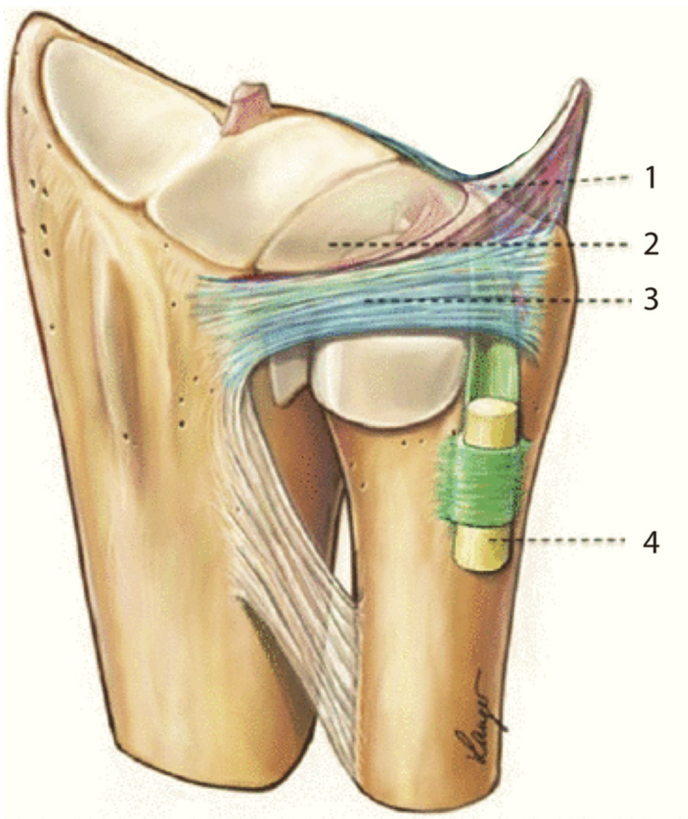


**Figure 3.3.** Dorsal view of the (1) meniscus homologue, (2) the articulating disc, (3) the dorsal radioulnar ligament (DRUL), and (4) the extensor carpi ulnaris (ECU) tendon in its tendon sheath.
Adapted from Haugstvedt et al. (2017).

### 3.6.4 The Interosseous Membrane

Ulna is the fixed element in the forearm as it is firmly connected to the humerus in the olecranon fossa. The IOM acts as an extrinsic ligament connecting the radius and ulna and transmits forces from one to another (Haugstvedt et al., 2017). As the radius rotates about the fixed ulna (Linscheid, 1992), the IOM is strained throughout forearm rotation motion. Obliquely running contrariwise descending and ascending reinforced fibers of the IOM serves to prevent both distal and proximal displacement of the radius from the fixed ulna (Pfaeffle et al., 2000; Poitevin, 2001).

Isolated IOM injury does not change the DRUJ kinematics significantly. Lesion of the distal oblique bundle (DOB) (Figure 3.4) of the IOM mainly add to DRUJ instability when also the TFCC is torn.

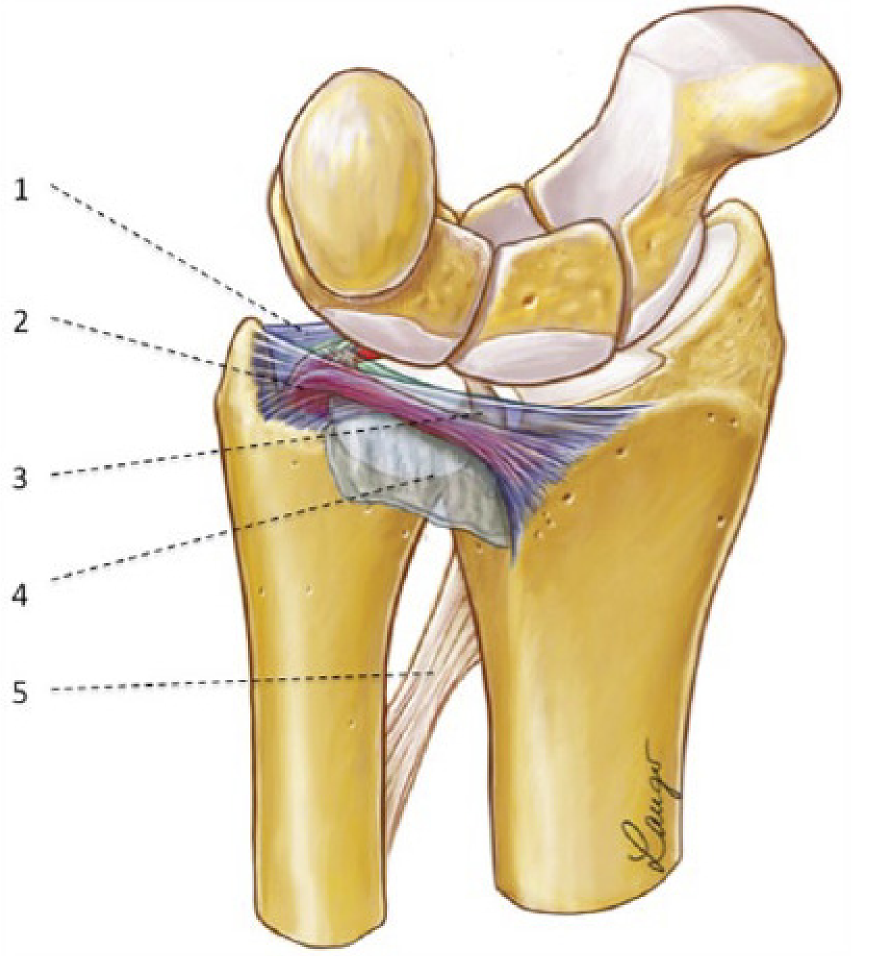


Figure 3.4. Palmar view of the (1) dorsal dc-TFCC, (2) pc-TFCC insertion in the ulnar fovea, (3) palmar dc-TFCC, (4) palmar capsule of the DRUJ, and (5) the distale oblique bundle (DOB) of the interosseus membrane. Adapted from Haugstvedt et al. (2017).

### 3.6.5 Anatomy of the Triangular Fibrocartilage Complex

In 1981, Palmer and Werner defined the term ‘Triangular Fibrocartilage Complex’ as a combined complex of ligamentous and cartilaginous structures interposed between the ulnar head and the carpus, acting to suspend the distal radius and ulnar carpus to the distal ulna. They described the TFCC as the major stabilizer of the DRUJ (Palmer and Werner, 1981).

The *anatomy* of the TFCC is complex (Figure 3.3 - 3.4). It is formed by:

- The avascular articulating disc (discus articularis) attached at the sigmoid notch rim and the radioulnar ligaments (RULs).
- The RULs originate from the medial border of the cartilaginous radius sigmoid notch, the palmar (PRUL) and dorsal (DRUL) osseus rim of the sigmoid notch.
  The RULs are vascularized and surround the articulating disc of which the peripheral 15–20% is vascularized. The RULs converge to attach at the ulnar bone (Berger and Landsmeer, 1990). This insertion has been described as two distinct sites of separate TFCC components on the ulna:
  - The superficial component inserting as a distal component of the TFCC (dc-TFCC), from the ulnar base and along the ulnar styloid process.
  - The deep component inserting as a proximal component of the TFCC (pc-TFCC), into the ulnar fovea at the axis of forearm rotation. The pc-TFCC is richly vascularized (Henle, 1871). Therefore, also often named ‘ligamentum subcruentum’ which means ‘bloodstained’.
- The ulnocarpal ligament complex (UCL) suspends the ulnar carpus and include the ulnotriquetral (UT) and the ulnolunate (UL) ligament (Semisch et al., 2016).
- The tendon sheath of the extensor carpi ulnaris (ECU), which have fibers connecting within both the radius and the RUL.

### 3.6.6 Functional anatomy of the TFCC

Analog concepts of the *functional anatomy* of the TFCC have been proposed:

- ‘The Hammock structure’ (Nakamura et al., 1996)
- ‘The Iceberg concept’ (Atzei and Luchetti, 2011), and
- ‘The 3-layer concept', which evolved from magnetic resonance imaging and dissection studies (Haugstvedt et al., 2017).

However, consensus exist on the following *functions of the TFCC*:

- Allows stable rotation of the radiocarpal unit about the fixed ulna.
- It provides gliding surfaces between the forearm bones and the carpal bones.
- Suspends the carpus and radius to the ulna.

- Act as cushion (the discus articularis) as force transmits from the hand through to the forearm and serves to maintain joint space between the carpal bones and the ulnar head during weight bearing but has limited impact on DRUJ stability (Semisch et al., 2016).

Nevertheless, the conclusions regarding the stabilizing function of the DRUL and PRUL during pronation and supination, has been contradicting (af Ekenstam and Hagert, 1985; Schuind et al., 1991). Later, in 1994 this 'Paradox of Af Ekenstam and Scheund' was clarified by Hagert. Both conclusions were valid as they described the function of the superficial part of the RULs inserting distally on the ulnar styloid (dc-TFCC) and the deep part of the RULs inserting proximally in the ulnar fovea (Hagert, 1994), respectively. Now a combined function of these TFCC components is generally accepted: the DRUL and PRUL work together as a dynamic stabilizers during forearm rotation; in pronation the distal superficial part of the DRUL is tight and the proximal deep part of the PRUL resist dorsal translation, and vice versa in supination (Figure 3.5) (Xu and Tang, 2009). The shearing forces of the DRUJ, affecting the DRUJ are utmost in full pronation and full supination (Ishii et al., 1998).

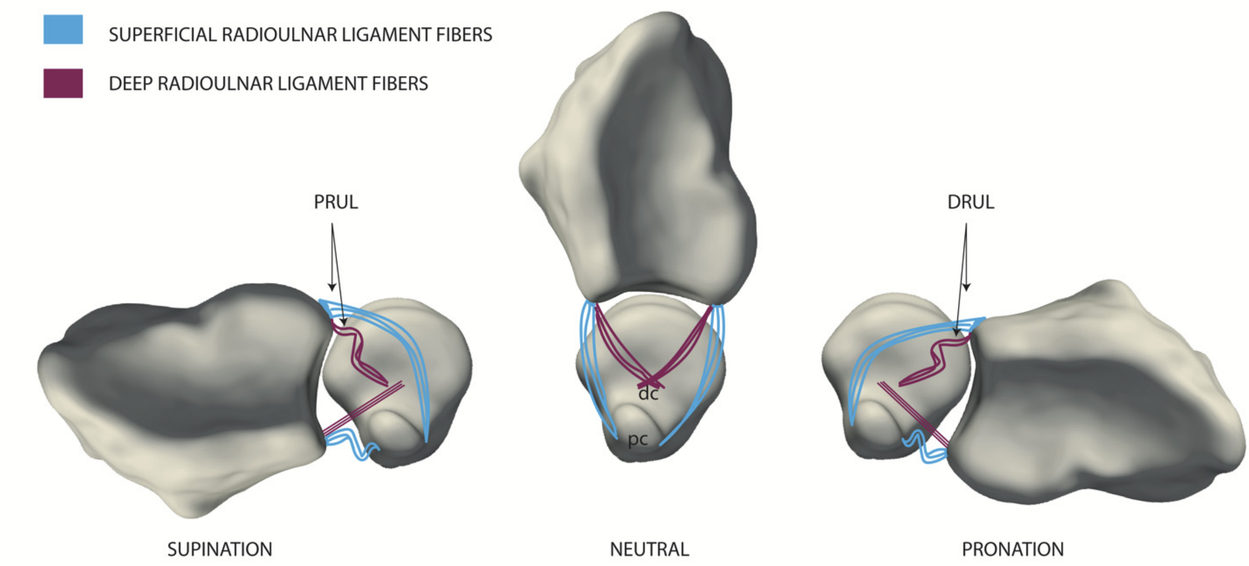


**Figure 3.5.** The superficial (distal component (dc)) and deep (proximal component (pc)) radioulnar ligaments (RUL) of the TFCC have stabilizing function in supination and pronation. The palmar radioulnar ligament (PRUL) and the dorsal radioulnar ligament (DRUL) originate from the radius and converge to insert at the ulna, but in two separate spots:

1) On the ulnar styloid the superficial RULs insert as a distal component (dc-TFCC).
2) In the ulnar fovea the deep RULs insert as a proximal component (dc-TFCC).

As the radius rotate around the ulna in supination, the superficial component of the PRUL tightens together with the deep fibers of the DRUL and prevent dorsal translation of the radius. Opposite, as the radius rotate around the ulna into pronation, the superficial component of the DRUL tighten together with the deep fibers of the PRUL and prevent volar translation of the radius. The figure display a DRUJ in a right forearm.

## 3.2 The 'black box'

The ulnar side of the wrist and the distal forearm include numerous anatomical structures including the TFCC. Thus, the cause of ulnar sided wrist pain can be challenging to diagnose as it can be related to many different types of injuries i.e., degenerative (DRUJ arthritis, central lesion in the TFCC meniscus, lunotriquetral ligament injury, ulnocarpal impaction or impingement, extensor carpi ulnaris tendonitis, flexor carpi tendonitis, pisotriquetral arthritis, ulnar nerve compression, ganglion cysts) or acute lesions (acute central lesion in the TFCC meniscus, traumatic lesions to the radioulnar ligaments of the TFCC, lunotriquetral ligament injury, ulnocarpal ligament injury, extensor carpi ulnaris tendon instability).

Therefore, by hand surgeons, ulnar sided wrist pain is often referred to, as the "black box'. Symptomatic degenerative TFCC lesions and especially acute TFCC lesions causing instability in the DRUJ may require treatment. DRUJ instability can either be the result of an isolated ligamentous TFCC injury (Trumble et al., 1997), but is also frequently seen in association with distal radius fractures (Lindau et al., 1997).
However, knowledge about TFCC injury symptoms and treatment is limited outside hand surgery circles and the diagnosis may be challenging to confirm. Therefore, TFCC related sequelae after distal radius fractures or simple wrist sprains may often be substantially delayed in referral for specialized hand surgical examination.

## 3.3 Anamnesis, etiology, and epidemiology

Patients suffering from ulnar sided wrist pain are often able to report if the pain has evolved slowly over time, as seen in chronic degenerative or inflammatory disorders, or was associated to a specific wrist trauma leading to an acute injury.
Nevertheless, clinical examination of acute ulnar sided wrist pain still can be challenging as several different disorders in the 'black box' produce similar symptoms. Further, subluxation in the DRUJ and varying degrees of DRUJ instability can be challenging to diagnose even for a trained hand surgeon.

### 3.3.1 Etiology and epidemiology of degenerative TFCC injuries

Chronic degenerative TFCC lesions in the central disc does not necessarily require treatment and is frequently asymptomatic (Iordache et al., 2012; Kinninmonth and Chan, 1990). The injuries occur as repeated ulnar deviation and axial force is transferred through the TFCC disc from the carpus through to the ulna. In individuals with normal ulnar variance, axial forces are transmitted from the carpus to the radius (80%), and from the carpus to the ulna (20%), via the TFCC (Palmer and Werner, 1984). Thus, congenital or acquired positive ulnar variance subject greater loading from the wrist to the forearm, through the TFCC, and increase the risk of degenerative TFCC wear and central disk perforation (Oda et al., 2013).

The prevalence of degenerative TFCC injuries has been reported to be 27% for patients younger than 30 years and increasing throughout life as age related TFCC changes develop (Chan et al., 2014; Kinninmonth and Chan, 1990; Kirschenbaum et al., 1995). Thus, in patients aged 70 years or older the prevalence of degenerative TFCC injuries is 49% (Chan et al., 2014).

### 3.3.2 Etiology and epidemiology of acute TFCC injuries with DRUJ instability

Traumatic injury of the TFCC may affect only the central TFCC disc, which does not result in DRUJ instability. Contrary, if the peripheral insertion of the ligaments surrounding the TFCC disc are injured, this may lead to DRUJ instability. These peripheral ligament injuries can be seen in athletes within spring gymnastics, martial arts, and racquet sports (Rettig, 2003).

The mechanisms causing acute TFCC injuries include the following:

- fall on outstretched hand i.e. hyper extended wrist and pronated forearm (Watanabe et al., 2010)
- rotational injuries i.e. power drill injuries (Watanabe et al., 2010)
- violent traction of the wrist/forearm (Atzei et al., 2017)
- TFCC injury concomitant with distal radius fracture (Andersson et al., 2014; Lindau et al., 1997).

The incidence of DRUJ instability after distal radius fractures is reported up to 42 % (Adolfsson, 1994; Geissler et al., 1996; Lindau et al., 2000; Tsai and Paksima, 2009; Wijffels and Ring, 2011) and is associated with pain and inferior patient reported outcomes (Lindau et al., 2000), but does not necessarily lead to symptomatic DRUJ instability (Mrkonjic et al., 2012). The incidence of isolated TFCC injuries (no fracture) is to my knowledge unknown.

## 3.4 Symptoms of TFCC injury

The following symptoms and complains are typical in patients with traumatic TFCC lesions and DRUJ instability and should call upon attention for TFCC injury as the cause:

- Ulnar sided wrist swelling
- Ulnar wrist clicking
- Ulnar wrist deformity or 'instability of the ulnar head'
- Ulnar sided wrist pain
- Aggravating pain when lifting
- Restricted or painful forearm rotation
- Weakness and reduced grip strength
- 'Giving way' of the wrist

## 3.5 Clinical evaluation

Ulnar wrist pain usually accompanies a TFCC injury and DRUJ instability, and a systematic clinical examination may give the diagnosis or differential diagnosis by means of special provocative maneuvers and diagnostic tests (Atzei et al., 2008; Kleinman, 2007). Nevertheless, provocative test was found to have limited diagnostic value in patients with suspected TFCC lesion, and most tests have not been validated.

### 3.5.1 Pain provocation tests

- *Passive forearm rotation,* leading to exacerbation of pain or occurrence of a 'click' may be associated with the presence of TFCC injuries, whereas *resisted forearm rotation* is often weakened on the injured side and painful as it reproduces the patient's functional complaints (Atzei and Luchetti, 2011). If 'crepitus,' or an intra-articular grinding sensation is present during forearm rotation DRUJ arthritis is suspected and can often be revealed on plain x-rays.
- *The Press test,* is positive when patients have ulnar sided pain as they push themselves up from the seated position, using the affected wrist, and has high sensitivity for detecting TFCC injuries (Lester et al.). However, not all kinds of TFCC injuries are associated with DRUJ instability (Lindau et al., 2000; Palmer, 1990) and the test specificity is unknown. Further, it does not grade the degree of DRUJ instability.

- *The ulnar fovea sign* is point tenderness, experienced by the patient, as the examiner with a thumb tip carefully palpate, between the ulnar styloid, the ulnar head, the pisiform bone and the flexor carpi ulnaris tendon (FCU). When tenderness is pinpointed in the 'soft spot' of the ulnar joint capsule, in comparison to the contra lateral side, the foveal sign is positive (Figure 3.6). The fovea sign is a reliable clinical sign in detecting foveal TFCC injuries, with a sensitivity of 96.2%, and a specificity of and 85.8%, Thus, the foveal sign can also be positive in other conditions with ulnar sided wrist pathology including central TFCC injury, superficial TCFF injury, ulnar impaction syndrome (abutment), lunotriquetral ligament injury, and DRUJ arthritis (Tay et al., 2007).

### 3.5.2 DRUJ provocation tests

- *The Piano key sign test* may reveal instability of the ulnar head relative to the radius. With pronated forearm, the wrist is stabilized in neutral position from the ulnar side. The examiner apply pressure onto the prominent ulnar head, which translate volar or is ballotable in cases with severe instability (Glowacki and Shin, 1999). The test bears resemblance with the keystroke and re-bounce of a Piano key, hence, the name 'Piano key sign'. The test is positive if the ulnar head translation is increased as evaluated relative to the contralateral wrist (Vezeridis et al., 2010) (Figure 3.7).

**Figure 3.6.** Foveal sign test

**Figure 3.7.** Piano Key test

- *Ballottement test*, is the most often used test. It is used to evaluate passive anteroposterior translation of the ulna with respect to the radius in comparison to the contralateral wrist. The examiner grasps and fix the radius and the radiocarpal joint (holding technique), while the distal ulna is held between the examiner's thumb and index finger and moved (translated) in anteroposterior and posteroanterior direction (Figure 3.8) (Moriya et al., 2009; Omokawa et al., 2017).

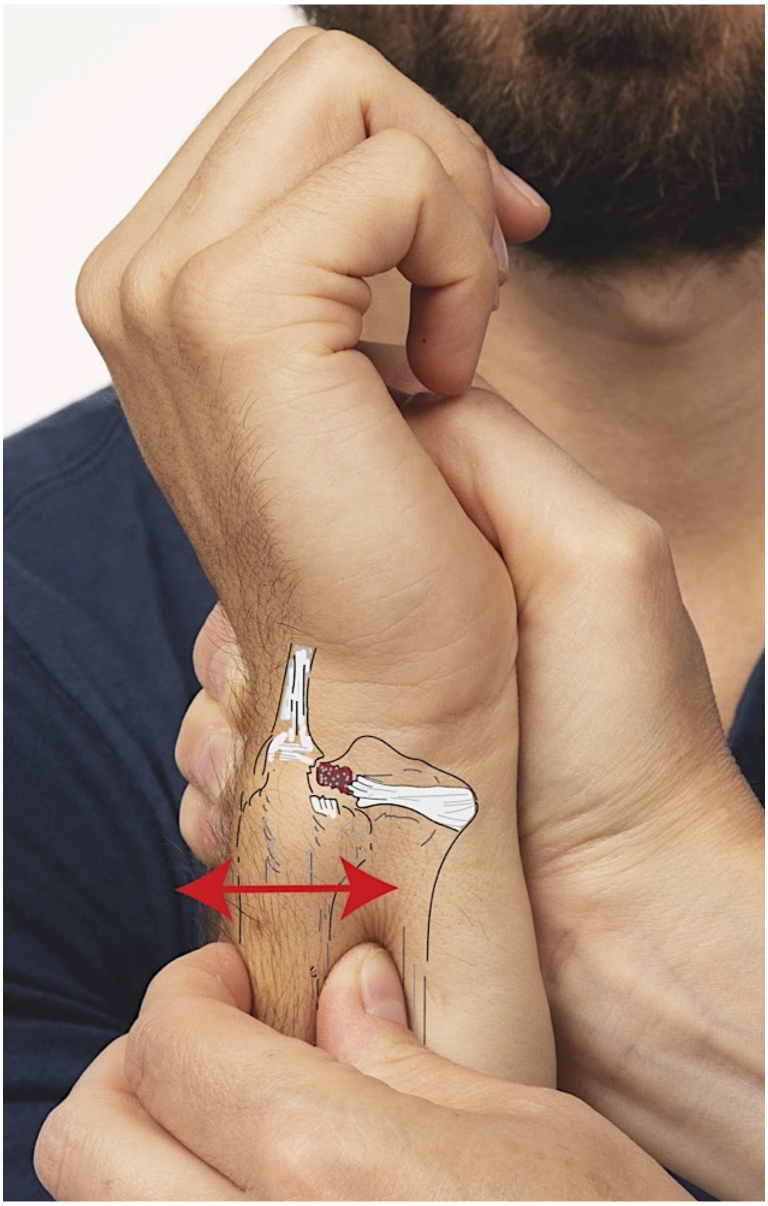

**Figure 3.8.** Ballottement test.

First, the test is performed in neutral rotation. Abnormally increased translation with a 'soft' end-point resistance, compared to the contralateral DRUJ, suggests TFCC ligament injury. The degree of DRUJ instability was proposed to be categorized as, normal to slight instability (<5 mm)/mild instability (5-10 mm)/severe instability (>10 mm) (Atzei et al., 2008).

Second, the Ballottement test is repeated with the forearm in full supination and full pronation, in an attempt to explore, which limb of the pc-TFCC is injured (Kleinman, 2007).

The Ballottement test is an easily applicable and simple test, to evaluate DRUJ stability.

However, there are significant shortcomings in clinical examination of DRUJ symptomatology and DRUJ instability as subjective testing, rely on the examiners experience and are difficult to quantify both between patients and between interventions and over time. Further, the tests are passive and static while used as an indication of a dynamic instability. Also, the reliability is dependent on relaxation of that the muscular stabilizers of the forearm, such as the ECU and the pronator quadratus, which yield protective contraction and provide a stabilizing effect on the DRUJ, which may mislead the examiner and result in false-negative conclusions (Atzei and Luchetti, 2011).

Despite this, clinical examination of the DRUJ stability, remains the most common outcome when surgeons evaluate the pre- and postoperative DRUJ stability when introducing new surgical methods for treatment of DRUJ instability.

### 3.5.3 AROM - Active Range of Motion

Evaluation of Active Range of motion (AROM) is commonly used during follow-up after hand surgical treatments. Various easurement techniques (placement of digital or manual goniometers) for the wrist joint exist (radial, ulnar, volar or dorsal). Using manual goniometry the volar and dorsal technique have good or excellent intra-rater and inter-rater reliability (Carter et al., 2009; LaStayo and Wheeler, 1994), and is recommended by 'The Danish National recommendations for measuring joint movement' (Helle Puggård, 2014).

However, some uncertainty in measures of wrist motion exist despite efforts to eliminate sources of error. The single-rater accuracy has been evaluated from 5 to 7 degrees for the dorsal measuring technique (Carter et al., 2009). The literature on precision and reliability of goniometer measured supination and pronation is sparce, but a minimal clinical important difference (MCID) of 5 degrees it in wrist motion is generally accepted (Muhlenhaupt, 1986; Therapists, 1992).

### 3.5.4 Grip strength

Hand surgeons and researchers frequently uses grip strength as a determining factor of upper extremity function. Grip strength measurement by a handheld dynamometer is easily applicable and have been proven equivalently good as work simulators (Beaton et al., 1995) and with high reliability and test-retest coefficients (ICC) of more than 0.90 (Beaton et al., 1995; Mathiowetz et al., 1984; Peolsson et al., 2001).

Normal values have been investigated in variety of populations (MacDermid et al., 1994; Mathiowetz et al., 1984; Peolsson et al., 2001). In patients suffering distal radius fractures the minimal clinically important difference (MCID) for grip strength has been reported to be 6.5 kg (equivalent to approximately 20% of the total strength) (Kim et al., 2014), however little is known about the extent of which grip strength is affected in patients with TFCC injuries and DRUJ instability.

Theoretically, grip strength measures may provoke pain in case of TFCC injury, as the forced grip dynamically increases the ulnar variance (Friedman et al., 1993). In patients with degenerative TFCC disk lesions a systematic review reported a significant improvement of surgical treatment with debridement. The preoperative grip strength was 65% and increased to 91% of the contralateral side (Saito et al., 2017)

Grip strength has been associated changes in 'Patient Rated Wrist Evaluation' (PRWE) in patients with distal radius fractures (Karnezis and Fragkiadakis, 2002). It is unknown if a similar association exist in patients with TFCC injuries and DRUJ instability, but currently only slight and non-significant improvements of grip strength has been found, both with open and arthroscopic TFCC stabilizing surgery (Anderson et al., 2008; Luchetti et al., 2014).

## 3.6 Patient-reported outcome measures

In order to evaluate upper extremity injuries and treatments, clinical evaluation of DRUJ stability, functional measurements of AROM and grip strength, and patient reported outcomes (PROMs), have traditionally been used to assess functional impairment. However, PROMs that have been developed and validated as measurements of functional impairment does not automatically reflect the patients experience of disability (Berkanovic et al., 1995). The answers are gathered directly form the patients; thus, observer bias is reduced. Today, PROMs are frequently used questionaries for gathering quantitative information to evaluate a patient disability (Wells et al., 2011), to evaluate progression in a patient cohort over time, and as a tool to facilitate cohort comparison between clinical trials (McPhail et al., 2012).

In upper extremity surgery, the 'Disabilities of the Arm, Shoulder, and Hand' questionnaire (DASH) as well as the shorted version, the 'Quick DASH' (QDASH) are commonly used region-specific PROMs. Further, the wrist specific 'Patient Rated Wrist Evaluation' questionnaire (PRWE), the hand specific 'Patient Rated Wrist and Hand Evaluation' questionnaire (PRWHE), and the 'Michigan Hand Outcomes Questionnaire' (MHOQ) are commonly used (Changulani et al., 2008; Hoang-Kim et al., 2011). The Numeric Rating Scale (NRS) or Visual Analog Scale (VAS) is widely used for assessment of pain during rest and defined activities.
In research related to wrist disorders and DRUJ instability, the DASH/QDASH and PRWE appear frequently, but no specific DRUJ related PROM questionnaire exists.

### 3.6.1 QDASH – Quick Disabilities of the Arm, Shoulder and Hand

The QDASH score is a shortened 11-item version of the original 30-item DASH outcome measure questionnaire for assessment of disability in patients with upper extremity disorders (Hudak et al., 1996). The QDASH is designed to measure pain and disability related to the whole upper extremity, as the name imply, which may influence the validity when evaluating specific disorders. The QDASH is a reliable and valid tool with excellent test-retest reliability ($r > 0.93$) and construct validity (correlated to DASH) (Beaton et al., 2005; Gummesson et al., 2006). Furthermore, a Danish version of the QDASH has been validated (Boeckstyns and Merser, 2014) (*Appendix 1*).

The QDASH allows patients to rate their:

1) ability to perform activities of daily living (ADL) (6 items)
2) social and work ability (2 items)
3) pain (1 item)
4) other symptoms (2 items).

The QDASH has a MCID of 14 points in patients with atraumatic conditions of the hand, wrist, and forearm (Sorensen et al., 2013) as well as for shoulder conditions (Budtz et al., 2018). The MCID for traumatic TFCC injury is not known.

In an asymptomatic population a mean QDASH score of 13 points (SD 15) has been reported (Jester et al., 2005). There is a close correlation between the DASH and QDASH score, both for those with little disability, and those with high disability in a general Norwegian population (Aasheim and Finsen, 2014).

### 3.6.2 PRWE – Patient-Rated Wrist Evaluation

The PRWE score is a 15-item questionnaire region-specific outcome measure initially developed for assessing and quantifying pain and function in individuals with distal radius fractures or scaphoid fractures. The English PRWE version was developed in 1996, and is a reliable and valid tool with excellent test-retest reliability ($r > 0.90$) (MacDermid et al., 1998).

Subsequent research has expanded the use of the PRWE to other wrist and hand conditions, thus a systematic review across many wrist/hand conditions has shown that the PRWE is a reliable upper extremity outcome instrument (Mehta et al., 2015), with high correlation to DASH and QDASH sores in patients treated for distal radius fractures (Gupta et al., 2014) and with wrist arthroplasties (Boeckstyns and Merser, 2014), respectively. PRWE is highly responsive for detecting effect of treatment ulnar wrist pain due to ulnar impaction syndrome (Omokawa et al., 2012).

A Danish version of the PRWE was validated in 2013 (Schonnemann et al., 2013) (*Appendix 2*). The PRWE allows patients to rate their levels of wrist pain and disability from 0 to 10 on two subscales:

1) The pain subscale (5 items and a maximum score of 50 points)
2) The function subscale (with a maximum score of 50 points) consisting of two sections regarding specific activities (6 items) and usual activities (4 items).

The total PRWE score equals the sum of the PRWE pain score and the PRWE function score. The highest total PRWE score, indicating severe impairment, is 100, and the best score, indicating no impairment, is 0.

The MCID for PRWE have been reported between 11.5 and 24 points for various upper extremity conditions (Schmitt and Di Fabio, 2004; Sorensen et al., 2013; Walenkamp et al., 2015), and in ulnar impaction syndrome a MCID of 17 was reported by Kim and Park (2013).

### 3.6.3 NRS – Numeric Rating Scale

The NRS can be administered verbally or graphically for self-completion to assess information on various items.

The NRS is a reliable and valid tool to assess pain, with excellent test-retest reliability ($r = 0.96$) and with high construct validity (correlated to the visual analog scale (VAS)) (Ferraz et al., 1990).

The NRS consists of a numeric version of the VAS, a horizontal line with an eleven-point numeric range, labeled from 0 to 10, where 0 represents no pain and 10 represent the most severe pain (Figure 3.9).

Reduction of approximately two points or a reduction of approximately 30% in pain NRS represent a MCID (Farrar et al., 2001; Salaffi et al., 2004).

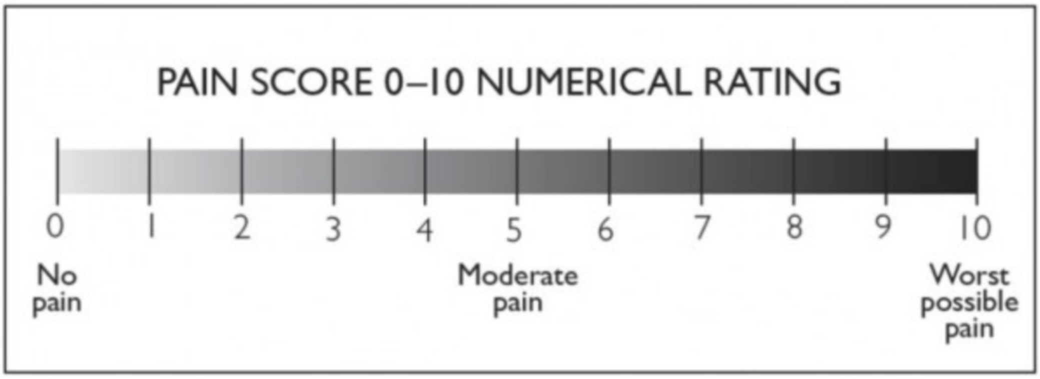


Figure 3.9. Example of the Numeric Pain Rating Scale

## 3.7 Forearm kinematics

### 3.7.1 Anatomical coordinate systems and axis

Kinematics of the forearm can be described from anatomical coordinate systems of the radius and ulna (McDonald et al., 2012) and a common RUJ axis for forearm rotation. Proximally, the RUJ axis pass through the center of the symmetrically shaped radial head and distally, through the foveal region of the ulnar head. In anatomical studies, the RUJ axis has been proposed to be a single RUJ axis (af Ekenstam, 1992; Hagert, 1992) (Figure 3.10). In imaging studies, a helical axis has been proposed to describe the complex forearm rotation axis (Tay et al., 2010), as the DRUJ and PRUJ together does not only act as a condyloid joint, but also include translation in the DRUJ and pistoning along the radioulnar axis. Thus, description of DRUJ kinematics is complex.

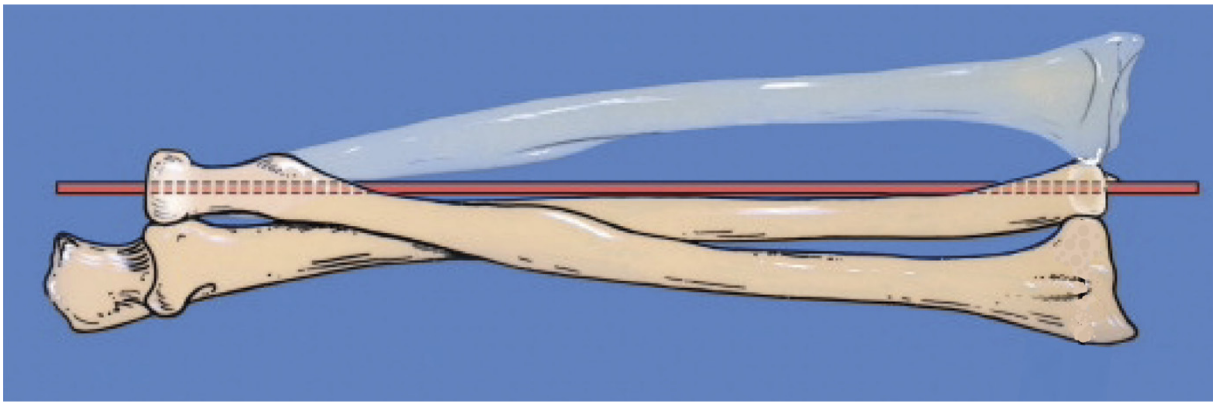

**Figure 3.10.** The single radioulnar rotation axis of the distal and proximal radioulnar joint. Adapted from Kleinman et. al. (2007).

### 3.7.2 DRUJ kinematics

First, *ex vivo* electromagnetic tracking devices were used to describe DRUJ kinematics. However, these invasive methods were not suited to be applied in vivo (Fischer et al., 2001; Gofton et al., 2004; Iida et al., 2012; Moriya et al., 2009).

Next, *in vivo* methods to evaluate the DRUJ kinematics utilizing two-dimensional (2D) slices of Computed Tomography (CT) (King et al., 1986; Mino et al., 1983) and Magnetic Resonance Imaging (MRI) (Nakamura et al., 1999) was described. Later, three-dimensional (3D) CT based registration techniques has been used to evaluate forearm kinematics in vivo from serial static images (Baeyens et al., 2006; Chen and Tang, 2013; Tay et al., 2010).

Studies describing and mapping *in vivo dynamic* forearm kinematics were sparse when this PhD thesis was initiated in 2015. Over the last decade radiographic 3D to 2D registration methods have been used in other joints, but to our knowledge only a few studies has described DRUJ kinematics (Matsuki et al., 2010) and PRUJ kinematics during in vivo dynamic rotation (Goto et al., 2004; Hemmingsen et al., 2020). The results confirmed the findings of previous static experimental and clinical examinations regarding simultaneous DRUJ translation and pistoning during forearm rotation about a RUJ axis. Thus, in healthy individuals it is generally accepted that the DRUJ allows for complex combined joint kinematics:

- An anteroposterior translation between the ulna head and the radius sigmoid notch due to their different radii (Figure 3.5) occurs simultaneously with forearm rotation (af Ekenstam and Hagert, 1985). The radius translates volar relative to the ulnar head in pronation and vice versa in supination (Ishii et al., 1998; King et al., 1986; Matsuki et al., 2010; Shaaban et al., 2007).
- Proximal to distal translation (pistoning) between the radius and the ulnar head occurs as the curved radius rotates around the fixed ulna. In pronation, the radius length decreases relative to the ulna, while increasing in supination (Palmer et al., 1988; Tay et al., 2010; Tay et al., 2008).

The radiographic position of the radius and ulna on posteroanterior (PA) x-rays is termed ulnar variance (Tomaino, 2000).

### 3.7.3 DRUJ translation

Translation in the DRUJ is considered to occur within a normal range due to the inherently instable DRUJ design. Increase in DRUJ translation in comparison to the contralateral joint is considered pathological and can indicate DRUJ instability i.e., owing to TFCC lesion. Therefore, objective methods to evaluate DRUJ translation has gained interest both in experimental settings (Iida et al., 2014; Moriya et al., 2009; Omokawa et al., 2017; Onishi et al., 2017), as imaging-based methods, as clinically applicable instruments (Nagata et al., 2013; Pickering et al., 2016).

## 3.8 Imaging of the TFCC

### 3.8.1 Magnetic Resonance Imaging and Arthrography

Imaging methods such as Magnetic Resonance Imaging (MRI) aim to indirectly visualize and diagnose TFCC injuries.

The field strength of wrist MRI during the past decade has been 1.5 T whereas new and stronger 3.0 T MRI scanners was first recently introduced. With improved image quality better diagnostic accuracy has been hypothesized (Saupe et al., 2005).

Magnetic Resonance Arthrography (MRA) with intraarticular injection of ionized contrast have can be utilized to increase visualization of TFCC injuries. Boer et al. (2018) and Lee et al. (2013) found MRA to have both higher sensitivity and specificity for TFCC injury detection compared to MRI. However, MRA does not sufficiently asses the TFCC injury size and component (Zanetti et al., 1997). Also, MRA has disadvantages as it is an invasive examination and comes with an additional risk.

The quality of all MR based examinations depend on the selected number of slices the MR settings and the use of a wrist coil. Consequently, MRI and MRA may reveal TFCC injuries, but offer limited information about injury location, size, and repairability.

MRI is of the performed in neutral forearm rotation and rarely in supination and pronation. Thus, dislocation or subluxation of the DRUJ is less likely to be demonstrated on axial MRI/MRA views and the method do not add information about the degree of dynamic DRUJ instability (Ehman et al., 2011).

## 3.9 Imaging of the DRUJ

### 3.9.1 Radiographs

Conventional radiography of the wrist includes *posteroanterior (PA) radiographs* and *lateral radiographs.*

On *PA radiographs (*obtained with 90° shoulder abduction, elbow flexion, and neutral forearm rotation), *g*apping in the DRUJ may indicate DRUJ instability but is rarely seen (Luchetti et al., 2014). However, clenched fist PA radiographs may detect DRUJ diastasis in comparison to the contralateral side, and is indicative of DRUJ instability (Iida et al., 2012). The ulnar variance is evaluated on PA radiographs, by projecting a line perpendicular on the radius length axis, from the distal end of the radius volar rim, and measuring the distance (mm) from this line to the distal ulna end (Figure 3.11) (Hulten, 1928). An ulnar styloid fracture may present as an isolated fracture (Logan and Lindau, 2008), but more frequently it accompanies a radial fracture (Buijze and Ring, 2010; Sammer et al., 2009). Basal styloid fractures or displaced styloid fractures may lead to DRUJ instability (Nakamura et al., 2014). Nevertheless, an ulnar styloid fracture is a poor prognostic factor for DRUJ instability (Kim et al., 2010; Wijffels et al., 2014) and has not been confirmed to be highly correlated to foveal TFCC injury in arthroscopic studies (Lindau et al., 1997; Lindau et al., 2000).

On *lateral radiographs (*obtained with 0° shoulder abduction, elbow flexion, and neutral forearm rotation), static DRUJ subluxation or dislocation can be diagnosed as prominence of the ulnar head. The correct lateral projection visualizes the palmar margin of the pisiform midway between the palmar margins of the distal pole of the scaphoid and the capitate head (Mino et al., 1983; Nakamura et al., 1995). However, a true a lateral view is difficult to obtain and as little as 10º of rotation can result in misinterpretation and incorrect diagnosis (Squires et al., 2014).

Thus, using radiographs to evaluate of DRUJ subluxation should be interpreted with caution and additionally, dynamic subluxation in supination and pronation cannot be detected.


**Figure 3.11.** The ulnar variance is evaluated on posterior-anterior radiographs, by projecting a line perpendicular on the radius length axis, from the distal end of the radius volar rim, and measuring the distance (mm) from this line to the distal ulna end (A).

### 3.9.2 Computed tomography scans

Computed tomography (CT) scans of the forearm can display the cross-sectional anatomy of the DRUJ. These examinations can be performed with the patient's forearm positioned in static supination, neutral forearm rotation and pronation. The clinical utility has been established for detecting DRUJ subluxation and is superior to conventional radiographs in evaluation of dynamic subluxation. Still, diagnosing DRUJ subluxation on axial CT is not without challenges. The positioning of the patient to allow for bilateral examination and ensure full pronation and supination has been challenging as positioning of patients on a CT scanner table does not permit the ideal position with 0° shoulder abduction and 90° elbow flexion. Thus, patients are often positioned prone on their belly in the 'superman position' with extended elbows (Mino et al., 1983), and the expected forearm rotation therefore may moreover be shoulder rotation.

Unilateral axial CT scans with 90° elbow flexion has been proposed to ensure full forearm pronation and supination, but repeated bilateral scans are required to allow comparison to normal dorsal or volar displacement of the ulnar head relative to the sigmoid notch of the contralateral forearm (Kim and Park, 2008; Park and Kim, 2008). As CT scans are associated with a relative high radiation dose, the need for repeated bilateral static examinations is a limitation of this CT based examination method.

A computer tomography based congruency method (Wechsler et al., 1987) and evaluation of subluxation across radioulnar lines were first described (Mino et al., 1985) for diagnosing DRUJ instability. Later, modifications of the 'Mino criteria' were proposed, i.e., the modified radioulnar line method (Nakamura et al., 1996), the epicenter method, the subluxation ratio method (Kim and Park, 2008), and the radioulnar ratio method (RUR) (Figure 3.12) (Lo et al., 2001).

All CT-based methods depend highly on standardized positioning during CT scanning and standardized degree of forearm pronation and supination as variation in rotation may influence the measured ulnar head subluxation. Lo et al. (2001) compared the validity of the radioulnar ratio method (RUR), with previously described techniques and reported normal values. In non-injured TFCCs, the mean RUR was 0.50 (SD 0.04) with neutral forearm rotation, and forearm pronation translated the ulnar head dorsally to a mean RUR of 0.60 (SD 0.05).

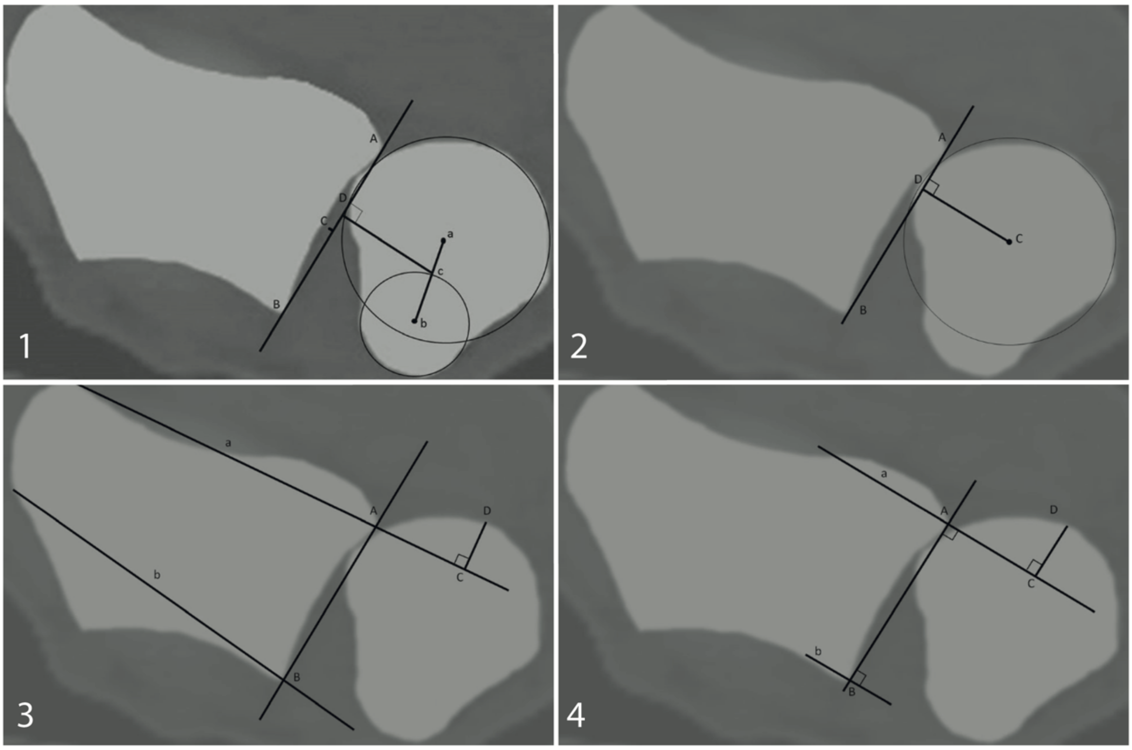


Figure 3.12. (1) The epicenter method =CD/AB, regard the halfway between the ulnar styloid center and the ulnar head center as the center or rotation (c). The orthogonal projection to the sigmoid notch line (AB) defines the point D. The midpoint of the sigmoid notch defines the point C. (2) The radioulnar ratio (RUR) method =AD/AB, regard the center of the ulnar head as the center of rotation (C). The orthogonal projection to the sigmoid notch line (AB) defines the point D. (3) The radioulnar line method = CD/AB, evaluate the amount of the ulnar head protruding (CD) volar (in supination) or dorsal (in pronation), from the radioulnar lines (a and b), and is calculated as a ratio of the sigmoid notch (AB). (4) The subluxation ratio method =CD/AB, evaluate the amount of the ulnar head protruding (CD) volar (in supination) or dorsal (in pronation), from the orthogonal to lines (a and b) of the sigmoid notch endpoints, and is calculated as a ratio of the sigmoid notch (AB). Adapted from Wijffels et al. (2016).

The intra-observer and inter-observer reliability was good with intraclass correlation coefficients of 0.89 (CI 95 0.85–0.92) and > 0.87 (CI 95 0.83–0.91), respectively. However, Kim and Park (2008) evaluated the level of agreement between CT findings and clinical DRUJ assessment and demonstrated poor agreement.

### 3.9.3 Ultrasonography

Ultrasonography (US) has been used as a non-invasive non-radiation dose producing tool to visualize TFCC injuries. The US has shown encouraging results compared to MRI and arthroscopy (Keogh et al., 2004) and MRA (Taljanovic et al., 2008), but is demanding and highly examiner dependent.

Hess et al. (2012) described a US based method to examine DRUJ translation. The US measures were made as axial views of the DRUJ while DRUJ translation was induced by the patient, who performed a volarly directed force of the ulnar palm. The active volar displacement of the ulnar head from the dorsal radius was estimated from static US images at rest and at maximum force. This test established a sensitivity of 88% and specificity of 81% for detecting DRUJ instability.

## 3.10 Classification of TFCC injuries

### 3.10.1 Palmer's classification

Palmer (1989) was the first to describe an arthroscopic classification system for TFCC injuries. It was based on the cause, location and degree of injury. Class 1 lesions being traumatic injuries (Figure 3.13), and Class 2 lesions being degenerative injuries associated with ulnar impaction syndrome.

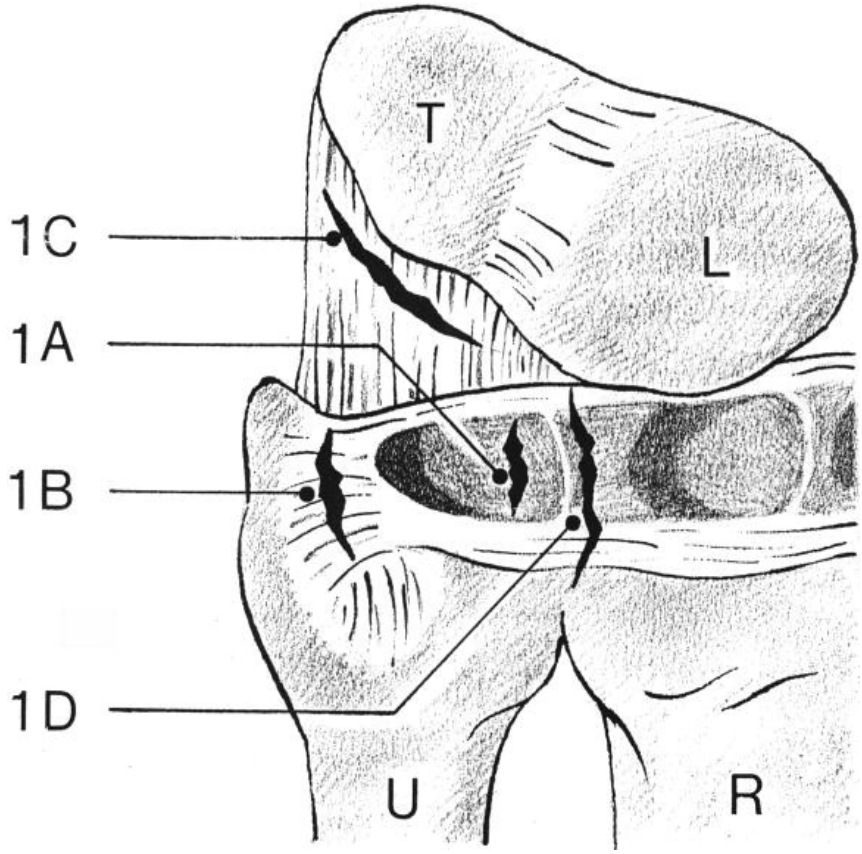


Figure 3.13. Palmer classification of traumatic class 1 injury subtypes including central perforation of the triangular fibrocartilage disc (1A), ulnar avulsion (with or without distal ulnar styloid fracture) that involve the proximal and/or distal TFCC insertion to the ulnar fovea and ulnar styloid, respectively (1B), distal avulsion involving ulnotriquetral and ulnolunate ligaments (1C), and radial avulsion of the TFCC with or without a sigmoid notch fracture (1D).
R: radius, L: lunate, T: triquetrum, U: ulna. Adapted from Bohringer et al. (2002)

The Palmer classification of Class 1 traumatic injuries has several limitations as lesion to the dorsal or volar radioulnar ligaments are not considered, and the peripheral 1B injuries lacks subclassification into foveal TFCC lesions or lesions with detachment of the distal TFCC insertion from the ulnar styloid. Further, different types of central 1A injuries have been documented arthroscopically; vertical slit tears, horizontal tears, and flap lesions in the disk (Abe et al., 2012; Watanabe et al., 2010). Further, it is not uncommon to see combined 1A and 1B tears by arthroscopic evaluation (Abe et al., 2018).

The Palmer classification does not reflect the surgical strategy of treating TFCC injuries. The healing potential in central disk perforations (Palmer 1A) is inadequate due to the absence of vascular supply but does not lead to DRUJ instability.

Contrary, Palmer 1B lesions can lead to symptomatic instability of the DRUJ, and therefore may need reinsertion of the well vascularized TFCC periphery and radioulnar ligaments (Ohmori and Azuma, 1998).

### 3.10.2 Atzei and Luchetti's classification of peripheral TFCC injuries

In 2008, Atzei proposed a classification of the Palmer 1B injuries (Atzei et al., 2008). Later, in 2011, Atzei and Luchetti further developed the comprehensive classification of peripheral TFCC injuries. The latter classifications are based om clinical findings, radiological findings, and arthroscopic findings (Figure 3.14) (Atzei and Luchetti, 2011).

### 3.10.3 Arthroscopic TFCC injury classification

The presence of a peripheral TFCC injury involving the *dc-TFCC* insertion on the ulnar styloid with or without associated styloid fracture can be directly visualized by radiocarpal arthroscopy and confirmed by 'the trampoline test' (Hermansdorfer and Kleinman, 1991), which evaluates the tension in the central TFCC disc. It has been recommended to perform the examination by wet arthroscopy as the TFFC resilience is absent with dry arthroscopy, probably due to lack of joint capsule distention by the fluid (Atzei and Luchetti, 2011).

The presence of a peripheral TFCC injury involving the *pc-TFCC* insertion from the ulnar fovea with or without associated styloid fracture cannot be directly visualized by radiocarpal arthroscopy unless the injury involves both the dc-TFCC and the pc-TFCC insertion.

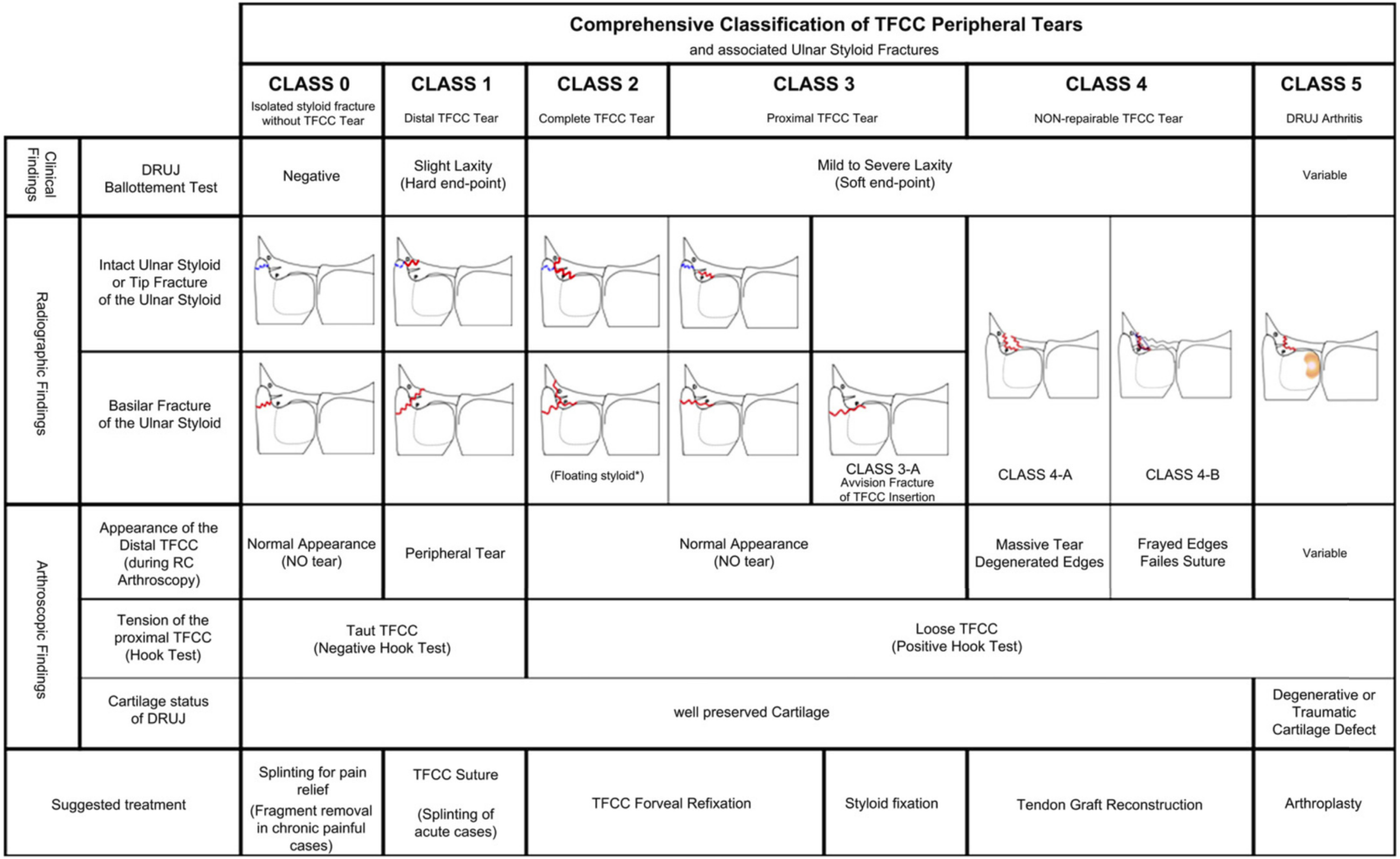


Figure 3.14. The comprehensive classification of TFCC peripheral tears. Clinical evaluation of DRUJ stability by the Ballottement test, radiographic styloid fracture evaluation, and arthroscopic inspection of dc-TFCC lesions, evaluation of the pc-TFCC by the Hook test, is considered. DRUJ arthroscopy can evaluate the DRUJ cartilage. Treatment is suggested according to the classification group (1-5). Adapted from Atzei and Luchetti, 2011.

Radiocarpal arthroscopy and 'the Hook test', however, allows for evaluation of the pc-TFCC as the intact ligamentum subcruentum prevent the TFCC to lift off an be dragged into the joint when tested by the hook of a probe through a 6-R portal, pulling the ulnar rim of the TFCC in a distal and radial direction (Figure 3.15) (Atzei, 2009; Ruch et al., 2003). Simultaneously, radiocarpal arthroscopy can be used to evaluate any other intraarticular injuries and to determine if a TFCC teat has degenerated edges which influence the decision of whether to proceed with TFCC repair or reinsertion (Atzei and Luchetti, 2011) .

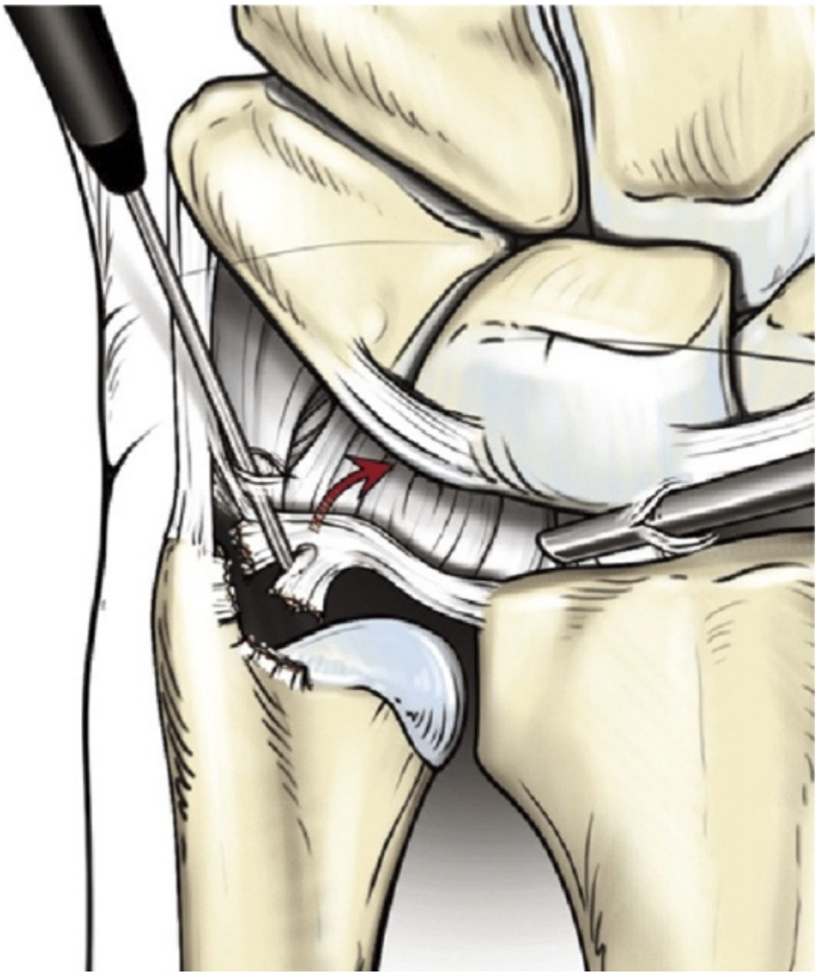

**Figure 3.15.** The Hook test of the foveal TFCC insertion by radiocarpal arthroscopy. Adapted from Atzei and Luchetti., (2011).

Arthroscopy of the DRUJ can directly visualize foveal detachment of the TFCC as well as the cartilage condition of the DRUJ. Today, arthroscopic evaluation of the TFCC is the recommended 'gold standard' diagnostic tool for definitive diagnosis of TFCC injuries (Atzei and Luchetti, 2011; Pederzini et al., 1992), but due to the cost and the invasive nature of the procedure it is nevertheless seldomly used as a 'stand-alone' diagnostic tool, or proceeded with unless surgical intervention is expected.

## 3.11 Surgical treatment of TFCC injuries

The past decades increased anatomical knowledge and biomechanical understanding of the TFCC and DRUJ has led to diverse surgical procedures in the treatment of TFCC injury.
In the acute phase, minor Class 1 dc-TFCC lesions may be sufficiently treated by conservative means with above elbow immobilization or arthroscopic debridement (Cardenas-Montemayor et al., 2013), whereas larger Class 1 dc-TFCC injuries may require arthroscopic capsular inside-out or outside-in suturing (Haugstvedt and Husby, 1999; Takagi et al., 2021) of the lesions due to lasting wrist pain and/or minor DRUJ instability (Atzei, 2009; Pederzini et al., 2007; Whipple and Geissler, 1993).

According to Atzei and Luchetti (2011) (Figure 3.14), Class 2 and 3 TFCC injuries involve the pc-TFCC insertion and may involve the dc-TFCC insertion or a styloid fracture. Symptomatic instability can be treated surgically with basal styloid fracture fixation (Hauck et al., 1996), open reinsertion of pc-TFCC to the fovea by a suture anchor via a dorsal approach through the 5th dorsal extensor compartment (Garcia-Elias et al., 2003; Hermansdorfer and Kleinman, 1991), or arthroscopic reinsertion of pc-TFCC to the fovea by a suture anchor (Kermarrec et al., 2020), transosseous mattress suturing techniques through dual bone tunnels (Nakamura et al., 2011; Shinohara et al., 2013) a single bone tunnel (Iwasaki and Minami, 2009; Kwon et al., 2020; Park et al., 2018) or creating a foot print by suturing through a single bone tunnel and the capsule (Chen, 2017). Debridement of scar tissue from the fovea by a shaver through the pre-styloid recess and careful refreshment of the peripheral TFCC edges is essential to create neovascularization in the TFCC periphery and allow for healing of the TFCC to its native footprint (Chen, 2017).
Class 4 injuries (Figure 3.14), with retracted TFCC edges or degeneration have poor healing potential and require open (Adams, 2000) or arthroscopic TFCC reconstruction (Atzei et al., 2017).

Lately, the arthroscopic techniques for foveal reinsertion of the pc-TFCC has gained increasing interest and general use. However, comparisons of open and arthroscopic reinsertion of repairable foveal TFCC lesions have shown similar results on AROM, grip strength, patient reported outcomes, pain, and clinical stability testing of DRUJ translation (Anderson et al., 2008; Andersson et al., 2018; Luchetti et al., 2014), and superiority with either method has yet to been documented (Robba et al., 2020).

## 3.12 Static radiostereometry

Radiostereometric analysis (RSA) was introduced in the 1970s by Göran Selvik and the first static RSA (sRSA) studies conducted on total hip arthroplasties (Baldursson et al., 1979; Selvik, 1989). The purpose was to quantify the motion of implants in the recipient bone by estimating the 3D position of the two objects over time using static stereoradiographs. This was enabled by using a setup with two converging x-ray sources and dual imaging of an object, which allowed for spatial calculations with reference to a calibration box. The radiolucent carbon box is still used and contain markers inserted in known patterns at the top and bottom layer. It is placed beneath the object, but above the image detectors, and thereby both the calibration box markers and the object are displayed on the RSA images (Figure 3.16).

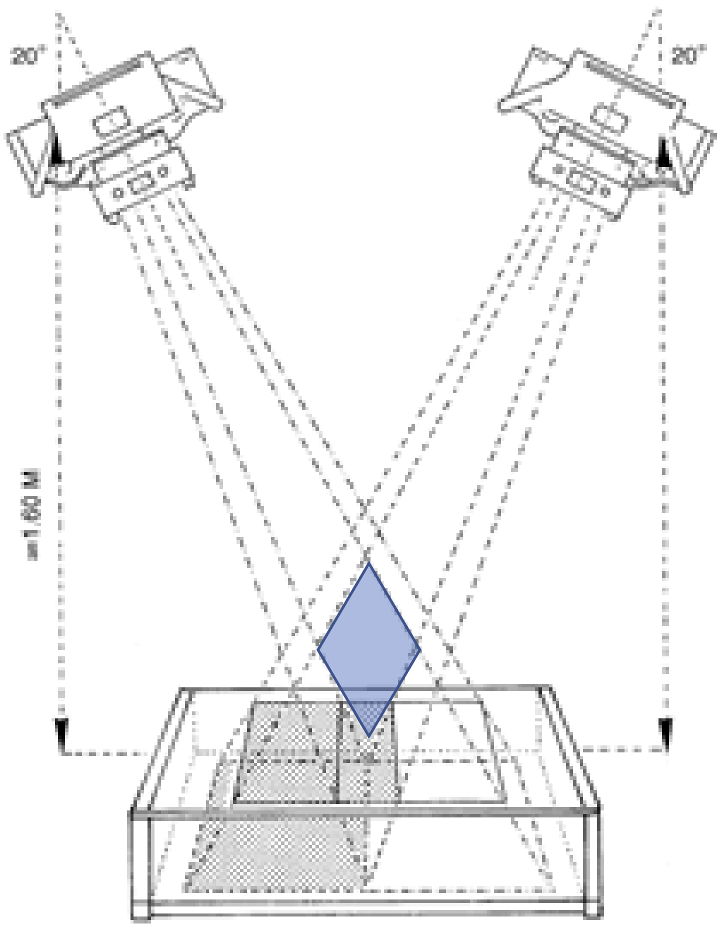


Figure 3.16. Radiostereometry set up with two converting x-ray tubes irradiating through a calibration box on to detectors slotted underneath the calibration box. The object of interest is placed centrally in the beam crossing (blue area) during examination. Adapted from Valstar et al. (2002).

### 3.12.1 Marker-based RSA

Initially, the investigated implant had small metal tantalum markers attached and further tantalum markers were inserted into the adjacent bone as a reference. From each single marker, a set of coordinates can be determined in the calibration box coordinate system. Using several markers (at least 3) it is possible to form a rigid body marker-model and define its 3D position and orientation.

### 3.12.2 Model-based RSA

In the 2000s Kaptein et al. developed a markerless RSA method for investigation of implant migration, but still, markers were used in the bone as reference. This model-based method depended on Computer-aided design (CAD) models of the implant, automated detection of implant edges, and finally complemented by manual selection of the relevant edges (Kaptein et al., 2003). The final RSA analysis to estimate the position of the CAD model was estimated automatically by mathematical algorithms in the model-based RSA software (MBRSA) (RSAcore, Leiden, Netherlands), which minimized the error between the model projections versus the marker-model in the radiographs (Kaptein et al., 2004).

Implant migration can be estimated by follow-up sRSA examinations and marker-based RSA or MBRSA image analysis can describe the implant displacement over time, calculated as the difference to a baseline reference image. Implant migration is reported in terms of translations along and rotations about the x, y, and z-axis in the implant coordinate system. High implant migration or continuous implant migration after the expected time of implant fixation indicate aseptic loosening and risk of implant loosening (Karrholm et al., 1994; Nieuwenhuijse et al., 2012; Pijls et al., 2012; Pijls et al., 2018; Pijls et al., 2012; Ryd et al., 1995). Thus, sRSA is ideal for pre-marked evaluation of the migration pattern of new implant designs and has been recommended before introduction of new implants to the commercial market (Nelissen et al., 2011).

## 3.13 Dynamic radiostereometry

Development of dynamic RSA (dRSA) imaging had the purpose of measuring joint kinematics during patient exercises with loaded joint movement, with or without implants. During the last decades, 3D surface bone models derived from computed tomography (CT) scans was used for bone registration using MBRSA (Anderst et al., 2009; Anderst and Tashman, 2003; Stentz-Olesen et al., 2017). This enabled non-invasive RSA examination and allowed for dRSA imaging of non-operated joints to estimate joint kinematics.

Various dynamic imaging methods have been used, including single-plane dynamic fluoroscopy (Banks and Hodge, 1996), bi-plane dynamic fluoroscopy (Bonanzinga et al., 2016; Guan et al., 2016; Tashman and Anderst, 2003; You et al., 2001), early semi-dynamic RSA (dRSA) imaging with film exchanging technique (Uvehammer and Karrholm, 2001). Later, dRSA imaging using highspeed digital detectors i.e. PIXIUM RF4343 detectors (Thales Electron Devices SA, Vélizy-Villacoublay, France) (Bragonzoni et al., 2019) and Canon CXDI-50RF detectors (Canon, Amstelveen, The Netherlands) (Hansen et al., 2017; Horsager et al., 2017) were published.

Dynamic RSA imaging requires high frequency synchronized radiation sources to expose digital image detectors with ability of high-speed data transfer. Today a 30 Hz image rate is possible in dRSA, but data transfer is currently the limiting factor, because high image rate comes at the expense of image size or resolution. The Adora RSA system (NRT X-Ray, Hasselager, Denmark) with Canon CXDI-50RF detectors (Canon, Amstelveen, The Netherlands) provides a resolution of 1104 × 1344 pixels (0.32 mm/pixel, 79 DPI) with an image frequency up to 15 Hz, when recording on the full detector size (37 cm x 42 cm). This is half of the resolution obtained by sRSA images in a similar setting (Nielsen et al., 2018; Stentz-Olesen et al., 2017).

Dynamic imaging entails an enormous number of dRSA images for analysis after a single patient exercise recording. Using conventional marker-based RSA or MBRSA for image analysis is extremely time consuming as manual assistance is necessary for analyzing each image frame and therefore the cost is prohibitive for a dRSA in a general use. Thus, for dRSA imaging to be efficient and to gain use in clinical practice an automated analyzing software with least possible manual interaction is essential (Stentz-Olesen et al., 2017).

### 3.13.1 Automated RSA software

The need for precise and accurate automated analysis of dRSA image series to estimate bone motion, led to development of new time saving and non-invasive software methods. These methods have been based on software generating 2-dimensional (2D) virtual digital reconstructed radiographs (DRR) from 3-dimensional (3D) computed tomography (CT) based bone models. A DRR is a projection of the 3D CT bone models on an 2D image plane, thus a virtual radiograph. A few research centers have developed their own algorithms for analysis, but no fully automated analysis software is currently commercially available for dynamic RSA analysis.

The use of individual 3D bone models, DRR and anatomical coordinate systems of each bone has benefits in relation to anatomical description of joint kinematics during active exercises. DRR based analysis methods have been used in vivo for evaluation of knee kinematics (Anderst et al., 2009; Christensen et al., 2020; You et al., 2001), hip kinematics (Hansen et al., 2018), and ex vivo elbow and forearm kinematics (Hemmingsen et al., 2020).

## 3.14 Accuracy and precision of RSA

The value of RSA for evaluation of implant migration is widely accepted due to its applicability in clinical practice and high accuracy and precision (Selvik, 1989).

Accuracy describes the closeness of agreement for the method under evaluation, against the true value, or an accepted reference. Examination of new methods in comparison to the 'gold standard' therefore does not reflect the difference to the true value, but the ability of a given method to measure the same value as the 'gold standard', which in theory should be zero. Precision describes the closeness of agreement between repeated measures with unchanged conditions.
Marker-based RSA was validated by using phantoms with known marker positions (Stilling et al., 2012) and marker-based RSA has been defined as the 'gold standard' RSA method as the accuracy and precision is high (Valstar et al., 2005). Validation of a methods precision rely on double examinations. The mean difference (dif) between double examinations, is an estimate of the systematic error, whereas the prediction interval (1.96 x SDdif) is a measure of the random error. The ideal method has a combination of high precision and high accuracy, that converge the repeated measurements close to the true value (Figure 3.17 (top left)).

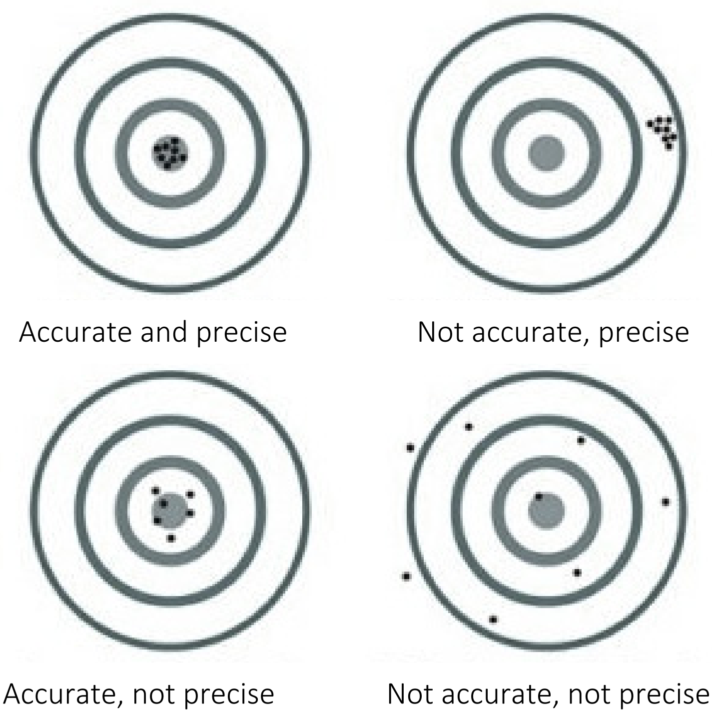


**Figure 3.17.** Description of precision and accuracy. An accurate method hits the true value with a small error. A precise method repeats the same value with small differences but does not necessarily hit the true value.

Ten Brinke et al. (2017) have reported the range of precision values in a systematic review on upper extremity RSA studies using marker-based or model-based RSA. The mean precision values (dif) ranged from 0.06–0.88 mm for translations and 0.05–10.7° for rotations in the shoulder, and from 0.05–0.34 mm translations and 0.16–0.76° rotations in the elbow. Precision values on the distal forearm has not been reported.

Stentz-Olesen et al., (2017) validated dRSA analysis with model-based RSA using marker-models of the bone and 3D surface bone-models in the knee joint. They reported sub-millimeter and sub-degree systematic errors and random errors for both translations and rotations of the 3D surface bone-models. Thus, the use of CT-based surface bone-models was encouraged, as a useful precise substitute to marker-based RSA methods for analyzing dRSA images.

The validity of RSA can, however, be affected by the calibration box, the x-ray source and detectors, the radiographic settings, positioning of the patient and the software for analysis (Bragdon et al., 2004; Cai et al., 2008; Lindgren et al., 2020). Also, a good tantalum marker distribution in the bone (condition number) plays a role. For hip and knee implants the acceptable condition number threshold is up to 150 (Valstar et al., 2005). Currently, such threshold limit is not defined in the upper limp. Due to the smaller bony anatomy in the upper limb compared to the lower extremity, wide marker distribution is much more challenging (Hansen and Stilling, 2013). To gain acceptable condition numbers attention to marker distribution is necessary If sufficiently low condition numbers are not obtained this increases the risk of lower accuracy and poorer precision in upper limb RSA studies compared to lower limb studies (Madanat et al., 2005).

Dynamic RSA analysis has additional challenges to static RSA due to limitations of simultaneously attaining good image quality, high image frequency (frames/sec) and full detector size. The latter often is of importance to record the full length of long bones in a moving limb, and image frequency is especially important when recording rapid moving limbs/exercises. During movement also the source to image distance (SID) needs to be approximately steady and with the limb centered in the beam crossing (Figure 3.16).

## 3.15 Summary of background

In summary, diagnosing DRUJ instability due to traumatic TFCC lesions can be difficult, both by clinical examination and imaging modalities. Thus, evaluation of DRUJ instability before and after surgical treatment to determine the stabilizing effect is challenging. Untreated DRUJ instability and insufficient effect of TFCC reinsertion may lead to persistent wrist pain and arthritis.

The number of described techniques for surgical treatment of TFCC lesions is growing as the challenge of treating TFCC injuries and DRUJ instability have gained increasing attention and interest the last decade. However, a common limitation is that objective evaluation of the preoperative and postoperative outcome in terms of DRUJ stability is sparse. Therefore, valid objective methods to assess in vivo DRUJ stability and help ensure timely diagnosis and appropriate treatment are warranted.

Static and dynamic RSA have proven accurate and precise for evaluation of joint kinematics and an automated analyzing method (AutoRSA) have been developed, which make extensive examination of different static and dynamic experimental ex vivo and patient performed in vivo tests of various joints realistic.

## 3.16 Motivation for the PhD thesis

The motivation for this PhD thesis was to develop, validate and apply dynamic RSA for measurement of DRUJ kinematics and fill the knowledge gap on normal kinematics in non-injured DRUJs, pathological kinematics in TFCC injured DRUJs, and reveal kinematic changes in the DRUJ after surgical treatments.

# 4 Aims & hypothesis

# 4

# Aims & hypotheses

The overall aims in this thesis are to use RSA for assessment in ex vivo and in vivo settings, to evaluate the DRUJ instability and investigate the DRUJ kinematics in normal joints, TFCC injured joints and the effect of surgical treatment (Figure 4.1).

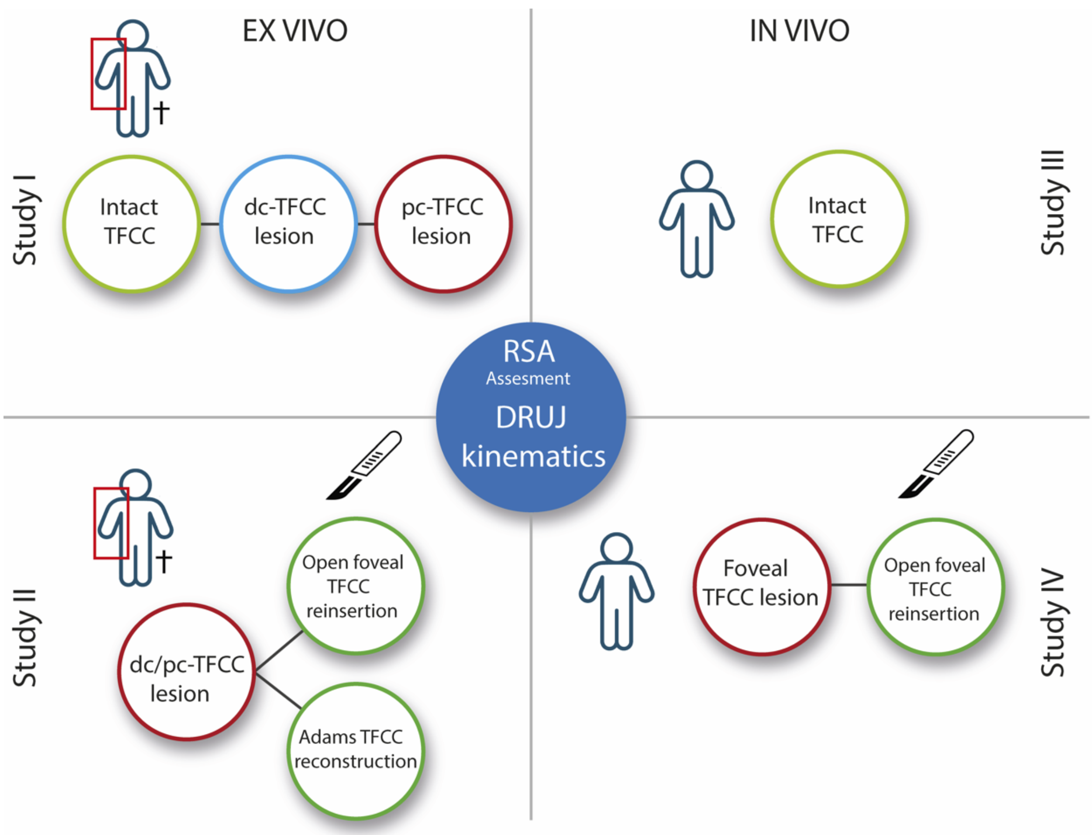


**Figure 4.1.** Schematic illustration of the different studies in the thesis.

## 4.1 Ex vivo studies

### 4.1.1 Study I

*Aim:* To use static RSA analysed by AutoRSA to evaluate DRUJ stability in intact donor arms and DRUJ instability after lesion of first the dc-TFCC and second after lesion of the pc-TFCC.

*Hypothesis:*

*H1:* The primary kinematic outcome, DRUJ translation, increase in with successive dc-TFCC and pc-TFCC lesion.

*H2:* Static RSA is a reliable and precise method to estimate DRUJ translation.

### 4.1.2 Study II

*Aim:* To use static RSA analysed by AutoRSA to compare surgical treatment of DRUJ instability with open foveal TFCC reinsertion and Adams TFCC reconstruction with palmaris longus graft.

*Hypothesis:*

*H0:* Open foveal TFCC reinsertion and Adams TFCC reconstruction have similar stabilizing effect on DRUJ stability evaluated by DRUJ translation.

## 4.2 In vivo studies

### 4.2.1 Study III

*Aim:* To use dynamic RSA analysed by AutoRSA to map normative data of kinematic values in non-injured symptom free participants DRUJs during a patient performed Press test.

*Hypothesis:*

H1: Dynamic RSA is a reliable and precise method to estimate normal DRUJ kinematics.

### 4.2.2 Study IV

*Aim:* To use dynamic RSA analysed by AutoRSA to evaluate the outcomes of DRUJ kinematics in foveal TFCC injured joints in comparison to the contralateral non-injured asymptomatic DRUJ at baseline and at 6-month and 1-year follow-up after surgical treatment, during a patient performed Press test.

*Hypothesis:*

H1: The primary kinematic outcome, DRUJ translation, was increased in foveal TFCC injured joints in comparison to the contralateral non-injured asymptomatic DRUJ.

H2: The secondary kinematic outcomes, in term of DRUJ position, DRUJ distance and ulnar pistoning was increased in foveal TFCC injured joints in comparison to the contralateral non-injured asymptomatic DRUJ.

H3: Surgical treatment normalize kinematic outcomes to normal values.

H4: Surgical treatment improve clinical outcome measures and PROMs.

H5: Dynamic RSA analysed by AutoRSA is a reliable and precise method to estimate pathological DRUJ kinematics.

# 5 Design

# 5

# Design

## 5.1 Ex vivo studies

### 5.1.1 Study I

Study I is a repeated measurement study design in an experimental setting on human doner arm.

### 5.1.2 Study II

Study II is a randomized controlled study design in an experimental setting on human doner arms.

## 5.2 In vivo studies

### 5.2.1 Study III

Study III is a clinical prospective cohort study, Evidence level IV.

### 5.2.2 Study IV

Study IV is a clinical prospective cohort study with 6-month and 1-year follow-up. Evidence level II.

# 6 Materials & methods

# 6

# Materials & methods

## 6.1 Ethical issues

### 6.1.1 Studies I & II

Studies I and II, were ex vivo studies on human donor arms. The Central Denmark Region Committees on Health Research Ethics approved the study (Casenr. 1-10-72-6-16 issued on February 24th, 2016).

### 6.1.2 Studies III & IV

Studies III and IV, were performed as in vivo studies of clinical patients.

In both studies, all participants received oral and written information about the research studies, the examination protocol including imaging and radiation dose, data collection, and surgical treatment including follow-up when appropriate. Prior to enrollment in the studies, all participants were offered time for reflection before informed written consent was obtained.

Prior to study initiation, the studies were registered with the Danish Data Protection Agency (Journal no.2012-58-006; issued May 2016) and approved by The Central Denmark Region Committees on Health Research Ethics (Journal no.1-10-72-146-16; issued August 2016). The ethical principles of the Declaration of Helsinki II regarding human experimentation were followed, and all data were handled according to the General Data Protection Regulation.

### 6.1.3 Radiation dose estimates Studies III & IV

Dynamic radiostereometry expose the participants in study III and the patients I study IV to ionizing radiation. In some centers CT is one of the diagnostic options to evaluate DRUJ subluxation, but in the following calculation of radiation dose it will be regarded as a part of the study radiation exposure, additional to background radiation.

To limit the additional radiation to which the participants and patients are exposed to, the examination field is reduced to least necessary anatomy of interest. The CT scans was only acquired once. The estimated effective dose for one CT of the forearm in adults was <0.1 mSv.

Estimation of the effective radiation dose of one dRSA stereoradiograph on the extremities is approximately 0.02 μSv (Medicotechnical advisors at Aarhus University Hospital). Dynamic series during the Press test examination depended on the speed of which the subject performed the test, but in average patients used up to 5 seconds and were examined twice (double examination for validation) at an image frame rate of 10 Hz (50 dRSA stereoradiographs /examination). The estimated effective radiation dose for participants in Study III was 2 μSv in addition to the 0.1 mSv CT dose (2 dbl. examinations x 1 forearms x 50 images x 0.02 μSv).

In Study IV, each patient was examined four times in total from inclusion to 1-year follow-up (bilateral preoperative, 6 months and 1 year). Thus, the estimated effective radiation dose, including double examinations for validation, was 8 μSv (2 dbl. examinations x (2 preoperative (bilat) + 2 postoperative examinations) x 50 images x 0.02 μSv) addition to the 0.1 mSv CT dose.

The accumulated effective radiation dose for the participants (2 μSv + 0.1 mSv = 0.102 mSv) and patients (8 μSv + 0.1 mSv = 0.108 mSv) in Studies III and IV, respectively, both falls into category IIa, according to the International Commission on Radiological Protection standard (2018).

The risk of inducing an incurable cancer disease increases by 5%/1 Sv radiation compared to the general population risk. The exposure to a dose of 0.1 mSV = 0.0001 Sv increases the risk by 5% x 0.0001 = 0.0001 % in addition to the 25% general risk of dying from cancer in Denmark.

## 6.2 Specimens and patients

### 6.2.1 Donor specimens in Studies I & II

Freshly frozen (not embalmed) donor arms from Department of Biomedicine, Aarhus University were used and included the hand, forearm, elbow and distal humerus. The donor arms were thawed for 48 hours at 5 °C before evaluation of eligibility.

In Study I, eight human donor arms from one woman and seven men with a mean age of 78 years (range 72 – 90) were used.

In Study II, ten human donor arms from two woman and eight men with a mean age of 78 years (range 63-90) were used.

### 6.2.2 Inclusion criteria in Studies I & II

Specimen inclusion criteria were: 1) normal fluoroscopy of the wrist, forearm and elbow, with no signs of previous fracture or malunion or DRUJ arthritis and 2) a normal Hook test on arthroscopic assessment. Degenerative lesions of the central TFCC meniscus were accepted (Palmer type 2A) (Palmer, 1989).

### 6.2.3 Patients in Studies III & IV

Participants in Studies III and IV were recruited prospectively at Aarhus University Hospital and Regional Hospital West.

In Study III, 33 consecutive subjects, nine-teen women and four-teen men were recruited between February 2017 and February 2020. They gave their informed consent to participate in a prospective cohort study on normative data of DRUJ kinematics.

In Study IV, 64 patients gave their informed consent to participate. In twenty-one patients, ten women and eleven men, wrist arthroscopy and Hook test confirmed traumatic foveal TCFF injury (Atzei, 2009). Between February 2017 and April 2020 these twenty-one patients were recruited. They were treated surgically by open foveal TFCC reinsertion and followed-up at 6 months and 1 year postoperatively. The study flow is described in detail in the next chapter 6.3. The patient's contralateral healthy arm was used for comparison.

### 6.2.4 Inclusion and exclusion criteria in Studies III & IV

Participants in Studies III and IV were eligible if aged 18 years to 50 years (both included).

In Study III, additional *inclusion criteria's* were: no ulnar sided wrist pain, no previous surgery or sequelae after upper limb injuries. To avoid paired data, only one non-injured forearm from each subject was included.

In Study IV, additional *inclusion criteria* were: 1) ulnar sided wrist pain with clinically evaluated DRUJ instability including increased DRUJ translation or radiological signs of TFCC injury or DRUJ instability such as gapping of the DRUJ on standard PA radiographs, MRI verified edema of or foveal TFCC injury and 2) finally, arthroscopic confirmation (reference standard) of foveal TFCC injury with a positive Hook test (Atzei, 2009). Further, 3) a non-injured contralateral forearm and DRUJ without any pain or history of wrist or forearm trauma or previous surgery was mandatory as this forearm was used for comparison with normal joint kinematics.

In Study IV, the *exclusion criteria* were: history of rheumatoid conditions, DRUJ and radiocarpal osteoarthritis, MRI verified signs of ulnocarpal impaction with ulnar variance >2 mm, arthroscopically verified intercarpal ligament injury, fracture malunion or surgical treatment of the wrist, DRUJ, forearm or elbow. Previous fractures below elbow level with remaining osteosynthesis material was an exclusion criterion because of metal artefacts on CT based bone models despite metal reduction protocols. Further, patients unable to communicate in Danish were excluded from the study. The flowchart of patients enrolled is displayed in Figure 6.1.

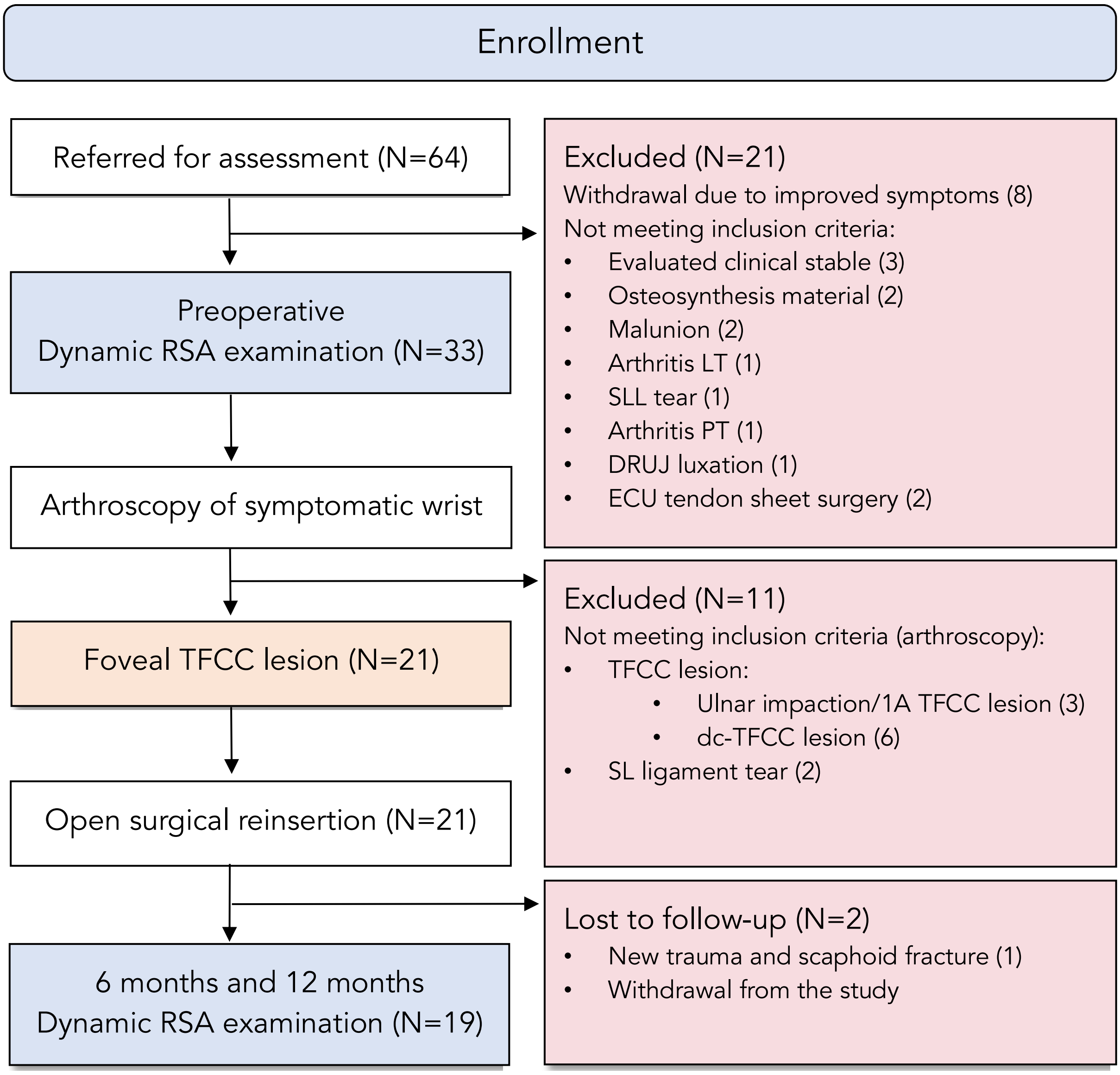


**Figure 6.1.** Flowchart of participants enrolled in the study at each timepoint.

## 6.3 Study flows and follow-up

The specimens in Studies I and II, were examined at baseline with fluoroscopy to exclude previous fracture, malunion or arthritis and by computer tomography (CT) to generate bone models for automated RSA analysis (AutoRSA).

### 6.3.1 Study I

The intact human donor arms DRUJ were assessed by the arthroscopic Hook test of the TFCC and clinical examination by Piano key test and Ballottement test at baseline (<5 mm translation in neutral position) and after each intervention to assess the TFCC status before static RSA examination was performed.

Small stapp-incisions were made in the skin and two cortical 4.2 mm drill holes were done, and through these eight tantalum beads (Ø: 1 mm) were inserted in the distal radius and ulna in a predefined pattern by use of a bead gun (Kulkanon, Wennberg Finmek, Gunnilse, Sweden).

Static RSA examinations were performed. First, with the forearm in neutral rotation, next, with pronated forearm, and finally after applying the Piano key test. The Study I flow is displayed in Figure 6.2.

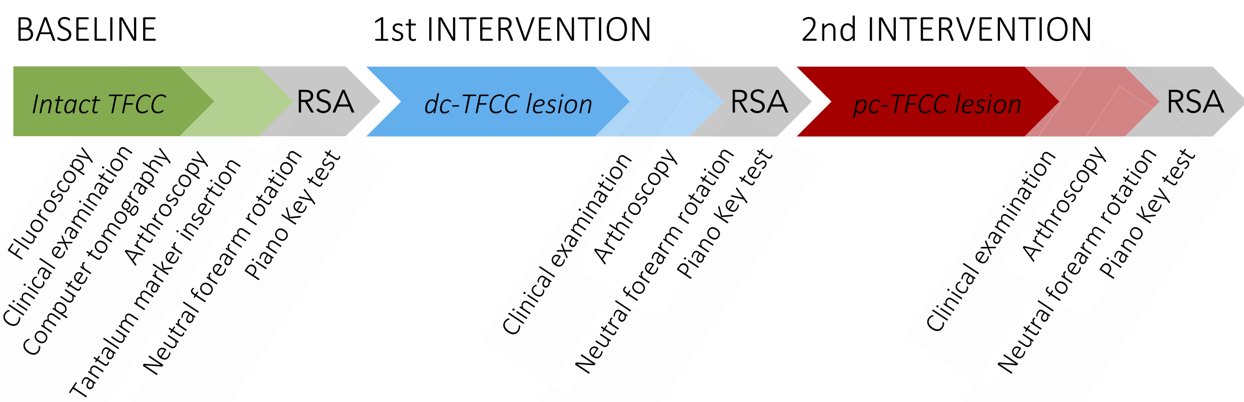


**Figure 6.2**. Study flow displaying interventions and examinations in Study I.

### 6.3.2 Study II

The human donor arms DRUJ with transected dc- and pc-TFCC were assessed loose by arthroscopic Hook test of the TFCC and unstable by Piano key test and Ballottement test (<5 mm translation in neutral position) at baseline.

Clinical examination was repeated after intervention with either open TFCC reinsertion (Hermansdorfer and Kleinman, 1991) or Adams TFCC reconstruction (Adams, 2000) as allocated by randomization. Static RSA examination in neutral forearm rotation and by the Piano key test was performed at baseline and after intervention. The Study II flow is displayed in Figure 6.3.

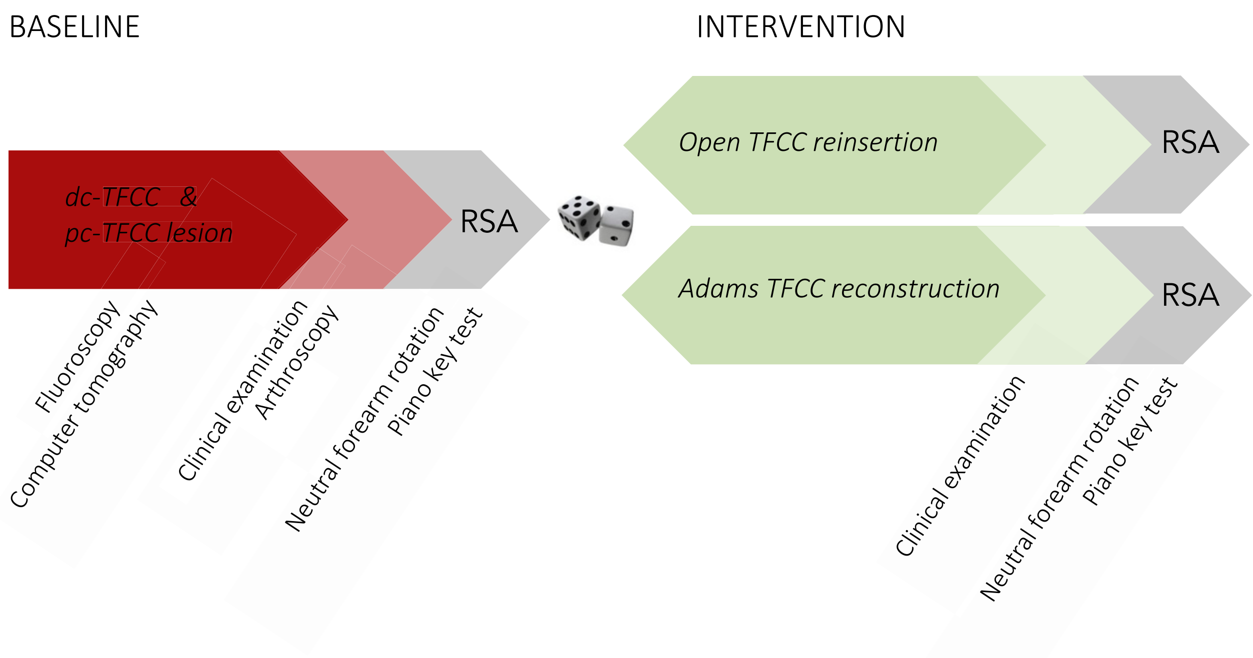


**Figure 6.3.** Study flow displaying interventions and examinations in Study II.

### 6.3.3 Study III

In study III, clinical examination of the participants non-injured pain-free forearm was performed. CT examination used to generate bone models for automated the RSA analysis. Dynamic RSA was recorded to collect data of normative DRUJ kinematics during a Press test.

### 6.3.4 Study IV

In study IV, patients referred to the outpatient clinics with ulnar wrist pain after a trauma were first evaluated by clinical examination.

When suspicion of TFCC injury and DRUJ instability was present, the patient was refereed for a '*imaging protocol*' including wrist radiographs, bilateral CT of the forearm for bone model generation, and MRI of the injured wrist. The patient's contralateral non-injured arm was used for comparison.

Patients returned for response on the imaging examinations and were enrolled in the study if arthroscopy was indicated, and they fulfilled the inclusion criteria.

At baseline, outcomes assessed by clinical examinations and bilateral ultrasonography measures (described in chapter 6.6.3) were recorded by the same observer in all patients. The patients returned after approximately 4 weeks for repeated ultrasonography examination and bilateral dynamic RSA imaging with two Press test cycles.

All questionnaires regarding PROMS were recorded before these examinations to reduce bias.

Arthroscopy was used to confirm injury of the pc-TFCC before open foveal TFCC reinsertion was performed.

At 6-month and 1-year follow-up, the patients returned for PROMs, clinical examination, US, and dynamic RSA imaging examination on the operated forearm. An overwiev of the study flow is dispayed in Figure 6.4.

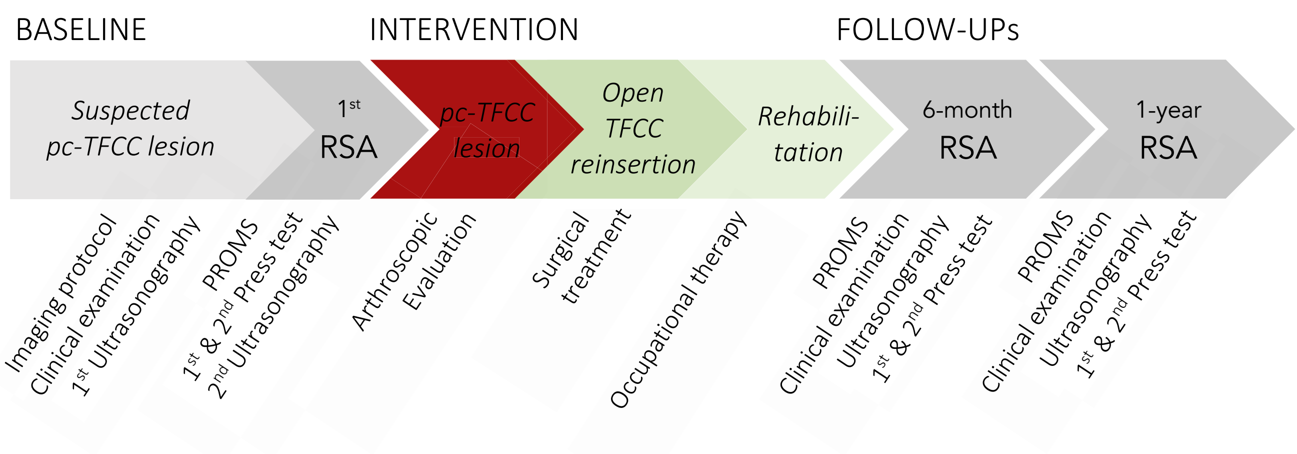


**Figure 6.4.** Study flow displaying examinations and interventions in Study IV.

## 6.4 Clinical examination

In Studies I and II, all specimens were examined to evaluate DRUJ stability before and after intervention. The Piano-key test and the Ballottement test in neutral rotation was performed by two hand surgeons (first and last author). A consensus was obtained as estimation of the DRUJ translation (stable: < 5 mm translation, unstable > 5 mm translation and soft endpoint).
In Study III and IV, all clinical examinations were performed by the principal investigator, who was not blinded to the history of the patients.

In Study III, clinical examination of the participants was performed to *rule out* ulnar sided wrist pain, signs of TFCC pathology, and DRUJ instability.
In Study IV, clinical examination of patients referred with ulnar wrist pain after a trauma were performed to confirm that the ulnar sided wrist pain was in the foval area (Foveal sign test and the Press test). Further, pain during passive and active forearm rotation added to the suspicion of specific TFCC injuries. Increased DRUJ translation evaluated by the Piano-key sign test and the Ballottement test was noted and compared to the contralateral asymptomatic/non-injured DRUJ.

In Studies III and IV, the AROM in wrist and forearm was measured in degrees with a goniometer as described in the Danish National recommendations for measuring joint movement (Helle Puggård, 2014). The examination of AROM was only performed by the principal investigator to increase reliability of the measures.
The grip strength was measured in kilograms with the DHD-1 digital Hand Dynamometer (SAEHAN Corporation, Gyeongsangnamdo, South Korea) allowing recording and displaying of the maximum pressure. The average of three measures was reported (Therapists, 1992). The Hand Dynamometer has 5 positions and position 2 was used for all examinations.

An overview of the baseline data and clinical findings collected in Studies I-IV are presented in Table 6.1.

| Table 6.1. Data collected in Studies I, II, III and IV | | | | |
|---|---|---|---|---|
| *Category* | *Studies I & II* | *Study III* | *Study IV* | |
| *Time* | *Preoperative* | | *Preoperative* | *6 and 12-month postoperative* |
| *Characteristics* | | | | |
| Age | + | + | + | + |
| Gender | + | + | + | + |
| Dominant side | | + | + | + |
| Injured side | | | + | + |
| *Clinical examinations* | | | | |
| Ballottement test | + | + | +* | +* |
| Piano key sign test | | | +* | |
| Active Range of motion | | + | +* | +* |
| Grip Strength | | + | +* | +* |
| *Patient reported outcome* | | | | |
| QDASH | | | + | + |
| PRWE | | | + | + |
| Pain on NRS | | | + | + |
| Treatment satisfaction | | | | + |
| Willingness to repeat | | | | + |
| *Imaging* | | | | |
| Ultrasonography | | + | +* | + |
| Static RSA | + | | | |
| Dynamic RSA | | + | +* | + |

**Bilateral*

## 6.5 Patient-Reported Outcome Measures

In Study IV, following paitent-reported outcome measures (PROMS) were recorded:

- The *QDASH* was used to assess ADL, social and work ability, pain and other symptoms. The total summative QDASH score ranging from 0 to 100, where 0 represents no disability and 100 represent the most severe disability, was calculated in the study.
- The *PRWE* was used to rate the patient's level of wrist pain and disability. These subscale scores and the summative total score ranging from 0 to 100, where 0 represents no disability and pain, and 100 indicating severe impairment.
- *Pain on NRS* was used to assess average information of pain intensity in rest, during pain provoking activities such as unloaded rotation of the forearm, loaded rotation of the forearm and lifting more than 5 kg.
- *Self-reported willingness to repeat* the surgical treatment and rehabilitation was reported at 1-year follow-up by the patients. This was assessed using a single question "would you undergo surgery again with the knowledge you have today about the course and the result'? The possible answers were "yes', "no ", and "I am not sure'.
- *Satisfaction with treatment* was reported at 1-year follow-up by the patients and answered as very dissatisfied, dissatisfied, neither satisfied, or very satisfied.

An overview of thePROMS collected in Studies IV, at baseline and at each follow-up are presented in Table 6.1.

## 6.6 Imaging protocol

### 6.6.1 Radiographs

Patients referred to Study IV was examined by standard lateral and PA wrist radiographs of the symptomatic wrist. Evaluation of the radiographs was done by the surgeon. Wrist pathology including fracture malunion, arthritis, DRUJ gapping, ulnar variance was evaluated and handled as described in the inclusion and exclusion criteria.

### 6.6.2 Computer Tomography (CT)

All arms were examined with CT scans to generate bone models (se chapter 6.14). Similar CT protocols for scanning of the wrist, forearm and elbow was conducted for specimens in Studies I and II, the non-injured forearms of the participants in Study III and both the injured and the non-injured forearm of patients participating in Study IV. All scans were acquired by a Philips Brilliance 64-slice CT scanner (Philips Medical Systems, Best, The Netherlands) with 120 kV, 100 mAs.

Images were reconstructed with a slice thickness of 0.9 mm, a slice increment of 0.45mm and an in-plane pixel size of 0.27 x 0.27 mm.

### 6.6.3 Magnetic Resonance Imaging

In Study IV at Hospital Unit West, the patient's injured wrist was examined by an Achieva 1.5 Tesla MRI unit (Philips Medical Systems). At Aarhus University Hospital the patient's injured wrist was examined with MRI on either an Optima 1.5T unit (GE) or a Skyra 3.0 Tesla unit (Siemens). A hand coil was used for all examinations. The MRI sequences is displayed in *Appendix 3*.

Evaluation of the MRI scans was done by an experienced consultant radiologist. Wrist pathology other than sings of TFCC injury was handled as described in the inclusion and exclusion criteria. Signs of TFCC injuries was evaluated and noted in case of radial injury to the radioulnar ligaments, superficial injury of the dc-TFCC, foveal detachment of the dc-TFCC, and any peripheral edema of the TFCC.

### 6.6.4 Ultrasonography

In Study III, ultrasonography examination of DRUJ translation was performed on the participants non-injured DRUJ, and in Study IV bilateral examination of the patients DRUJ was performed. The patients were examined in at standardized setting as described by Hess et al. (2012), by using a custom-made positioner that abducted the upper arm 60° from the vertical plane and pronated the forearm 30°, as the hand was resting on a block (Figure 6.5).

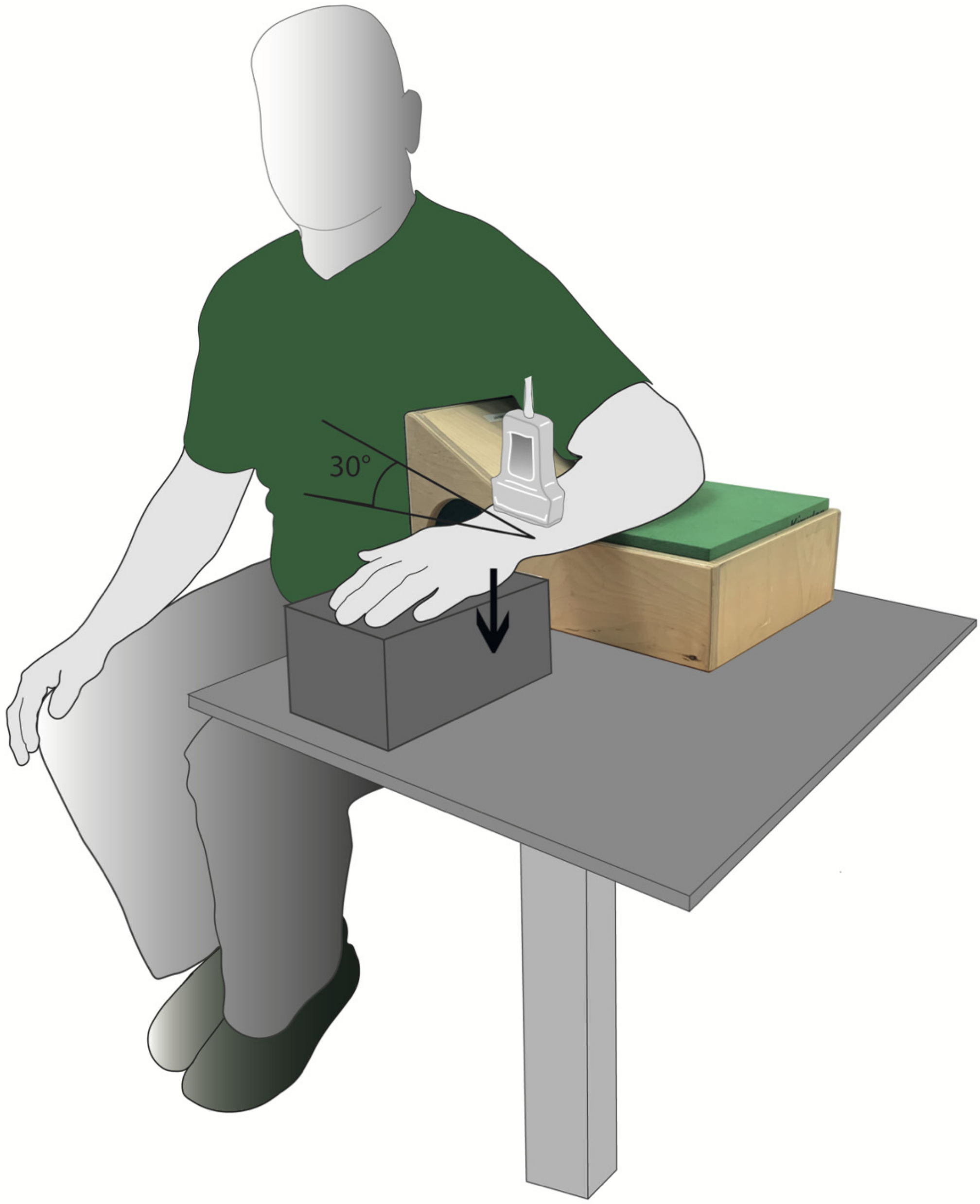


Figure 6.5. Standardized patient position during ultrasonography.
Adapted from Thillemann et al. (2021b).

Ultrasonography measures were made perpendicular to the longitudinal axis of the ulna, placing the transducer dorsally over the DRUJ at the level of the Lister tubercle (LT) displaying axial views of the distal radius (DR) and the ulnar head (UH).

First, static measurement of the perpendicular distance from an extended line through the floor of the 4$^{th}$ extensor compartment of the distal radius (DR) to the top of the ulnar head (UH) was recorded at rest ($X_1$) (Figure 6.6a).
Second, this measure was repeated ($X_2$) after a palmar shift of the ulnar head pressure was induced by applying pressure by the pisiform bone area of the palm onto the leveled block (Figure 6.6b). The DRUJ translation ($T = X_1\text{-}X_2$) and the Hess Quotient ($Q = [X_1\text{-}X_2] / X_1$) was calculated.

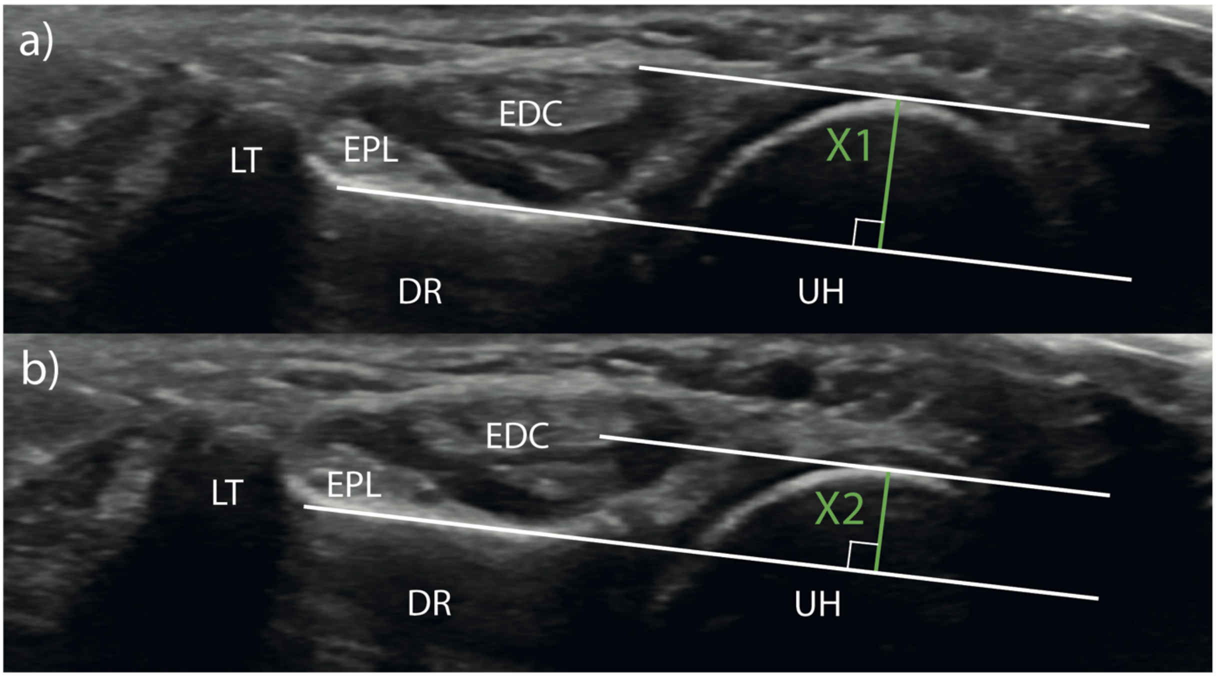


**Figure 6.6.** (a) Resting ultrasonography DRUJ measure ($X_1$) and (b) loaded DRUJ translation measure ($X_2$) was used to calculate the DRUJ translation ($T = [X_1\text{-}X_2]$) and the Hess Quotient ($Q= [X_1\text{-}X_2] / X_1$.). Adapted from Thillemann et al. (2021b).

## 6.7 Arthroscopic evaluation

In the experimental Studies I and II, human donor arms were examined at baseline with wrist arthroscopy and after each intervention.
In Study I, first wrist arthroscopy was used to verify the TFCC to be intact at baseline. Second, to confirm dc- and pc-TFCC lesions in terms of a positive trampoline test (Hermansdorfer and Kleinman, 1991) and a positive Hook test (Atzei, 2009), after each intervention.
In the intact cadaver specimens, we observed more laxity of the TFCC as tested with the trampoline test compared to a wrist arthroscopy in vivo. Therefore, the status after the dc-TFCC lesion was not assessed by the trampoline test.
The Hook test *was* used to assess the status of the pc-TFCC in all three phases of the study.

In Study II, wrist arthroscopy including the Trampoline test and the Hook test was used to verify the pc-TFCC lesion before intervention with TFCC reinsertion or TFCC reconstruction.

In Study VI, patients with clinically assessed DRUJ instability was re-examined by the ballottement test in general anesthesia before the wrist arthroscopy was performed. Prior to intervention with surgical treatment, wrist arthroscopy was used to rule out concomitant lesions as described in the exclusion criteria and finally, to apply the Hook test and confirm lesion of the pc-TFCC from the ulnar fovea.

## 6.8 Randomization

In Study II, the specimens were randomly assigned into two intervention groups: open surgery with foveal TFCC reinsertion (Hermansdorfer and Kleinman, 1991); or Adams TFCC reconstruction, with palmaris longus graft (Adams, 2000).
Specimens were numbered and ten opaque envelopes were prepared with an equal 1:1 ratio distribution of intervention labels and sealed. Randomization was conducted by sequentially drawing envelopes that randomly assigned the specimens to the two intervention groups.

## 6.9 Interventions

In Study I, a skin incision proximal to the TFCC on the dorsal aspect of the DRUJ was used to assess the posterior DRUJ capsule of the specimens. Through a 1 cm transverse opening proximal to the TFCC, the first intervention was detachment of the dc-TFCC insertion on the ulnar styloid, and second intervention, detachment of the pc-TFCC insertion in the ulnar fovea under fluoroscopic visualization (Figure 6.7).

The remaining soft tissue and DRUJ stabilizing structures, including the interosseous membrane, were kept intact to mimic the in vivo anatomy and kinematics as good as possible.

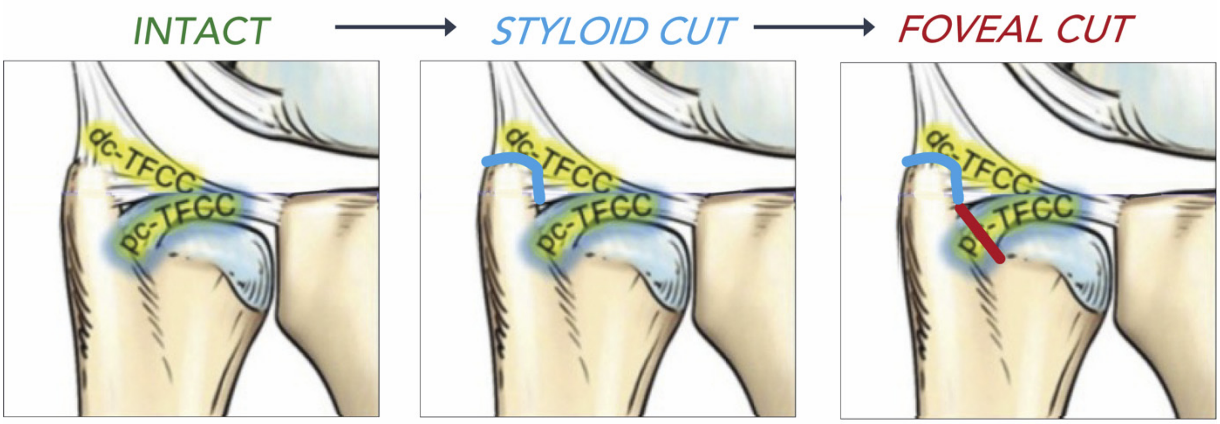


Figure 6.7. Detachment of the dc-TFCC and the pc-TFCC. Modified from Atzei et al., (2011).

In Study II, detachment of the dc-TFCC and pc-TFCC were performed to prepare the specimens to the baseline examination. Thereafter, intervention with TFCC reinsertion (Hermansdorfer and Kleinman, 1991) or TFCC reconstruction (Adams, 2000) as assigned by randomization, was performed (Figure 6.8).

In Study III, the normative DRUJ kinematics is described. The study was without interventions.

In Study IV, the intervention was open TFCC reinsertion of the TFCC in patients with arthroscopic confirmed non-retracted foveal pc-TFCC detachment.

The baseline TFCC status, interventions and outcomes of all four studies are listed in Table 6.3.

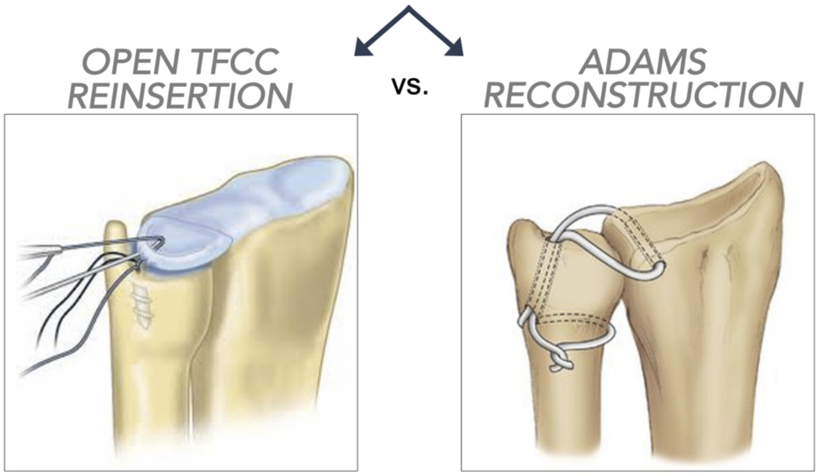


Figure 6.8. Interventions in Study II included open TFCC reinsertion or Adams TFCC reconstruction as assigned by randomization. Adapted from Atzei (2008) and Adams and Berger (2002).

### 6.9.1 Open TFCC reinsertion

The extensor retinaculum over the distal ulna was exposed through a longitudinal dorsal skin incision. The 5th extensor compartment was identified, opened and accessed to longitudinally release the DRUJ capsule 1-2 mm from the insertion on the ulnar aspect of the radius, preserving the radial insertion of the TFCC and the extensor digiti minimi. On the proximal side of the dorsal radioulnar ligament, an L-shaped extension of the capsular opening were extended to the extensor carpi ulnaris tendon sheet, which was preserved.

The ulnar fovea was identified and controlled by fluoroscopy, before removing any DRUJ synovitis in the ulnar fovea before ligament reinsertion. The ulnar fovea was prepared for a Mitec Mini QUICKANCHOR® (DePuy Mitek, Raynham, MA, USA) by predrilling. The distal side of the TFCC was approached through an additional 1 cm transverse incision in the wrist capsule.

The non-absorbable 2-0 Mitec sutures was passed through the TFCC from proximal to distal, and the TFCC was reinserted by a mattress suture and tied with 5 knots, while the DRUJ was positioned in neutral forearm rotation and compressed by the assistant. The L-shaped capsular opening was closed by absorbable braided 3–0 sutures before skin closure. An above elbow back-slap plaster was applied to protect the repair.

### 6.9.2 Adams TFCC reconstruction

The fovea of the distal ulnar head was exposed through a longitudinal dorsal skin incision, an opening of the DRUJ capsule through the 5$^{th}$ extensor compartment with a L-shaped extension, as described above for open TFCC reinsertion.

A skin incision extending 3 cm promimal from the proximal wrist crease was used to expose the volar exit point of a fluoroscopy guided radius tunnel. A k-wire was placed for over-drilling of a 4 mm radius tunnel with an even 3 mm distance to the radius lunate fossa and the sigmoid notch. An additional incision over the distal ulnar neck was used to assess the exit point of a 4 mm oblique ulnar tunnel made by over-drilling a second k-wire placed from the lateral ulnar neck and emerging in the ulnar fovea.

Reconstruction of the TFCC with a palmaris longus graft was performed as described by Adams (Adams, 2000) as a harvested palmaris graft was passed through the radius tunnel from the dorsal to the volar aspect of the wrist with a straight tendon grasper. The volar limb of the graft was passed through the DRUJ capsule proximal to the TFCC remnant and the dorsal limb through the L-shaped capsular opening, before the two tendon limbs were passed through the oblique ulnar tunnel. Finaly, the volar tendon limb was passed around the ulnar neck, close to the volarly aspect of the bone.

With the DRUJ in neutral forearm rotation, the two tendon limbs were tied dorsally with the first half of a surgeons knot while the assistant compressed the DRUJ. Three 3-0 fiberwire mattress sutures secured the tendon knot before a second tendon knot was tied and secured Finaly, the L-shaped dorsal capsular opening was closed by absorbable braided 3–0 sutures before skin closure. An above elbow back-slap plaster was applied to protect the repair.

## 6.10 Rehabilitation program

In Study IV, the patients treated with foveal TFCC reinsertion followed a standardized rehabilitation program and were followed during the first postoperative year.

At two to three weeks postoperatively all patients returned to the nurse outpatient clinic for suture removal and the above elbow back-slap plaster was replaced and worn for a total of 6 weeks.

Six weeks postoperatively all patients continued protecting the wrist using a removable splint (another 4 weeks) and followed a staged protocolled 3-month rehabilitation program, supervised by an occupational therapist. First, the rehabilitation training program involved normalization of active joint movement in the upper extremity and gentle specific isometric muscle strengthening exercises.

Eight weeks postoperatively additional proprioceptive and neuromuscular exercises for the wrist was included in the training.

Ten weeks postoperatively strengthening of the wrist by increased loading during neuromuscular exercises were allowed. Splinting was discontinued and only recommended during activities with risk of burdening the wrist.

Six months postoperatively, unlimited use of the upper extremity was allowed if tolerated. The surgeon followed patients in the outpatient clinic as they returned at 6-weeks, 3-month, 6-month and 1-year follow-ups during the rehabilitation period.

## 6.11 Validation and reliability

In Study I, static RSA images in varying positions were analyzed and AutoRSA data was compared to marker-based RSA data (reference standard) to validate the analysis method. The systematic bias (absolute mean difference) and prediction interval (SD x 1.96) was estimated.

In Studies III and VI, ultrasonography and dynamic RSA imaging of the Press test was repeated for examination of test-retest reliability of the kinematic RSA outcomes and the ultrasonography measured translation. Further, the systematic bias (absolute mean difference) and prediction interval (SD x 1.96) of the pressure applied on the weight platform and the kinematic RSA outcomes, was measured.

## 6.12 Radiostereometric test setups

In Studies I and II, the human donor arms were examined in a standardized setting mimicking the Piano key test by a custom-made fixture (Figure 6.9). Static RSA imaging was used to record the DRUJ in neutral forearm rotation, and before and after pressure application by the Piano key test.

In Studies III and IV, the participants were examined while actively performing a Press test in at standardized setting, using a custom-made weight-platform.
Synchronized dynamic RSA imaging recorded the patients DRUJ during active Press test application.
Using a Raspberry Pi, a custom-made device was designed to log, timestamp and relate the pressure exposure (measured in kg) on the weight-platform and the simultaneously recorded dynamic RSA images.

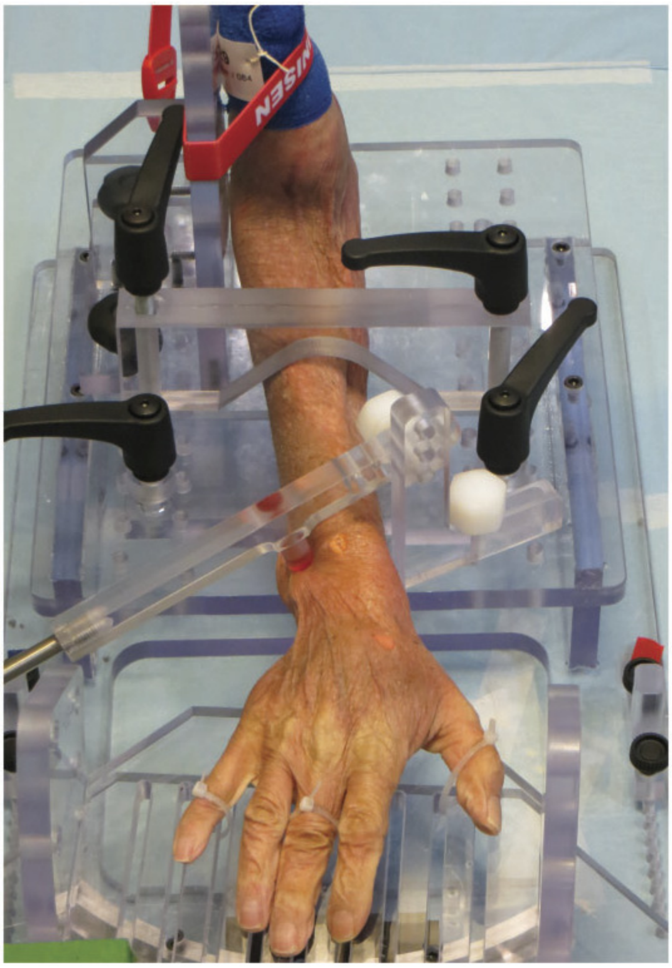

**Figure 6.9.** Customized radiolucent fixture for application of the Piano key test.
Adapted from Thillemann et al., (2020).

### 6.12.1 Test in neutral forearm rotation

With neutral wrist deviation and neutral wrist flexion, the 1st, 3rd and 5th fingers of the human donor arms were secured to a horizontal radiolucent plate. The elbow was in 90° flexion and the forearm in neutral rotation as the humeral shaft was secured in a horizontal position to the fixture. Static RSA imaging of the neutral rotated forearm was obtained.

### 6.12.2 Piano key test

With the hand of the human donor arm secured as described above, the forearm was rotated into pronation, as the humeral shaft was elevated from a horizontal to a vertical position and secured to the fixture.
In this test setup, first, a static RSA recording of the unloaded pronated forearm was obtained. Second, a static RSA recording was obtained, while a fixture lever induced a 7 kg pressure on the ulnar head to simulate the clinical Piano-key test (Cooney et al., 1980) (Figure 6.10). This load resembles the thumb load we could manually apply to the ulnar head, during a clinical Piano key test. Further, this load do not disrupt the soft tissues and the anatomical structures (Stuart et al., 2000).

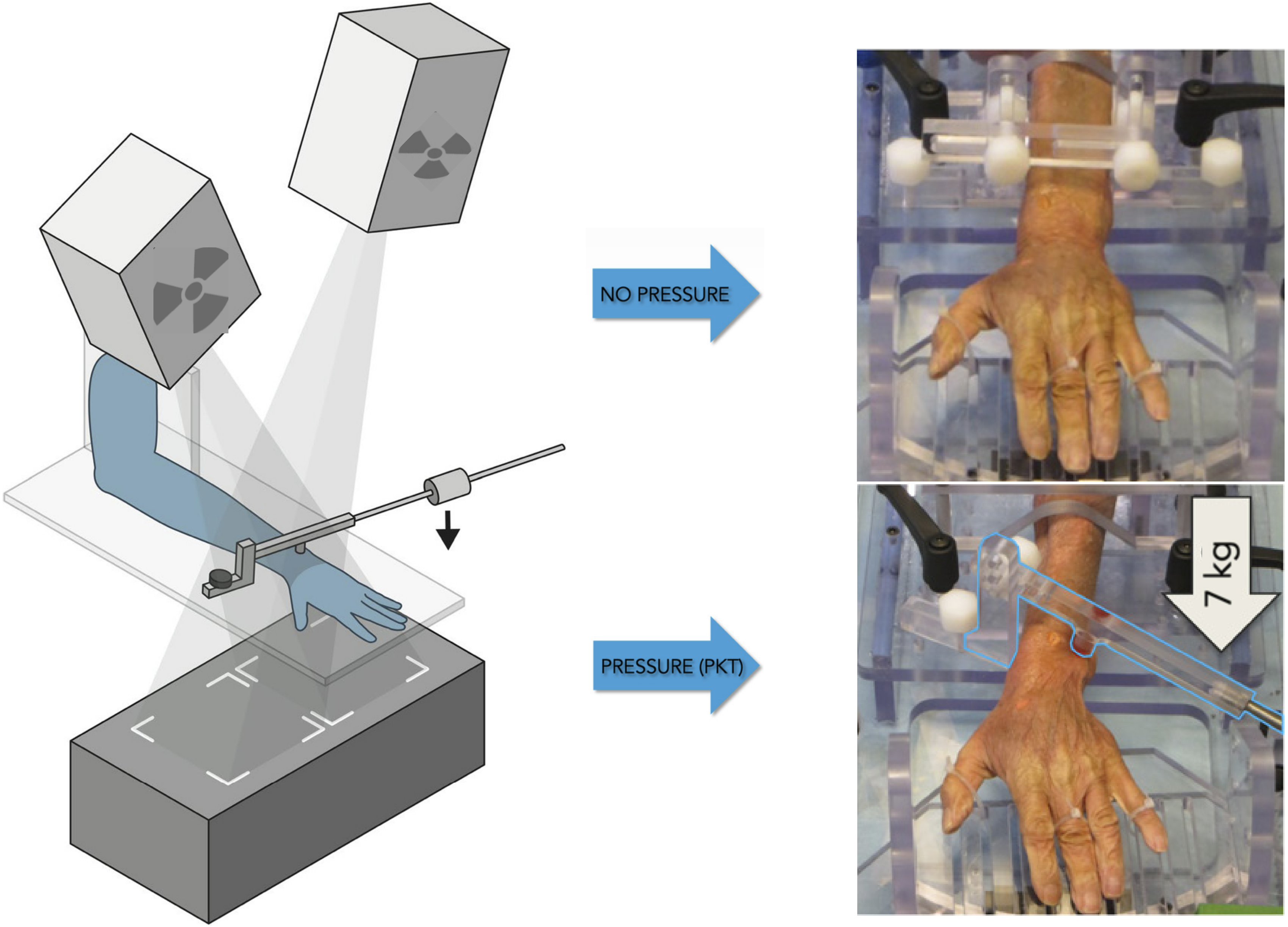


**Figure 6.10.** Fixture designed for standardized Piano key test examination, first without pressure and second with 7 kg pressure application. Adapted from Thillemann et al. (2020) and (2021a).

### 6.12.3 Press test

A standardized modification of the Press test described by Lester et al. (1995) was performed. The participants were seated with the shoulder in slight flexion, the upper arm adducted, the elbow flexed, and the forearm pronated. The hand was resting flat on a radiolucent plate mounted for pressure application on a custom-made uni-directional weight-platform (Figure 6.11). To induce volar translation of the ulnar head, the participants were instructed in gradually to apply pressure to their maximum, and release pressure gradually until no pressure. The test was repeated to evaluate the test precision.

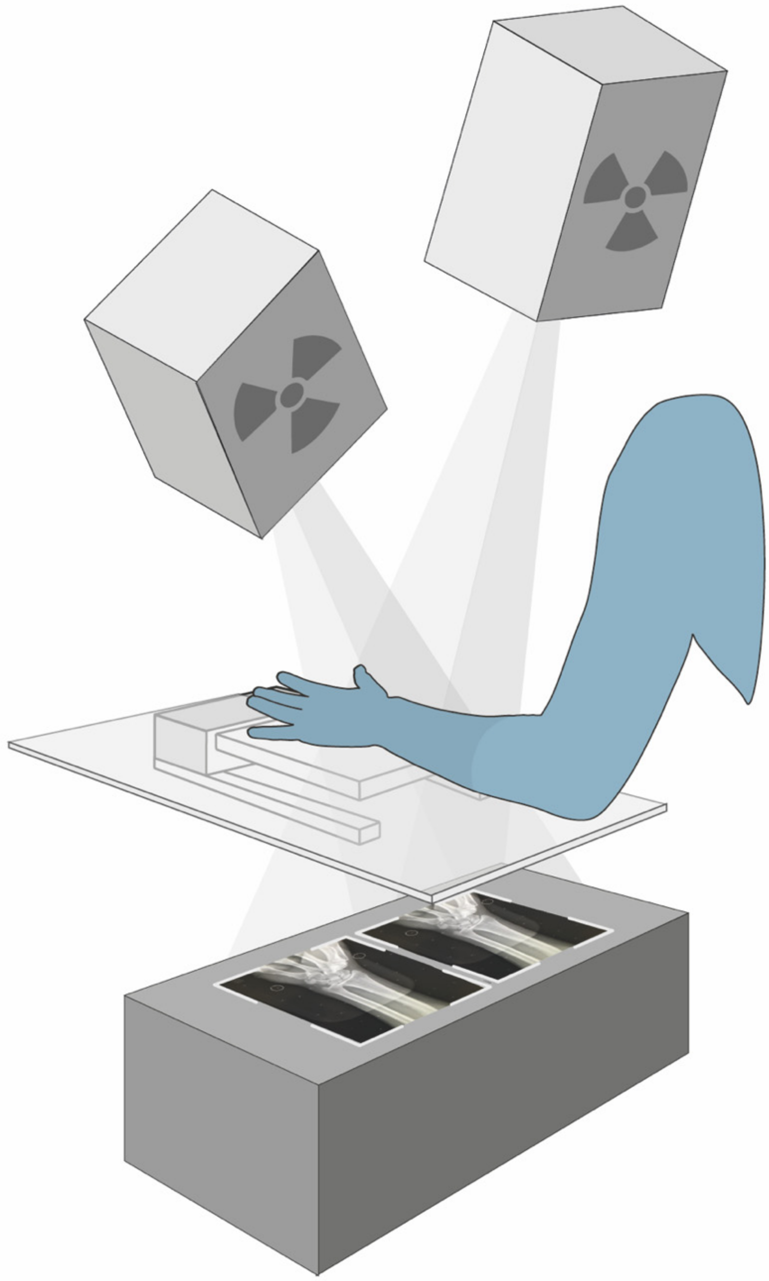

**Figure 6.11.** Press test examination set-up recorded by dynamic radiostereometric imaging. Adapted from Thillemann et al. (2021b).

## 6.13 Static RSA imaging

In Studies I and II, the human donor arms were recorded during the Piano key test by static RSA.

Synchronized static RSA images were recorded with a digital Adora RSA system (NRT X-Ray, Hasselager, Denmark). The images were obtained with the two ceiling mounted X-ray tubes in a 20° – 20° tube position on the vertical plane. The exposure settings were 60 kV and 2.5 mAs. The source to images Distance (SID) was 150 cm, and the source to skin distance (SSD) was 100 cm. Beneath a uniplanar carbon calibration box (Carbon box 19, Medis Specials, Leiden, The Netherlands) two digital Canon CXDI-50RF image detectors were slotted and recorded images with a 2208 x 2688 pixels resolution (0.16 x 0.16 mm/pixel). DICOM files of the images were exported.

## 6.14 Dynamic RSA imaging

In Studies III and IV, the participants were recorded during the Press test by dynamic RSA.

Synchronized dynamic RSA images were recorded with a digital Adora RSA system (NRT X-Ray, Hasselager, Denmark) at a rate of 10 images/second (10 Hz). The images were obtained with the two ceiling mounted X-ray tubes in a 20°-20° tube position on the vertical plane. The exposure settings were 60 kV, 630 mA and 2.0 ms exposuretime. The source to images Distance (SID) was 150 cm, and the source to skin distance (SSD) was 100 cm. Beneath a uniplanar carbon calibration box (Carbon box 19, Medis Specials, Leiden, The Netherlands) two digital Canon CXDI-50RF image detectors were slotted and recorded images with a 2208 x 2688 pixels resolution (0.16 x 0.16 mm/pixel).

Multi-frame DICOM files of the image series were exported. Individual image frames were extracted for analysis.

## 6.15 Bone models and Digital Reconstructed Radiographs

In all studies three-dimensional (3D) volume and surface bone models were used for analyzing the static and dynamic RSA recordings as the position of the radius and ulna in the calibration box coordinate system was transformed to the standardized anatomical coordinate systems of each bone.

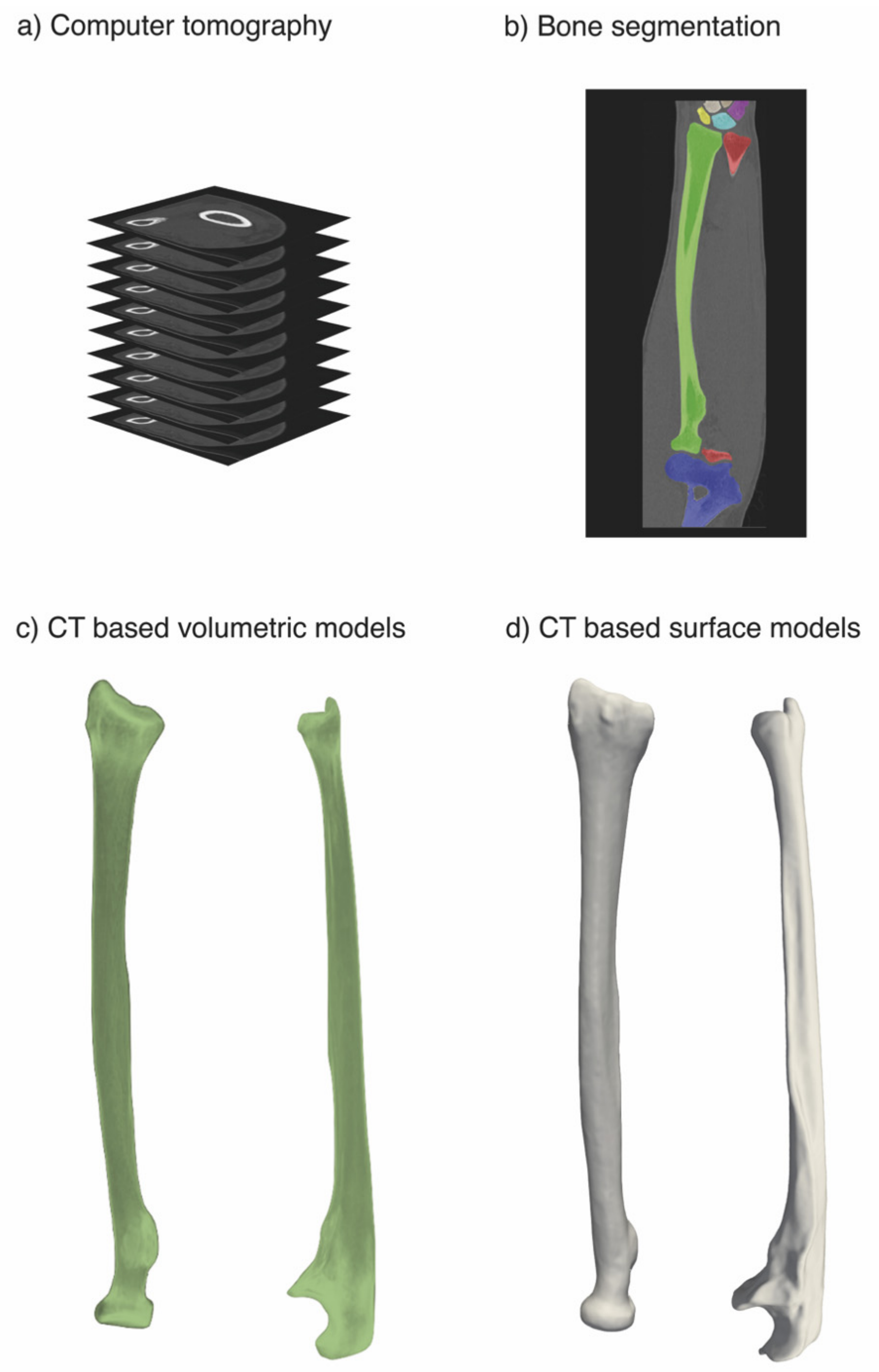


Figure 6.12. Bone models generated by bone segmentation of computer tomography scans. Adapted from Thillemann et al. (2021b).

First, each human donor forearm or participant forearm, was CT-scanned (Figure 6.12.a). Second, greyscale information was extracted from the CT scans and an automated method of graph-cut segmentation (Hansen et al., 2018) (Figure 6.12.b) was used to generate individualized volume and surface bone models of the radius and ulna (Figure 6.12.c-d). All image processing was performed as described by Hansen er al. (2018)  with custom implemented software based on the Insight Toolkit and the Visualization Toolkit (Kitware, New York, USA).

### 6.15.1 Surface models

The 3D surface bone models of the radius and the ulna were simplified to approximately 10,000 triangles. The 3D surface bone models were used to define anatomical landmarks, the anatomical coordinate system, and the radioulnar axis.

### 6.15.2 Volume models

The 3D volume bone models were extracted using the greyscale information from the CT scan. The 3D volume bone models were used in combination with the 3D surface bone models to generate DRRs.

### 6.15.3 Digital Reconstructed Radiograph

Combined 3D volume and surface bone models were used to generate the DRRs (Figure 6.13), utilized for analysis of the static and dynamic RSA recordings.

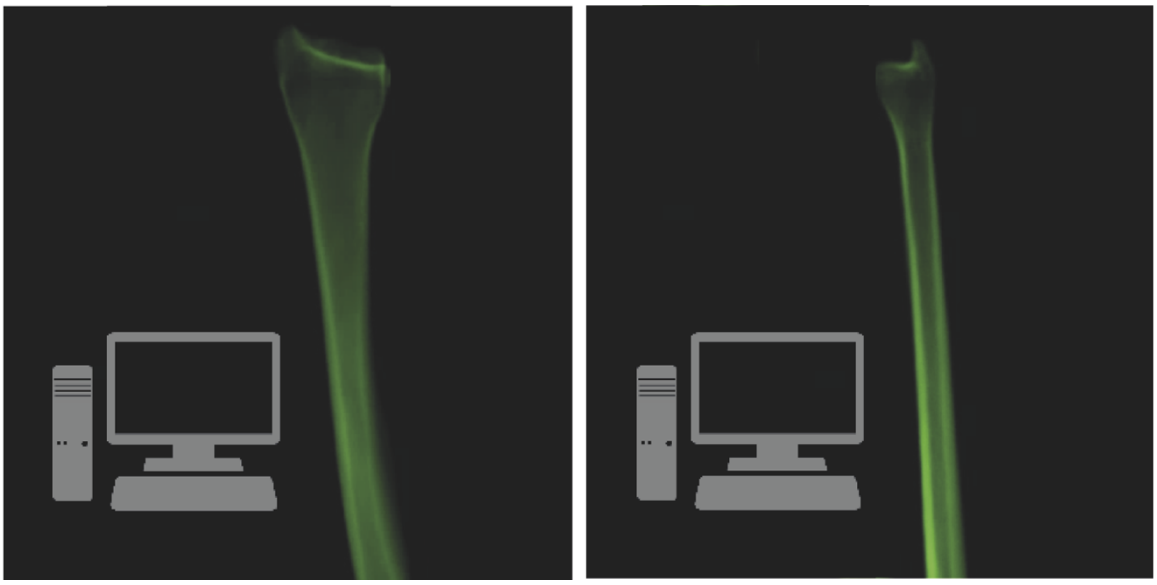

**Figure 6.13.** Digital Reconstructed Radiographs (DRR) of radius and ulna generated from bone models. Adapted from Thillemann et al. (2021b).

## 6.16 RSA analysis

In Studies I and II, *Model-based RSA* software (MBRSA) was used to calibrate each the static RSA image and to initialize the ulna and radius bone models (Kaptein et al., 2004). Next, a custom made automated radiostereometry software (AutoRSA) was used for the final estimation of bone position in the calibration box coordinate system. Finaly, the static RSA recordings from various positions were finally re-analyzed using *marker-based RSA*. Thus, the precision (absolute mean difference) and the prediction interval of the radius and ulna pose analysed by AutoRSA analysis was evaluate with reference to the *marker-based* RSA as the reference standard.

In Studies III and IV, an averaged calibration image was created from all image frames from each dynamic RSA examination (average of 50 frames). Thereby, image noise from the moving arm was reduced and the calibration box fiducial and control markers were viewed more clearly (Figure 6.14).

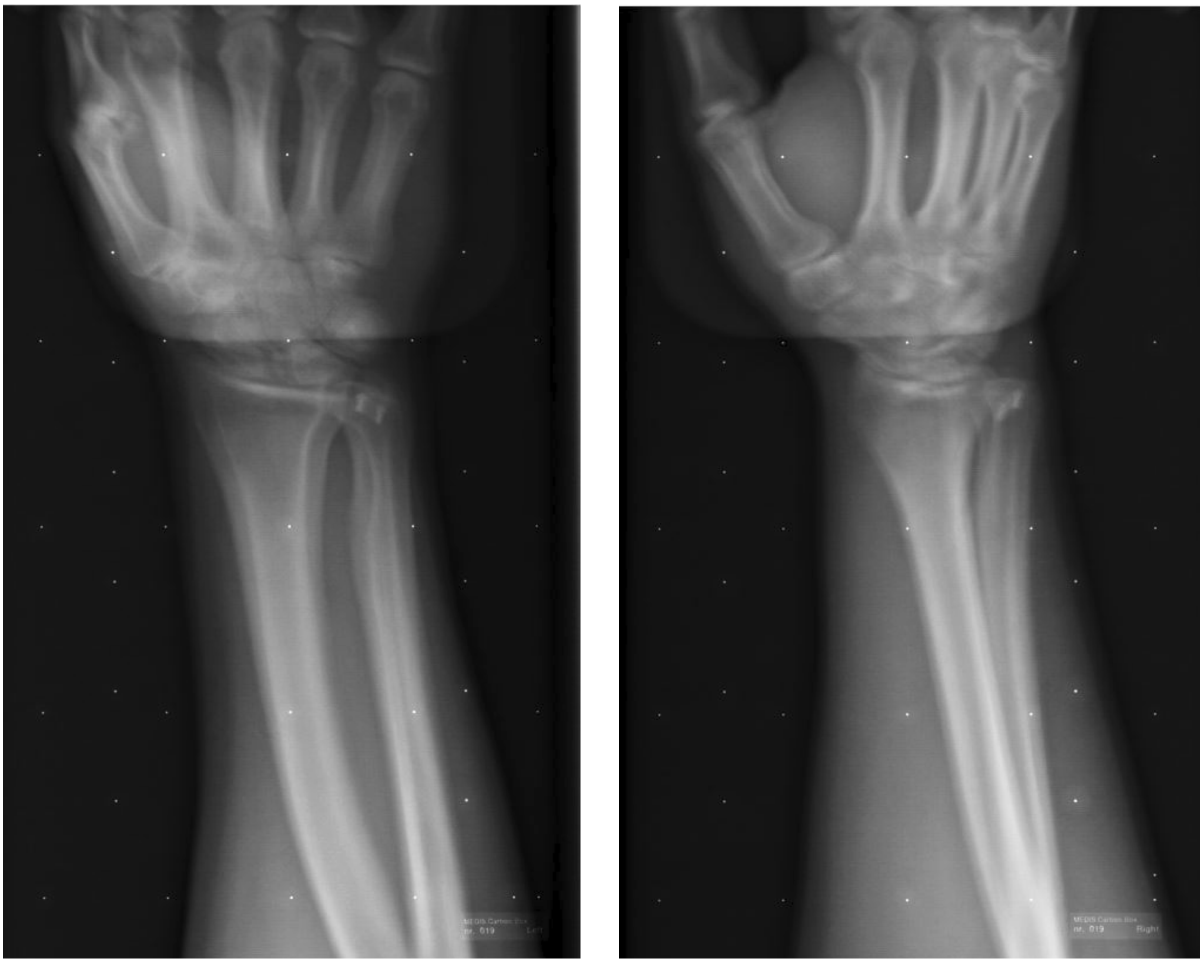

Figure 6.14. Averaged calibration images from the dual x-rays created from all dynamic RSA image frames.

*Model-based RSA* was used to calibrate the averaged calibration image and next *AutoRSA* was used for both primary manual initialization of the DRR of the radius and ulna bone models to approximately fit the initial RSA image.
Finally, automated AutoRSA analysis fitting the DRR to the RSA images was performed with the remaining dynamic RSA images for the final estimation of bone position in the calibration box coordinate system.

**6.16.1 Marker-based RSA**

Static RSA images in various positions were selected for repeated marker-based RSA analysis (reference standard). The images were imported in the MBRSA program (MBRSA 4.11, RSAcore, Leiden, The Netherlands) and the tantalum markers inserted in the radius and ulna were detected to estimate the bone position in the calibration box coordinate system.
Data was recorded to estimate the precision and prediction interval of the AutoRSA analysis on the same static RSA image.
The condition number in the radius and ulna was good despite marker spread in these small slim radial and ulnar bones was challenging. The mean condition numbers for the radius (70.4) and ulna (83.8) were well below the acceptable threshold (<150) in lower extremity (Valstar et al., 2005)

**6.16.2 Model-based RSA**

Static RSA images were imported in the MBRSA program (MBRSA 4.11, RSAcore, Leiden, The Netherlands) and bone edges of the radius and ulna were detected automatically. The pertinent bone edges were selected manually (Figure 6.15).

The CT-based 3D surface bone models of the radius and the ulna were imported into the MBRSA program and the initial positioning was performed manually. Thereafter, the MBRSA software estimated the best position of the bones automatically by minimizing the error of the bone model projections versus the manually detected bone edges on the radiographs.
This estimated bone position in the calibration box coordinate system was used as an initial position in the final analysis of the RSA image with the AutoRSA software.

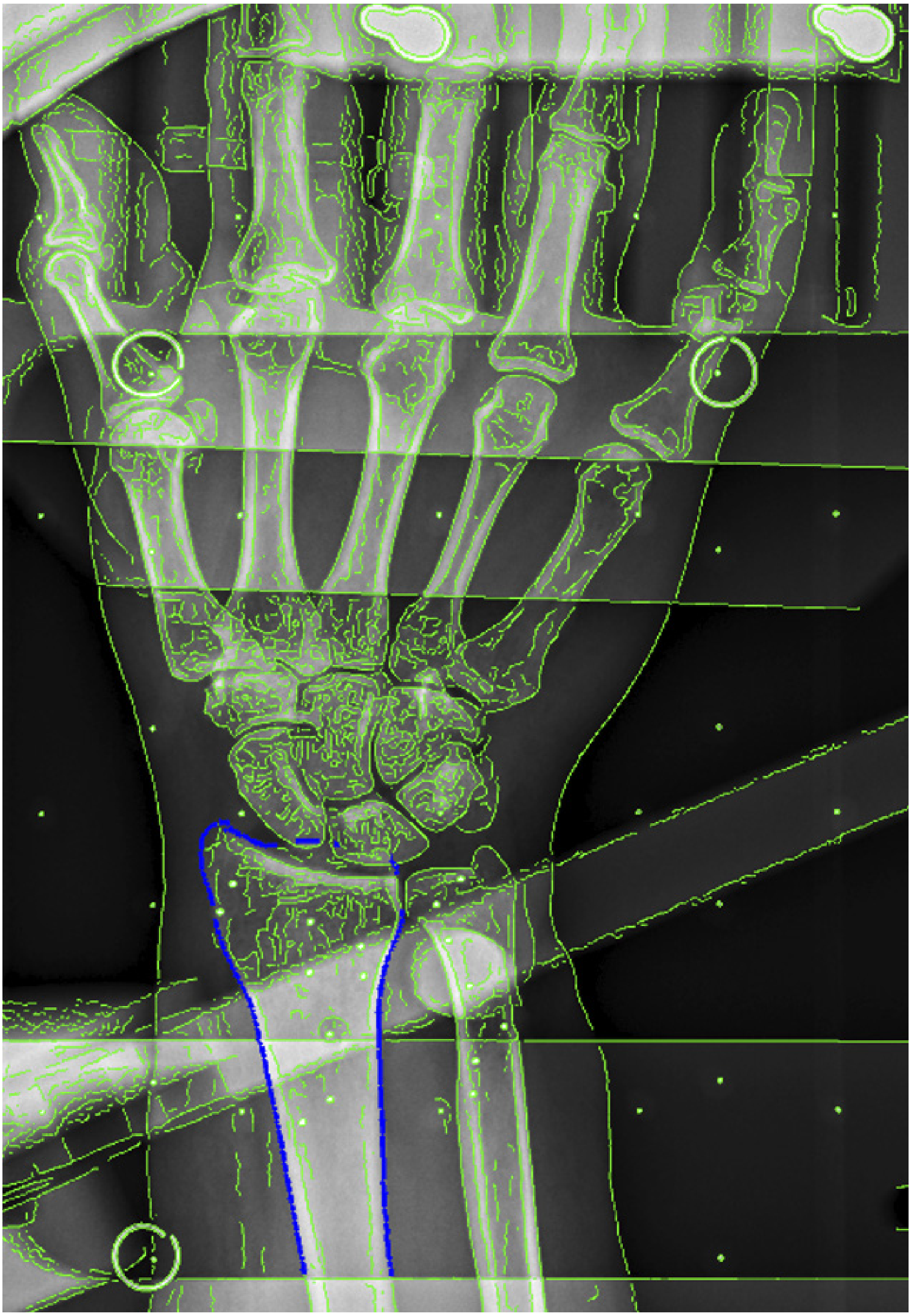

Figure 6.15. Edges of the radius and ulna detected by model-based RSA. Adapted from Thillemann et al., (2021a).

### 6.16.3 Automated radiostereometry analysis (AutoRSA)

The first image of dynamic RSA examinations was used for primary manual initialization (Figure 6.16.1-3) of the DRR using the AutoRSA program (AutoRSA software, Orthopaedic Research Unit, Aarhus, Denmark). When the DRR approximately fit the initial RSA image, AutoRSA calculated the optimal pose of the bone models by repeated comparison between the simulated DRR and the RSA images until no further improvements could be made on this first image (Figure 6.16).

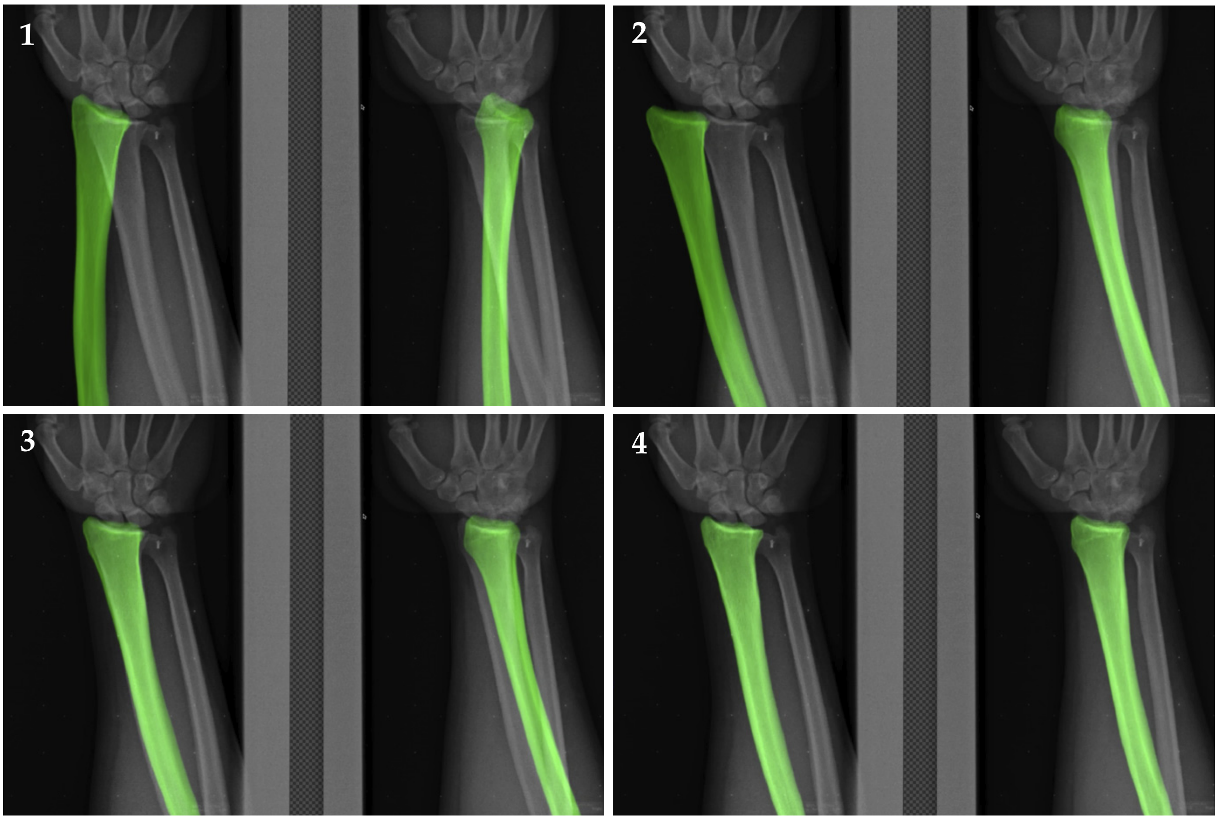


Figure 6.16. Manual initialization (1-3) before automated optimal fit of the radius and ulna DRR (green) to the dual RSA images by AutoRSA (4).

The bone registration area was focused on the next RSA image with an automatically produced mask projected from the position of the previous DRR. On the following dynamic RSA images of the dynamic press-test recording, the AutoRSA software automatically set the initialization of the next DRR image by extrapolation from the previous movement. The final 3D position and orientation (pose) of the ulna and radius bone in the calibration box coordinate system was estimated from virtually generated projections using mathematical optimization algorithms (Christensen et al., 2020; Hansen et al., 2018; Hemmingsen et al., 2020) and transformed to the standardized bone specific coordinate systems.

## 6.17 Anatomical Landmarks and Coordinate system

### 6.17.1 Anatomical landmarks

In all studies, the anatomical landmarks of each bone model were picked at baseline and represent exactly the same anatomical landmarks and axis in all repeated RSA examinations throughout each study. Thus, the picking of landmarks does not affect the precision.

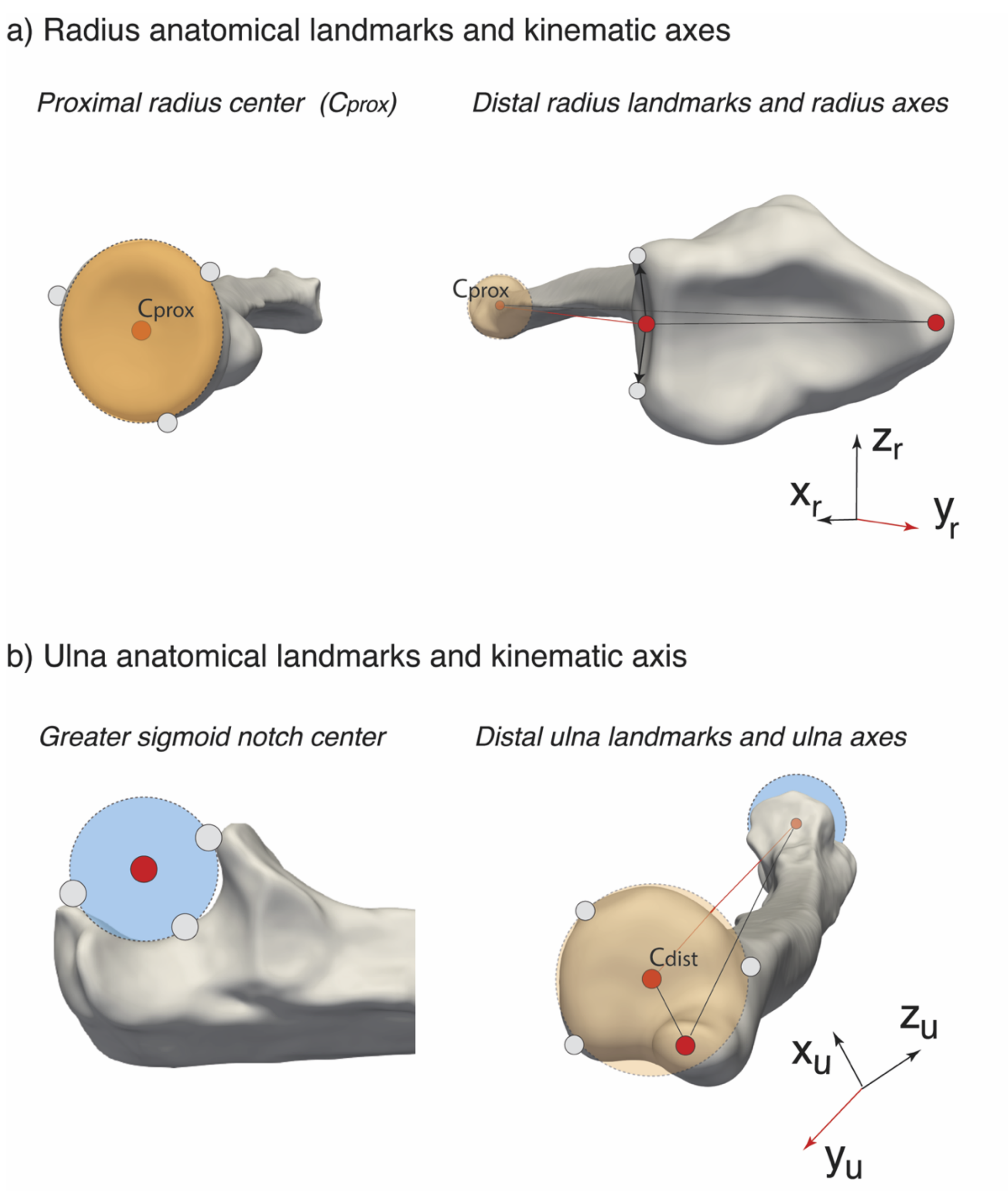


Figure 6.17. Bone specific anatomical landmarks (red) and anatomical kinematic axes of the radius and ulna (x, y and z). Adapted from Thillemann et al. (2021b).

The center point landmarks of the ulna greater sigmoid notch, the radial head ($C_{prox}$), and the ulnar head ($C_{dist}$), were computed as the center of the best fitted sphere of three points picked on the olecranon trochlear ridge, the radial head articulating surface and the ulnar head articulating surface (Figure 6.17).
The *radius landmarks* were: the tip of the radius styloid, the center of the distal radioulnar joint surface and the center point of the radial head ($C_{prox}$) (Figure. 6.17.a).
The *ulna landmarks* were: the center point of the ulnar head ($C_{dist}$), the tip of the distal ulnar styloid, and the center point of the greater sigmoid notch (Figure 6.17.b).

### 6.17.2 Anatomical coordinate system

In all studies, the three anatomical landmarks on each individual 3D surface bone model were used to define bone specific orthogonal x, y and z-axes of the radius and ulna (Figure 6.17), determining a standardized anatomical coordinate system as described by McDonald et al. (2012).

The estimated positions of the radius and ulna in the calibration box coordinate system were transformed to the standardized anatomical coordinate system for each bone and used to calculate the DRUJ kinematic outcomes.

## 6.18 Radiostereometry based Kinematic measures

The single *radioulnar axis* (RUJ axis) of forearm rotation as described by Hagert et al. (1992) was used to calculate the DRUJ kinematics, including anterior posterior *DRUJ translation* and the *DRUJ position ratio* along a *radius sigmoid notch line*, the change in ulnar variance along the RUJ axis the and *forearm rotation* about the RUJ axis. An overview of RSA based kinematic outcomes in each study is outlined in Table 6.3.

### 6.18.1 Radioulnar Joint Axis

The RUJ axis extend from the center point of the radial head ($C_{prox}$) to the center point of the ulnar head ($C_{dist}$) (Figure 6.18).

### 6.18.2 Radius Sigmoid Notch line

The bony components of the DRUJ include the ulnar head and the sigmoid notch (SN) on the distal radius. The articulation is limited by a volar and dorsal rim supporting the DRUJ stability in supination and pronation, respectively.

The radius sigmoid notch line was defined as a connecting line from the midpoint of the volar rim (A) to the dorsal rim (Figure 6.19). The length of the SN was measured in millimeters.

### 6.18.3 DRUJ position

The orthogonal projection of the RUJ axis *on* the radius sigmoid notch line was defined as the DRUJ position and measured in millimeters from the volar rim point of the SN (Figure 6.19).

### 6.18.4 DRUJ position ratio

Individual differences in sigmoid notch-length were taken into account calculating the DRUJ position ratio defined as DRUJ position / SN length (Figure 6.19).

### 6.18.5 DRUJ translation

Anterior posterior translation of the RUJ axis orthogonal projection *along* the radius sigmoid notch line defined the DRUJ translation measured in millimeters (Figure x).

### 6.18.6 Ulnar variance

Changes of the ulnar variance along the RUJ axis was defined as DRUJ pistoning and
calculated as translation of the distal center point of the ulnar head ($C_{dist}$) along the RUJ axis (Figure 6.19).

### 6.18.7 Forearm rotation

Pronation and supinating rotation of the forearm was calculated as the angle between a line from the radial styloid tip landmark to the midpoint of the sigmoid notch line, and a line from the ulnar head center ($C_{dist}$) and the distal ulnar styloid tip, with reference to the RUJ axis (Figure 6.19).

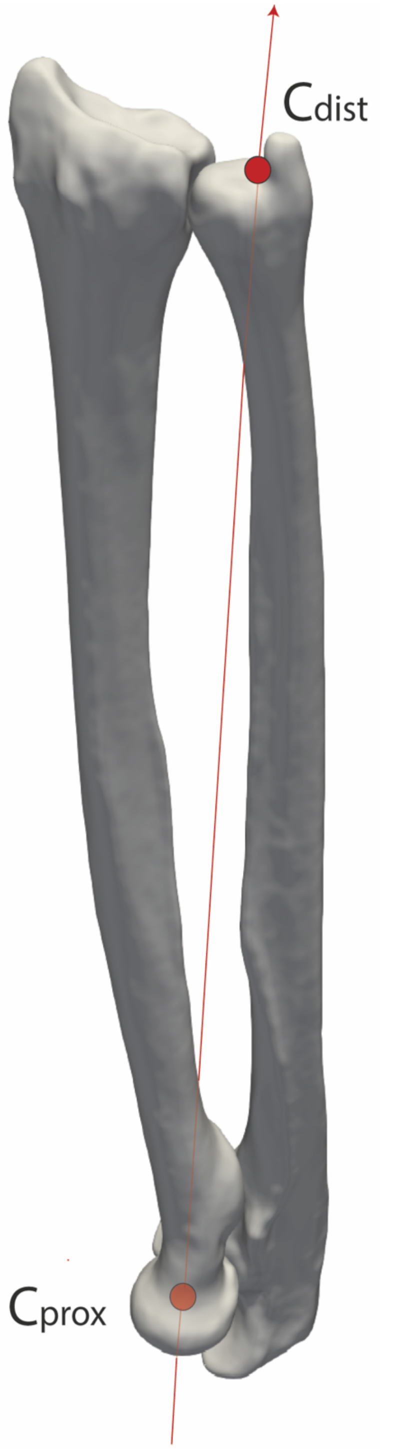


**Figure 6.18.** The radioulnar axis. From Thillemann et al. (2021b).

### 6.18.8 DRUJ distance

The DRUJ distance was estimated as the orthogonal projected distance from the RUJ axis to the SN line (Figure 6.19).

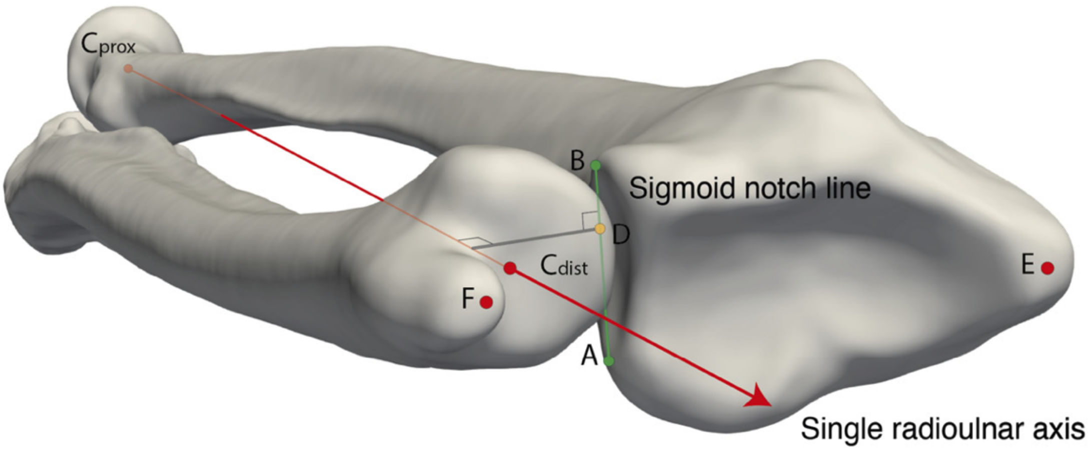


Figure 6.19. Anatomical landmarks and the radioulnar axis ($C_{dist}$ to $C_{prox}$) used to compute kinematic outcomes including the sigmoid notch line length (AB), DRUJ position (D) measured from the volar rim (A), DRUJ position ratio (AD/AB), DRUJ translation (D movement on AB), change in ulnar variance (translation of $C_{dist}$ on the radioulnar joint axis) and forearm rotation (the angle between F and $C_{dist}$ and a line from the midpoint of AB to E. The DRUJ distance was estimated as the orthogonal projected distance (grey line) from the RUJ axis to the SN line. Adapted from Thillemann et al., (2022).

## 6.19 Outcomes

In Studies I-IV, the primary outcome was DRUJ translation measured by static or dynamic RSA during test application.

### 6.19.1 Studies I-II

In these experimental cadaver studies DRUJ translation was evaluated during the Piano Key test. Secondary outcomes are listed in Table 6.3.

### 6.19.2 Study III

In this study on non-injured participant forearms DRUJ translation was evaluated during the dynamic Press test. Secondary clinical outcomes, pressure force and ultrasonography outcomes are listed in Table 6.3.

### 6.19.3 Study IV

In this study on patients with arthroscopic verified pc-TFCC injury, the DRUJ translation was evaluated during the dynamic Press test. Secondary clinical outcomes, pressure force, PROMs and ultrasonography outcomes are listed in Table 6.3. Further, preoperative MRI examinations were evaluated.

**Table 6.3**. Overview of interventions and outcomes in Studies I to IV

| *Baseline TFCC status* | *Follow-up* | *Intervention* | *Clinical Outcome(s) PROM outcomes* | *Kinematic outcomes* |
|---|---|---|---|---|
| *Study I* | | | | |
| Intact TFCC | - | -<br>dc-TFCC lesion<br>*pc*-TFCC lesion | | *Static RSA:*<br>DRUJ translation<br>DRUJ position ratio<br>Forearm pronation |
| *Study II* | | | | |
| *pc-TFCC lesion* | - | TFCC reinsertion<br>or<br>TFCC reconstruction | *Clinical examination:*<br>Ballottement test | *Static RSA:*<br>DRUJ translation<br>DRUJ position ratio<br>Forearm pronation |
| *Study III* | | | | |
| Intact TFCC | - | Not relevant<br>Normative data | *Clinical examination:*<br>Ballottement test<br>Grip strength<br>AROM | *Ultrasonography:*<br>DRUJ translation<br>Hess Quotient<br><br>*Dynamic RSA:*<br>DRUJ translation<br>DRUJ position ratio<br>Forearm pronation<br>DRUJ pistoning |
| *Study IV* | | | | |
| *pc-TFCC injury* | 6-month<br>12-month | Open TFCC reinsertion | *Clinical examination:*<br>Ballottement test<br>Piano key test<br>Grip strength<br>AROM<br><br>*PROMS:*<br>QDASH<br>PRWE<br>NRS pain<br>Patient satisfaction<br>Willingness to repeat | *Ultrasonography:*<br>DRUJ translation<br>Hess Quotient<br><br>*Dynamic RSA:*<br>DRUJ translation<br>DRUJ position ratio<br>Forearm pronation<br>DRUJ pistoning<br>DRUJ distance |

*Primary outcome was DRUJ translation in all four studies.*

## 6.20 Data management of dynamic Press test data

In Studies III and IV, the pressure force applied on the custom-made weight-platform and the dynamic RSA images of the Press test were timestamped. Thus, after analyzing the dynamic RSA examinations, the calculated kinematic outcomes and the corresponding pressure force was related.

The pressure data (force in kg) and the calculated kinematic outcome measures were merged before handling subject individual delay of pressure application. A customized software automatically identified the pressure start- and endpoint of each Press test motion cycle, defined as the point just before the pressure force exceeded a threshold value of +0.1 kg relative to course start- and endpoints.
Next, the maximum pressure force of each cycle was defined as the 50 % mark of the motion cycle and divide the motion cycle in a pressure and release phase. To normalize the varying number of data points in each pressure and release phase, each phase was normalized to 50% of a motion cycle by linear interpolation (Figure 6.20).

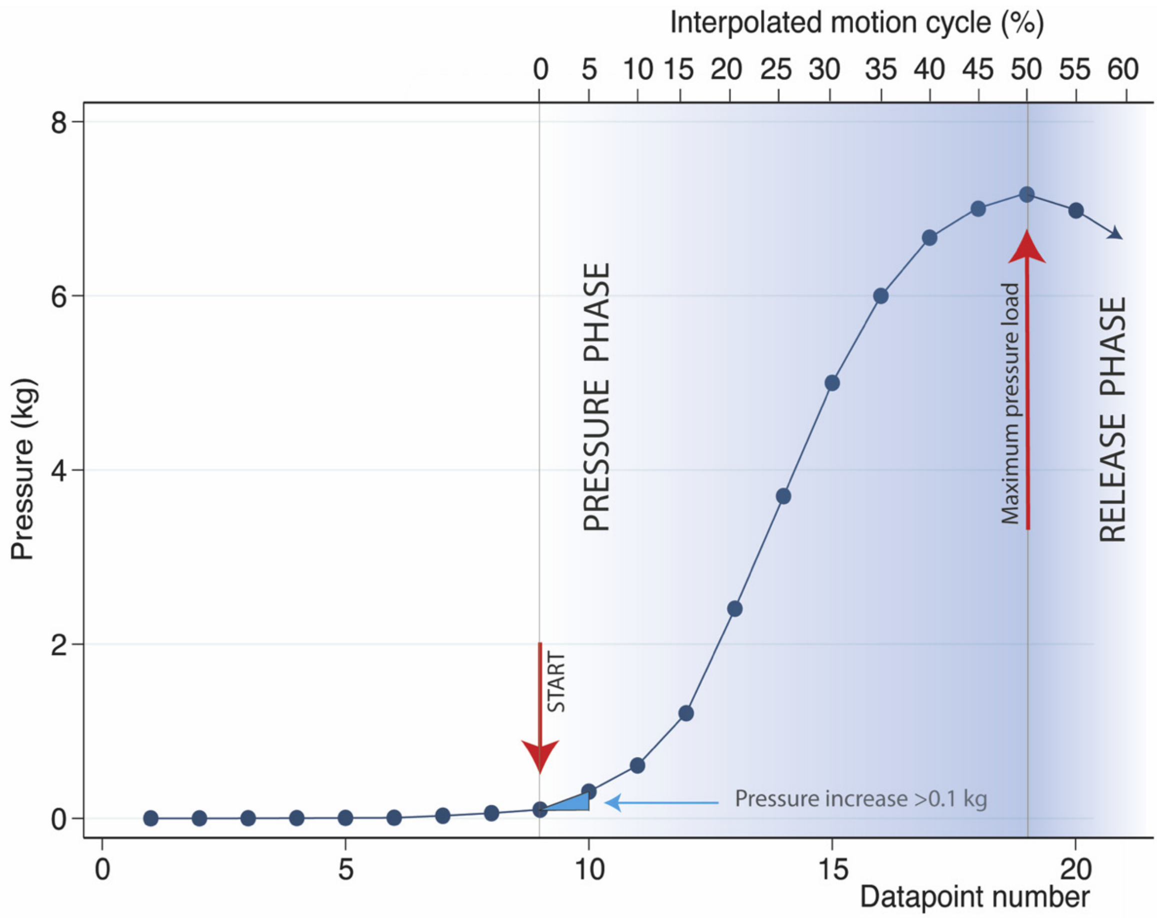


**Figure 6.20.** Definition of motion cycle start point, maximum pressure, and pressure phase.

The Press test was repeated twice and the maximum pressure force and corresponding kinematic outcome values from the two normalized motion cycles were used for examination of reliability.
The normalized motion cycle with the highest maximum pressure force was used for data analysis of the corresponding kinematic outcomes.

## 6.21 Sample-Size

As the study set out, only few publications on DRUJ translation existed. Omokawa et al. (2017) evaluated DRUJ translation by the Ballottement test and a magnetic tracking system for measurement of anterior-posterior DRUJ translation in neutral forearm rotation. Pickering et al. (2016) developed and used externally mounted rig to measure DRUJ translation on pronated forearms in normal and clinically unstable populations.

### 6.21.1 Study I

The sample size calculation was based on an estimated DRUJ translation of 7 mm (SD 3) in intact wrists, and 14 mm (SD 4) after experimental TFCC lesion (Omokawa et al., 2017).
The estimated sample size was 7 human donor arms for two-sample comparison of paired-means as the power was set to of 0.80 and alpha to 0.05 and the correlation > 0. Eight human donor arms eligible and fulfilled the inclusion criteria.

### 6.21.2 Study II

As the DRUJ translation on pronated forearms in Study I was considerably lower compared to the measures reported in neutral forearm rotation by Omokawa et al. (2007), the sample size calculation was based on estimated DRUJ translations with pronated forearm although measured by external means. Pickering et al. (2016) found a DRUJ translation on pronated forearm of 4.2 mm (SD 0.5) in non-injured controls, and 7.0 mm (SD 0.5) in a clinically unstable patient group.
The estimated sample size was 3 human donor arms per group for a two-sample comparison of unpaired means as the power was set to of 0.90 and alpha to 0.05.
Ten human donor arms were eligible and fulfilled the inclusion criteria. Therefore, a sample size of 5 patients per group was selected to allow for incomplete data collection/imaging errors.

### 6.21.3 Study IV

The initial sample size calculation was based on the estimated DRUJ translation in study I. In pronation the DRUJ translation was 1.36 mm (SD 1.42) in intact wrists, and 2.3 mm (SD 1.07) after experimental dc- and pc-TFCC lesion (Thillemann et al., 2020). The correlation between DRUJ translation before and after experimental dc- and pc-TFCC lesion was 0.79. The estimated sample size was 12 patients for a two-sample comparison of paired-means as the power was set to of 0.90 and alpha to 0.05.

A conservative sample size of 20 patients was selected to allow for incomplete follow-up, data collection and imaging errors.

In April 2020, twenty-one patients were included in the study after arthroscopic assessment and confirmation of a foveal TFCC injury.

## 6.22 Statistics

In all studies, continuous data were cheeked for normality by inspection of frequency and probability plots (quantile-quantile plots). Parametric continuous data were reported as means with 95% confidence intervals (95% CI). Paired data (i.e., outcome before and after intervention) was compared using the depended sample *t*-test. Unpaired data (i.e., comparison of groups receiving two different interventions) was compared using the independent sample *t*-test.

Non-parametric continuous data were reported as medians with Inter Quartile Ranges (IQR) and compared using the Wilcoxon signed-rank test or Mann as appropriate. Categorical data were reported as numbers and compared between groups using the chi-squared test.

In Study I, DRUJ kinematics was analyzed using mmultivariate repeated measurements ANOVA with outcome data and intervention status (non-injured, dc-TFCC injury and dc/pc-TFCC injury) as factors.

The precision of AutoRSA analysis was calculated with, MBRSA as reference standard, and reported as systematic bias (absolute mean difference) and prediction interval (SD x 1.96).

In Study IV, DRUJ kinematics across the entire Press test motion cycle was analyzed using multivariate repeated measurements ANOVA with outcome data and injury status (injured forearm vs. contralateral non-injured forearm) as factors, at baseline and throughout follow-up.

Model validation of the multivariate repeated measurements ANOVA was performed by assessing and comparing the standard errors and correlations of the relevant groups by the likelihood-ratio test. Unequal standard errors and correlations were taken into account in the analyses. Normal distribution of the mixed-model residuals was tested probability plots (quantile-quantile plots). Pairwise comparisons between the relevant groups were used to specify any differences.

In Studies III and IV, descriptive analyses of participant and patient demographics were performed.
In Studies III and IV, repeatability of the dynamic RSA press-test was evaluated in order to approximate the precision and reported as absolute mean difference of the systematic bias (absolute mean difference) and prediction interval (SD x 1.96).
Inter-rater agreement of RSA and US double-examination outcomes was calculated as Intraclass Correlation Coefficients based on an assumption of a single rater, absolute-agreement, two-way mixed-effects model (ICC 2,1). The rater consistency (r) was reported with 95% confident intervals and evaluated as described by Koo and Li (Koo and Li, 2016).

In all studies the level of significance was set at $p<0.05$ and all analyses were computed using Stata 16.0 software (StataCorp LP, Texas).

# 7 Results

# 7

# Results

## 7.1 Demographics

The demographics of the human cadaver arms in in Study I and II, of the participants in Study III, and of the patients included in Study IV, is displayed in Table 7.1.

In Study II, the two groups randomised to Foveal TFCC reinsertion or Adams TFCC reconstruction had comparable preoperative characteristics (Table 7.1).

| Table 7.1. Characteristics and demographics in Studies I, II, III, and IV | | |
|---|---|---|
| *Studies* | *Units* | *Value* |
| *Study I, N = 8 donor arms* | | |
| Age | Mean years (range) | 78 (72 – 90) |
| Gender | Male % | 88 |
| Ballottement test[n] | Unstable (>5 mm translation %) | 0 |
| Arthroscopic Hook test | Unstable foveal insertion % | 0 |
| *Study II, N = 10 donor arms (5/5)* | | *Foveal reinsertion / Adams reconstruction* |
| Age | Mean years (range) | 77 (72–90) / 79 (63–90) |
| Gender | Male % | 100/ 60 |
| Side | Right hands % | 80 / 20 |
| Ballottement test[n] | Unstable (>5 mm translation %) | 100 / 100 |
| Arthroscopic Hook test | Unstable foveal insertion % | 100 / 100 |
| *Study III, N = 33 participants non-injured forearm* | | |
| Age | Mean years (range) | 31 (19 – 50) |
| Gender | Male % | 42 |
| Dominant hand | Right % | 94 |
| Investigated hand | Dominant hands % | 58 |
| Ballottement test[n] | Unstable (>5 mm translation %) | 0 |
| Piano key test | Instability sign % | 0 |
| Grip strength | Mean kg (95% CI) | 42 (37 – 46) |
| Women | | 33 (30 – 36) |
| Men | | 53 (49 – 58) |
| Wrist motion | Mean degrees (95% CI) | |
| Flexion | | 79 (75 – 82) |
| Extension | | 74 (71 – 77) |
| Radial | | 23 (20 – 25) |
| Ulnar | | 36 (34 – 38) |
| Forearm rotation | Mean degrees (95% CI) | |
| Supination | | 84 (82 – 87) |
| Pronation | | 81 (78 – 84) |
| *Study IV, N = 21 patients injured forearm* | | |
| Age | Mean years (range) | 34 (22 – 50) |
| Time since injury | Median month (IQR) | 9 (6–58) |
| Gender | Male % | 52 |
| Dominant hand | Right% | 95 |
| Investigated injured hand | Dominant % | 48 |
| Ballottement test [n] | Unstable (>5 mm translation %) | 100 |
| Piano key test | Instability sign % | 57 |

*n: Ballottement test in neutral position*

## 7.2 The Sigmoid Notch

### 7.2.1 Sigmoid notch length

The anterior–posterior sigmoid notch (SN) length measured from the midpoint of the anterior sigmoid notch rim to the midpoint of the posterior sigmoid notch rim of the radius had individual variation.

In Studies I, III and IV the mean SN length ranged from 13.4 mm to 13.8 mm for the examined study populations.

In Study III, statistically significant gender differences on SN length was found ($p$ = 0.005) (Table 7.2). This emphasized the need for taking the individual SN length into account in evaluation of DRUJ translation.

In Study IV, the injured DRUJ was equally distributed between dominant (48%) and non-dominant hands (52%) (Table 7.1), and the SN length was similar on the injured side compared to the non-injured ($p$ = 0.57) (Table 7.2).

Table 7.2. Radiostereometry measured sigmoid notch length, Studies I, III, and IV

| *Sigmoid notch (SN) length* | *Units* | *Value* |
|---|---|---|
| *Study I, N= 8 donor arms* | | |
| SN length | Mean mm (95% CI) | 13.8 (12.5 – 15.2) |
| *Study III, N = 33 participants non-injured forearm* | | |
| SN length | Mean mm (95% CI) | 13.4 (13.0 – 13.8) |
| Men *(N = 14)* | | 14.1 (13.3 – 14.8) |
| Women (*N = 19)* | | 12.9 (12.4 – 13.4)* |
| *Study IV, N = 21 patients injured forearm* | | |
| SN length | Mean mm (95% CI) | |
| Non-injured hand | | 13.4 (12.9 – 14.0) |
| Injure hand | | 13.7 (13.0 – 14.4) |

**Statistically significant difference comparing men and women (p=0.005).*

### 7.2.2 Tolat type

In Study IV, the Tolat type of the sigmoid notch in injured DRUJs was equally distributed between dominant and non-dominant hands. All Tolat types were represented, but with the C-type as the most frequent (43%) (Figure 7.1).

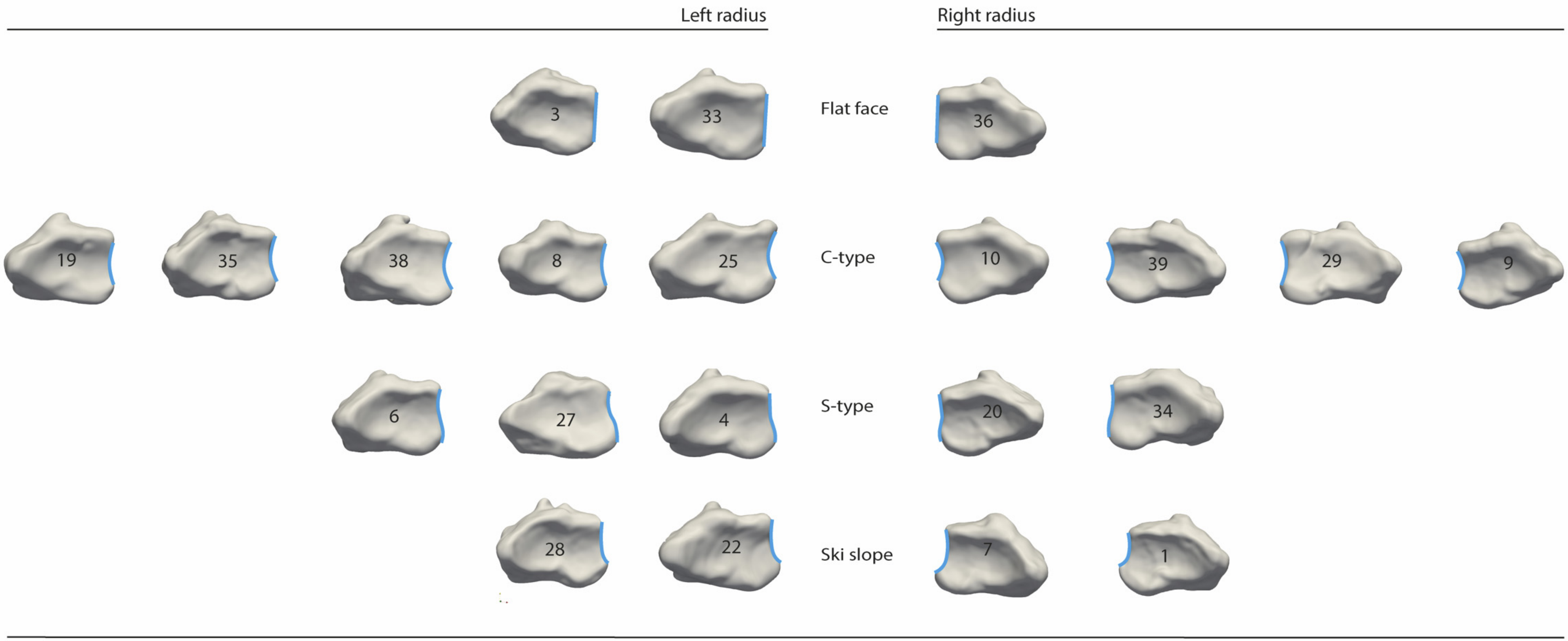


**Figure 7.1.** Sagittal view of the distal radius and sigmoid notch in all patients (Study IV), displaying notch type according to Tolat et al. (1996). (Numbers refer to anonymized patient IDs).

## 7.3 Study I

### 7.3.1 Clinical examination

The Ballottement test evaluated by 2 surgeons was less than 5 mm before treatment in all specimens, and more than 5 mm DRUJ translation after the last intervention performing combined dc/pc-TFCC lesion (Table 7.1).

### 7.3.2 DRUJ translation

In Study I, during the Piano key test the DRUJ translation on the intact human cadaver arms was mean 1.36 mm (95% CI 0.17–2.5) in intact wrists, mean 1.96 mm (95% CI 1.05 – 2.86) after lesion of the dc-TFCC and mean 2.30 mm (95% CI 1.41–3.20), after combined dc/pc-TFCC lesion. Each intervention significantly increased the DRUJ translation compared to the intact situation ($p < 0.04$) (Table 7.3).

Table 7.3. DRUJ translation and DRUJ position ratio after Piano Key test in Study I

| *Kinematic outcome*<br>*N = 8 donor arms* | *Intact TFCC* | *dc-TFCC lesion* | *dc-TFCC lesion* |
|---|---|---|---|
| *Pronated forearm* | | | |
| Forearm pronation (°) | 80 (76 – 85) | 83 (79 – 87) | 81 (75 – 88) |
| DRUJ position ratio | 0.72 (0.65 – 0.78) | 0.71 (0.65 – 0.76) | 0.67 (0.58 – 0.76) |
| *Piano key test* | | | |
| DRUJ translation (mm) | 1.36 (0.17 – 2.55) | 1.96 (1.05 – 2.86)* | 2.30 (1.41 – 3.20)* |
| DRUJ position ratio | 0.61 (0.55 – 0.67) | 0.56 (0.49 – 0.63)* | 0.50 (0.41 – 0.60)* |

**Statistically significant difference compared to the intact TFCC. Values are displayed as means with 95% CI. DRUJ: Distal radioulnar joint, dc distal component, pc proximal component, TFCC triangular fibrocartilage complex. Adapted from Thillemann et al., (2020).*

### 7.3.3 DRUJ position

The DRUJ position in Study I, before and after the Piano key test in intact human cadaver arms and after lesion to the dc-TFCC and after combined dc/pc-TFCC lesion is presented in Figure 7.2.

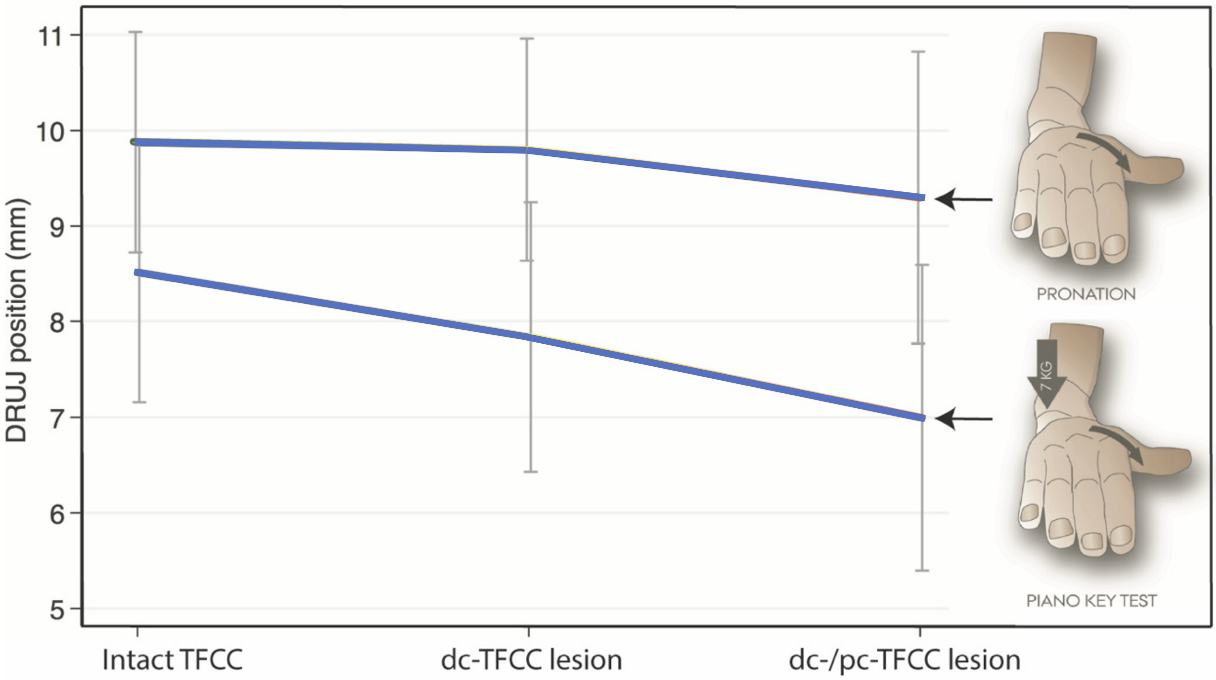


Figure 7.2. Graph displaying the distal radioulnar joint (DRUJ) position in pronation and after the Piano key test, with the intact triangular fibrocartilage complex (TFCC), after lesion of the distal component (dc-TFCC) and after combined lesions of the distal and proximal components (dc/pc-TFCC) of the TFCC. The mean (95% CI) DRUJ position is displayed as millimeters measured from the volar rim of the sigmoid notch. Adapted from Thillemann et al., (2020).

### 7.3.4 DRUJ position ratio

To take the individual variation and gender differences of the SN length into account, the DRUJ position of the ulnar head was presented as a ratio of the SN length (DRUJ position ratio).

Initially, at neutral forearm rotation the DRUJ position ratio was mean 0.54 (95% CI 0.48–0.59) and by pronating the forearm to mean 80 degrees (95% CI 76 – 85) a statistically significant dorsal glide of the ulnar head to a mean 0.72 (95% CI 0.65–0.78) DRUJ position ratio was detected ($p = 0.0001$)

After lesion to the dc-TFCC and finally the pc-TFCC, the DRUJ position ratio decreased to a mean 0.67 (95% CI 0.58–0.76). Compared to the intact situation this decrease was borderline significant ($p = 0.07$).

At each lesion-stage the Piano key test was applied. After dc-TFCC and pc-TFCC lesion the DRUJ position ratio decreased compared to the intact situation ($p < 0.02$) and was 0.50 (95% CI 0.41–0.60) after the combined dc/pc-TFCC lesion (Table 7.3).

### 7.3.5 Validation of AutoRSA

In Study I, the AutoRSA based RSA analysis vas validated against the marker-based RSA analysis as the reference standard. The pose of the bone models measured with AutoRSA and marker-based RSA analysis, showed no statistical difference in mean translation along or mean rotations about the x, y and z-axis for the distal radius and ulna (p >0.05) (Figure 7.3).

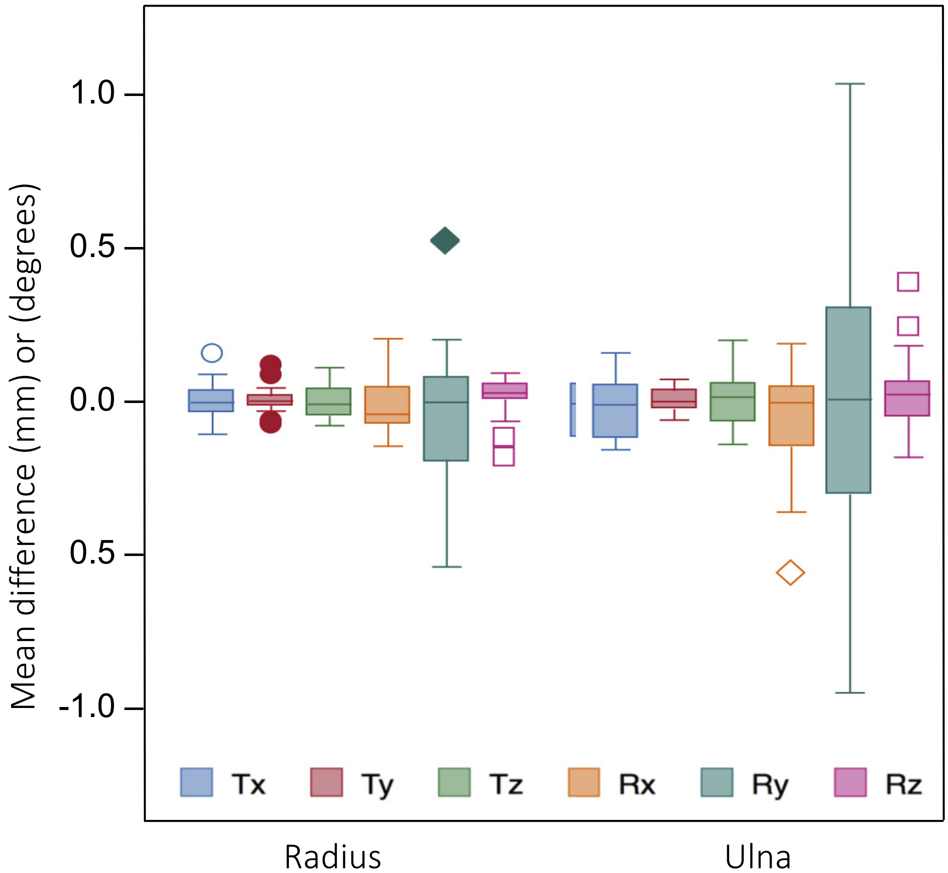


**Figure 7.3.** Mean difference of AutoRSA analysis in the distal radius and ulna compared to marker-based RSA.

The AutoRSA precision (prediction interval (1.96 x SD)) was below 0.12 mm for translation of the radius, below 0.18 mm for translation of the ulna, and less than 0.98 degrees in rotations for both the radius and ulna, compared to marker-based RSA analysis (Table 7.4).

**Table 7.4.** Prediction interval (1.96 x SD) of AutoRSA analysis in the distal radius and ulna compared to marker-based RSA.

| *Bone* | *Translations* | | | *Rotations* | | |
|---|---|---|---|---|---|---|
| | *Tx* | *Ty* | *Tz* | *Rx* | *Ry* | *Rz* |
| Radius | 0.12 | 0.08 | 0.10 | 0.17 | 0.50 | 0.13 |
| Ulna | 0.18 | 0.07 | 0.17 | 0.36 | 0.97 | 0.26 |

Translations (T) displayed in mm and rotations (R) in degrees of 22 double examinations.

## 7.4 Study II

### 7.4.1 Clinical examination

In Study II, the Ballottement test estimated the DRUJ translation was evaluated as more than 5 mm before treatment in all specimens, and as less than 5 mm DRUJ translation after ended intervention (Table 7.1).

### 7.4.2 DRUJ translation

In Study II, using static RSA examinations, the DRUJ translation induced by applying the Piano key test in human cadaver arms after lesion to dc/pc-TFCC, and after open foveal TFCC reinsertion or Adams TFCC reconstruction was evaluated. Before surgery, the DRUJ translation was mean 1.86 mm (95% CI 0.84–2.89) in the Foveal TFCC reinsertion group and reduced to 0.08 mm (95% CI -0.48–0.64) after surgery ($p$ = 0.007). The DRUJ translation was 3.05 (95% CI 1.78–4.32) in the Adams TFCC reconstruction group before surgery and reduced to 2.04 mm (95% CI -0.81–4.89) after surgery ($p$ = 0.17) (Figure 7.4). The preoperative DRUJ translation in the two groups was comparable (p = 0.08) but was reduced by mean 1.78 mm (95% CI 0.82–2.74) in the foveal TFCC reinsertion group ($p$ = 0.007) and mean 1.01 mm (95% CI -1.58–3.60) in the Adams TFCC reconstruction group ($p$ = 0.17). The reduced DRUJ translation were similar ($p$ = 0.31), but with greater variation in the Adams TFCC reconstruction group (Figure 7.4).

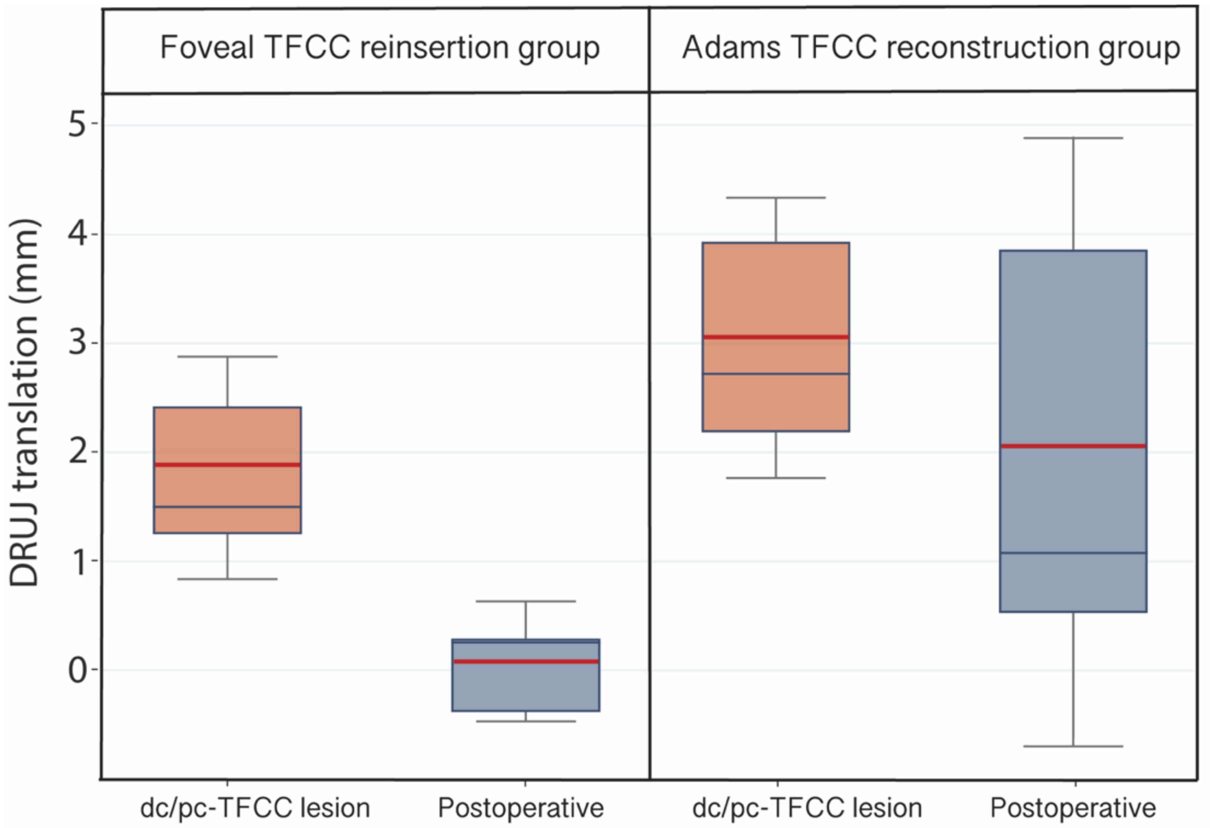


Figure 7.4. Graph displaying distal radioulnar joint (DRUJ) translation induced by the Piano key test in the open foveal TFCC reinsertion group and the Adams TFCC reconstruction group, before and after intervention. The mean (red line) and 95% CI is displayed (whiskers). The median (blue line) and IQR (box) is displayed for visualization of variation.
Adapted from Thillemann et al., (2021a).

### 7.4.3 DRUJ position ratio

In Study II, the DRUJ position ratio was used to express the preoperative DRUJ position before applying the Piano key test. The forearm pronation ($p = 0.87$) as well as the DRUJ position ratio was comparable between treatment groups before applying the Piano key test ($p = 0.21$).

At the stage with dc/pc-TFCC lesion, the Piano key test moved the ulnar head to comparable DRUJ position ratios of mean 0.51 (95% CI 0.45–0.57) in the open foveal TFCC reinsertion group and mean 0.48 (05% CI 0.28–0.68) in the Adams TFCC reconstruction group ($p = 0.72$).

After surgical treatment, the Piano key test induced less translation to reach a similar DRUJ position ratio in the foveal reinsertion group of mean 0.60 (95% CI 0.57 – 0.63) and mean 0.61 (95% CI 0.41–0.81) in the Adams TFCC reconstruction group (p = 0.87) (Table 7.5).

Table 7.5. DRUJ translation and DRUJ position ratio after Piano key test in Study II.

| *Kinematic outcome* | *With dc/pc-TFCC lesion* | | | *After surgical treatment* | | |
|---|---|---|---|---|---|---|
| | *Foval TFCC reinsertion* | *Adams TFCC reconstruction* | *p-value* | *Foval TFCC reinsertion* | *Adams TFCC reconstruction* | *p-value* |
| *N= 10 donor arms (5 reinsertion/5 reconstruction)* | | | | | | |
| *Pronated forearm* | | | | | | |
| Forearm pronation (°) | 81 (68 – 93) | 82 (72 – 91) | 0.87 | 58 (44 – 73) | 68 (49 – 88) | 0.31 |
| DRUJ position ratio | 0.63 (0.52 – 0.75) | 0.72 (0.60 – 0.84) | 0.21 | 0.60 (0.57 – 0.63) | 0.77 (0.65 – 0.89) | 0.005 |
| *Piano key test* | | | | | | |
| DRUJ translation (mm) | 1.86 (0.84 – 2.89) | 3.05 (1.78 – 4.32) | 0.08 | 0.08 (-0.48 – 0.64) | 2.04 (-0.81 – 4.89) | 0.10 |
| DRUJ position ratio | 0.51 (0.45 – 0.57) | 0.48 (0.28 – 0.68) | 0.72 | 0.60 (0.57 – 0.63) | 0.61 (0.41 – 0.81) | 0.87 |

*Values are displayed as means with 95% confidence intervals (CI).*

*DRUJ: Distal radioulnar joint, dc: distal component, pc: proximal component, TFCC: triangular fibrocartilage complex.*

*Table adapted from Thillemann et al., (2021a).*

## 7.5 Study III

### 7.5.1 Clinical examination

The DRUJ of all participants was evaluated as stable (<5 mm translation) by the Ballottement test performed in neutral forearm rotation (Table 7.1).

### 7.5.2 Press test pressure force

The maximum pressure force (at 50% of the motion cycle) applied onto the weight platform during the Press test motion cycle is displayed in Table 7.6. Men and women applied a similar pressure force ($p$ = 0.55). The maximum pressure force for all participants was mean of 6.0 kg (95% CI 5.1–6.9).

The Press test decreased the DRUJ position ratio, but a floor effect was seen after 5 kg force application (Figure 7.5).

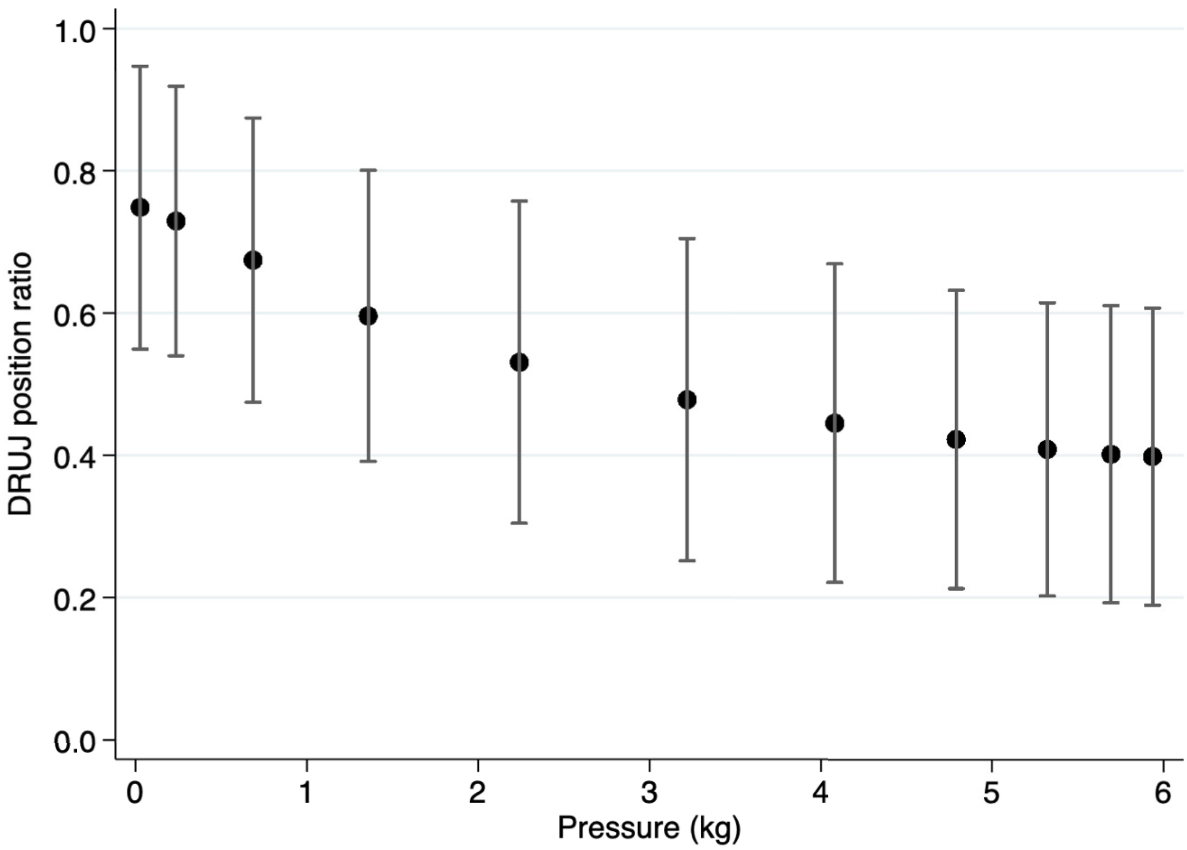


Figure 7.5. Graph displaying the relation between the applied press test pressure (kg) and the mean DRUJ position ratio with 95% confidence intervals.
Adapted from Thillemann et al. (2021b).

### 7.5.3 DRUJ pronation

Before initiation of pressure application onto the weight platform (0% of the motion cycle) the degree of DRUJ pronation was significantly higher in women as compared to men ($p = 0.03$) (Table 7.6).

After pressure application to the maximum pressure force the DRUJ pronation and the kinematic outcomes for men and women were similar ($p > 0.08$) (Table 7.6).

### 7.5.4 DRUJ translation

The maximum pressure force (induced a DRUJ translation of mean 4.7 mm (95% CI 4.2 – 5.5) for all participants (Table 7.6).

Table 7.6. Dynamic radiostereometry (dRSA) outcome measures of the distal radioulnar joint (DRUJ) in asymptomatic forearms in Study III.

| *Kinematic outcome*<br>*N = 33 participants non-injured arm* | *Men* | *Women* | *p-value*[1] | *All participants* |
|---|---|---|---|---|
| *At 0 % of the motion cycle* | | | | |
| Forearm pronation (°) | 57 (53 – 61) | 65 (59 – 71) | 0.03 | 62 (58 – 66) |
| DRUJ position ratio | 0.72 (0.65 – 0.79) | 0.77 (0.73–0.81) | 0.23 | 0.75 (0.71–0.78) |
| *At 50 % of the motion cycle* | | | | |
| Maximum force (kg) | 6.3 (4.7 – 7.9) | 5.8 (4.8 – 6.8) | 0.55 | 6.0 (5.1 – 6.9) |
| Forearm pronation (°) | 48 (42 – 54) | 56 (50 – 63) | 0.08 | 53 (48 – 57) |
| DRUJ position ratio | 0.42 (0.37–0.47) | 0.38 (0.33–0.44) | 0.32 | 0.40 (0.33–0.44) |
| *From 0 to 50% of the motion cycle* | | | | |
| DRUJ translation (mm) | 4.3 (3.5 – 5.0) | 4.9 (4.4 – 5.5) | 0.15 | 4.7 (4.2 – 5.1) |
| Change in ulnar variance (mm) | 1.1 (0.8 – 1.3) | 1.1 (0.9 – 1.3) | 0.94 | 1.1 (1.0 – 1.2) |

*[1]Independent t-test comparing men and women.*
*TFCC triangular fibrocartilage complex. DRUJ: distal radioulnar joint, RUJ: radioulnar joint.*
*Numbers are reported as means with 95% confidence intervals (CI).*
*Adapted from Thillemann et al. (2021b).*

### 7.5.5 DRUJ position ratio

Before pressure application onto the weight platform was initiated the DRUJ position ratio was mean 0.75 (95% CI 0.71 – 0.78) for all participants. At maximum pressure force, the center of the ulnar head moved below the sigmoid notch center to a mean 0.40 (95% CI 0.33 – 0.44) DRUJ position ratio for all participants (Table 7.6).

### 7.5.6 Ulnar variance

The mean 6.0 kg (95% CI 5.1 – 6.9) pressure application on the weight platform increased the mean ulnar variance by 1.1 mm (95% CI 1.0 – 1.2) (Table 7.6).

### 7.5.7 Press test repeatability

Repeatability of the Press test induced maximum pressure force was estimated. The absolute mean difference between double examinations was 0.80 kg (SD 0.69) and within a prediction interval (1.96 x SD) of ±1.35 kg.
The absolute mean differences of the corresponding kinematic outcomes are displayed in Table 7.7. The repeatability of the DRUJ translation was within a prediction interval of ±0.53 mm, the DRUJ position ratio was within a prediction interval of ±0.04 and the change in ulnar variance was within a prediction interval of ±0.18 mm (Table 7.7.).

The Intraclass Coefficient (2,1) of absolute agreement evaluating test-retest consistency between the double examinations was good ($r = 0.87$, 95% CI 0.76 – 0.94) for the applied pressure force. The ICC consistency was excellent for the corresponding kinematic outcomes ($r > 0.93$) (Table 7.7).

Table 7.7. Precision of kinematic outcomes and maximum force recorded by dynamic radiostereometry (dRSA) during the Press test in non-injured DRUJs in Study III. (N = 2 x 33)

| | *Mean difference* | *Prediction interval* | *ICC* |
|---|---|---|---|
| Maximum force (kg) | 0.80 (0.69) | 1.35 | 0.87 (0.76 – 0.94) |
| DRUJ translation (mm) | 0.39 (0.27) | 0.53 | 0.93 (0.86 – 0.96) |
| DRUJ position ratio | 0.02 (0.02) | 0.04 | 0.95 (0.91 – 0.98) |
| Ulnar variance (mm) | 0.10 (0.09) | 0.18 | 0.996 (0.99 – 1.00) |

*Systematic bias reported as absolute mean differences with standard deviations (SD) and prediction intervals (SD × 1.96).*
*DRUJ: distal radioulnar joint, ICC: Intraclass Coefficient (2,1) calculated as two-way mixed effects, absolute agreement to evaluate rater consistency between first and second examinations, with 95% confidence intervals. Adapted from Thillemann et al. (2021b).*

### 7.5.8 Ultrasonography and repeatability

The DRUJ translation (T) measured by the first US was mean 2.3 mm (95% CI 1.7 – 2.8) and the Hess Quotient mean 0.59 (95% CI 0.44 – 0.74). Six of the 33 participants had a Hess Quotient above the proposed cut-off value of 0.80 on their asymptomatic forearm (specificity 82%).

Precision of the US measured DRUJ translation and the Hess Quotient was estimated. The absolute mean difference of the DRUJ translation between double examinations was 0.77 mm (SD 0.74) and within a prediction interval (1.96 x SD) of ±1.44 mm, whereas the Hess Quotient had a mean difference of 0.21 (SD 0.52) and a prediction interval (1.96 x SD) of ±1.01 (Table 7.8).

The Intraclass Coefficient (2,1) of absolute agreement evaluating rater consistency of the US measured DRUJ translation double examinations indicated moderate reliability ($r$ = 0.74, 95% CI 0.53 – 0.87) (Table 7.8).

Table 7.8. Precision of ultrasonography measured outcomes of the participants non-injured forearm in Study III. (N=2 x 33)

| | *Mean difference* | *Prediction interval* | *ICC* |
|---|---|---|---|
| DRUJ translation | 0.77 (0.74) | 1.44 | 0.74 (0.53 – 0.87) |

*Systematic bias reported as absolute mean differences with standard deviations (SD) and prediction intervals (SD × 1.96). DRUJ: distal radioulnar joint, ICC: Intraclass Coefficient (2,1) calculated as two-way mixed effects, absolute agreement to evaluate rater consistency between first and second examinations with 95% confidence interval. Adapted from Thillemann et al. (2021b).*

### 7.5.9 Dynamic kinematic outcomes during the Press test

Figure 7.6. display the normal values of dynamic DRUJ kinematics during the Press test examination, in the participants with asymptomatic forearms.

The maximum pressure force (kg) applied onto the weight platform was defined as at the 50% of the motion cycle, the downstroke pressure phase was displayed as 0 – 50 % of the motion cycle, and release phase as 51 – 100 % of the motion cycle (Figure 7.6.a). Figure 7.6.b-d display the corresponding dynamic kinematic outcomes.

The maximum/minimum outcomes were reached as the pressure was at the maximum pressure force (at 50% of the motion cycle).

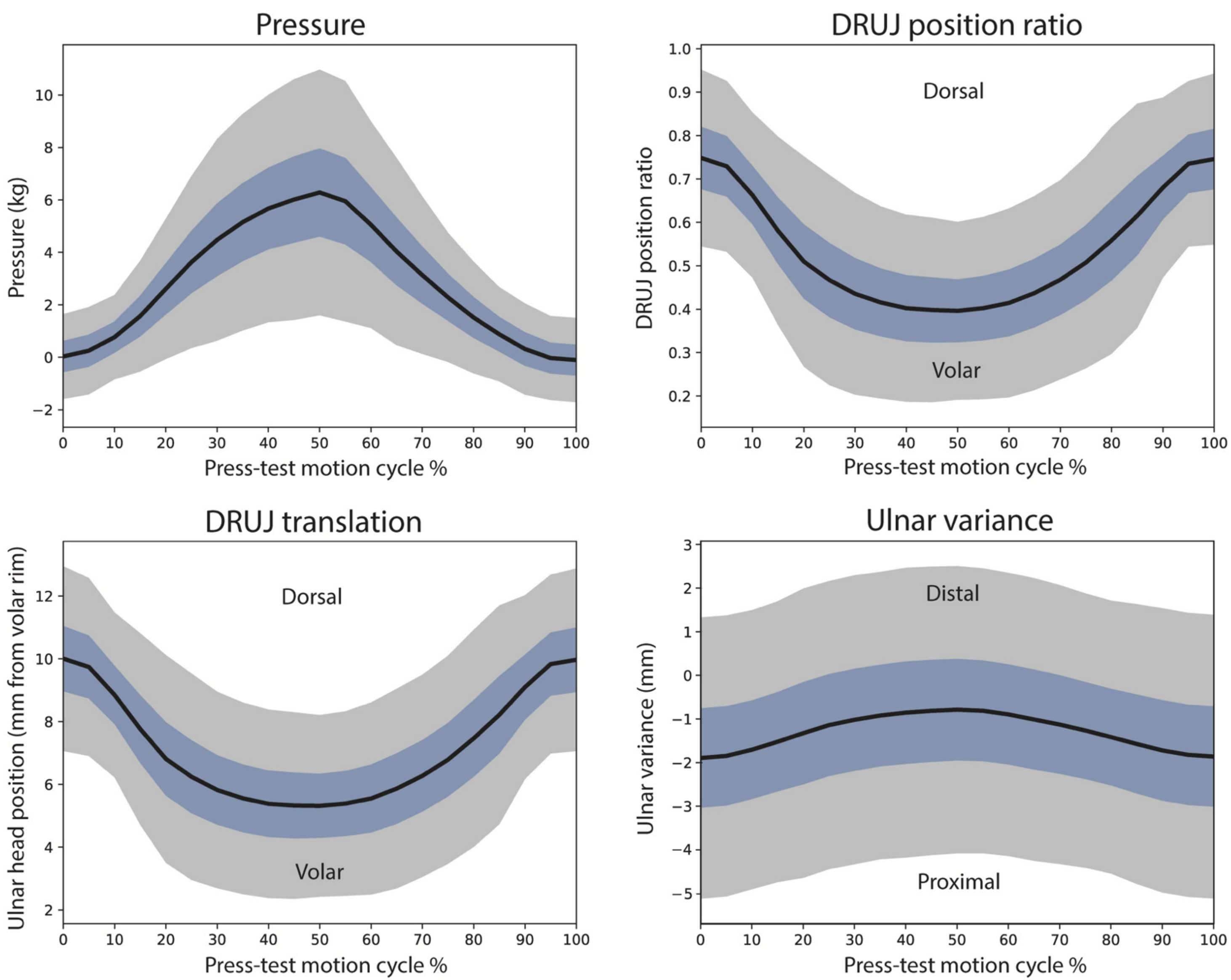


**Figure 7.6.** Graphs display the force applied during the Press test (a), the corresponding DRUJ position ratio (b), the resulting DRUJ translation (c), and the changes in ulnar variance (d). The mean of the kinematic outcomes (black line) with 95% confidence intervals (blue area) during the Press test motion cycle (0%–100%) recorded by dynamic RSA and the prediction interval (PI = 1.96 x SD) (grey area). The maximum force is defined as 50% of the motion cycle, the downstroke and pressure phase as 0–50% of the cycle, and the release phase as 51–100% of the cycle.
Adapted from Thillemann et al. (2021b).

## 7.6 Study IV

### 7.6.1 Clinical examination

Table 7.9. display the results from the *preoperative* clinical examination.
Twelve patients were classified as unstable by Piano key test, whereas all patients had more than 5 mm translation evaluated with the Ballottement test in neutral forearm rotation. Preoperatively 14 DRUJ´s were unstable in pronation compared to 8 in supination ($p$ = 0.06).
The mean grip strength was 5.7 kg (95% CI 1.8 – 9.6) less in the injured hand compared to the contralateral healthy hand ($p$ = 0.006). This difference was most pronounced in women ($p$ = 0.002). Wrist AROM and forearm rotation was reduced in the forearms with foveal TFCC injury, compared to the contralateral non-injured wrist and forearm ($p$<0.04) (Table 7.9).

*After surgical treatment*, clinical examination of the DRUJ stability by the Piano key test and the Ballottement test indicated improvement of the stability after surgical treatment (Table 7.10).
The mean grip strength was lower at the 6-month FU but was regained at the preoperative level at 1-year FU ($p$ = 0.93) but did not reach the level of the non-injured hand ($p$=0.002).
Wrist AROM and forearm rotation in the arms with foveal TFCC injury, did not improve during the first postoperative year (Table 7.10).

Table 7.9. Preoperative clinical examination of non-injured and injured forearm in Study IV.

| *Examination* | *Units* | *Baseline value* | | |
|---|---|---|---|---|
| *N = 21 patients* | | *Non-injured forearm* | *Injured forearm* | *p-value*[1] |
| *Clinical examination* | | | | |
| Grip strength | Mean kg (95% CI) | 45 (39 – 51) | 39 (32 – 47) | 0.006 |
| Women (*N = 10*) | | 33 (28 – 38) | 25 (20 – 30) | 0.002 |
| Men (*N = 11*) | | 56 (52 – 60) | 52 (46 – 58) | 0.26 |
| Wrist motion | Mean degrees (95% CI) | | | |
| Flexion | | 78 (73 – 82) | 70 (65 – 76) | 0.001 |
| Extension | | 74 (70 – 78) | 67 (61 – 73) | 0.004 |
| Radial | | 22 (19 – 25) | 18 (16 – 20) | 0.01 |
| Ulnar | | 37 (34 – 40) | 28 (25 – 30) | 0.01 |
| Forearm rotation | Mean degrees (95% CI) | | | |
| Supination | | 84 (81 – 87) | 78 (75 – 82) | 0.001 |
| Pronation | | 81 (77 – 85) | 79 (74 – 83) | 0.04 |
| Ballottement test[2] | Number | | | |
| Neutral | | 21/0/0 | 0/15/6 | < 0.001 |
| Pronation | | 21/0/0 | 7/14/0 | < 0.001 |
| Supination | | 21/0/0 | 13/8/0 | < 0.05 |
| Piano key test | Number unstable | 0 | 12 | 0.00 |

*[1] Preoperative comparison between the non-injured forearm and the foveal TFCC injury arm using either a t-test, Wilcoxon sing-rank or a chi-square test as appropriate, [2] Normal to slight instability (<5 mm)/mild instability (5-10mm)/severe instability (>10 mm). Adapted from Thillemann et al. (2022).*

Table 7.10. Clinical examination of the injured forearm before and after surgical treatment in Study IV

| *Examination* | *Units* | *Value* | | | |
|---|---|---|---|---|---|
| | | *Preoperatively* | *6-month follow-up* | *1-year follow-up* | *p-value*[1] |
| *Clinical examination* | | *(N = 21)* | *(N = 19)* | *(N = 19)* | |
| Weeks of follow-up | Mean weeks (range) | 0 | 32 (25 – 41) | 59 (51 – 73) | |
| Grip strength injured hand | Mean kg (95% CI) | 39 (32 – 47) | 36.1 (29.9 – 42.4) | 39.5 (31.7 – 47.3) | 0.04** |
| Women | | 25 (20 – 30) | 23.0 (17.2 – 28.8) | 25.0 (17.1 – 32.9) | 0.30 |
| Men | | 52 (46 – 58) | 47.6 (44.1 – 51.1) | 52.5 (46.0 – 58.9) | 0.048** |
| Wrist motion | Mean degrees (95% CI) | | | | |
| Flexion | | 70 (65 – 76) | 67 (62 – 72) | 68 (62 – 73) | 0.59 |
| Extension | | 67 (61 – 73) | 68 (64 – 72) | 66 (61 – 71) | 0.63 |
| Radial | | 18 (16 – 20) | 18 (16 – 20) | 19 (17 – 22) | 0.13 |
| Ulnar | | 28 (25 – 30) | 28 (25 – 30) | 32 (28 – 37) | 0.02* |
| Forearm rotation | Mean degrees (95% CI) | | | | |
| Supination | | 78 (75 – 82) | 76 (72 – 80) | 74 (70 – 78) | 0.17 |
| Pronation | | 79 (74 – 83) | 77 (73 – 81) | 79 (75 – 83) | 0.49 |
| Ballottement test[2] | | | | | |
| Neutral | | 0/15/6 | 13/6/0 | 13/6/0 | < 0.001*/** |
| Pronation | | 7/14/0 | 17/2/0 | 17/2/0 | < 0.01*/** |
| Supination | | 13/8/0 | 17/2/0 | 17/2/0 | 0.04*/** |

*[1] Comparison of the foveal TFCC injury arm over time, from preoperative, 6 month and 1-year follow-up with Kruskal Wallis test of non-parametric repeated measures. [2] Normal to slight instability (<5 mm)/mild instability (5-10mm)/severe instability (>10 mm). Statistical significance compared to the preoperative examination of the foveal TFCC injury arm.*

** Statistical significance between preoperative examination and 6-month follow-up*

*** Statistical significance between preoperative examination and 1-year follow-up*

*Adapted from Thillemann et al. (2022).*

### 7.6.2 Patient-reported Outcomes

*Preoperatively* the patients reported no statistically significant pain on NRS score at rest and during unloaded foream rotation, as the median NRS scores were 0 (IQR 0 – 3) and 1 (IQR 0 – 5) respectively. Contrary, lifting above 5 kg and loaded forearm rotation was reported to produce pain ($p > 0.05$).

*After surgical treatment*, the NRS pain score was reduced during activity ($p < 0.007$). The pain reduction experienced by the patients during lifting and loaded forearm rotation was statistically significantly reduced during the first postoperative year ($p < 0.001$), but also clinically relevant as the improvement was above the MCID for pain (2 points) (Farrar et al., 2001; Salaffi et al., 2004) (Figure 7.7, Table 7.11).

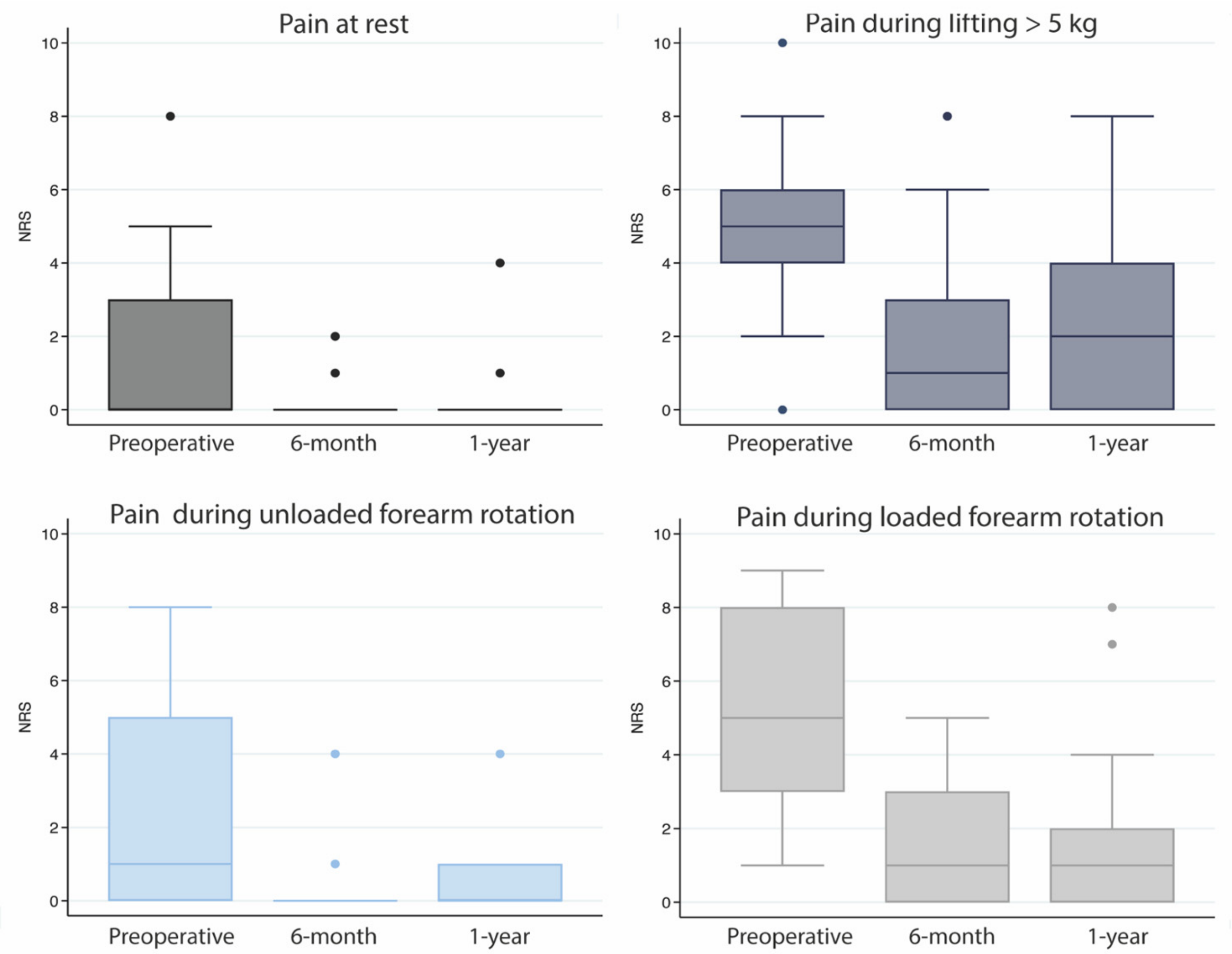


**Figure 7.7.** Patient reported pain on Numeric Rating Scale in patients' forearm with foveal TFCC injury. Boxplots of the patient reported pain at rest, during lifting more than 5 kg, with loaded- and unloaded forearm rotation, from the preoperatively throughout the 6-month and 1-year follow-up.
Boxplots display median pain, with inter quartile ranges (IQR), whiskers (1.5 x IQR) and outliers.
Adapted from Thillemann et al. (2022).

**Table 7.11**. Patient reported outcomes in the patients injured forearm before and after surgical treatment in Study IV

| *Patient reported outcome* | *Units* | *Value* | | | |
|---|---|---|---|---|---|
| | | *Preoperative (N=21)* | *6-month follow-up (N = 19)* | *1-year follow-up (N = 19)* | *p-value* |
| DRUJ pain [1] | Median NRS score (range) | | | | |
| At rest | | 0 (0 – 3) | 0 (0 – 0) | 0 (0 – 0) | 0.162 |
| Unloaded rotation | | 1 (0 – 5) | 0 (0 – 0) | 0 (0 – 1) | 0.007* |
| Resisted rotation | | 5 (3 – 8) | 1 (0 – 3) | 1 (0 – 2) | < 0.001* |
| Lifting >5 kg | | 5 (4 – 6) | 1 (0 – 3) | 2 (0 – 4) | < 0.001* |
| QDASH [2] | Mean score (95% CI) | 39 (32 – 47) | 29 (22 – 36) | 25 (16 – 35) | < 0.000* |
| Pain PRWE [2] | Mean score (95% CI) | 29 (25 – 33) | 17 (14 – 20) | 18 (13 – 23) | < 0.000* |
| Function PRWE [2] | Mean score (95% CI) | 20 (15 – 24) | 12 (8 – 15) | 10 (6 – 14) | < 0.000* |
| Total PRWE [2] | Mean score (95% CI) | 49 (41 – 57) | 29 (23 – 35) | 28 (19 – 37) | < 0.000* |

*[1] Kruskal Wallis test of non-parametric repeated measures; [2] ANOVA repeated measures (MIXED MODEL) for comparison of repeated parametric measures. Statistical significance compared to the preoperative examination of the foveal TFCC injury arm (*). Adapted from Thillemann et al. (2022).*

The *preoperative* patient reported QDASH score improved throughout the 1-year follow-up, by 14 points (95% CI 7 – 21) ($p = 0.000$) (Figure 7.8, Table 7.11).
The *preoperative* patient reported total PRWE score improved throughout the 1-year follow-up, by 21 points (95% CI 13 –29) ($p = 0.000$) (Figure 7.9, Table 7.11).

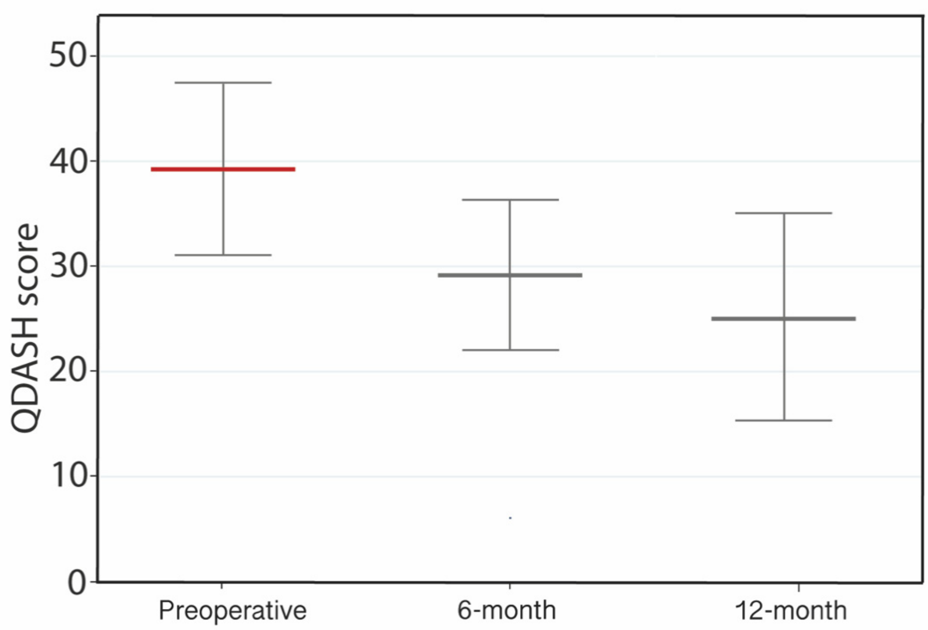


**Figure 7.8.** Quick DASH score reported by patients with foveal TFCC injury from preoperative (red), throughout the 6-month and 1-year follow-up. The graph display means with 95% confidence intervals.

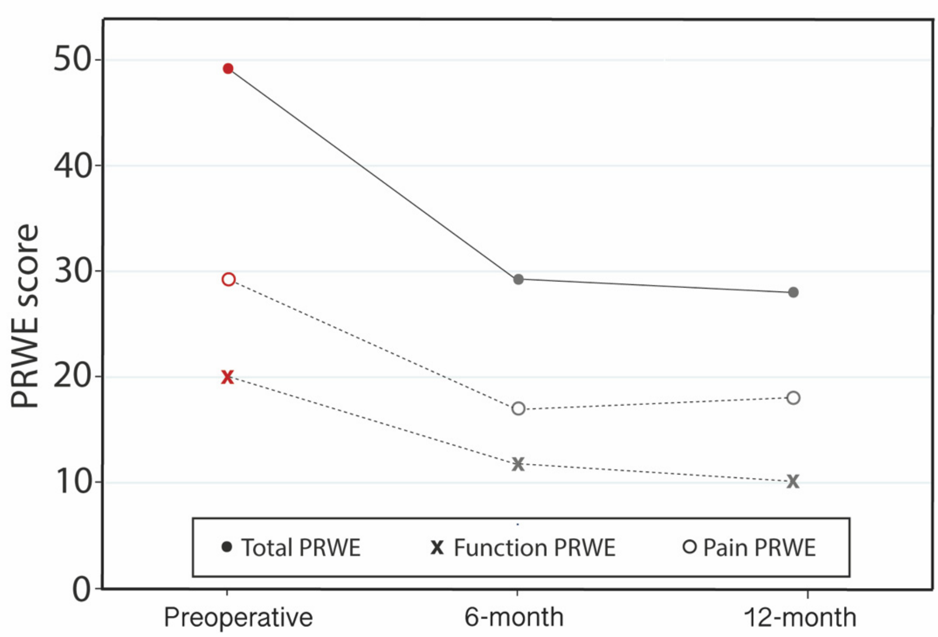


**Figure 7.9.** Total PRWE score, function PRWE and pain PRWE sub scores reported by patients with foveal TFCC injury from preoperative (red), throughout the 6-month and 1-year follow-up.

Seventy-nine percent of patients reported *willingness to repeat* the surgical treatment and rehabilitation at 1-year. Eighty-five percent of patients reported to be satisfied with treatment and 5% were dissatisfied (Figure 7.10).

At 1-year follow-up, no patients were reoperated, but one patient had suffered a new trauma and was treated with a cast due to suspected scaphoid fracture. This patient had persisting DRUJ pain and instability after scaphoid fracture was disclaimed, and after 1-year she was reoperated using tendon graft and Adams TFCC reconstruction.

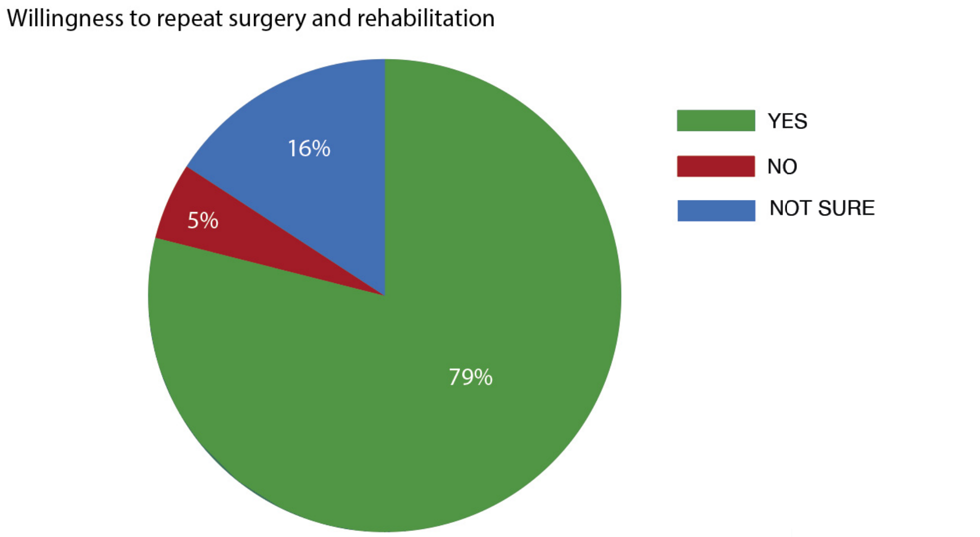


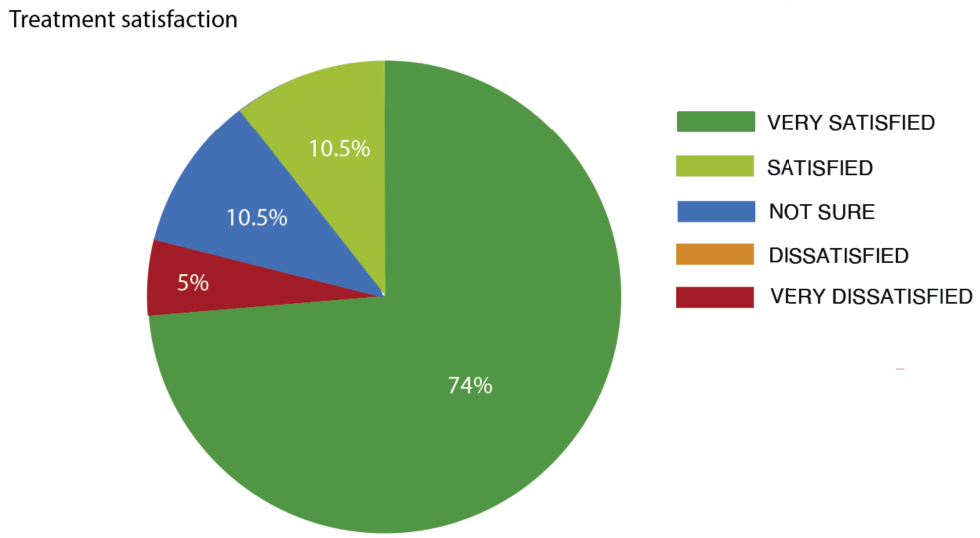


**Figure 7.10.** Pie charts of patient's (N=19) willingness to repeat treatment and their treatment satisfaction.

### 7.6.3 Press test pressure force

In the healthy and injured forearms, the *preoperative* maximum pressure force applied onto the weight platform was similar (Table 7.12).

Table 7.12. Preoperative dynamic radiostereometry (dRSA) outcome measures of the distal radioulnar joint (DRUJ) in asymptomatic forearms in Study IV.

| *Kinematic outcome* | *Baseline value* | | *p-* |
|---|---|---|---|
| *N = 21 patients* | *Non-injured forearm* | *Injured forearm* | *value[1]* |
| *At 0 % of the motion cycle* | | | |
| Forearm pronation (°) | 61 (56 – 67) | 59 (54 – 65) | 0.61 |
| DRUJ position ratio | 0.72 (0.68 – 0.76) | 0.68 (0.61 – 0.75) | 0.28 |
| DRUJ distance (mm) | 9.9 (9.4 – 10.4) | 10.6 (10.0 – 11.1) | 0.07 |
| *At 50 % of the motion cycle* | | | |
| Maximum force (kg) | 6.7 (5.6 – 7.7) | 6.9 (5.7 – 8.1) | 0.71 |
| Forearm pronation (°) | 52 (47 – 58) | 50 (44 – 57) | 0.64 |
| DRUJ position ratio | 0.39 (0.34 – 0.44) | 0.29 (0.21 – 0.37) | 0.02 |
| DRUJ distance (mm) | 9.1 (8.5 – 9.7) | 10.6 (9.9 – 11.4) | 0.002 |
| *From 0 to 50% of the motion cycle* | | | |
| DRUJ translation (mm) | 4.4 (3.9 – 5.0) | 5.3 (4.4 – 6.1) | 0.09 |
| Change in ulnar variance (mm) | 1.14 (0.95 – 1.32) | 0.96 (0.75 – 1.07) | 0.14 |
| Pain during the Press test | | | |
| Pain on NRS (median, IQR) | 0 (0 – 0) | 1 (0 – 4) | 0.000 |

*[1]Paired t-test or Wilcoxon signed-rank test as appropriate comparing healthy and injured forearm. Numbers are reported as means with 95% confidence intervals (CI) or medians with inter quartile range (IQR). DRUJ: distal radioulnar joint, RUJ: radioulnar joint. Adapted from Thillemann et al. (2022).*

*After surgical treatment* the maximum pressure force was similar for the arms with foveal TFCC injury at all FU times (Table 7.13).

Table 7.13. Dynamic radiostereometry (dRSA) outcome measures of the distal radioulnar joint (DRUJ) in patients injured forearm before and after surgical treatment in Study IV.

| *Kinematic outcome* | *Value* | | | |
|---|---|---|---|---|
| *N = 21 patients* | *Preoperative (N=21)* | *6-month follow-up (N = 19)* | *1-year follow-up (N = 19)* | *p-value[1]* |
| *At 0 % of the motion cycle* | | | | |
| Forearm pronation (°) | 59 (54 – 65) | 60 (55 – 65) | 59 (54 – 64) | 0.46 |
| DRUJ position ratio | 0.68 (0.61 – 0.75) | 0.69 (0.62 – 0.75) | 0.70 (0.63 – 0.77) | 0.53 |
| DRUJ distance (mm) | 10.6 (10.0 – 11.1) | 10.6 (10.0 – 11.1) | 10.7 (10.1 – 11.2) | 0.22 |
| *At 50 % of the motion cycle* | | | | |
| Maximum force (kg) | 6.9 (5.7 – 8.1) | 7.4 (6.2 – 8.6) | 7.5 (6.0 – 9.1) | 0.65 |
| Forearm pronation (°) | 50 (44 – 57) | 54 (49 – 59) | 53 (48 – 59) | 0.23 |
| DRUJ position ratio | 0.29 (0.21 – 0.37) | 0.32 (0.24 – 0.39) | 0.31 (0.22 – 0.40) | 0.53 |
| DRUJ distance (mm) | 10.6 (9.9 – 11.4) | 10.5 (9.9 – 11.2) | 10.5 (9.7 – 11.2) | 0.21 |
| *From 0 to 50% of the motion cycle* | | | | |
| DRUJ translation (mm) | 5.3 (4.4 – 6.1) | 5.1 (4.3 – 5.8) | 5.3 (4.5 – 6.1) | 0.65 |
| Change in ulnar variance (mm) | 0.96 (0.75 – 1.07) | 0.94 (0.74 – 1.13) | 1.03 (0.85 – 1.2) | 0.31 |
| *Pain during the Press test* | | | | |
| Pain on NRS (median, IQR) | 1 (0 – 4) | 0 (0 – 1) | 0 (0 – 0) | 0.0001 |

*[1] Kruskal Wallis test of non-parametric repeated measures or ANOVA repeated measures (mixed model) for comparison of repeated parametric measures, as appropriate.*
*Significance compared to the preoperative examination of the foveal TFCC injury arm (*).*
*Significance between 6-month and 1-year follow-up (FU) in the foveal TFCC injury arm (**).*
*Adapted from Thillemann et al. (2022).*

Likewise, repeated measurement analysis of the force applied during the Press test motion cycle, showed similar force application throughout the entire motion cycle, with a mean difference of less than 0.9 kg between non-injured forearms and forearms with foveal TFCC injury at all FU times ($p > 0.28$) (Figure 7.11).

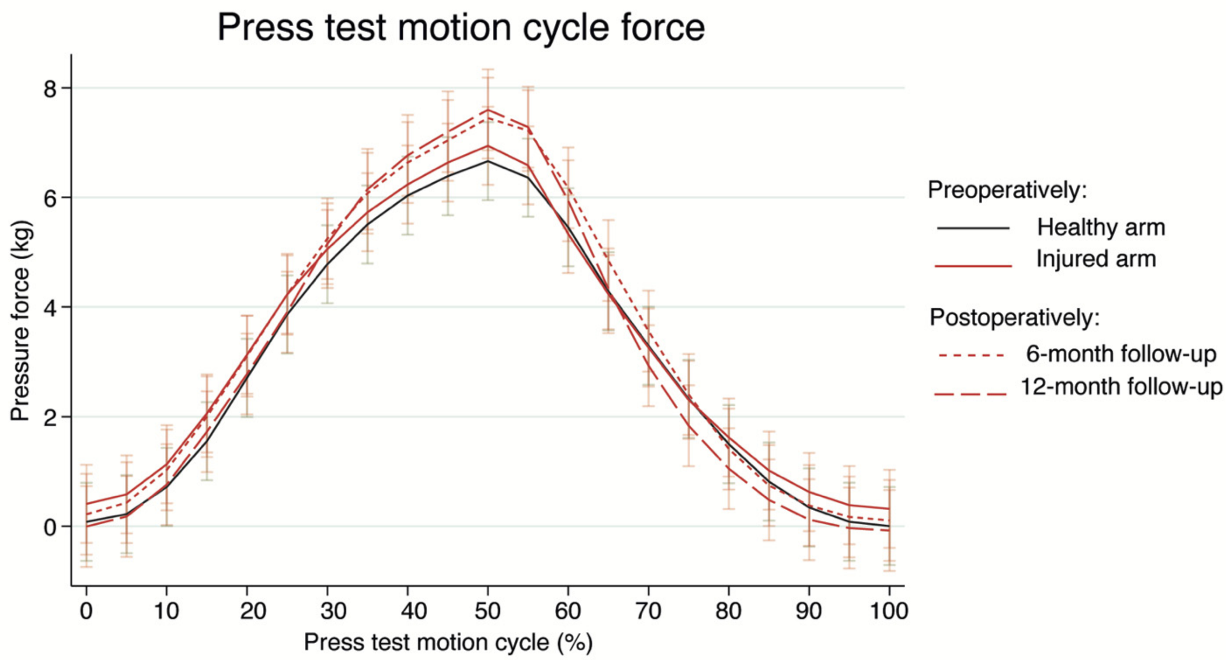


**Figure 7.11.** Dynamic pressure force during the Press test motion cycle. Preoperative force is displayed in non-injured forearms (black) and in forearms with foveal TFCC injury (red). Postoperative force at the 6-month and 12-month follow-up is displayed (dashed red lines). Graph's display (means with 95% confidence intervals). Adapted from Thillemann et al. (2022).

### 7.6.4 DRUJ pronation

The *preoperative* forearm pronation in the non-injured forearms and the injured forearms was similar as the Press test motion cycle was initiated and when the maximum pressure was applied ($p > 0.61$) (Table 7.12). Likewise, *after surgical treatment* the forearm pronation was similar in the injured forearm at alle follow-ups. ($p > 0.23$) (Table 7.13).

### 7.6.5 DRUJ translation

The *preoperative* mean difference in DRUJ translation during the motion cycle pressure phase in forearms with foveal TFCC injury, compared to the non-injured forearms was 0.9 mm (95% CI -0.2 – 1.7). *Surgical treatment* did not significantly decrease the DRUJ translation during the motion cycle pressure phase ($p$ = 0.65) (Table 7.12 and 7.13).

### 7.6.6 DRUJ position ratio

Taking the individual sigmoid notch size into account, the unloaded (0% of the cycle) *preoperative* mean DRUJ position ratio in non-injured joints was 0.72 (SD 0.09) and the foveal TFCC injured joints at a 0.68 (SD 0.15) ratio. At maximum pressure force the *preoperative* mean DRUJ position ratio at was at a 0.10 (95% CI 0.01 – 0.19) more volar ratio in the forearms with foveal TFCC injury, compared to the non-injured DRUJs ($p$=0.02) (Table 7.12).

Repeated measurement analysis of the *preoperative* mean DRUJ position ratio showed a significant difference from 15% to 75% of the dynamic motion cycle, between the forearms with foveal TFCC injury and the non-injured DRUJs (Figure 7.12.a).

At 6-month follow-up *after surgical treatment,* the DRUJ position ratio maximum pressure force was slightly more dorsal, but no significant difference was detected between the 6-month, or 12-month FU, and the preoperative examination of the injured forearm ($p$ = 0.53) (Table 7.13).

Repeated measurement analysis of the entire dynamic motion cycle showed no significant differences of the DRUJ position ratio in the pressure phase, but shortly, as the release phase was initiated (at 55% of the Press test motion cycle), a significant difference of 0.08 (95% CI 0.00 – 0.16) was present ($p$ = 0.045) (Figure 7.12.b).

The DRUJ position ratio at 6-month and 12-month follow-up was similar throughout the entire Press test motion cycle ($p > 0.44$) (Figure 7.12.c).

In healthy DRUJs the mean DRUJ position ratio was generally above a 0.4 ration throughout the motion cycle, and foveal TFCC injured forearms translated below this level (Figure 7.12a)

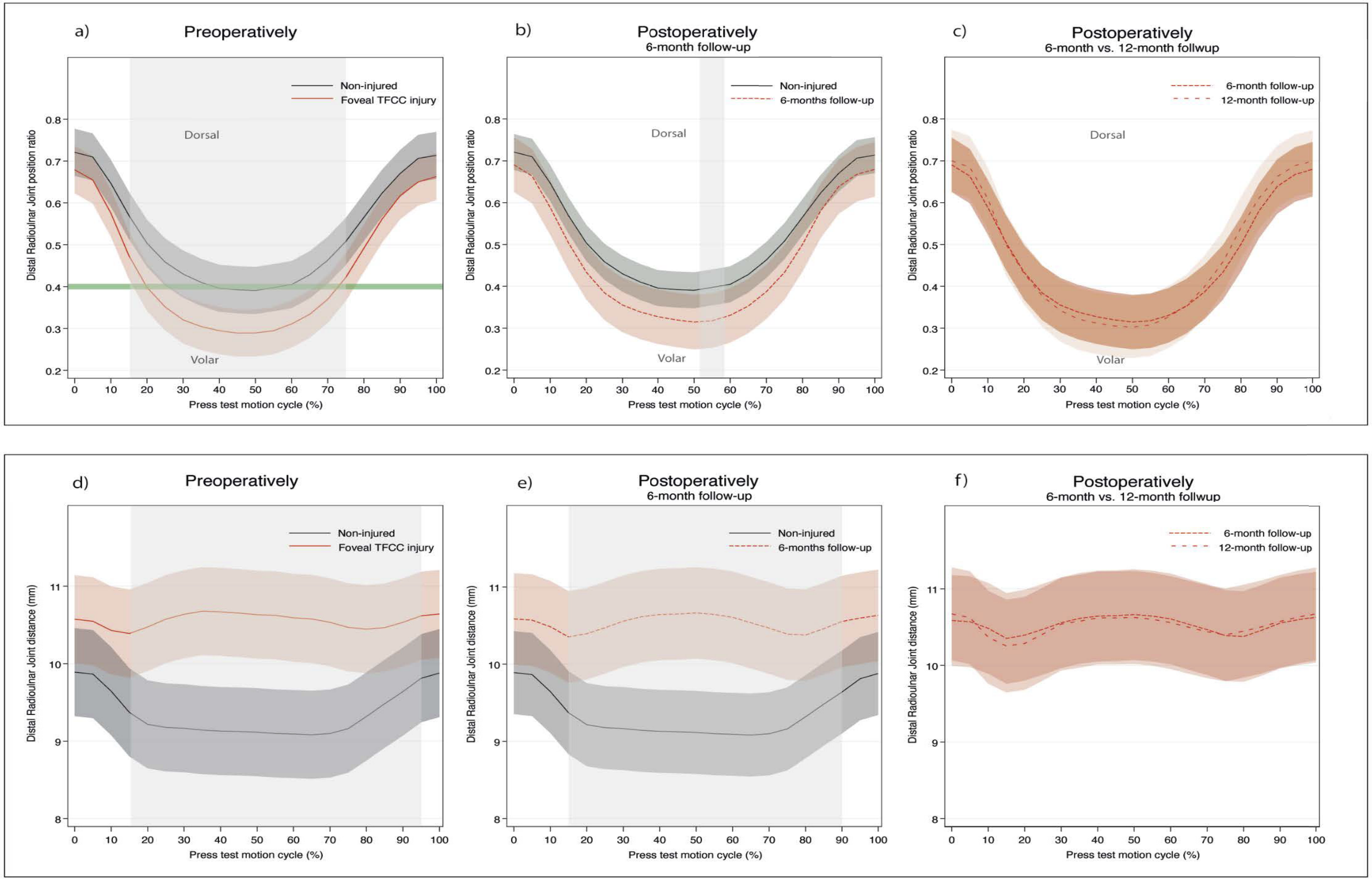


**Figure 7.11.** Dynamic kinematic outcomes including DRUJ position ratio and DRUJ distance during the Press test.
Preoperative and postoperative comparison of the distal radioulnar joint position ratio (a) and distal radioulnar joint distance (b) of patient forearms with foveal TFCC injury (red) and the contralateral asymptomatic non-injured arm (black) (means with 95% confidence intervals). Mixed model statistics was used to define parts of the Press test motion cycle with significant differences (displayed as light grey areas). Adapted from Thillemann et al. (2022).

### 7.6.7 DRUJ distance

The *preoperative* mean difference in DRUJ distance was 0.7 mm (95% CI -0.05 –1.4) wider in the arms with foveal TFCC injury compared to the non-injured forearms as the Press test was initiated (p=0.07) and maximum pressure the difference of 1.5 mm (95% CI 0.6 – 2.4) was statistically significant (p=0.002) (Table 7.12).

Repeated measurement analysis of the *preoperative* mean DRUJ distance showed a significant difference from 15% to 95% of the dynamic motion cycle, between the arms with foveal TFCC injury and the non-injured forearms (Figure 7.12.d).

*Surgical treatment* did not normalize the DRUJ distance at maximum pressure ($p > 0.21$) (Table 7.13).

Repeated measurement analysis of the entire dynamic motion cycle continuously showed a significant difference of the DRUJ distance in the downstroke pressure phase and release phase from 15% to 90% of the dynamic motion cycle, between the arms with foveal TFCC injury and the non-injured forearms (Figure 7.12.e).

The DRUJ distance at 6-month and 12-month follow-up was similar throughout the entire Press test motion cycle ($p > 0.05$) (Figure 7.12.f).

### 7.6.8 Ulnar variance

The *preoperative* increase of ulnar variance during the pressure phase was similar in arms with foveal TFCC injury, compared to the non-injured forearms ($p = 0.14$), and remained unchanged throughout follow-ups ($p = 0.31$) (Table 7.12 and 7.13).

### 7.6.9 Press test repeatability

The absolute mean difference (systematic bias) of Press test double examinations was below 0.80 kg pressure and within a prediction interval of 1.35 kg and 1.38 kg for non-injured forearms and forearms with foveal TFCC injury, respectively (p=0.80). The resulting differences of kinematic outcomes between double examinations were small and comparable for non-injured forearms and forearms with foveal TFCC injury (p>0.29).

ICC rater consistency of the kinematic outcomes were excellent ($r > .90$), with a lower limit 95% confidence interval indicating good or excellent consistency ($r > .80$) (Table 7.14).

| Table 7.14. Precision of dynamic radiostereometry (dRSA) recorded kinematic outcomes and maximum force in DRUJs with foveal TFCC injury during Press test in Study IV. | | | |
|---|---|---|---|
| *Outcome*<br>*N = 21 double examinations* | *Mean difference*<br>*(SD)* | *Prediction interval*<br>*(SD × 1.96)* | *ICC*<br>*(95% CI)* |
| Maximum force (kg) | 0.80 (0.70) | 1.38 | 0.93 (0.80 – 0.97) |
| DRUJ translation (mm) | 0.30 (0.31) | 0.62 | 0.97 (0.94 – 0.99) |
| DRUJ position ratio | 0.02 (0.03) | 0.06 | 0.98 (0.94 – 0.99) |
| Ulnar variance (mm) | 0.12 (0.09) | 0.29 | 0.91 (0.79 – 0.96) |
| DRUJ distance | 0.23 (0.18) | 0.35 | 0.97 (0.93 – 0.99) |

*The systematic biases are reported as absolute mean differences with standard deviations (SD) and prediction intervals (SD × 1.96).*
*DRUJ: distal radioulnar joint, ICC: Intraclass Coefficient (2,1) calculated as two-way mixed effects, absolute agreement to evaluate rater consistency between first and second examinations, CI: confidence interval. Adapted from Thillemann et al. (2022).*

### 7.6.10 Ultrasonography and repeatability

The ICC (2,1) rater consistency of the measured DRUJ translation by US double examinations, indicated good reliability in non-injured forearms ($r = 0.87$ (95% CI 0.72–0.95)) and moderate reliability in forearms with foveal TFCC injury ($r$ = 0.62 (95% CI 0.29–0.83)) (Table 7.15).

| Table 7.15. Precision of ultrasonography measured DRUJ translation in Study IV. | | | |
|---|---|---|---|
| <br>*N = 21 double examinations* | *Mean difference*<br>*(SD)* | *Prediction interval*<br>*(SD × 1.96)* | *ICC*<br>*(95% CI)* |
| DRUJ translation | | | |
| Healthy | 0.64 (0.50) | 0.97 | 0.87 (0.72 – 0.94) |
| Injured | 1.06 (1.04) | 2.04 | 0.62 (0.29 – 0.83) |

*Systematic bias reported as absolute mean differences with standard deviations (SD) and prediction intervals (SD × 1.96). DRUJ: distal radioulnar joint, ICC: Intraclass Coefficient (2,1) calculated as two-way mixed effects, absolute agreement to evaluate rater consistency between first and second examinations, CI: confidence interval. Adapted from Thillemann et al. (2022).*

The preoperative US measured DRUJ translation quotient (Q) for evaluation of DRUJ stability, was median 0.5 (IQR 0.3 – 0.7) in non-injured forearms and median 1.1 (0.6, 2.5) in forearms with foveal TFCC injury (p=0.02) and decreased to median 0.8 (0.4 – 1.6) one year postoperatively.

Preoperatively, the US measured DRUJ translation ($T = X_1$-$X_2$), was mean 1.7 mm (95% CI 0.6–2.9) higher in forearms with foveal TFCC injury compared to the contralateral healthy arm ($p$=0.004). DRUJs with foveal TFCC injury had a mean DRUJ translation of 3.9 (95% CI 2.9–4.9) which significantly decreased to 3.1 (95% CI 2.3–4.0) and 2.7 (95% CI 2.0–3.3), 6 months and 1 year after surgical treatment, respectively.

The DRUJ translation ratio was below the recommended pathological laxity detection cut-off (Q = 0.8) in 17 of 21 non-injured forearms (specificity 85%) and above in 12 of 21 forearms with arthroscopically confirmed foveal TFCC injury (sensitivity 57%) (Table 7.16). The positive predictive value (PPV) was 75% and the negative predictive value (NPV) was 65%.

### 7.6.11 Magnetic Resonance Imaging

Foveal TFCC injury was diagnosed on preoperative MRI of the injured wrist in 7 of 21 patients (sensitivity 33%), whereas MRI visualized foveal TFCC injury or peripheral edema was present in 15 of 21 patients (sensitivity 71%). Additionally, two patients had MRI suspected isolated distal TFCC component injury, but arthroscopy revealed a positive Hook test and lesion to the proximal TFCC component.

Table 7.16. Kinematic outcomes and agreement of ultrasonography at maximum force during the Press test in the patient's healthy DRUJ and injured DRUJ before and after surgical treatment.

| | *Non-injured* | *TFCC lesion* | | | $p$ [1] | $p$ [2] |
|---|---|---|---|---|---|---|
| | *Preoperative (n=21)* | *Preoperative (n=21)* | *6-month (n=19)* | *12-month (n=19)* | | |
| *DRUJ translation (mm)* | 2.2 (1.5–2.9) | 3.9 (2.9–4.9) | 3.1 (2.3–4.0) | 2.7 (2.0–3.3) | 0.004 | 0.01 |
| ICC (2,1) | 0.87 (0.72–0.95) | 0.62 (0.29–0.83) | | | | |
| *Hess Q-ratio (median (IQR))* | 0.5 (0.3–0.7) | 1.1 (0.6–2.5) | 0.8 (0.5–1.1) | 0.8 (0.4–1.6) | 0.02 | 0.47 |
| Specificity (Q-ratio < 0.8) | 85% | - | - | - | - | - |
| Sensitivity (Q-ratio $\geq$ 0.8) | - | 57% | - | - | - | - |

*Numbers are displayed as means with 95% confidence intervals (CI) or medians with inter quartile ranges (IQR).*

*ICC: Intraclass Coefficient (2,1) calculated as two-way mixed effects, absolute agreement to evaluate rater consistency between preoperative double examinations*

[1] *Paired t-test or Wilcoxon signed-rank test as appropriate. Preoperative comparison of healthy and injured forearm.*

[2] *Mixed or Kruskal Wallis test as appropriate. Comparison of injured forearm over time. Adapted from Thillemann et al. (2022).*

# 8 Discussion

# 8

# Discussion

## 8.1 The story of the thesis

Diagnosing DRUJ instability can be a difficult task. On one side, severe DRUJ instability is easily 'felt during the surgeons manual test. On the other side, patients typically present with less stability, which is far more difficult to 'sense' during manual tests and may cause doubt about the diagnosis.

Often, I see patients after years of complaints and persisting ulnar wrist pain. Patients who have repeatedly been reassured by medical staff, that a wrist sprain may persist for a long time or that it is an expected consequence after distal radius fracture. This may in part be owing to the challenges of evaluating the TFCC and DRUJ by clinical examination, but also due to a lack of knowledge about the TFCC as a DRUJ stabilizer and lack of valid imaging techniques for diagnosing TFCC injuries and grading of DRUJ instability.

When surgeons succeed in diagnosing DRUJ instability and treating patients by TFCC reinsertion, normal DRUJ stability may not by accomplished. This could relate to challenges in restoring the complexity of the TFCC, and numerous surgical techniques have been presented. Yet, comparing these is difficult because of the poor validity of the main outcome - manual assessment of DRUJ stability.

In this thesis, I introduce static and dynamic RSA as a new, precise, non-invasive, low radiation methodology to examine DRUJ stability and DRUJ kinematics ex vivo and in vivo. However, analyzing dRSA images is a user-intensive and time-consuming task. Thus, careful selection and validation of a single clinically relevant test (Piano

key/Press test) for evaluation of DRUJ stability in both an experimental and a clinical setting was a necessity. Using this single Piano key/Press test I described the effect on DRUJ stability of different degrees of TFCC lesion, effect of two different TFCC reinsertion/reconstruction methods, normal DRUJ kinematics in patients, and DRUJ stability before and after open TFCC reinsertion in patients.
During my 5-6 years spent on this thesis work, a lot of development and automatization with the AutoRSA software has been accomplished, which opens for investigation of more complex and functional DRUJ loaded exercises in the future.

## 8.2 Key findings

**8.2.1 Ex vivo DRUJ kinematics during a Piano key test**

Study I demonstrated the feasibility and validity of AutoRSA for analysis of RSA imaging of DRUJ translation and showed that first a lesion of the dc-TFCC and a next a combined dc/pc-TFCC lesion led to increasing DRUJ translation during a Piano key test.

**8.2.2 Ex vivo DRUJ kinematics after open TFCC reinsertion or Adams TFCC reconstruction**

Study II demonstrated that surgical treatment with foveal TFCC reinsertion stabilized the DRUJ and reduced DRUJ translation during a Piano key test whereas the Adams TFCC reconstruction did not prove a statistically significant reduction of DRUJ translation. This could potentially be reasoned by a broader variation on the DRUJ stabilizing effect with the Adams reconstruction.

**8.2.3 In vivo normal DRUJ kinematics during a hand Press test**

Study III demonstrated that the participants with asymptomatic DRUJs repeated the Press test reliably and the maximum DRUJ kinematic outcomes corresponding to maximum pressure was expected to be reached at 5 kg force application. The Press test induced a mean DRUJ translation of 4.7 mm (95% CI 4.2 – 5.5) as the ulnar head center translated from a dorsal DRUJ position ratio of 0.75 (95% CI 0.71 – 0.78) to a volar DRUJ position ratio of 0.40 (95% CI 0.33 – 0.44) (Figure 8.1 (right hand)). The ICC test-retest correlation was good or excellent for pressure application and the corresponding kinematic outcomes, respectively.

### 8.2.4 In vivo DRUJ kinematics and PROMs in foveal TFCC injured patients examined during hand Press test before and after open TFCC reinsertion

Study IV demonstrated significant changes of the DRUJ position ratio in foveal TFCC injured DRUJs compared to the asymptomatic side. The Press test induced DRUJ translation in the foveal TFCC injured DRUJs was mean 5.3 mm (95% CI 4.4 – 6.1) as the ulnar head center translated from a dorsal DRUJ position ratio of 0.68 (95% CI 0.61–0.75) to a volar DRUJ position ratio of 0.29 (95% CI 0.21–0.37) (Figure 8.1 (left hand)), which was 10 percent points more volar compared to the contralateral asymptomatic DRUJ. Furthermore, open foveal reinsertion had a stabilizing effect towards normal values at 6-month and 1-year follow-up. The ICC test-retest correlation was good or excellent for pressure application and the corresponding kinematic outcomes, and with similar precision for the injured and asymptomatic side.

The clinical results regarding grip strength and AROM were decreased in the foveal TFCC injured side compared to the asymptomatic side. After surgery, the grip strength and AROM of the injured side was not normalize to the level of the asymptomatic contralateral side, but at 1-year follow-up, the preoperative level was regained and PROMs in term of QDASH, PRWE and pain during activity were improved to the level of the minimal clinically important difference (MCID).

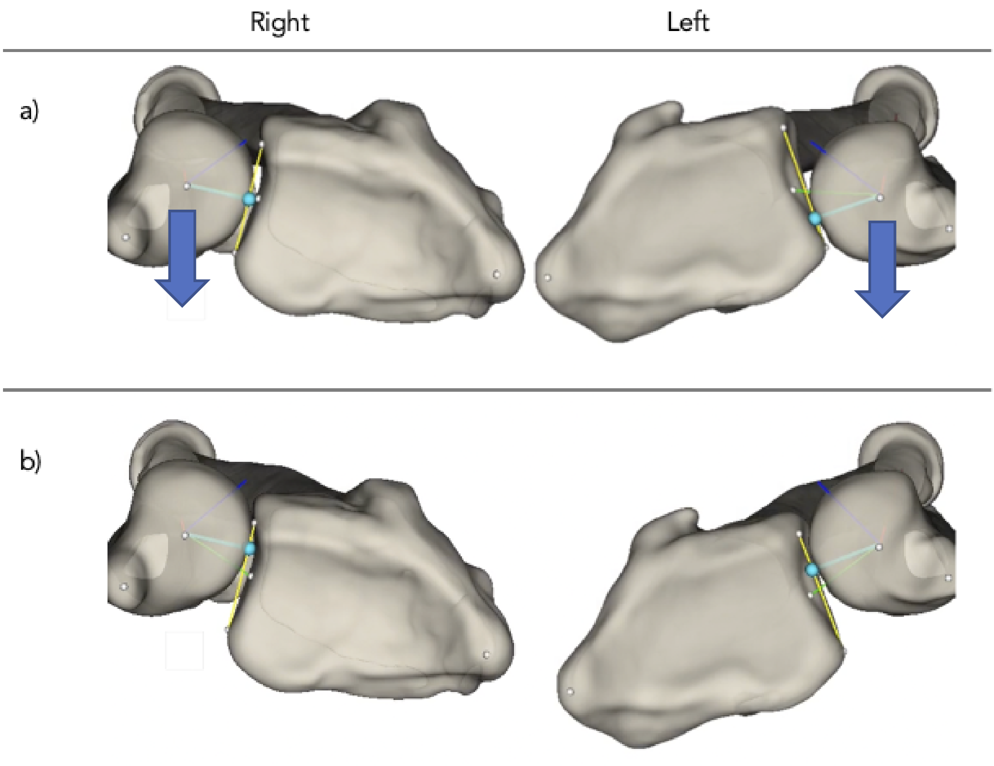


Figure 8.1. Example of DRUJ position during the Press test. The applied force result in a more volar ulnar head position in the sigmoid notch in DRUJs with foveal TFCC injury (left) compared to asymptomatic DRUJs (right). (a) Maximal force after downstroke on the weight platform and (b) with no pressure.

## 8.3 Diagnosing TFCC injury

This section includes a discussion of some of the clinical examinations, imaging modalities, PROMS and surgical options used in my daily practice and in the thesis, when evaluating patients with ulnar wrist pain and potential DRUJ instability.

There are no local or international clinical recommendations for establishing the diagnosis of TFCC injury and DRUJ instability by use of clinical examination techniques and imaging modalities. The reason may be inferiority of clinical examination and imaging, compared to arthroscopy. Even improvement of MRI scanners to 3.0 Tesla units has not improved the sensitivity and specificity of this imaging modality for TFCC diagnostics. Thus, arthroscopy remains the recommended 'gold standard' for final diagnosis of TFCC lesions despite the fact that arthroscopy is an invasive and expensive 'test'. Arthroscopy enables evaluation of the TFCC edges, retraction, and repairability, and is deemed crucial in determination of the best treatment (Figure 3.14) (Atzei et al., 2017). Proficient patient selection is highly important to limit the number of patients assigned to diagnostic arthroscopy and treatment to those with true DRUJ instability and abnormal DRUJ kinematics. Thereby, the preoperative planning including patient information and expected sick leave, time reserved for surgery, and surgical technique can be optimized.

The availability of diagnostic imaging tools is diverging and influence the clinical practice in each hospital unit. A schematic example of frequently used diagnostic tools including clinical examinations and imaging modalities is displayed in Figure 8.2.
Examination by RSA is an example of advanced diagnostics, that enable precise unbiased evaluation of DRUJ kinematics and stability before and after surgery. Despite the fact that dynamic RSA equipment including image processing methods is only available in a few centers worldwide, dynamic RSA have a justification for investigation of the precise objective DRUJ stabilizing effect of different or new surgical methods for TFCC reinsertion/reconstruction. RSA has been recommended in the phased introduction for new joint implants or surgical techniques before introduction to the commercial marked (Nelissen et al., 2011).

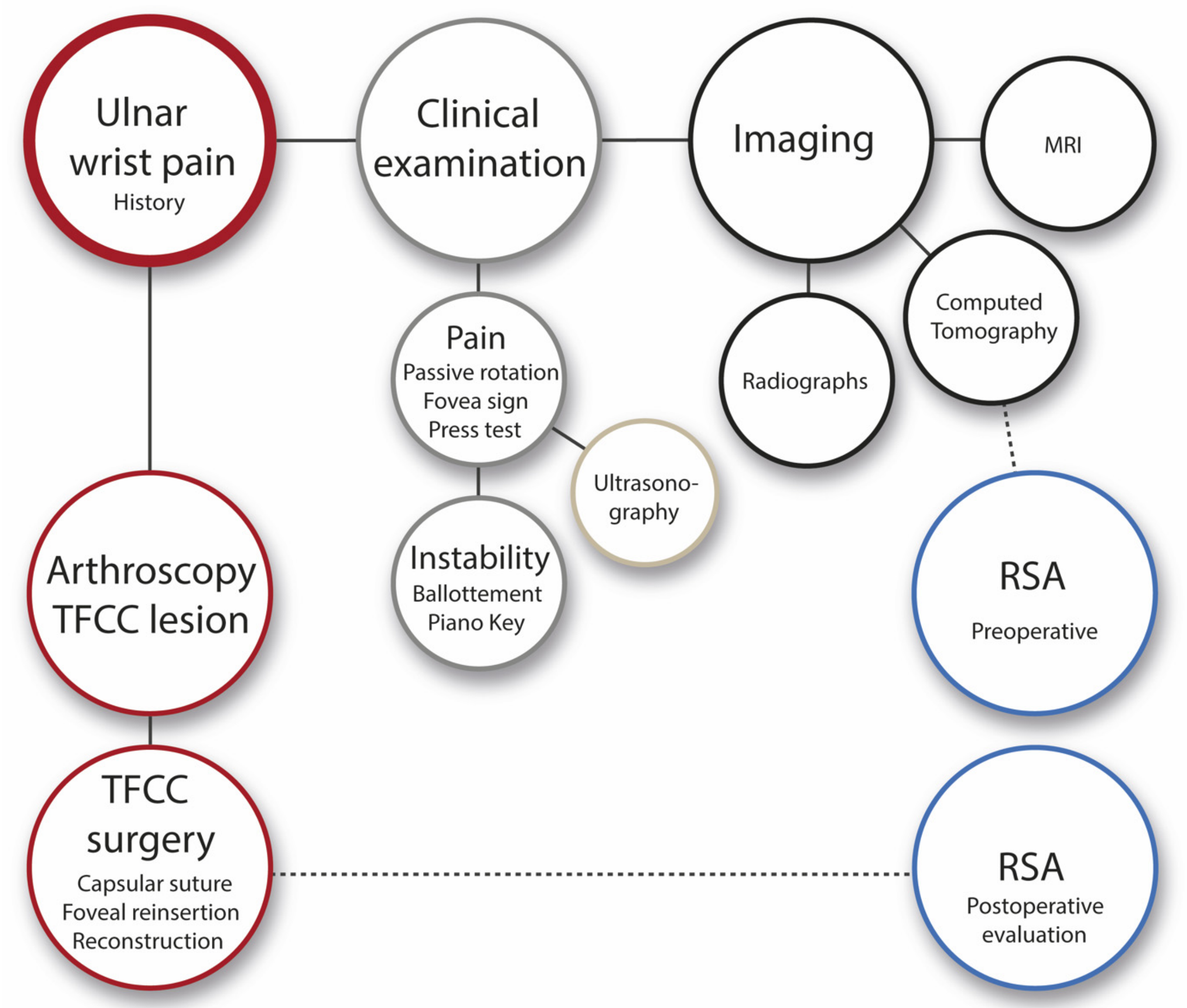


Figure 8.2. Schematic illustration of a clinical pathway to diagnose and treat a patient with ulnar wrist pain due to TFCC lesion. Solid lines indicate an example on a patient examination flow. RSA may be a useful 'ad on' for evaluation of surgical treatments or as a new diagnostic tool.

### 8.3.1 Clinical examination of DRUJ instability

Clinical examination is always available and 'right by the hand'. Many diagnostic tests for ulnar wrist pain exist. The *Ballottement test* is the most widely used test to diagnose and grade DRUJ instability by evaluation of DRUJ translation (anterior to posterior) in neutral forearm rotation, supination, and pronation. However, all three forearm positions are rarely described in publications. The detected grade of DRUJ instability is highly observer depended. Thus, the repeatability for one examiner and reproducibility between different examiners are disappointing, and the diagnostic value of the test, remains debated (Jupiter, 2009; Kim and Park, 2008; Lindau et al., 2000; Szabo, 2006).

Lindau et al., (2002) reported a moderate inter-rater agreement of the Ballottement test to detect DRUJ instability ($k$ = 0.66; 95%CI 0.36–0.95), and in comparison with arthroscopic findings the Ballottement test had moderate ability to diagnose instability due to complete foveal TFCC injuries (sensitivity=0.59), but excellent ability to rule out instability in wrists without foveal TFCC injury (specificity=0.96) (Lindau et al., 2000). In Study IV, clinical suspicion of DRUJ instability by the *Ballottement test* and arthroscopic foveal TFCC lesion were inclusion criteria. Thus, there is a risk of having excluded patients due to a misinterpreted negative Ballottement, as all patients did not undergo arthroscopy, and the true sensitivity and specificity cannot be evaluated in this study.

In Study IV, the sensitivity of the *Piano key sign test* was 57% as only 12 of 21 patients was evaluated as positive. The *Piano key sign test* was performed in full pronation. According to Hagert et al. (1994) and Xu and Tang (2009), the pronated DRUJ is stabilized mainly by the proximal component (pc) of the volar RUL that prevents dorsal ulnar head protrusion. Any lesions with instability owing predominantly to the proximal component (pc) of the dorsal RUL, which is the main stabilizer in supination, may therefore not be revealed during *Piano key sign test*, which may in turn explain the reduced Piano key sign sensitivity.

In conclusion, clinical examination must be focused on examining both proximal and distal, dorsal and volar TFCC components. Among hand surgeons DRUJ instability testing has received increasing attention during the last decade. The modest sensitivity and reliability of the *Ballottement test and Piano key test* may be explained by the fact that TFCC lesions have different injury patterns and cannot be regarded as simple as positive or negative. Rather, the lesion types must be differentiated and appreciated in the treatment planning. Likewise, the stability achieved after surgery, can likely not be evaluated as positive or negative. Nevertheless, this is the most common way to report effect on DRUJ stability after surgical interventions in the literature. Robba et al. (2020) conducted a systematic review and in the 7 included studies the postoperative DRUJ stability after open TFCC repair was reported to be achieved (by a variety of different testing techniques) in 84% (76/90) of patients and in 86% (129/150) following arthroscopic repair.

### 8.3.2 Clinical examination of grip strength

*Grip strength* is an easy quantitative test to apply in the clinical setting and frequently used to evaluate upper extremity function after hand surgical interventions. DRUJ instability can lead to pain and decreased *grip strength* (Adams and Berger, 2002; Adams and Lawler, 2007). Since grip strength and pain typically correlate well, grip strength can be a reliable tool to follow patient's postoperative outcome. The test-retest reliability is excellent ($r > 0.90$). In distal radius fractures, the grip strength MCID is

20% of the non-injured contralateral side (Kim et al., 2014). However, in TFCC injured populations the MCID in has not been reported.

In Study IV, the grip strength of the hand with foveal TFCC injury was mean 39 kg, and 87% of the asymptomatic contralateral hand. At 1-year after surgery the grip strength was similar to the preoperative level, but the grip strength of the asymptomatic contralateral hand (45 kg (95% CI 39-51)) was not reached (Table 8.1) (Thillemann, 2022).

The reported grip strength in studies with *open foveal TFCC reinsertion* is divergent. Often the grip strength improves above the 20% MCID level but reach only 87%-91% of the grip strength in the asymptomatic contralateral hand, and is in line with the findings reported in Study IV (Table 8.1) (Chou et al., 2003; Hermansdorfer and Kleinman, 1991; Moritomo et al., 2010).

Table 8.1. List of studies reporting clinical outcomes and PROMS after open foveal TFCC reinsertion.

| *Author* | *Year* | *Method* | *N* | *FU* | *Preoperative* | | | *Postoperative* | | |
|---|---|---|---|---|---|---|---|---|---|---|
| | | | | | *Grip[1]* | *DASH[2]* | *Pain[3]* | *Grip[1]* | *DASH[2]* | *Pain[3]* |
| Study IV | (2021) | Open | 19 | 14 | 39kg/87% | 39* | 5** | 40kg/89% | 25* | 2** |
| *Randomizes studies comparing open and arthroscopic treatment* | | | | | | | | | | |
| Anderson et al. | (2008) | Bone tunnels | 39 | 53 | 72% | - | - | 73% | - | - |
| Luchetti et al. | (2014) | Bone anchor | 24 | *31* | 20kg | 58 | 7 | 22kg | 36 | 4 |
| *Prospective cohorts/retrospective cohorts* | | | | | | | | | | |
| Hermansdorfer | (1991) | Bone tunnels[5] | 10 | 25 | - | - | - | 87% | - | - |
| Chou et al. | (2003) | Mini open | 11 | 48 | 23kg | - | - | 37kg/88% | - | - |
| Morimoto et al. | (2010) | Bone anchor | 10 | 28 | 18kg/52% | - | - | 91% | - | - |
| *Open TFCC reconstruction (resembling Adams reconstruction (2000))* | | | | | | | | | | |
| Adams & Berger | (2002) | Tendon graft | 14 | 26 | - | - | - | 85% | - | - |
| Gills et al. | (2019) | Tendon graft | 95 | 65 | 22kg/69% | - | - | 24kg/77% | - | - |
| Seo et al. | (2009) | Tendon graft | 16 | 19 | 32kg | 34.5 | - | 37kg | 10.5 | - |
| Meyer et al. | (2017) | Tendon graft | 37 | 16 | 39kg | - | - | 39kg | - | - |
| Shih & Lee | (2005) | Tendon graft | 37 | 36 | 65% | - | - | 90% | - | - |
| Hess et al. | (2016) | Tendon graft | 11 | 12 | - | - | - | 35kg/82% | - | - |

*FU: Mean Follow-up time after surgical treatment I month.*

[1] *Reported in kg or percentage of the contralateral non-injured hand,* [2] *Reported as DASH score or QDASH* score,*

[3] *Pain reported on VAS or NRS scale at maximum stress (ranging from 0 to 10, with 0 being no pain and 10, maximum pain),*

[4] Additional stabilizing k-vires. ***Pain reported as median NRS score during lifting >5 kg*

Contrary, *arthroscopic foveal TFCC reinsertion* has been reported to increase the grip strength to the level of the contralateral hand (98%-106%) (Atzei, 2009; Atzei et al., 2008; Iwasaki et al., 2011; Kim et al., 2013; Park et al., 2018; Shinohara et al., 2013) (Table 8.2). This finding, favoring arthroscopic treatment, was however not confirmed in the single randomized controlled trial that has compared open and arthroscopic foveal TFCC reinsertion (osseous). No significant improvement of grip strength was reported 31 months after surgery, with neither the open and nor the arthroscopic approach (Luchetti et al., 2014).

Table 8.2. List of studies reporting clinical outcomes and PROMS after arthroscopic foveal TFCC reinsertion.

| *Author* | *Year* | *Method* | *N* | *FU* | *Preoperative* | | | *Postoperative* | | |
|---|---|---|---|---|---|---|---|---|---|---|
| | | | | | *Grip* [1] | *DASH*[2] | *Pain* [3] | *Grip* [1] | *DASH*[2] | *Pai3*[4] |
| *Randomizes studies comparing open and arthroscopic treatment* | | | | | | | | | | |
| Anderson et al.[4] | (2008) | Capsular | 37 | 32 | 66% | - | - | 71% | - | - |
| Luchetti et al. | (2014) | Anchor DF portal | 25 | 31 | 22kg | 39 | 7 | 24kg | 23 | 3 |
| *Prospective cohorts/retrospective cohorts* | | | | | | | | | | |
| Atzei et al. | (2008) | Anchor DF portal | 18 | 18 | 73% | - | 8.3 | 90% | 10.5 | 1.2 |
| Iwasaki et al. | (2011) | One tunnel | 12 | 30 | 93% | 60 | | 106% | 8 | - |
| Shinohara et al. | (2013) | Two tunnels | 11 | 30 | 84% | - | - | 98% | - | - |
| Kim et al. | (2013) | Anchor DF portal | 15 | 29 | 79% | 28 | - | 83% | 17 | - |
| Atzei et al. | (2015) | Anchor DF portal | 44 | 33 | 93% | 42 | - | 103% | 15 | - |
| Park et al. | (2018) | One tunnel | 16 | 31 | 57% | 35* | 3.7 | 80% | 10* | 0.8 |
| Kwon et al. | (2020) | One tunnel | 8 | 15 | - | 47* | 5.9 | - | 12* | 1.5 |
| Kermarrec et al. | (2020) | All inside anchor | 5 | 29 | - | 59* | 6.8 | 36kg/94% | 18* | 0.4 |
| *Open TFCC reconstruction (resembling Adams reconstruction (2000))* | | | | | | | | | | |
| Tse et al. | (2013) | Tendon graft | 15 | 86 | 56% | - | 6.6 | 77% | - | 3.2 |
| Mak and Ho | (2017) | Tendon graft | 28 | 62 | 59% | - | 5.9 | 72% | - | 3 |
| Luchetti & Atzei | (2017) | Tendon graft | 11 | 68 | 13kg/54% | 48 | 4 | 20kg/96% | 25 | 2 |
| Yeh & Shih | (2021) | Tendon graft | 67 | 32 | 37% | - | 6.2 | 83% | - | 1.6 |

*DF: Direct foveal portal; FU: Follow-up time after surgical treatment, DF: distal foveal, FU: Mean Follow-up time after surgical treatment I month.*

*[1] Reported in kg or percentage of the contralateral non-injured hand.*

*[2] Reported as DASH score or QDASH* score.*

*[3] Pain reported on a VAS or NRS scale at maximum stress (ranging from 0 to 10, with 0 being no pain and 10, maximum pain*

*[4]Randomized trial comparing Open vs. Arthroscopic outside-in suture of the TFCC to the capsule (not foveal reinsertion).*

Anatomical *TFCC reconstruction* of chronic unrepairable TFCC lesions as described by Adams (2000) is commonly performed by an open approach (Gillis et al., 2019; Hess et al., 2016; Meyer et al., 2017; Seo et al., 2009; Shih and Lee, 2005), but has also been modified to less invasive arthroscopically assisted approaches (Chu-Kay Mak and Ho, 2017; Luchetti and Atzei, 2017; Tse et al., 2013; Yeh and Shih, 2021). However, normalization of grip strength to the level of the contralateral non-injured hand after TFCC reconstruction is rarely reported (Tables 8.1 and 8.2).

In conclusion clinical examination of *grip strength* in DRUJ instable patients is expected to remain reduced in comparison to the contralateral hand. Surgical treatment by arthroscopic foveal TFCC reinsertion and TFCC reconstruction is gaining more interest and is used increasingly over open surgical TFCC reinsertion, but it has yet to be proven to provide benefits in terms of grip strength, when compared to open surgery. Alternatively, forearm torque strength may be more suitable for evaluation of DRUJ pathology than grip strength as Axelson et al. (2020) recently concluded that forearm torque strength was more responsive to change after DRUJ arthroplasty than grip strength.

**8.3.3 Ultrasonography examination of DRUJ instability**

*Ultrasonography* is also an easily accessible examination option for the clinician.
Hess et al. (2012) found good inter-observer correlation ($r = 0.83$) of US measured DRUJ translation. The method relies on static imaging to capture the endpoints of the true dynamic DRUJ translation excursions. In Study IV, the intra-rater repeatability of US was evaluated in TFCC injured patients ($r = 0.62$), but the level of correlation estimated by Hess et. al ($r = 0.83$) was not reproduced as only moderate agreement was found.
Hess et al. proposed a ratio ($Q = [X_1\text{-}X_2]/X_1)$) to determine the presence of DRUJ instability. By setting a cut-off level at Q = 0.8 they reported a sensitivity of 88% and a specificity of 81%. In study IV the specificity was similar (85%), but the sensitivity for detecting foveal TFCC injuries and DRUJ instability was less good (57%).
In clinical practice the impression of dorsal ulnar head protrusion and increased DRUJ translation during the Press test can be seen in DRUJ unstable wrists compared to the contralateral healthy. Thus, an active patient performed test, would expectedly reveal such increased DRUJ translation. However, the US examination of the Press test depend on capturing maximum DRUJ translation in one static image, exactly at maximum press force, and with the transducer in the same position as during rest. This may lead to underestimation as well as unprecise measurements.

**8.3.4 MRI examination of TFCC lesions**

The field strength of wrist MRI has been 1.5 Tesla during the past decade whereas new and stronger 3.0 Tesla MRI scanners first recently has been introduced in Danish institutions. As image quality is improved by 3.0 Tesla MRI, better diagnostic accuracy has been hypothesized (Saupe et al., 2005) but not uniformly been confirmed (Anderson et al., 2008; Boer et al., 2018).

In Study IV, all patients were diagnosed with foveal TFCC lesion by arthroscopy. However, the preoperative MRI scans visualized high intensity areas (peripheral edema) at the fovea on T2 weighted images and detected up to 71% of these TFCC lesions. All scans were performed using dedicated hand coils on 1.5 Tesla or 3.0 Tesla MRI scanners. In other studies using 1.5 Tesla MRI units, dedicated wrist coils, and specific TFCC protocols, TFCC lesions were visualized with varying sensitivity ranging from 67% up to 100% and a specificity from 71% up to 100% when compared to the 'gold standard', wrist arthroscopy (Andersson et al., 2015; Boer et al., 2018; Lee et al., 2013; Zlatkin and Rosner, 2006).

In clinical practice the combination of clinical examination and MRI examination is often used to diagnose and classify TFCC lesions and the resultant instability. Prosser et al. (2011) evaluated the accuracy of clinical examination and the incremental value of adding an MRI examination when patients presented with ulnar sided wrist pain. They found a statistically significant increase in the percentage of patients diagnosed correctly with suspected TFCC lesion (from 73% to 86%) and the number needed to MRI scan to make one additional correct diagnosis was 8 patients. However, diagnosing DRUJ instability did not benefit from supplemental static MRI scans (from 73% to 71%). The reference standard was wrist arthroscopy.

In conclusion, *MRI* is subjective as it depends on the observer and demand dedicated radiologist to detect TFCC lesions with high sensitivity. However, MRI does play an important role in hand surgical diagnostics - despite varying sensitivity for TFCC lesions and inability to evaluate DRUJ instability - because MRI is useful for detecting or ruling out other pathological findings causing wrist pain and disability.

#### 8.3.5 Computed tomography scans for detection of DRUJ instability

Axial reconstruction of CT scans is another imaging modality used to evaluate subluxation and instability of the DRUJ. The scans are performed with patients either seated or in the supine 'superman position' and visualize static axial reconstructions of the DRUJ in passive supinated and pronated positions. Most CT based methods for evaluation of DRUJ subluxation has limited inter-observer reliability (Lo et al., 2001; Park and Kim, 2008; Wijffels et al., 2016) and the congruency and Mino methods have been associated with high false positive rates (Chiang et al., 1998; Nakamura et al., 1996).

The RUR method use the ulnar head center for evaluation of DRUJ subluxation. In an ex vivo study, Lo et al. found the RUR method superior to the Mino and Epicenter methods for detection of slight instability in the DRUJ when the TFCC structures was sectioned successively (Lo et al., 2001). The RUR method is based on 2D axial anatomical landmarks resembling the exact same landmarks as used in this thesis to define the DRUJ position ratio, however as 3D anatomical landmarks.
The CT based RUR method for detection of DRUJ subluxation was not reported in this thesis, as static imaging of an unprovoked joint may not reveal the instability in patients with minor instability or dynamic instability (Tay et al., 2007), but as the RUR method (Figure 8.3) resembles the DRUJ position ratio, it will be discussed further in the following section on DRUJ kinematics.

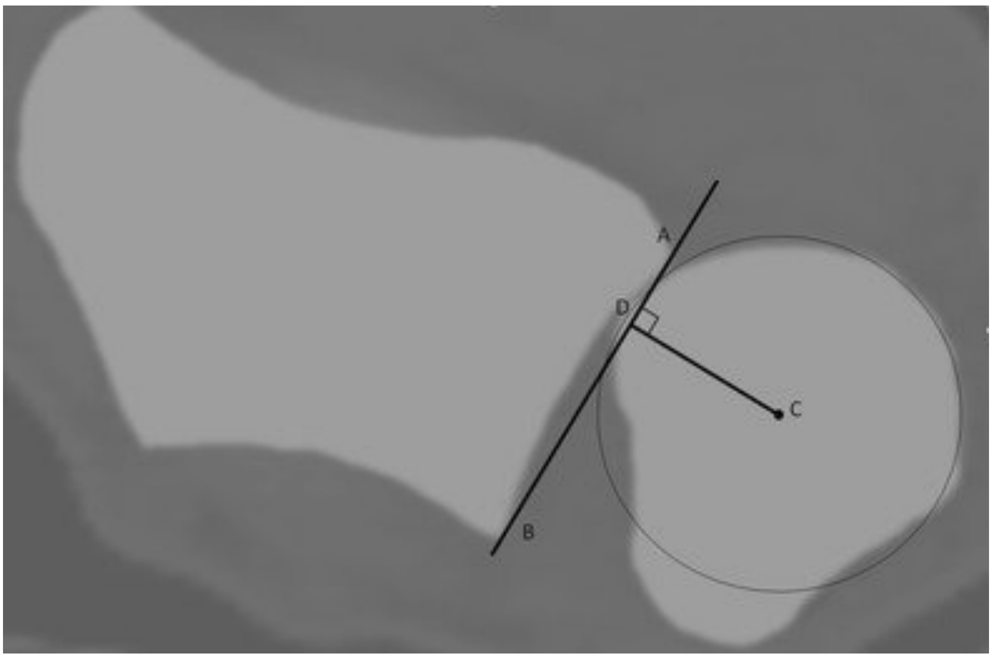


Figure 8.3. The radioulnar ratio method (RUR). The ratio is calculated as RUR=AD/AB. The sigmoid notch length is measured (length AB) and a perpendicular line from the ulnar head center defines the point D. (Wijffels et al., 2016).

## 8.4 Evaluation of DRUJ kinematics

The selection of a test/exercise to be examined by RSA in this thesis, was influenced by practical feasibility of sRSA in the experimental setting, and the feasibility of patients to actively perform the test while simultaneously being recorded by dRSA imaging. Further, the consideration was to select a test/exercise that resembled a clinical examination (i.e., the Piano key test) or patient performed symptom giving exercise (i.e., the Press test - pushing up from a chair or forearm rotation). The assumption was that dynamic recording of an active patient performed test by dRSA would capture the extremes of the motion range and the positions associated with 'giving way' symptoms. Further, the kinematic outcomes selected for evaluation should resemble the DRUJ motions allowed by the joint anatomy and be equivalent to measures used to evaluate clinical examination (DRUJ translation) and imaging (DRUJ position ratio and ulnar pistoning). These kinematic outcomes will be discussed in the following section.

### 8.4.1 DRUJ translation

The DRUJ translation has been studied ex vivo in cadavers and in vivo, by numerus methods using i.e., magnetic tracking devises, external mounted rigs, and ultrasound (Hess et al., 2012; Iida et al., 2014; Nagata et al., 2013; Omokawa et al., 2017; Onishi et al., 2017; Pickering et al., 2016).

*The Ballottement test* is the most often used test in clinical examination of DRUJ stability. In unstable DRUJs, the feeling of endpoint resistance is 'soft' compared to the 'firm' feeling in the stable DRUJ. The DRUJ translation is used as a measure to evaluate whether the DRUJ is stable or unstable. The following grading categories of the Ballottement test have been proposed (Atzei et al., 2008):

1) normal or slight instability (<5 mm)
2) mild instability (between 5-10 mm)
3) severe instability (above 10 mm)

In an *ex vivo study* Onishi et al., (2017) reported a 9.8 mm (SD 4.1) DRUJ translation by the Ballottement test in neutral rotated forearms on five TFCC intact wrists. Electromagnetic tracking devices were placed on the examiners thumb nails and the measures may include rotation and soft tissue movement. Iida et al. (2014) and Omokawa et al. (2017) inserted electromagnetic sensors into the distal radius and ulna after removal of the soft tissues, but sparing of the TFCC. The translation by the

Ballottement test in neutral rotated forearms ranged from 6.7 mm (SD 2.3) to 7 mm (SD 3). Rigo et al. (2021) applied up to 50N force by an Hydraulic Machine (Instron 8871, Canton, MA), and after removing soft tissues, but sparing the TFCC, 7.3 mm (SD 2.4) AP translation was detected in neutral rotated forearms.
Nagata et al. (2013) designed a custom '*rig*', inspired by the KT1000 manual arthrometer used for assessment of cruciate ligament stability in knees, and used it to measure DRUJ translation. However, *'the rig'* does not allow for evaluation of end-point resistance. '*The rig'* was validated ex vivo and thereafter used to asses' normal values in non-injured DRUJs and DRUJ instability in patients. The intra-tester consistency was good ($r$ = 0.83) and the inter-observer correlation was excellent ($r$ = 0.91). In neutral forearm rotation, the DRUJ translation was mean 6.5 mm (SD 1.0) in patients non-injured DRUJs. With the forearm maximally pronated, *'the rig'* measured DRUJ translation was 4.2 mm (SD 0.6) in non-injured DRUJs and 7.0 mm (SD 0.5) in unstable DRUJs (Nagata et al., 2013; Pickering et al., 2016). Despite good reliability, these measures may be an overestimation of DRUJ translation as they include soft tissue movement and a degree of forearm rotation.
In general ex vivo estimates of DRUJ translation in neutral forearm rotation were above the 5 mm limit for normal DRUJ translation suggested by Atzei et al. (2008).

The *ultrasonography* based method for evaluation of DRUJ translation was first described by Hess et al. (2012), with the patient seated in a standardized position with approximately $30^0$ forearm pronation. The inter-observer correlation was reported as good ($r$ = 0.83). In non-injured DRUJs the translation (unidirectional measure) was 2.5 mm (SD 1.03) and 5.1 mm in unstable DRUJs. A difference of 1 mm was suggested to be pathological. Using the US method for evaluation of TFCC reconstructed patients, surgery improved the DRUJ translation from 5.2 mm (SD 1.5) to 3.5 mm (SD 1.7).
Later, Yoshii et al. (2019) used US for estimation of DRUJ translation to assess healthy volunteers but induced the translation by a 'pressure-monitor ultrasound system'. The estimated DRUJ translation was below 1 mm. Thus, this passive testing system may not resemble the DRUJ translation well, but the force/DRUJ translation ratio estimate may be useful for evaluation of endpoint resistance, as displacement may be induced with less force in DRUJs without sufficient ligament stability.

The *radiostereometry* based method evaluated DRUJ translation during the Piano key test (unidirectional measure). In *Study I,* only 1.36 mm translation of the ulnar head was induced with intact TFCC in the pronated forearm, which increased to 2.3 mm after foveal TFCC lesion. All soft tissues were spared, and ligament lesions were performed minimally invasive under fluoroscopic guidance.

In *Study II,* the DRUJ translation induced by the Piano key test was reduced significantly (by 1.78 mm (95% CI 0.82–2.74)) after foveal TFCC reinsertion, but not after Adams TFCC reconstruction (1.01 mm (95% CI -1.58–3.60)). The Adams reconstruction had high variation in the stabilizing effect and no statistically significant difference was found between the two methods. In an ex vivo study on forearms with neutral rotation, Rigo et al. (2021) used a hydraulic machine to test and compare the stabilizing effect of two Adams TFCC reconstruction tecniques:
Adams TFCC reconstruction with suture tape augmentation of the tendon graft and DX SwiveLock SL anchor fixation (Arthrex, Naples, FL) had a significantly better stabilizing effect and reduced DRUJ translation by 2.51 mm (SD 1.31) mm, compared to Adams TFCC reconstruction with tendon graft alone, which reduced DRUJ translation by 0.46 mm (SD 1.94).
Using an Electromagnetic tracking device in at cadaver set-up with pronated forearms, Heitner et al. (2020) detected an improvement of DRUJ translation of 8.4 mm (SD 3.6) after Adams reconstruction of TFCC and IOM injured.

In Study III and IV, the *ultrasonography-based* evaluation of DRUJ translation was 2.2 - 2.3 mm in non-injured joints and 3.9 mm in unstable DRUJs. Surgical reinsertion of the foveal TFCC improved the DRUJ translation to 2.7 mm at 1-year follow-up.
The test-retest agreement of dRSA was excellent both in non-injured DRUJs ($r$ = 0.93) and in DRUJs with foveal TFCC injury ($r$ = 0.97) and resemble or exceed the test-retest coefficients reported for 'the rig' (Nagata et al., 2013) and US-based measurements (Hess et al., 2012).
In *Study IV*, the Press test induced DRUJ translation measured by dRSA was 4.4 mm in the non-injured DRUJ and 5.3 mm in the DRUJ with foveal TFCC injury. Surgical reinsertion of the foveal TFCC in patients did not change the DRUJ translation statistically significantly at 1-year follow-up (Thillemann, 2022; Thillemann, 2021b).

DRUJ translation measures varies much in the literature. Ex vivo studies resemble the time zero stability achieved in patients, and DRUJ stability testing after TFFC surgery in cadavers will induce some stretching on the area of repair. However, it is unknown and questionable if the measured stabilizing effect ex vivo is translational to what can be achieved in patients using live tissue that change of biomechanical properties postoperatively. It has been shown that tendon grafts undergo histological and microarchitectural changes in vivo during a 'ligamentization' period (Claes et al., 2011). Reinsertion of the TFCC remnant to the fovea on the ulnar head is a direct repair and it is unknown if biomechanical properties change in the repair area over time and if the stability that is achieved during surgery is maintained its over time.

The dRSA method only assess bone kinematics and thus overcomes the soft tissue bias seen in other methods. However, active patient performed testing relies on patient compliance and ability to 'relax and allow instability and discomfort to happen' during the test. Despite careful instructions to perform the Press test with a relaxed DRUJ using active elbow extension, patients may involuntarily activate DRUJ muscular stabilizers and avoid a 'giving way' pain. This may reduce the measured DRUJ translation during testing in clinical studies.
The flooring effect detected when applying the Press test in Study III indicate that the test can be simplified to static measures in the unloaded pronated position and at maximum pressure exceeding 5 kg (Figure 7.5.). However, there is a risk of missing the outmost extreme DRUJ positions during static testing.

In conclusion, examinations based on bony measures eliminate soft tissue bias and consequently the translation estimates are lower. Using US and dRSA based measures on the same participant/patient cohort and a similar press-test activity revealed higher DRUJ translation measures were achieved with the dRSA method. Contrary to US, dRSA is semi-automated and operator and experience independent. Ultrasonography bears the advantage of easy accessibility to evaluate DRUJ translation in vivo, but the true endpoint and maximum translation may not be captured and dynamic DRUJ kinematics cannot be derived and mapped with US.

### 8.4.2 DRUJ position ratio

Several studies have used *CT-based methods* (described in chapter 8.2.5) to evaluate DRUJ subluxation as a diagnostic criterion of DRUJ instability. Lo et al. (2001) reported the radioulnar ratio (RUR) method to be superior compared to other CT based measuring methods, as the intra-observer and inter-observer reliability was higher. The intraclass correlation coefficients for the RUR method were 0.89 and 0.87, respectively.
The RUR method is a 2D axial slice dependent method that resemble the 3D measured DRUJ ratio in this thesis, as similar anatomical landmarks are used. The 2D detection of anatomical landmarks can however be challenging. The axial slice displaying the

largest sigmoid notch including Lister's tubercle should be selected (Wijffels et al., 2016), but in practice this does not uniformly represent a well-defined ulnar head, and slice thickness may further challenge the selection of a representative slice for measurements (Figure 8.4). In patients with malunion, previous fracture or abnormal ulnar variance this may be even more difficult.

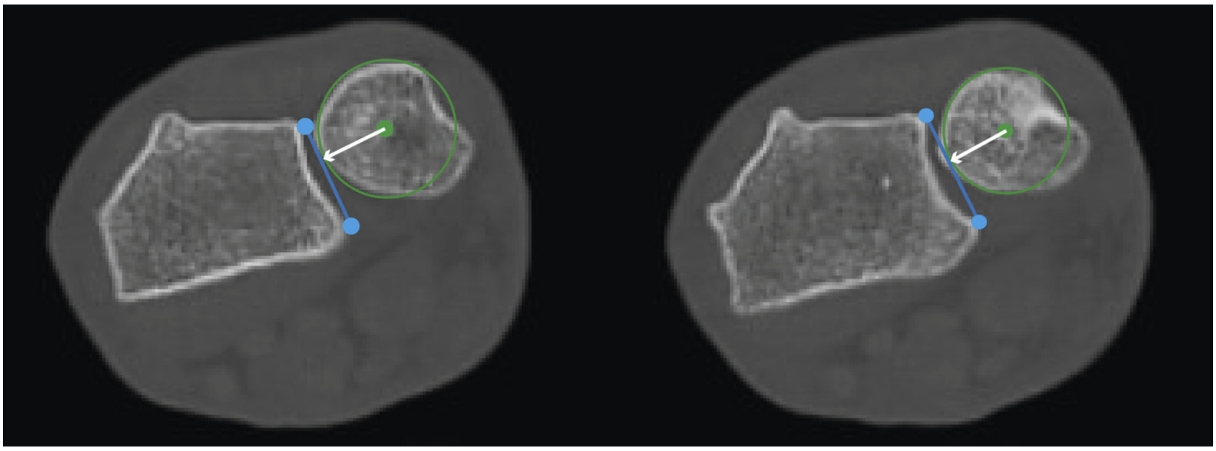

**Figure 8.4.** The radioulnar ratio (RUR)method applied on two different axial CT slices of the same patient and examination sequence, both represent a large sigmoid notch and including Lister's tubercle, but the RUR is diverging.

In non-injured DRUJs Lo et al. reported a RUR normal value of 0.60 (+/- 2SD: 0.50-0.71) in pronated forearms. Others reported a higher upper prediction interval limit for RUR normal values in non-injured forearms (Park and Kim, 2008; Wijffels et al., 2016) (Table 8.3).

Table 8.3. List of in vivo studies reporting DRUJ translation based on static axial CT reconstructions of the DRUJ with forearm pronation

| *Author* | *Year* | *Radio-ulnar ratio (RUR)* | | | | *ICC (95% CI)* | |
|---|---|---|---|---|---|---|---|
| | | *N* | *Mean* | *Min* | *Max* | *Inter-observer* | *Intra-observer* |
| *Non-injured DRUJs* | | | | | | | |
| Study IV[1,4] | 2021 | 21 | 0.72 | 0.55 | 0.89 | 0.95 (0.91 – 0.98) | |
| Lo et al. [2] | 2001 | 13 | 0.60 | 0.50 | 0.71 | 0.87 (0.83-0.91) | 0.89 (0.85-0.92) |
| Park and Kim[2, 3] | 2008 | 45 | 0.66 | 0.48 | 0.86 | 0.72 | 0.86 |
| Wijffels et al. [2, 3] | 2016 | 46 | 0.58 | 0.39 | 0.77 | 0.30 (-0.10-0.62) | 0.65 (0.45-0.79) |
| *Instable DRUJs* | | | | | | | |
| Study IV[1,4] | 2022 | 21 | 0.68[*] | 0.38 | 0.98 | 0.98 (0.94 – 0.99) | |

[1] Measured by RSA in 3D (ICC values only reported at maximum pressure), [2] Measured by axial CT slices in 2D, [3] Report upper and lower 95% confidence interval, not prediction interval, [4] ICC at maximum force during Press test is displayed. Min/Max: mean +/- 2SD.

[*]No significant difference compared to the contralateral DRUJ.

Following the diagnostic criterion of the CT based RUR method, dorsal subluxation is present if the RUR value is above the normal upper prediction interval, in pronation. Thus, Park and Kim (2008) recommended to use the broader range of normal values described in their study to reduce the risk false positive findings.

In Study IV, the *pronated and unloaded* mean DRUJ position ratio in non-injured DRUJs, exceeded the reported mean RUR values, but the normal prediction interval resembled the normal values suggested by Park and Kim (2008) (Table 8.3.) (Figure 8.5.)

In Study IV, the patients with foveal TFCC injured DRUJs had an even broader prediction interval of the DRUJ position ratio (Figure 8.5.).

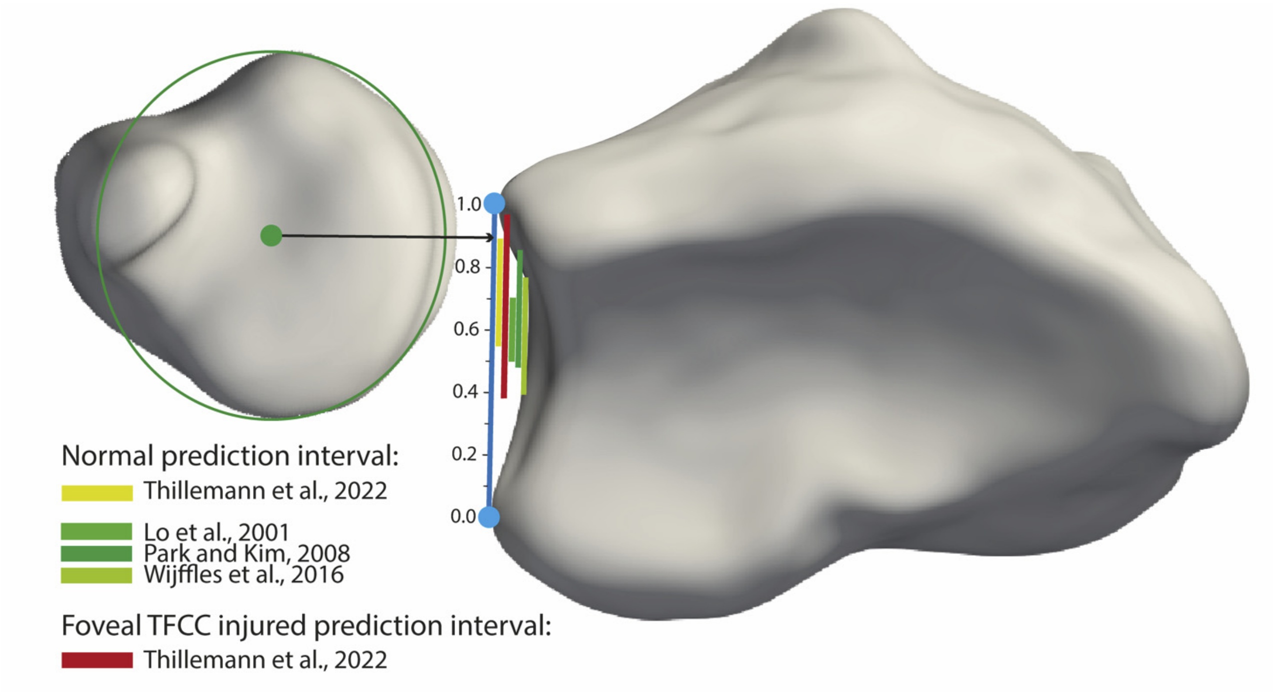


**Figure 8.5.** Normal values of the 2D CT based radioulnar ratio (RUR) and the equivalent 3D dRSA based DRUJ position ratio.

No studies in vivo have previously reported the predictive RUR values in unstable DRUJs with arthroscopic confirmation as a reference standard. Further, the degree of forearm pronation during the examination is not reported in CT-based studies. In pronation, the DRUJ articulation point slides dorsally in sigmoid notch and vice versa in supination (Chen and Tang, 2013; Gammon et al., 2018; Matsuki et al., 2010). Thus, diversity of RUR values and DRUJ position ratios could be an effect of differences in degree of forearm pronation.

The mean DRUJ position ratio of the TFCC injured DRUJs did not translate dorsally in the studies of this thesis. This discrepancy of RSA based findings compared to the normal conception of dorsal subluxation and ulnar head prominence in patients with DRUJ instability, add concern about the threshold value and sensitivity of the CT based methods, as foveal TFCC lesion was confirmed by arthroscopy in Study I, II and IV. However, the surgically applied injuries by the dorsal approach in Study I and II, may influence the kinematic findings, and does not exactly reflect in vivo injuries.
The increasing focus on different lesions of the foveal TFCC component, leading to instability in opposite directions (Figure 3.5), may be important to stratify when evaluating DRUJ instability and kinematics. In study IV, the distribution of instability patterns evaluated by the Ballottement test in supination and pronation, was with similar distribution (Table 7.9). Stratified evaluation of kinematic patterns in patients with volar directed instability and dorsal directed instability, has not been examined in this thesis as the number of patients is too small.

In study III and IV, the active patient performed *Press test* induced a volar directed glide of the ulnar head in the radius SN. The change of the DRUJ kinematics described as a ratio, has to my knowledge not previously been used in kinematic studies. This was previously recommended to consider anatomical differences of SN size i.e., between small and larger individuals as well as men and women (Thillemann, 2021b). Mapping of the DRUJ position ratio kinematics during the Press test pressure and release phase, revealed that foveal TFCC injured DRUJs translate to a significantly more volar DRUJ position ratio, as compared to the patient's contralateral non-injured DRUJ. Open surgical treatment generally normalized the kinematics of the DRUJ position ratio, but the kinematic pattern was not restored to normal kinematic levels of the contralateral non-injured DRUJ (Thillemann, 2022).

**8.4.3 Ulna variance and pistoning**

*Ulnar variance* is evaluated by standard PA radiographs (Figure 3.11) (Hulten, 1928). Proximal to distal translation (pistoning) of the radius relative to the ulnar head, occurs during forearm rotation (Tay et al., 2008), as the curved radius rotates around the fixed ulna. In pronation, the ulna length increases relative to the radius (King et al., 1986; Palmer et al., 1988; Tay et al., 2010). Detailed mapping of ulnar pistoning during forearm rotation has been evaluated by sequential CT scans ($30^{o}$ rotation increment) and estimated a 1.6 mm relative increase of the ulnar variance during forearm pronation from the neutral position (Chen and Tang, 2013).

In ex vivo studies, increased ulnar variance has been associated with TFCC lesion and DRUJ instability (Shen et al., 2005). In vivo, increased ulnar variance increase the risk of ulnar impaction syndrome (Friedman and Palmer, 1991), but vice versa TFCC pathology has also been related to increased ulnar variance (Ozer et al., 2018).
In non-injured DRUJs, *loaded gripping* increased the ulnar variance by 1.34 mm (Jung et al., 2001), whereas heavy *axial loading* increased the ulnar variance by 0.2 mm to 1.95 mm measured by radiographs (Friedman et al., 1993; Ozer et al., 2018) or CT (Hojo et al., 2019).
Evaluations of changes in ulnar variance during a *posterior-anterior applied force* has to my knowledge only been reported in Study III and IV. The Press test increased the ulnar variance by 1.1 mm in non-injured DRUJs and with similar pistoning in foveal TFCC injured DRUJs as well as DRUJs with surgical reinserted foveal TFCC lesion (Thillemann, 2022; Thillemann, 2021b).

**8.4.4 DRUJ distance**

Gapping in the DRUJ on conventional PA radiographs indicate DRUJ instability (Luchetti et al., 2014). Clenched fist views revealing DRUJ diastasis in comparison to the contralateral side has been proposed as imaging method to detect DRUJ instability (Iida et al., 2012) as the intact TFCC employ compressive forces and maintain 'congruency' in the DRUJ (Hagert and Hagert, 2010). Thus, gapping is not expected in the stable DRUJ, but submillimeter diastasis may not be visible.

In study IV, a volar gliding of the ulnar head in the radius SN was mapped during the Press test. In DRUJs with foveal TFCC lesion, the DRUJ distance from the ulnar head center to the straight SN line increased as the DRUJ position ratio decrease below a 0.4 level. This finding, however, does not reflect true gaping between the articulation joint surfaces and comparison of gapping distances to other studies is inappropriate.
In the DRUJ multiple movements occur simultaneously, and gapping cannot easily be documented as translation along a single axis. Other methods using *pressure-sensitive films* have been used to evaluate articular contact points and contact area in the DRUJ and in the PRUJ (Hemmingsen et al., 2020; Malone et al., 2015; Nishiwaki et al., 2008; Shaaban et al., 2007). These direct techniques are only feasible ex vivo and normal kinematics may be affected by insertion of the film through the capsuloligamentous structures of the joint. Another option to achieve insight in in vivo DRUJ kinematics could be non-invasive *motion capturing systems and skin surface* markers. This method has been widely used in gait analysis and have provided important insight into healthy and pathological kinematics in the lower extremity. However, accurate

dynamic arthrokinematics cannot be achieved by these optical systems, as the accuracy is naturally limited due to skin motion errors relative to the underlying bones (Leardini et al., 2005; Miranda et al., 2013). Instead, precise joint kinematics and the closest contact point (proximity) between the subchondral bone of the articulating surfaces, can be estimated by matching participant-specific 3D bone models to either uni-planar (fluoroscopic) or bi-planar (RSA) dynamic radiographic 2D imaging (3D to 2D image registration methods) (Figure 8.6.) (Anderst and Tashman, 2003; Matsuki et al., 2010).

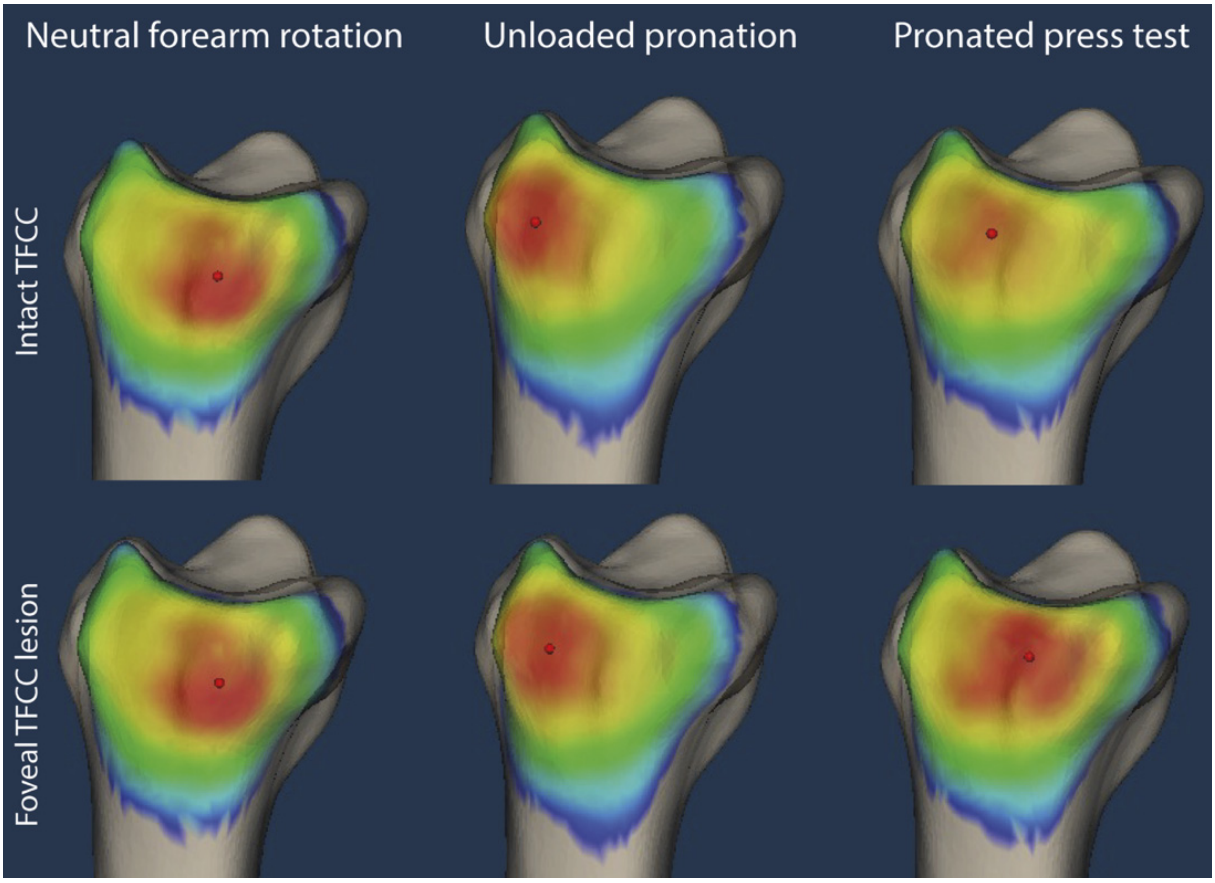


Figure 8.6. Example of proximity mapping in a patient from Study IV.
The closest proximity is mapped by red and the least proximity by dark blue in the DRUJ with foveal TFCC lesion and the non-injured contralateral DRUJ (mirrored). Similar closest contact point was detected in neutral forearm rotation and unloaded pronation. At maximum pressure during the Press test the DRUJ with foval TFCC lesion translated volar compared to the non-injured side with intact TFCC.

To increase accuracy of the registration process bi-planar imaging is preferable. Also, 4D-CT examination of in vivo joint kinematics exists but the freedom of movement is limited within the CT tube (Chen et al., 2020).

Combined CT based bone models and MRI based cartilage models, may provide improved precision of estimating the contact point, contact area or the closest distance (Akpinar et al., 2019). Such model segmentation is however challenging.

## 8.5 Surgical treatment

Technical reports dominate the literature and many different surgical techniques in terms of repair of the TFCC have been presented in the literature over the last decades. The surgical techniques used in Study II (Adams reconstruction (Adams, 2000)) and Study IV (open reinsertion of pc-TFCC to the fovea by a suture anchor (Hermansdorfer and Kleinman, 1991)) were the commonly used methods at the Departments of Hand Surgery at Aarhus University Hospital and Hospital Unit West as this thesis was initiated in 2015. These surgical techniques or their modifications (Garcia-Elias et al. (2003)) have been used worldwide.

In the last decade arthroscopic reinsertion techniques have gained increasing interest for treatment of Atzei Class 2 and 3 lesions (Figure 8.7):

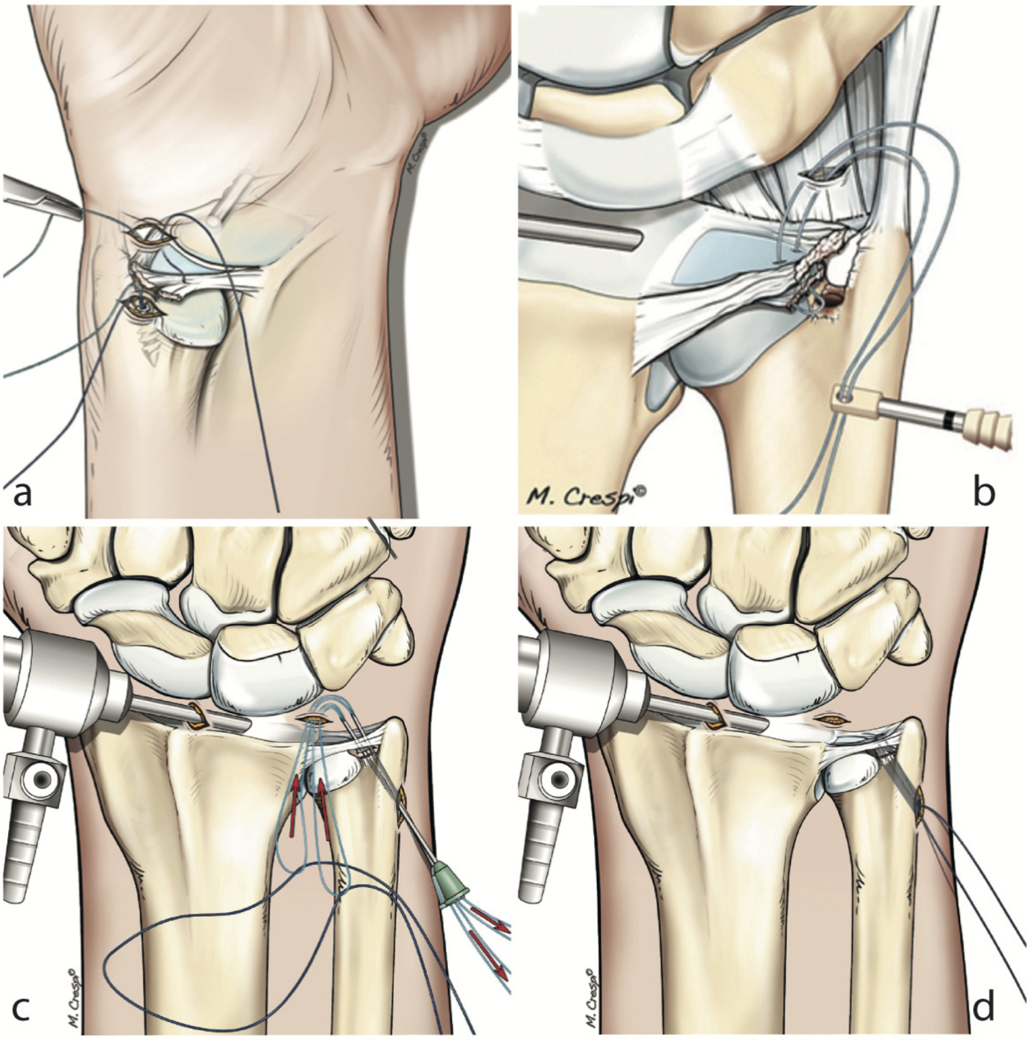


Figure 8.7. Examples of arthroscopic approaches to foveal TFCC reinsertion:
Mini open direct foveal portal (a) (Atzei et al., 2008). All inside bone anchor reinsertion (b) (Kermarrec et al., 2020). Transosseous mattress suturing through dual bone tunnels (c) (Nakamura, 2012). Transosseous mattress suturing through a single bone tunnel (d) (Iwasaki and Minami, 2009).

- Mini open direct foveal portal bone anchor suture (Figure 8.7a) (Atzei et al., 2008)
- All inside bone anchor reinsertion (Figure 8.7b) (Geissler, 2015; Kermarrec et al., 2020).
- Transosseous mattress suturing through dual bone tunnels (Figure 8.7c) (Nakamura et al., 2011; Shinohara et al., 2013)
- Transosseous mattress suturing through a single bone tunnel (Figure 8.7d) (Iwasaki and Minami, 2009; Kwon et al., 2020; Park et al., 2018)
- Single bone tunnel foot print and capsule suture (Chen, 2017).

One of the latest surgical technique for Atzei Class 2 and 3 lesions is an arthroscopic approach to foveal TFCC reinsertion using a single bone tunnel and suturing the TFCC to the fovea by a tendon graft (Zhang et al., 2021). For Atzei Class 4 lesions, arthroscopic assisted TFCC reconstruction using tendon grafts have been developed (Chu-Kay Mak and Ho, 2017; Luchetti and Atzei, 2017; Tse et al., 2013).

**8.5.1 PROMS after surgical treatment**

In Study IV, at 1-year follow-up, open foveal TFCC reinsertion improved pain on NRS during lifting from median 5 to 2, the quick DASH score improved from mean 39 points to 25 points, and the total PRWE improved from mean 49 to 28 points. These PROM measures all improved statistically significant and to the level of the currently available MCID for each PROM (Farrar et al., 2001; Kim and Park, 2013; Salaffi et al., 2004; Sorensen et al., 2013).

Few studies have reported QDASH/DASH scores and pain scores after open TFCC reinsertion or reconstruction surgery. Two randomized controlled trials have been conducted to compare open and arthroscopic TFCC reinsertion. Two randomized controlled trials have been conducted to compare open and arthroscopic TFCC reinsertion. Anderson et al. (2008) used both arthroscopic capsular suture and osseous foveal reinsertion of lesions in the 'peripheral TFCC' but found similar outcomes between groups in terms of pain, DASH and PRWE scores, compared to open foveal TFCC reinsertion. Luchetti et al. (2014) investigated a heterogenous patient group with DRUJ instability confirmed by clinical testing and arthroscopic confirmation (Hook test) and compared arthroscopic osseous foveal TFCC reinsertion and open foveal TFCC reinsertion. Both treatments had a significant effect on improvement of pain during loading, DASH and PRWE score, but without improvement of grip strength. In the arthroscopic group, the DASH score and PRWE improved to significantly lower levels compared to the open group.

The MCID of QDASH in TFCC injured DRUJ instable patients has not previously been established. In Study IV the improvement of QDASH was to the level of the 14 points MCID (Sorensen et al., 2013) as well as the 17 points PRWE MCID detected in ulnar impaction syndrome (Kim and Park, 2013).

Recent retrospective and prospective non-randomized cohort studies using arthroscopic foveal TFCC reinsertion have more frequently reported PROMs before and after foveal TFCC reinsertion. In these arthroscopic reports, there is a tendency of grip strength improvement towards the strength of the contralateral hand. Further, both the pain scores (range 0.4-1.5 (on a 0–10-point scale)) and QDASH/DASH scores (range 8-18) were reported at a lower level compared to the results after open foveal reinsertion in Study IV. Contrary, studies on TFCC reconstruction generally seem to report less improvement of the postoperative grip strength, QDASH/DASH and pain scores (Table 8.1. and 8.2.). However, pain score is not uniformly reported (i.e., at rest or during specific activities) and must be compared across studies with precaution. Pain scores before and after surgical treatment is displayed in the Tables 8.1 and 8.2 and a pain reduction of approximately two points or a reduction of approximately 30% in pain NRS represent a MCID (Farrar et al., 2001; Salaffi et al., 2004).

Due to diversity in patient material and lesion type of published studies, comparison of results of surgical treatments across studies must be done with precaution. The most recent systematic review on open versus arthroscopic treatment of foveal TFCC injuries was published by Robba et al. (2020), and they concluded that superiority of either method had yet to been documented.

Evaluation of postoperative results by PROMs may also be challenged by the specificity of the PROM score for the functional problems of the condition that is studied. Many questions in the DASH and QDASH questionnaire are related to elbow and shoulder function whereas the PRWE score was developed for wrist disorders. Thus, neither the PRWE nor the DASH questionnaires were developed with focus on evaluation of the DRUJ symptoms and TFCC injuries. Preferably, a new focused questionnaire should be developed and validated for evaluation of PROM in TFCC injured and DRUJ instable patients, i.e., ulnar wrist pain, pain in relation to forceful forearm rotation, and pain when lifting away from the core. A PROM focused on TFCC injuries and the DRUJ, may be superior to elucidate differences between treatments.

## 8.6 Methodological considerations and limitations

Important limitations to the results of this thesis relates to the method, design, and generalizability of the studies.

### *8.6.1* Generalizability, bias, and sample size

*Studies I and II:* Using *cadaver* specimens in experimental studies have limitations such as loss of tissue elasticity and absence of muscular stabilization, and the kinematic findings and therefore the results cannot be directly transferred to patients. Further, the cadaver specimens were from an old study-population (range 72 – 90 years), which may not resemble younger patients due to cartilage wear and TFCC degeneration with increasing age. The cadavers were freshly frozen to minimize tissue changes and all soft tissue were kept intact. The homogeneity of the cadavers was ensured, and *bias* due to degenerative lesions and trauma related injuries were reduced by performing fluoroscopy, CT, and arthroscopy, to exclude specimens with pathology listed in the study criteria, which could potentially influence DRUJ kinematics and DRUJ stability.

In Studies I and II, the manually applied TFCC lesions of the foveal attachment may not exactly resemble in vivo traumatic TFCC injuries. However, the foveal TFCC lesion was confirmed and validated using arthroscopic Hook test in each specimen.
Randomization to intervention in study II aimed to distribute specimens randomly. However, the pre-operative instability of the specimens in the group had variation. Further, in a cadaver study, the effect of surgical treatment only tests the direct stability of the surgical techniques directly after surgery. In vivo stabilizing effects of adhesions, scar tissue formation and ligamentization develop over time and contrary, laxity developed during rehabilitation, is not tested in experimental settings, but likely would be expected to affect DRUJ stability at longer-term clinical follow-up.
In study II, the *sample size* calculation estimates were performed using the best available data at the time. A larger cohort would expectedly reduce the risk of diverging baseline characteristics in the groups. Further, a larger cohort might have displayed statistically significant differences of DRUJ stability with the two surgical procedures (type 2 error).
The surgical procedures were performed as a joint venture by two surgeons (JKT and MS) and cannot be generalized beyond that particular group of specimens and surgeons, the latter however ensured uniformly performed surgical treatment.

*Studies III and IV:* In vivo DRUJ translation in normal joints with an intact TFCC can be seen with broad variability ranging from hypermobility to highly stable joints and inability to relax the DRUJ-supporting muscular stabilizers during testing. Also, age and gender may influence joint kinematics. Patient individual differences in perception of DRUJ symptoms, functional demands and symptom provoking activities also affect the answers given in PROMs.

In Study III, normal kinematics should preferably be examined on numerous individuals, optioning age clusters, gender clusters, and maybe even sub-grouped by 'Tolat' sigmoid notch types. As dRSA is time consuming, despite assisted by semiautomated AutoRSA analysis software, the number of non-injured DRUJs included in Study III cohort during the study period, is limited. The kinematic results cannot be directly transferred to populations outside the study criteria.

In Study IV, the size of the study cohort is similar to many other studies on foveal TFCC surgery (Table 8.1 and 8.2). However, a relatively small cohort size may potentially affect the results (type II error) and generalization to patients with diverging characteristics and patients outside the study criteria. Examples are; patients with malunion following distal radius fractures and concomitant DRUJ instability and patients with combined lesions (i.e. simultaneous scapholunate ligament lesion) as those were not included in study IV.

Patient selection may be influenced by the clinical evaluation performed by the only surgeon and principal investigator (JKT). To reduce risk of *selection bias*, foveal TFCC lesion was confirmed arthroscopically by a Hook test (study criteria), but as for the clinical evaluation this was performed also by the principal investigator and thus, may be biased by the clinical examination findings. However, misinterpretation of the clinical examination (Ballottement test and Piano Key clinical tests) by referring colleagues may have resulted in false negative conclusions (no TFCC lesion suspicion), which may have excluded patients from the study cohort. Yet, all symptomatic patients with suspected TFCC lesion (including evaluations of slight instability by Ballottement test) were offered participation and were finally excluded if the arthroscopic findings did not fulfill the study criteria (positive Hook test). In total, 6 patients with arthroscopic verified dc-TFCC lesions were excluded (positive trampoline test and negative Hook test), which were treated by out-side in capsular suture. Patients primarily evaluated as DRUJ stable, with other clinical or MRI verified diagnosis and persisting wrist pain, were offered wrist arthroscopy if relevant, but this was not performed solely by the principal investigator and patients were initially excluded from the study (no follow-up data).

A single surgeon (JKT) performed all arthroscopic evaluations of TFCC instability (Hook test) and the open foveal TFCC reinsertions and therefore results cannot be generalized beyond that particular group of patients and the surgeon. At initiation of Study IV, the surgeon experience with arthroscopy and TFCC surgery was graded as levels III according to Tangs classification on 'Levels of experience of surgeons in clinical studies' (Tang, 2009) and no learning curve was expected for JKT.

To reduce *information-bias* all preoperative, 6-month and 1-year questionnaires were handed out and filled by the patient before clinical examination/RSA imagining.

**8.6.2 Confounding**

Potentially, the results in the thesis can be affected by confounders. To limit the impact from other conditions influencing the clinical outcomes, the kinematic outcomes and PROMs, all patients underwent MRI before study inclusion to rule out concomitant pathology (exclusion criteria).

It is debated if ulnar variance is a contraindication for foveal TFCC reinsertion. Nakamura et al. (2011) have proposed ulnar variance exceeding 2 mm as a contraindication to foveal TFCC reinsertion. In contrast, Kim et al. (2013) showed no correlation to secondary ulnocarpal impaction syndrome if patients did not experience such symptoms prior to their TFCC injury. Thus, they did not find positive ulnar variance to be a contraindication for foveal TFCC reinsertion.

Positive ulnar variance was not defined as an exclusion criterion as the thesis began, but according to Nakamura et al (2011), the clinical practice in both including departments was not to perform foveal TFCC reinsertion to patients with a > 2 mm positive ulnar variance on PA radiographs, a history of ulnar wrist pain prior to trauma, and signs of ulnocarpal impaction on MRI. Rather such patients were offered an ulnar shortening osteotomy and a foveal TFCC reinsertion at the same time or later if needed. Patients treated with ulna shortening were not included in the study because of metal artefacts from ulna shortening plate which would disturb the RSA image analysis, and the chanced ulna length and thus, patient follow-up by dRSA will be encumbered with errors.

In Study IV, kinematic data could have been adjusted by i.e., gender, age, ulnar variance, concomitant Palmer 1A TFCC lesion, or pressure applied during the Press test. This however 'blur' the actual kinematics achieved, and preferably a larger cohort with possibility of stratification is preferred, but time consuming, as dRSA still demand assistance in calibrating and initializing the analyzes.

### 8.6.3 Other DRUJ stabilizers

Non-diagnosed concomitant lesions influencing DRUJ instability may also have impact on the results in Study IV.

The *interosseus membrane (IOM)* play a role in stabilizing the DRUJ. Lesions of the IOM has not been a focus in the current thesis and MRI has not routinely been conducted as proximal as to include the central band of the IOM.

In experimental studies, intact RULs in isolation preserved normal kinematics despite lesion of the IOM (Gofton et al., 2004). Contrary, TFCC tendon reconstruction provide less stability compared to IOM reconstruction (Riggenbach et al., 2013) and TFCC tendon reconstruction may be an incomplete treatment in patients with concomitant rupture of the IOM (Heitner et al., 2020).

Combined IOM lesions and foveal TFCC lesions would expectedly result in severe DRUJ instability (Kihara et al., 1995) and may increase the risk of non-restored stability in the postoperative phase. It is unknown, if some of the patients in Study IV with severe DRUJ instability would have benefitted from additional IOM repair in addition to TFCC to improve DRUJ stability.

The *ulnocarpal ligament complex (UCL)* suspends the ulnar carpus (Semisch et al., 2016) but knowledge about lesions of the UCL and influence on DRUJ stability was not in focus when the thesis was initiated. Potentially, a combined Ballottement test using both the 'holding' and 'non-holding' technique with and without radial wrist deviation would add suspicion to UCL lesions in severely unstable DRUJs (Omokawa et al., 2017).

### 8.6.4 Method limitations

*Marker-based RSA* is considered the RSA 'gold standard' and has high accuracy for as well as precision for evaluation of joint arthroplasty fixation and wear, and high precision for evaluation of kinematics of native joints (Stilling et al., 2012). A prerequisite for marker-based RSA is a good marker-model with sufficient number and dispersion of markers in the bone and in similar anatomical positions between the studied cases. The dispersion of markers is expressed by the condition number (CN) and the upper limit for the CN is 150 in knee and hip arthroplasty (Valstar et al., 2005). The CN was mean 70.4 in the radius and mean 83.8 in the ulna despite the anatomical limitations of these small slim bones that limit marker dispersion. In average eight tantalum markers were inserted in each bone.

In Study I, marker-based RSA was not used for analysis, but to evaluate the precision of *RSA analysis based on DRR* (AutoRSA) to marker-based RSA. The precision was high and within PIs of ±0.18 mm and 0.98 degrees, for translations and rotations, respectively (Thillemann et al., 2020). A previous dynamic RSA study using DRR (AutoRSA) on knees presented high precision within PIs of ±0.42 mm and 0.33 degrees, for translations and rotations, respectively (Christensen et al., 2020).
Using *AutoRSA* on bones from aged donors that are likely to have osteoporosis or osteopenia (Boskey and Coleman, 2010), may affect the intensity of cortical and trabecular bone in the CT-based DRR models. Since the DRR method use intensity levels in the models and x-rays it may affect the accuracy of DRR registration in the cadaver studies, yet precision was acceptable. However, the DRRs are constructed from CT scans using information on the whole bone volume models including the trabecular bone structure and therefore the sum of information available for matching to the RSA image is very high, whereas markers-based RSA depend on more limited (minimum 3 markers) information. Using AutoRSA, kinematic measurements are determined by bone model coordinate systems. Anatomical coordinate systems represent the bones and joints of the studied individual patients best possible, whereas marker-models are not representative of the anatomy.
At best, precision and accuracy may have improved using AutoRSA in clinical studies on younger subjects (Studies III and IV). Further, it is unknown if marker-based RSA or AutoRSA analysis is closer to the true value, as accuracy studies have not been conducted for the latter (Christensen et al., 2020).

*Anatomical landmarks* were essential to estimate the kinematic outcomes of the RSA analysis in the thesis. The anatomical landmarks (points) combined define anatomical relevant axis and coordinate systems used to represent the true joint kinematics. Such relevant coordinate systems has previously been defined (McDonald et al., 2012), but point picking induce a potential error regardless of whether they are applied manually or selected by automated algorithms. This is due to the varying inter-individual bony anatomy and may be important for comparisons across subjects. However, these landmarks and anatomical coordinate systems needs only to be defined once in each bone and therefore does not affect within-subject comparisons over time (because the same bone model can be used).
Nevertheless, the combination of AutoRSA imaging and anatomical kinematic axis, exclude overestimations due to soft tissue components and most importantly, the kinematic estimates are free of observer bias.

Furthermore, the degree of forearm rotation influences the DRUJ stability, but DRR based dRSA enable estimation of the forearm rotation in any test. This may be an important key for comparison of kinematic outcomes across studies.

In Study III and IV, the patients performed the *Press test* in a systematic way using elbow flexion and neutral wrist extension. However, this does not exactly resemble the clinical Press test, where the patient push himself up from an armchair. The Press test produced less pain than expected (median 1 (IQR 0 – 4)). The test may therefore not be the ideal test for reflecting the patient's sensation of painful DRUJ instability and 'give way'.

The *dynamic setup* with 10 Hz imaging intended to capture the most extreme DRUJ positions during testing, but it is unknown if 10 Hz was sufficiently high to obtain the outlying fluctuations of the Press test kinematics. A sampling frequency of 15 Hz with the same image resolution and recording on full detector size became possible during the course of this thesis, but it was decided to keep the set-up unchanged for studies III and IV.

In gait cycle analysis recommendations on sampling rate is defined to avoid insufficient sampling and aliasing (Lévesque, 2014). Insufficient sampling with data lost at discrete time points lead to inability of reproducing the true trajectory of the motion kinematics, but as the motion range during the Press test is rather narrow and the patients were instructed to 'relax – gradually press - hold the pressure for a second – and release the force gradually', the discrete timepoints was most likely imaged by a 10 Hz dRSA sampling frequency. However, potential discrete kinematic points may not be exhibited in patients who were unable to relax the muscular DRUJ stabilizers sufficiently during the test. Likewise, in theory, preoperative pain might have limited the ability to produce a forceful excursion on the force plate, on the injured site. This does however not seem to be the case, as similar force was applied by the non-injured side and the injured side preoperatively, and at all follow-ups (Figure 7.11). The patient's execution of the Press test might be subjected to learning curve, but this is less likely as the test validation showed small and non-significant mean difference between the first and second test (Tables 7.7 and 7.14).

# 9 Conclusion

# 9

# Conclusions

## 9.1 Conclusions

### 9.1.1 Study I

- Static RSA was applied on cadaver arms and AutoRSA analysis with CT based bone model registration was validated in comparison to the marker-based RSA 'gold standard' and small systematic errors and high precision was found.

- The DRUJ translation increased during Piano key test with successive TFCC lesions and confirmed significant and increasing DRUJ instability with detachment of first the dc-TFCC and next also the pc-TFCC insertion.

### 9.1.2 Study II

- Open foveal TFCC reinsertion and Adams TFCC reconstruction with palmaris longus tendon graft had a stabilizing effect on the DRUJ, but the effect of the Adams reconstruction was heterogeneous.

- This cadaver study supports foveal TFCC reinsertion in patients suffering from symptomatic DRUJ instability due to repairable lesions but remains to be confirmed in vivo.

### 9.1.3 Study III

- Kinematics of the DRUJ during dynamic patient applied Press test was estimated with high test-retest agreement, small systematic errors, and high precision of double examinations by dRSA imaging in non-injured DRUJs.

- The normative DRUJ kinematics during the Press test were mapped by dRSA imaging. Anatomical differences of the articulating sigmoid notch length and shape were documented, and consequently individual differences of the articulation length were considered. In asymptomatic participants, the calculated DRUJ position ratio mean value was above a 0.40 ratio (0 equals the volar rim, and 1 equals the dorsal rim) throughout the Press test examination.

### 9.1.4 Study IV

- Pathokinematics in patients with symptom giving DRUJ instability due to arthroscopically verified foveal TFCC lesion displayed a statistically significant altered pattern, with a up to 10 percent points decrease of the DRUJ position in the force-loaded part (>2.3kg) of the Press test, compared to the contralateral non-injured DRUJ. At maximum Press test force, the DRUJ position ratio mean value was decreased to 0.29 in DRUJs with foveal TFCC lesion.

- The *ulnar variance* increased bilaterally by approximately 1 mm with induced maximum force. Evaluation of DRUJ distance revealed an inverse pattern in injured joints, which reflect the decreased DRUJ position ratio.

- *Surgical treatment* by open foveal reinsertion had a stabilizing effect on the DRUJ and improved the DRUJ position ratio pattern towards normal values up 12 months follow-up.

- *Patient reported outcomes* in terms of pain, QDASH and PRWE scores were significantly improved during the first postoperative year and to the level of the minimal clinically important difference (MCID) levels available for wrist and hand conditions.

- Pathokinematics of the DRUJ during dynamic patient applied Press test was estimated with high test-retest agreement, small systematic errors, and high precision of double examinations by dRSA imaging in foveal TFCC injured DRUJs.

- The Press test repeatability with dynamic RSA was superior to ultrasonography measured DRUJ translation. *Observer bias* was limited using DRR based kinematic estimates of the DRUJ and excluded overestimations due to soft tissue components.

# 10 Future perspectives

# 10

# Perspectives

## 10.1 Clinical perspectives

This thesis proved AutoRSA analysis to be a precise method for analyzing and estimating DRUJ kinematics in sRSA and dRSA image recordings. Thus, objective measurement of DRUJ instability and mapping of normative kinematics as well as pathokinematics during dynamic testing is now possible. How can we benefit from this in the future?

Long term stability in relation to patient satisfaction after TFCC surgery is an important issue. A planned midterm evaluation (5 years) of DRUJ kinematics and PROMS will provide important new evidence on the lasting effect the open foveal repair technique.

The Press test was simple to visualize and record with dRSA and mimics the clinical stability test, but it is unknown if it shows the full trajectory of DRUJ instability. Likely, recording and analysis of more complex tests using active symptom provoking exercises such as torque loaded forearm rotation may contribute with new knowledge of DRUJ pathokinematics. Importantly, the tests should be standardized and performable for all patients. Thus, the feasibility and diagnostic value of new tests for evaluation of DRUJ instability is mandatory. This is now possible with dRSA and AutoRSA.

There is an abundant amount of different surgical techniques for DRUJ instability and dRSA imaging and AutoRSA analysis can be used in future studies to document, which techniques provide a better normalization of DRUJ kinematics and stability. Furthermore, dRSA imaging and AutoRSA analysis can be used as a quality control for a stepwise introduction of new methods to ensure their safety, efficacy, and superiority compared to established methods before a general application in patients (Nelissen et al., 2011).

In selected cases, individualized dRSA examinations of DRUJ pathomechanics may be very helpful for the clinician to understand the functional deficit resulting from radius and ulna fracture malunion (Figure 10.1). Thus, dRSA imaging and AutoRSA analysis can help the clinician to understand the functional effect of anatomical deformity and provide appropriate and sufficient treatments in complex cases.

## 10.2 Technical perspectives

During the PhD study the AutoRSA analysis software package has gradually been developed and improved. This open new doors of opportunities and usability of dRSA.
At initiation of the thesis, we were unable to analyze dRSA images with overlapping bones, but today AutoRSA can track the bones during image series despite overlap of the radius and ulna during forearm rotation.

For a more widespread clinical use and research application of dRSA for evaluation of DRUJ kinematics a fully automated analysis package of dRSA images is demanded and this is in progress within the AutoRSA Research Group. Once accomplished, it will allow future studies to examine larger patient cohorts with DRUJ stability problems and use more patient active exercise tests without concerns about the analysis workload.

Patient specific bone models for AutoRSA analyses were segmented from CT scans of the forearm, which is an additional time-consuming and radiation dose producing examination. In the future usage of statistical shape models (averaged models from multiple forearm CT scans) may alleviate the need for individual CT scans, reduce radiation dose, and increase the applicability and dissemination of the dRSA method for evaluation of DRUJ stability.

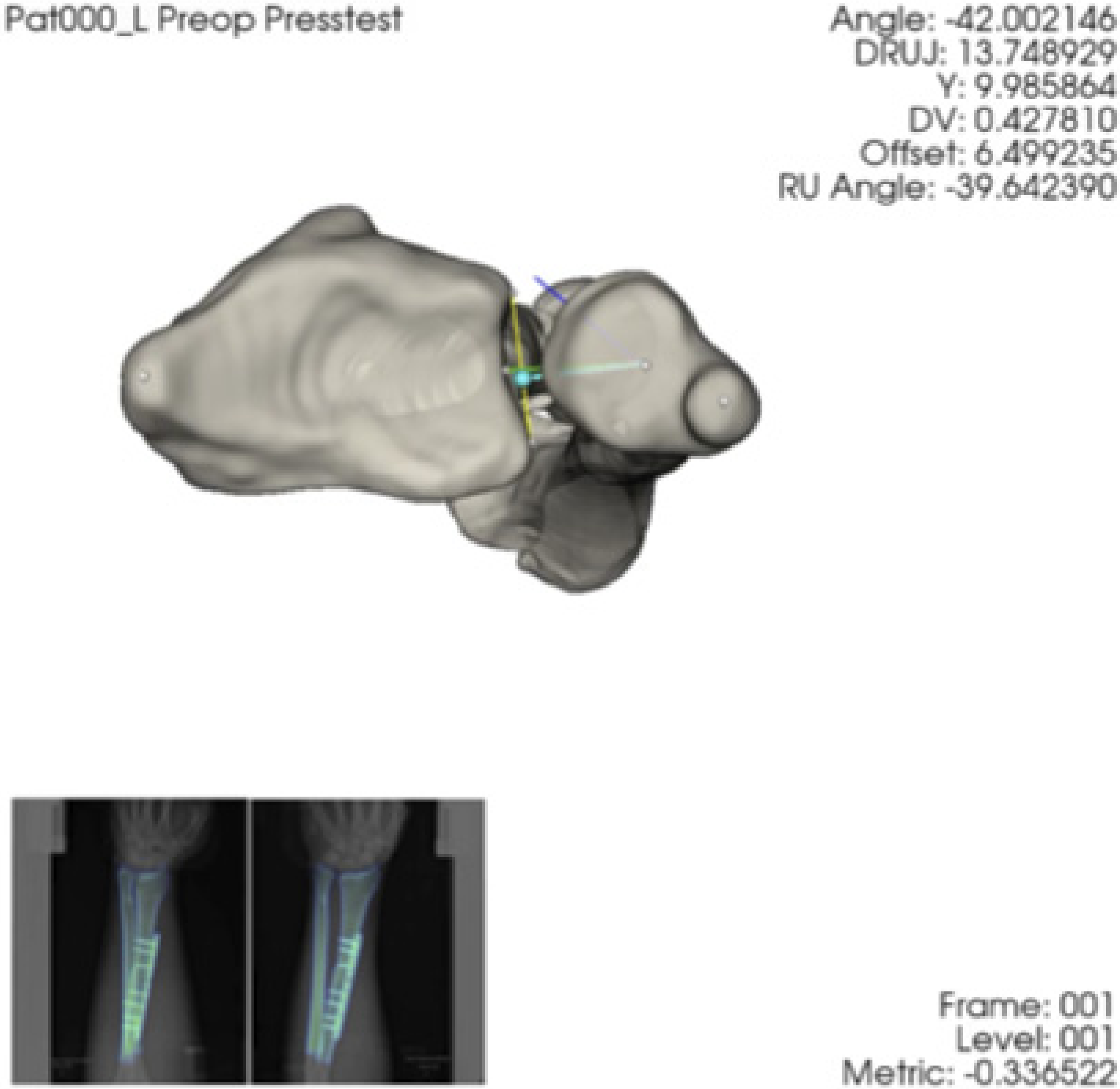


Figure 10.1. Example of dynamic RSA examination of a malunion of the radius, resulting from incorrect osteosynthesis of a midshaft fracture and TFCC injury (Galleazi fracture), leading to DRUJ incongruency.

# 11 References

# 11

# References


1. Guidelines on the use of ionising radiation in health research projects - appendix 2. The Danish National Committee on Health Research Ethics, 2018.

2. Abe Y, Fujii K, Fujisawa T. Midterm results after open versus arthroscopic transosseous repair for foveal tears of the triangular fibrocartilage complex. J Wrist Surg. 2018, 7: 292-7.

3. Abe Y, Tominaga Y, Yoshida K. Various patterns of traumatic triangular fibrocartilage complex tear. Hand Surg. 2012, 17: 191-8.

4. Adams BD. Anatomic reconstruction of the distal radioulnar ligaments for druj instability. Techniques in hand & upper extremity surgery. 2000, 4: 154-60.

5. Adams BD, Berger RA. An anatomic reconstruction of the distal radioulnar ligaments for posttraumatic distal radioulnar joint instability. The Journal of hand surgery. 2002, 27: 243-51.

6. Adams BD, Lawler E. Chronic instability of the distal radioulnar joint. J Am Acad Orthop Surg. 2007, 15: 571-5.

7. Adolfsson L. Arthroscopic diagnosis of ligament lesions of the wrist. J Hand Surg Br. 1994, 19: 505-12.

8. af Ekenstam F. Anatomy of the distal radioulnar joint. Clin Orthop Relat Res. 1992: 14-8.

9. af Ekenstam F, Hagert CG. Anatomical studies on the geometry and stability of the distal radio ulnar joint. Scand J Plast Reconstr Surg. 1985, 19: 17-25.

10. Akpinar B, Thorhauer E, Tashman S, Irrgang JJ, Fu FH, Anderst WJ. Tibiofemoral cartilage contact differences between level walking and downhill running. Orthop J Sports Med. 2019, 7: 2325967119836164.

11. Anderson ML, Larson AN, Moran SL, Cooney WP, Amrami KK, Berger RA. Clinical comparison of arthroscopic versus open repair of triangular fibrocartilage complex tears. The Journal of hand surgery. 2008, 33: 675-82.

12. Anderson ML, Skinner JA, Felmlee JP, Berger RA, Amrami KK. Diagnostic comparison of 1.5 tesla and 3.0 tesla preoperative mri of the wrist in patients with ulnar-sided wrist pain. The Journal of hand surgery. 2008, 33: 1153-9.

13. Andersson JK, Ahlen M, Andernord D. Open versus arthroscopic repair of the triangular fibrocartilage complex: A systematic review. Journal of experimental orthopaedics. 2018, 5: 6.

14. Andersson JK, Andernord D, Karlsson J, Friden J. Efficacy of magnetic resonance imaging and clinical tests in diagnostics of wrist ligament injuries: A systematic review. Arthroscopy. 2015, 31: 2014-20 e2.

15. Andersson JK, Axelsson P, Stromberg J, Karlsson J, Friden J. Patients with triangular fibrocartilage complex injuries and distal radioulnar joint instability have reduced rotational torque in the forearm. The Journal of hand surgery, European volume. 2016, 41: 732-8.

16. Andersson JK, Lindau T, Karlsson J, Friden J. Distal radio-ulnar joint instability in children and adolescents after wrist trauma. The Journal of hand surgery, European volume. 2014, 39: 653-61.

17. Anderst W, Zauel R, Bishop J, Demps E, Tashman S. Validation of three-dimensional model-based tibio-femoral tracking during running. Med Eng Phys. 2009, 31: 10-6.

18. Anderst WJ, Tashman S. A method to estimate in vivo dynamic articular surface interaction. J Biomech. 2003, 36: 1291-9.

19. Atzei A. New trends in arthroscopic management of type 1-b tfcc injuries with druj instability. The Journal of hand surgery, European volume. 2009, 34: 582-91.

20. Atzei A, Luchetti R. Foveal tfcc tear classification and treatment. Hand Clin. 2011, 27: 263-72.

21. Atzei A, Luchetti R, Braidotti F. Arthroscopic foveal repair of the triangular fibrocartilage complex. J Wrist Surg. 2015, 4: 22-30.

22. Atzei A, Luchetti R, Garagnani L. Classification of ulnar triangular fibrocartilage complex tears. A treatment algorithm for palmer type ib tears. The Journal of hand surgery, European volume. 2017, 42: 405-14.

23. Atzei A, Rizzo A, Luchetti R, Fairplay T. Arthroscopic foveal repair of triangular fibrocartilage complex peripheral lesion with distal radioulnar joint instability. Techniques in hand & upper extremity surgery. 2008, 12: 226-35.

24. Axelsson P, Sollerman C, Karrholm J. Validity and responsiveness of forearm strength measurements in the evaluation of distal radioulnar joint implant arthroplasty. The Journal of hand surgery. 2020, 45: 778 e1- e7.

25. Baeyens JP, Van Glabbeek F, Goossens M, Gielen J, Van Roy P, Clarys JP. In vivo 3d arthrokinematics of the proximal and distal radioulnar joints during active pronation and supination. Clin Biomech (Bristol, Avon). 2006, 21 Suppl 1: S9-12.

26. Baldursson H, Egund N, Hansson LI, Selvik G. Instability and wear of total hip prostheses determined with roentgen stereophotogrammetry. Arch Orthop Trauma Surg. 1979, 95: 257-63.

27. Banks SA, Hodge WA. Accurate measurement of three-dimensional knee replacement kinematics using single-plane fluoroscopy. IEEE Trans Biomed Eng. 1996, 43: 638-49.

28. Beaton DE, O'Driscoll SW, Richards RR. Grip strength testing using the bte work simulator and the jamar dynamometer: A comparative study. Baltimore therapeutic equipment. The Journal of hand surgery. 1995, 20: 293-8.

29. Beaton DE, Wright JG, Katz JN. Development of the quickdash: Comparison of three item-reduction approaches. The Journal of bone and joint surgery American volume. 2005, 87: 1038-46.

30. Berger RA, Landsmeer JM. The palmar radiocarpal ligaments: A study of adult and fetal human wrist joints. The Journal of hand surgery. 1990, 15: 847-54.

31. Berkanovic E, Hurwicz ML, Lachenbruch PA. Concordant and discrepant views of patients' physical functioning. Arthritis Care Res. 1995, 8: 94-101.

32. Boeckstyns ME, Merser S. Psychometric properties of two questionnaires in the context of total wrist arthroplasty. Dan Med J. 2014, 61: A4939.

33. Boer BC, Vestering M, van Raak SM, van Kooten EO, Huis In 't Veld R, Vochteloo AJH. Mr arthrography is slightly more accurate than conventional mri in detecting tfcc lesions of the wrist. Eur J Orthop Surg Traumatol. 2018, 28: 1549-53.

34. Bohringer G, Schadel-Hopfner M, Petermann J, Gotzen L. A method for all-inside arthroscopic repair of palmer 1b triangular fibrocartilage complex tears. Arthroscopy. 2002, 18: 211-3.

35. Bonanzinga T, Signorelli C, Bontempi M et al. Evaluation of rsa set-up from a clinical biplane fluoroscopy system for 3d joint kinematic analysis. Joints. 2016, 4: 121-5.

36. Boskey AL, Coleman R. Aging and bone. J Dent Res. 2010, 89: 1333-48.

37. Bragdon CR, Estok DM, Malchau H et al. Comparison of two digital radiostereometric analysis methods in the determination of femoral head penetration in a total hip replacement phantom. Journal of orthopaedic research : official publication of the Orthopaedic Research Society. 2004, 22: 659-64.

38. 'Bragonzoni L, Marcheggiani Muccioli GM, Bontempi M et al. New design total knee arthroplasty shows medial pivoting movement under weight-bearing conditions. Knee Surg Sports Traumatol Arthrosc. 2019, 27: 1049-56.

39. Budtz CR, Andersen JH, de Vos Andersen NB, Christiansen DH. Responsiveness and minimal important change for the quick-dash in patients with shoulder disorders. Health Qual Life Outcomes. 2018, 16: 226.

40. Buijze GA, Ring D. Clinical impact of united versus nonunited fractures of the proximal half of the ulnar styloid following volar plate fixation of the distal radius. The Journal of hand surgery. 2010, 35: 223-7.

41. Cai R, Yuan X, Rorabeck C, Bourne RB, Holdsworth DW. Development of an rsa calibration system with improved accuracy and precision. J Biomech. 2008, 41: 907-11.

42. Cardenas-Montemayor E, Hartl JF, Wolf MB et al. Subjective and objective results of arthroscopic debridement of ulnar-sided tfcc (palmer type 1b) lesions with stable distal radio-ulnar joint. Arch Orthop Trauma Surg. 2013, 133: 287-93.

43. Carter TI, Pansy B, Wolff AL et al. Accuracy and reliability of three different techniques for manual goniometry for wrist motion: A cadaveric study. The Journal of hand surgery. 2009, 34: 1422-8.

44. Chan JJ, Teunis T, Ring D. Prevalence of triangular fibrocartilage complex abnormalities regardless of symptoms rise with age: Systematic review and pooled analysis. Clin Orthop Relat Res. 2014, 472: 3987-94.

45. Changulani M, Okonkwo U, Keswani T, Kalairajah Y. Outcome evaluation measures for wrist and hand: Which one to choose? Int Orthop. 2008, 32: 1-6.

46. Chen H, Kluijtmans L, Bakker M et al. A robust and semi-automatic quantitative measurement of patellofemoral instability based on four dimensional computed tomography. Med Eng Phys. 2020, 78: 29-38.

47. Chen WJ. Arthroscopically assisted transosseous foveal repair of triangular fibrocartilage complex. Arthrosc Tech. 2017, 6: e57-e64.

48. Chen YR, Tang JB. In vivo gliding and contact characteristics of the sigmoid notch and the ulna in forearm rotation. The Journal of hand surgery. 2013, 38: 1513-9.

49. Chiang CC, Chang MC, Lin CF, Liu Y, Lo WH. Computerized tomography in the diagnosis of subluxation of the distal radioulnar joint. Zhonghua Yi Xue Za Zhi (Taipei). 1998, 61: 708-15.

50. Chou KH, Sarris IK, Sotereanos DG. Suture anchor repair of ulnar-sided triangular fibrocartilage complex tears. J Hand Surg Br. 2003, 28: 546-50.

51. Christensen R, Petersen ET, Jurgens-Lahnstein J et al. Assessment of knee kinematics with dynamic radiostereometry: Validation of an automated model-based method of analysis using bone models. Journal of orthopaedic research : official publication of the Orthopaedic Research Society. 2020.

52. Chu-Kay Mak M, Ho PC. Arthroscopic-assisted triangular fibrocartilage complex reconstruction. Hand Clin. 2017, 33: 625-37.

53. Claes S, Verdonk P, Forsyth R, Bellemans J. The "ligamentization" process in anterior cruciate ligament reconstruction: What happens to the human graft? A systematic review of the literature. Am J Sports Med. 2011, 39: 2476-83.

54. Cooney WP, 3rd, Dobyns JH, Linscheid RL. Complications of colles' fractures. J Bone Joint Surg Am. 1980, 62: 613-9.

55. Ehman EC, Hayes ML, Berger RA, Felmlee JP, Amrami KK. Subluxation of the distal radioulnar joint as a predictor of foveal triangular fibrocartilage complex tears. The Journal of hand surgery. 2011, 36: 1780-4.

56. Farrar JT, Young JP, Jr., LaMoreaux L, Werth JL, Poole MR. Clinical importance of changes in chronic pain intensity measured on an 11-point numerical pain rating scale. Pain. 2001, 94: 149-58.

57. Ferraz MB, Quaresma MR, Aquino LR, Atra E, Tugwell P, Goldsmith CH. Reliability of pain scales in the assessment of literate and illiterate patients with rheumatoid arthritis. J Rheumatol. 1990, 17: 1022-4.

58. Fischer KJ, Manson TT, Pfaeffle HJ, Tomaino MM, Woo SL. A method for measuring joint kinematics designed for accurate registration of kinematic data to models constructed from ct data. J Biomech. 2001, 34: 377-83.

59. Fliegel BE, Ekblad J, Varacallo M. Anatomy, shoulder and upper limb, elbow annular ligament. *Statpearls*. Treasure Island (FL), 2021.

60. Friedman SL, Palmer AK. The ulnar impaction syndrome. Hand Clin. 1991, 7: 295-310.

61. Friedman SL, Palmer AK, Short WH, Levinsohn EM, Halperin LS. The change in ulnar variance with grip. The Journal of hand surgery. 1993, 18: 713-6.

62. Gammon B, Lalone E, Nishiwaki M, Willing R, Johnson J, King GJW. Arthrokinematics of the distal radioulnar joint measured using intercartilage distance in an in vitro model. The Journal of hand surgery. 2018, 43: 283 e1- e9.

63. Garcia-Elias M, Smith DE, Llusa M. Surgical approach to the triangular fibrocartilage complex. Techniques in hand & upper extremity surgery. 2003, 7: 134-40.

64. Geissler WB. Arthroscopic knotless peripheral ulnar-sided tfcc repair. J Wrist Surg. 2015, 4: 143-7.

65. Geissler WB, Fernandez DL, Lamey DM. Distal radioulnar joint injuries associated with fractures of the distal radius. Clin Orthop Relat Res. 1996: 135-46.

66. Gillis JA, Soreide E, Khouri JS, Kadar A, Berger RA, Moran SL. Outcomes of the adams-berger ligament reconstruction for the distal radioulnar joint instability in 95 consecutive cases. J Wrist Surg. 2019, 8: 268-75.

67. Glowacki KA, Shin LA. Stabilization of the unstable distal ulna: The linscheid-hui procedure. Techniques in hand & upper extremity surgery. 1999, 3: 229-36.

68. Gofton WT, Gordon KD, Dunning CE, Johnson JA, King GJ. Soft-tissue stabilizers of the distal radioulnar joint: An in vitro kinematic study. The Journal of hand surgery. 2004, 29: 423-31.

69. Goto A, Moritomo H, Murase T et al. In vivo elbow biomechanical analysis during flexion: Three-dimensional motion analysis using magnetic resonance imaging. J Shoulder Elbow Surg. 2004, 13: 441-7.

70. Guan S, Gray HA, Keynejad F, Pandy MG. Mobile biplane x-ray imaging system for measuring 3d dynamic joint motion during overground gait. IEEE Trans Med Imaging. 2016, 35: 326-36.

71. Gummesson C, Ward MM, Atroshi I. The shortened disabilities of the arm, shoulder and hand questionnaire (quickdash): Validity and reliability based on responses within the full-length dash. BMC musculoskeletal disorders. 2006, 7: 44.

72. Gupta S, Halai M, Al-Maiyah M, Muller S. Which measure should be used to assess the patient's functional outcome after distal radius fracture ? Acta orthopaedica Belgica. 2014, 80: 116-8.

73. Hagert CG. The distal radioulnar joint in relation to the whole forearm. Clin Orthop Relat Res. 1992: 56-64.

74. Hagert CG. Distal radius fracture and the distal radioulnar joint--anatomical considerations. Handchir Mikrochir Plast Chir. 1994, 26: 22-6.

75. Hagert E, Hagert CG. Understanding stability of the distal radioulnar joint through an understanding of its anatomy. Hand Clin. 2010, 26: 459-66.

76. Hansen L, de Raedt S, Jorgensen PB, Mygind-Klavsen B, Kaptein B, Stilling M. Dynamic radiostereometric analysis for evaluation of hip joint pathomechanics. Journal of experimental orthopaedics. 2017, 4: 20.

77. Hansen L, De Raedt S, Jorgensen PB, Mygind-Klavsen B, Kaptein B, Stilling M. Marker free model-based radiostereometric analysis for evaluation of hip joint kinematics: A validation study. Bone & joint research. 2018, 7: 379-87.

78. Hansen TB, Stilling M. Equally good fixation of cemented and uncemented cups in total trapeziometacarpal joint prostheses. A randomized clinical rsa study with 2-year follow-up. Acta orthopaedica. 2013, 84: 98-105.

79. Hauck RM, Skahen J, 3rd, Palmer AK. Classification and treatment of ulnar styloid nonunion. The Journal of hand surgery. 1996, 21: 418-22.

80. Haugstvedt JR, Husby T. Results of repair of peripheral tears in the triangular fibrocartilage complex using an arthroscopic suture technique. Scand J Plast Reconstr Surg Hand Surg. 1999, 33: 439-47.

81. Haugstvedt JR, Langer MF, Berger RA. Distal radioulnar joint: Functional anatomy, including pathomechanics. The Journal of hand surgery, European volume. 2017, 42: 338-45.

82. Heitner HD, Werner FW, Cavallaro SM, Willsey SR, Harley BJ. Biomechanical evaluation of distal radioulnar joint instability and adams procedure. The Journal of hand surgery. 2020, 45: 909-17.

83. Helle Puggård KCP, Alice Ørts. National målestandard ledmåling - kraftmåling. 2014.

84. Hemmingsen CK, Thillemann TM, Elmengaard B et al. Elbow biomechanics, radiocapitellar joint pressure, and interosseous membrane strain before and after radial head arthroplasty. Journal of orthopaedic research : official publication of the Orthopaedic Research Society. 2020, 38: 510-22.

85. Hermansdorfer JD, Kleinman WB. Management of chronic peripheral tears of the triangular fibrocartilage complex. The Journal of hand surgery. 1991, 16: 340-6.

86. Hess F, Farshad M, Sutter R, Nagy L, Schweizer A. A novel technique for detecting instability of the distal radioulnar joint in complete triangular fibrocartilage complex lesions. J Wrist Surg. 2012, 1: 153-8.

87. Hess F, Sutter R, Nagy L, Schweizer A. Stability and clinical outcome after reconstruction of complete triangular fibrocartilage disruption. J Wrist Surg. 2016, 5: 124-30.

88. Hoang-Kim A, Pegreffi F, Moroni A, Ladd A. Measuring wrist and hand function: Common scales and checklists. Injury. 2011, 42: 253-8.

89. Hojo J, Omokawa S, Iida A, Ono H, Moritomo H, Tanaka Y. Three-dimensional kinematic analysis of the distal radioulnar joint in the axial-loaded extended wrist position. The Journal of hand surgery. 2019, 44: 336 e1- e6.

90. Horsager K, Kaptein BL, Romer L, Jorgensen PB, Stilling M. Dynamic rsa for the evaluation of inducible micromotion of oxford uka during step-up and step-down motion. Acta orthopaedica. 2017, 88: 275-81.

91. Hudak PL, Amadio PC, Bombardier C. Development of an upper extremity outcome measure: The dash (disabilities of the arm, shoulder and hand) [corrected]. The upper extremity collaborative group (uecg). American journal of industrial medicine. 1996, 29: 602-8.

92. Hulten O. Über anatomische variationen der hand-gelenkknochen. Acta Radiol 1928, 9: 155–69.

93. Iida A, Omokawa S, Akahane M, Kawamura K, Takayama K, Tanaka Y. Distal radioulnar joint stress radiography for detecting radioulnar ligament injury. The Journal of hand surgery. 2012, 37: 968-74.

94. Iida A, Omokawa S, Moritomo H et al. Biomechanical study of the extensor carpi ulnaris as a dynamic wrist stabilizer. The Journal of hand surgery. 2012, 37: 2456-61.

95. Iida A, Omokawa S, Moritomo H et al. Effect of wrist position on distal radioulnar joint stability: A biomechanical study. Journal of orthopaedic research : official publication of the Orthopaedic Research Society. 2014, 32: 1247-51.

96. Iordache SD, Rowan R, Garvin GJ, Osman S, Grewal R, Faber KJ. Prevalence of triangular fibrocartilage complex abnormalities on mri scans of asymptomatic wrists. The Journal of hand surgery. 2012, 37: 98-103.

97. Ishii S, Palmer AK, Werner FW, Short WH, Fortino MD. Pressure distribution in the distal radioulnar joint. The Journal of hand surgery. 1998, 23: 909-13.

98. Iwasaki N, Minami A. Arthroscopically assisted reattachment of avulsed triangular fibrocartilage complex to the fovea of the ulnar head. The Journal of hand surgery. 2009, 34: 1323-6.

99. Iwasaki N, Nishida K, Motomiya M, Funakoshi T, Minami A. Arthroscopic-assisted repair of avulsed triangular fibrocartilage complex to the fovea of the ulnar head: A 2- to 4-year follow-up study. Arthroscopy. 2011, 27: 1371-8.

100. Jester A, Harth A, Germann G. Measuring levels of upper-extremity disability in employed adults using the dash questionnaire. The Journal of hand surgery. 2005, 30: 1074 e1- e10.

101. Jung JM, Baek GH, Kim JH, Lee YH, Chung MS. Changes in ulnar variance in relation to forearm rotation and grip. J Bone Joint Surg Br. 2001, 83: 1029-33.

102. Jupiter JB. Commentary: The effect of ulnar styloid fractures on patient-rated outcomes after volar locking plating of distal radius fractures. The Journal of hand surgery. 2009, 34: 1603-4.

103. Kaptein BL, Valstar ER, Stoel BC, Rozing PM, Reiber JH. A new model-based rsa method validated using cad models and models from reversed engineering. J Biomech. 2003, 36: 873-82.

104. Kaptein BL, Valstar ER, Stoel BC, Rozing PM, Reiber JHC. Evaluation of three pose estimation algorithms for model-based roentgen stereophotogrammetric analysis. P I Mech Eng H. 2004, 218: 231-8.

105. Karnezis IA, Fragkiadakis EG. Association between objective clinical variables and patient-rated disability of the wrist. J Bone Joint Surg Br. 2002, 84: 967-70.

106. Karrholm J, Borssen B, Lowenhielm G, Snorrason F. Does early micromotion of femoral stem prostheses matter - 4-7-year stereoradiographic follow-up of 84 cemented prostheses. Journal of Bone and Joint Surgery-British Volume. 1994, 76b: 912-7.

107. Keogh CF, Wong AD, Wells NJ, Barbarie JE, Cooperberg PL. High-resolution sonography of the triangular fibrocartilage: Initial experience and correlation with mri and arthroscopic findings. AJR Am J Roentgenol. 2004, 182: 333-6.

108. Kermarrec G, Cohen G, Upex P, Fontes D. Arthroscopic foveal reattachment of the triangular fibro cartilaginous complex. J Wrist Surg. 2020, 9: 256-62.

109. Kihara H, Short WH, Werner FW, Fortino MD, Palmer AK. The stabilizing mechanism of the distal radioulnar joint during pronation and supination. The Journal of hand surgery. 1995, 20: 930-6.

110. Kim B, Yoon HK, Nho JH et al. Arthroscopically assisted reconstruction of triangular fibrocartilage complex foveal avulsion in the ulnar variance-positive patient. Arthroscopy. 2013, 29: 1762-8.

111. Kim JK, Koh YD, Do NH. Should an ulnar styloid fracture be fixed following volar plate fixation of a distal radial fracture? J Bone Joint Surg Am. 2010, 92: 1-6.

112. Kim JK, Park ES. Comparative responsiveness and minimal clinically important differences for idiopathic ulnar impaction syndrome. Clin Orthop Relat Res. 2013, 471: 1406-11.

113. Kim JK, Park MG, Shin SJ. What is the minimum clinically important difference in grip strength? Clin Orthop Relat Res. 2014, 472: 2536-41.

114. Kim JP, Park MJ. Assessment of distal radioulnar joint instability after distal radius fracture: Comparison of computed tomography and clinical examination results. The Journal of hand surgery. 2008, 33: 1486-92.

115. King GJ, McMurtry RY, Rubenstein JD, Gertzbein SD. Kinematics of the distal radioulnar joint. The Journal of hand surgery. 1986, 11: 798-804.

116. King GJ, McMurtry RY, Rubenstein JD, Ogston NG. Computerized tomography of the distal radioulnar joint: Correlation with ligamentous pathology in a cadaveric model. The Journal of hand surgery. 1986, 11: 711-7.

117. Kinninmonth AW, Chan KM. A study of age-related changes of the articular disc of the wrist in hong kong chinese. J Hand Surg Br. 1990, 15: 358-61.

118. Kirschenbaum D, Sieler S, Solonick D, Loeb DM, Cody RP. Arthrography of the wrist. Assessment of the integrity of the ligaments in young asymptomatic adults. J Bone Joint Surg Am. 1995, 77: 1207-9.

119. Kleinman WB. Stability of the distal radioulna joint: Biomechanics, pathophysiology, physical diagnosis, and restoration of function what we have learned in 25 years. The Journal of hand surgery. 2007, 32: 1086-106.

120. Kleinman WB, Graham TJ. The distal radioulnar joint capsule: Clinical anatomy and role in posttraumatic limitation of forearm rotation. The Journal of hand surgery. 1998, 23: 588-99.

121. Koo TK, Li MY. A guideline of selecting and reporting intraclass correlation coefficients for reliability research. J Chiropr Med. 2016, 15: 155-63.

122. Kwon YW, Park JH, Choi IC, Lee JS, Park JW. Revisional triangular fibrocartilage complex (tfcc) repair using arthroscopic one-tunnel transosseous suture: Preliminary results. Arch Orthop Trauma Surg. 2020.

123. LaStayo PC, Wheeler DL. Reliability of passive wrist flexion and extension goniometric measurements: A multicenter study. Phys Ther. 1994, 74: 162-74; discussion 74-6.

124. Leardini A, Chiari L, Della Croce U, Cappozzo A. Human movement analysis using stereophotogrammetry. Part 3. Soft tissue artifact assessment and compensation. Gait Posture. 2005, 21: 212-25.

125. Lee YH, Choi YR, Kim S, Song HT, Suh JS. Intrinsic ligament and triangular fibrocartilage complex (tfcc) tears of the wrist: Comparison of isovolumetric 3d-thrive sequence mr arthrography and conventional mr image at 3 t. Magn Reson Imaging. 2013, 31: 221-6.

126. Lester B, Halbrecht J, Levy IM, Gaudinez R. "Press test" for office diagnosis of triangular fibrocartilage complex tears of the wrist. Ann Plast Surg. 1995, 35: 41-5.

127. Lévesque L. Nyquist sampling theorem: Understanding the illusion of a spinning wheel captured with a video camera. Phys Educ. 2014, 49: 697-705.

128. Lindau T, Adlercreutz C, Aspenberg P. Peripheral tears of the triangular fibrocartilage complex cause distal radioulnar joint instability after distal radial fractures. The Journal of hand surgery. 2000, 25: 464-8.

129. Lindau T, Arner M, Hagberg L. Intraarticular lesions in distal fractures of the radius in young adults. A descriptive arthroscopic study in 50 patients. J Hand Surg Br. 1997, 22: 638-43.

130. Lindau T, Hagberg L, Adlercreutz C, Jonsson K, Aspenberg P. Distal radioulnar instability is an independent worsening factor in distal radial fractures. Clin Orthop Relat Res. 2000: 229-35.

131. Lindau T, Runnquist K, Aspenberg P. Patients with laxity of the distal radioulnar joint after distal radial fractures have impaired function, but no loss of strength. Acta Orthop Scand. 2002, 73: 151-6.

132. Lindgren L, Jorgensen PB, Morup RMS et al. Similar patient positioning: A key factor in follow-up studies when using model-based radiostereometric analysis of the hip. Radiography (Lond). 2020, 26: e45-e51.

133. Linscheid RL. Biomechanics of the distal radioulnar joint. Clin Orthop Relat Res. 1992: 46-55.

134. Lo IK, MacDermid JC, Bennett JD, Bogoch E, King GJ. The radioulnar ratio: A new method of quantifying distal radioulnar joint subluxation. The Journal of hand surgery. 2001, 26: 236-43.

135. Logan AJ, Lindau TR. The management of distal ulnar fractures in adults: A review of the literature and recommendations for treatment. Strategies Trauma Limb Reconstr. 2008, 3: 49-56.

136. Luchetti R, Atzei A. Arthroscopic assisted tendon reconstruction for triangular fibrocartilage complex irreparable tears. The Journal of hand surgery, European volume. 2017, 42: 346-51.

137. Luchetti R, Atzei A, Cozzolino R, Fairplay T, Badur N. Comparison between open and arthroscopic-assisted foveal triangular fibrocartilage complex repair for post-traumatic distal radio-ulnar joint instability. The Journal of hand surgery, European volume. 2014, 39: 845-55.

138. MacDermid JC, Kramer JF, Woodbury MG, McFarlane RM, Roth JH. Interrater reliability of pinch and grip strength measurements in patients with cumulative trauma disorders. J Hand Ther. 1994, 7: 10-4.

139. MacDermid JC, Turgeon T, Richards RS, Beadle M, Roth JH. Patient rating of wrist pain and disability: A reliable and valid measurement tool. J Orthop Trauma. 1998, 12: 577-86.

140. Madanat R, Makinen TJ, Moritz N, Mattila KT, Aro HT. Accuracy and precision of radiostereometric analysis in the measurement of three-dimensional micromotion in a fracture model of the distal radius. Journal of orthopaedic research : official publication of the Orthopaedic Research Society. 2005, 23: 481-8.

141. Malone PS, Cooley J, Morris J, Terenghi G, Lees VC. The biomechanical and functional relationships of the proximal radioulnar joint, distal radioulnar joint, and interosseous ligament. The Journal of hand surgery, European volume. 2015, 40: 485-93.

142. Mathiowetz V, Weber K, Volland G, Kashman N. Reliability and validity of grip and pinch strength evaluations. The Journal of hand surgery. 1984, 9: 222-6.

143. Matsuki KO, Matsuki K, Mu S et al. In vivo 3d kinematics of normal forearms: Analysis of dynamic forearm rotation. Clin Biomech (Bristol, Avon). 2010, 25: 979-83.

144. McDonald CP, Moutzouros V, Bey MJ. Measuring dynamic in-vivo elbow kinematics: Description of technique and estimation of accuracy. J Biomech Eng. 2012, 134: 124502.

145. McPhail SM, Bagraith KS, Schippers M, Wells PJ, Hatton A. Use of condition-specific patient-reported outcome measures in clinical trials among patients with wrist osteoarthritis: A systematic review. Adv Orthop. 2012, 2012: 273421.'

146. Mehta SP, MacDermid JC, Richardson J, MacIntyre NJ, Grewal R. A systematic review of the measurement properties of the patient-rated wrist evaluation. J Orthop Sports Phys Ther. 2015, 45: 289-98.

147. Meyer D, Schweizer A, Nagy L. Anatomic reconstruction of distal radioulnar ligaments with tendon graft for treating distal radioulnar joint instability: Surgical technique and outcome. Techniques in hand & upper extremity surgery. 2017, 21: 107-13.

148. Mino DE, Palmer AK, Levinsohn EM. The role of radiography and computerized tomography in the diagnosis of subluxation and dislocation of the distal radioulnar joint. The Journal of hand surgery. 1983, 8: 23-31.

149. Mino DE, Palmer AK, Levinsohn EM. Radiography and computerized tomography in the diagnosis of incongruity of the distal radio-ulnar joint. A prospective study. J Bone Joint Surg Am. 1985, 67: 247-52.

150. Miranda DL, Rainbow MJ, Crisco JJ, Fleming BC. Kinematic differences between optical motion capture and biplanar videoradiography during a jump-cut maneuver. J Biomech. 2013, 46: 567-73.

151. Moritomo H, Masatomi T, Murase T, Miyake J, Okada K, Yoshikawa H. Open repair of foveal avulsion of the triangular fibrocartilage complex and comparison by types of injury mechanism. The Journal of hand surgery. 2010, 35: 1955-63.

152. Moriya T, Aoki M, Iba K, Ozasa Y, Wada T, Yamashita T. Effect of triangular ligament tears on distal radioulnar joint instability and evaluation of three clinical tests: A biomechanical study. The Journal of hand surgery, European volume. 2009, 34: 219-23.

153. Mrkonjic A, Geijer M, Lindau T, Tagil M. The natural course of traumatic triangular fibrocartilage complex tears in distal radial fractures: A 13-15 year follow-up of arthroscopically diagnosed but untreated injuries. The Journal of hand surgery. 2012, 37: 1555-60.

154. Muhlenhaupt M. Measurement of joint motion - a guide to goniometry, 1st edition - norkin,cc, white,dj. Am J Occup Ther. 1986, 40: 369-70.

155. Nagata H, Hosny S, Giddins GE. In-vivo measurement of distal radio-ulnar joint translation. Hand Surg. 2013, 18: 15-20.

156. Nakamura R, Horii E, Imaeda T, Nakao E. Criteria for diagnosing distal radioulnar joint subluxation by computed tomography. Skeletal Radiol. 1996, 25: 649-53.

157. Nakamura R, Horii E, Imaeda T, Tsunoda K, Nakao E. Distal radioulnar joint subluxation and dislocation diagnosed by standard roentgenography. Skeletal Radiol. 1995, 24: 91-4.

158. Nakamura T. Druj instability: Arthroscopic repair of the detached tfcc to the fovea of the ulna. In: Del piñal f. (eds) arthroscopic management of ulnar pain. Springer, Berlin, Heidelberg, 2012.

159. Nakamura T, Iwamoto T, Matsumura N, Sato K, Toyama Y. Radiographic and arthroscopic assessment of druj instability due to foveal avulsion of the radioulnar ligament in distal radius fractures. J Wrist Surg. 2014, 3: 12-7.

160. Nakamura T, Sato K, Okazaki M, Toyama Y, Ikegami H. Repair of foveal detachment of the triangular fibrocartilage complex: Open and arthroscopic transosseous techniques. Hand Clin. 2011, 27: 281-90.

161. Nakamura T, Yabe Y, Horiuchi Y. Functional anatomy of the triangular fibrocartilage complex. J Hand Surg-Brit Eur. 1996, 21b: 581-6.

162. Nakamura T, Yabe Y, Horiuchi Y, Yamazaki N. In vivo motion analysis of forearm rotation utilizing magnetic resonance imaging. Clin Biomech. 1999, 14: 315-20.

163. Nelissen RG, Pijls BG, Karrholm J, Malchau H, Nieuwenhuijse MJ, Valstar ER. Rsa and registries: The quest for phased introduction of new implants. J Bone Joint Surg Am. 2011, 93 Suppl 3: 62-5.

164. Nielsen ET, Stentz-Olesen K, de Raedt S et al. Influence of the anterolateral ligament on knee laxity: A biomechanical cadaveric study measuring knee kinematics in 6 degrees of freedom using dynamic radiostereometric analysis. Orthop J Sports Med. 2018, 6: 2325967118789699.

165. Nieuwenhuijse MJ, Valstar ER, Kaptein BL, Nelissen RG. Good diagnostic performance of early migration as a predictor of late aseptic loosening of acetabular cups: Results from ten years of follow-up with roentgen stereophotogrammetric analysis (rsa). J Bone Joint Surg Am. 2012, 94: 874-80.

166. Nishiwaki M, Nakamura T, Nagura T, Toyama Y, Ikegami H. Ulnar-shortening effect on distal radioulnar joint pressure: A biomechanical study. The Journal of hand surgery. 2008, 33: 198-205.

167. Oda T, Wada T, Iba K, Aoki M, Tamakawa M, Yamashita T. Reconstructed animation from four-phase grip mri of the wrist with ulnar-sided pain. The Journal of hand surgery, European volume. 2013, 38: 746-50.

168. Ohmori M, Azuma H. Morphology and distribution of nerve endings in the human triangular fibrocartilage complex. J Hand Surg Br. 1998, 23: 522-5.

169. Omokawa S, Iida A, Kawamura K et al. A biomechanical perspective on distal radioulnar joint instability. J Wrist Surg. 2017, 6: 88-96.

170. Omokawa S, Imaeda T, Sawaizumi T et al. Responsiveness of the japanese version of the patient-rated wrist evaluation (prwe-j) and physical impairment measurements in evaluating recovery after treatment of ulnocarpal abutment syndrome. J Orthop Sci. 2012, 17: 551-5.

171. Onishi T, Omokawa S, Iida A et al. Biomechanical study of distal radioulnar joint ballottement test. Journal of orthopaedic research : official publication of the Orthopaedic Research Society. 2017, 35: 1123-7.

172. Ozer K, Zhu AF, Siljander B, Lawton JN, Waljee JF. The effect of axial loading on ulnar variance. J Wrist Surg. 2018, 7: 247-52.

173. Palmer AK. Triangular fibrocartilage complex lesions: A classification. The Journal of hand surgery. 1989, 14: 594-606.

174. Palmer AK. Triangular fibrocartilage disorders: Injury patterns and treatment. Arthroscopy. 1990, 6: 125-32.

175. Palmer AK, Werner FW. The triangular fibrocartilage complex of the wrist--anatomy and function. The Journal of hand surgery. 1981, 6: 153-62.

176. Palmer AK, Werner FW. Biomechanics of the distal radioulnar joint. Clin Orthop Relat Res. 1984: 26-35.

177. Palmer AK, Werner FW, Glisson RR, Murphy DJ. Partial excision of the triangular fibrocartilage complex. The Journal of hand surgery. 1988, 13: 391-4.

178. Park JH, Kim D, Park JW. Arthroscopic one-tunnel transosseous foveal repair for triangular fibrocartilage complex (tfcc) peripheral tear. Arch Orthop Trauma Surg. 2018, 138: 131-8.

179. Park MJ, Kim JP. Reliability and normal values of various computed tomography methods for quantifying distal radioulnar joint translation. J Bone Joint Surg Am. 2008, 90: 145-53.

180. Pederzini L, Luchetti R, Soragni O et al. Evaluation of the triangular fibrocartilage complex tears by arthroscopy, arthrography, and magnetic resonance imaging. Arthroscopy. 1992, 8: 191-7.

181. Pederzini LA, Tosi M, Prandini M, Botticella C. All-inside suture technique for palmer class 1b triangular fibrocartilage repair. Arthroscopy. 2007, 23: 1130 e1-4.

182. Peolsson A, Hedlund R, Oberg B. Intra- and inter-tester reliability and reference values for hand strength. J Rehabil Med. 2001, 33: 36-41.

183. Pfaeffle HJ, Fischer KJ, Manson TT, Tomaino MM, Woo SL, Herndon JH. Role of the forearm interosseous ligament: Is it more than just longitudinal load transfer? The Journal of hand surgery. 2000, 25: 683-8.

184. Pickering GT, Nagata H, Giddins GEB. In-vivo three-dimensional measurement of distal radioulnar joint translation in normal and clinically unstable populations. J Hand Surg-Eur Vol. 2016, 41: 521-6.

185. Pijls BG, Nieuwenhuijse MJ, Fiocco M et al. Early proximal migration of cups is associated with late revision in tha: A systematic review and meta-analysis of 26 rsa studies and 49 survivalstudies. Acta orthopaedica. 2012, 83: 583-91.

186. Pijls BG, Plevier JWM, Nelissen R. Rsa migration of total knee replacements. Acta orthopaedica. 2018, 89: 320-8.

187. Pijls BG, Valstar ER, Nouta KA et al. Early migration of tibial components is associated with late revision: A systematic review and meta-analysis of 21,000 knee arthroplasties. Acta orthopaedica. 2012, 83: 614-24.

188. Poitevin LA. Anatomy and biomechanics of the interosseous membrane: Its importance in the longitudinal stability of the forearm. Hand Clin. 2001, 17: 97-110, vii.

189. Prosser R, Harvey L, Lastayo P, Hargreaves I, Scougall P, Herbert RD. Provocative wrist tests and mri are of limited diagnostic value for suspected wrist ligament injuries: A cross-sectional study. J Physiother. 2011, 57: 247-53.

190. Rettig AC. Athletic injuries of the wrist and hand. Part i: Traumatic injuries of the wrist. Am J Sports Med. 2003, 31: 1038-48.

191. Riggenbach MD, Conrad BP, Wright TW, Dell PC. Distal oblique bundle reconstruction and distal radioulnar joint instability. J Wrist Surg. 2013, 2: 330-6.

192. Rigo IZ, Riano F, Kalapos R, Haugstvedt JR. Biomechanical comparison of modified adams-berger and dx technique in druj reconstruction. Journal of Wrist Surgery. 2021, 10: 516-22.

193. Robba V, Fowler A, Karantana A, Grindlay D, Lindau T. Open versus arthroscopic repair of 1b ulnar-sided triangular fibrocartilage complex tears: A systematic review. Hand (N Y). 2020, 15: 456-64.

194. Ruch DS, Yang CC, Smith BP. Results of acute arthroscopically repaired triangular fibrocartilage complex injuries associated with intra-articular distal radius fractures. Arthroscopy. 2003, 19: 511-6.

195. Ryd L, Albrektsson BEJ, Carlsson L et al. Roentgen stereophotogrammetric analysis as a predictor of mechanical loosening of knee prostheses. Journal of Bone and Joint Surgery-British Volume. 1995, 77b: 377-83.

196. Saito T, Malay S, Chung KC. A systematic review of outcomes after arthroscopic debridement for triangular fibrocartilage complex tear. Plast Reconstr Surg. 2017, 140: 697e-708e.

197. Salaffi F, Stancati A, Silvestri CA, Ciapetti A, Grassi W. Minimal clinically important changes in chronic musculoskeletal pain intensity measured on a numerical rating scale. Eur J Pain. 2004, 8: 283-91.

198. Sammer DM, Shah HM, Shauver MJ, Chung KC. The effect of ulnar styloid fractures on patient-rated outcomes after volar locking plating of distal radius fractures. The Journal of hand surgery. 2009, 34: 1595-602.

199. Saupe N, Prussmann KP, Luechinger R, Bosiger P, Marincek B, Weishaupt D. Mr imaging of the wrist: Comparison between 1.5- and 3-t mr imaging--preliminary experience. Radiology. 2005, 234: 256-64.

200. Schmitt JS, Di Fabio RP. Reliable change and minimum important difference (mid) proportions facilitated group responsiveness comparisons using individual threshold criteria. J Clin Epidemiol. 2004, 57: 1008-18.

201. Schonnemann JO, Hansen TB, Soballe K. Translation and validation of the danish version of the patient rated wrist evaluation questionnaire. J Plast Surg Hand Surg. 2013, 47: 489-92.

202. Schuind F, An KN, Berglund L et al. The distal radioulnar ligaments: A biomechanical study. The Journal of hand surgery. 1991, 16: 1106-14.

203. Selvik G. Roentgen stereophotogrammetry. A method for the study of the kinematics of the skeletal system. Acta Orthop Scand Suppl. 1989, 232: 1-51.

204. Semisch M, Hagert E, Garcia-Elias M, Lluch A, Rein S. Histological assessment of the triangular fibrocartilage complex. The Journal of hand surgery, European volume. 2016, 41: 527-33.

205. Seo KN, Park MJ, Kang HJ. Anatomic reconstruction of the distal radioulnar ligament for posttraumatic distal radioulnar joint instability. Clin Orthop Surg. 2009, 1: 138-45.

206. Shen J, Papadonikolakis A, Garrett JP, Davis SM, Ruch DS. Ulnar-positive variance as a predictor of distal radioulnar joint ligament disruption. The Journal of hand surgery. 2005, 30: 1172-7.

207. Shih JT, Lee HM. Functional results post-triangular fibrocartilage complex reconstruction with extensor carpi ulnaris with or without ulnar shortening in chronic distal radioulnar joint instability. Hand Surg. 2005, 10: 169-76.

208. Shinohara T, Tatebe M, Okui N, Yamamoto M, Kurimoto S, Hirata H. Arthroscopically assisted repair of triangular fibrocartilage complex foveal tears. The Journal of hand surgery. 2013, 38: 271-7.

209. Shaaban H, Giakas G, Bolton M et al. Contact area inside the distal radioulnar joint: Effect of axial loading and position of the forearm. Clin Biomech (Bristol, Avon). 2007, 22: 313-8.

210. Sorensen AA, Howard D, Tan WH, Ketchersid J, Calfee RP. Minimal clinically important differences of 3 patient-rated outcomes instruments. The Journal of hand surgery. 2013, 38: 641-9.

211. Spinner M, Kaplan EB. Extensor carpi ulnaris. Its relationship to the stability of the distal radio-ulnar joint. Clin Orthop Relat Res. 1970, 68: 124-9.

212. Squires JH, England E, Mehta K, Wissman RD. The role of imaging in diagnosing diseases of the distal radioulnar joint, triangular fibrocartilage complex, and distal ulna. AJR Am J Roentgenol. 2014, 203: 146-53.

213. Stentz-Olesen K, Nielsen ET, De Raedt S et al. Validation of static and dynamic radiostereometric analysis of the knee joint using bone models from ct data. Bone & joint research. 2017, 6: 376-84.

214. Stilling M, Kold S, de Raedt S, Andersen NT, Rahbek O, Soballe K. Superior accuracy of model-based radiostereometric analysis for measurement of polyethylene wear: A phantom study. Bone & joint research. 2012, 1: 180-91.

215. Stuart PR. Pronator quadratus revisited. J Hand Surg Br. 1996, 21: 714-22.

216. Stuart PR, Berger RA, Linscheid RL, An KN. The dorsopalmar stability of the distal radioulnar joint. The Journal of hand surgery. 2000, 25: 689-99.

217. Szabo RM. Distal radioulnar joint instability. J Bone Joint Surg Am. 2006, 88: 884-94.

218. Takagi T, Nakamura T, Fukuoka M. Arthroscopic capsular repair for triangular fibrocartilage complex tears. J Wrist Surg. 2021, 10: 249-54.

219. Taljanovic MS, Sheppard JE, Jones MD, Switlick DN, Hunter TB, Rogers LF. Sonography and sonoarthrography of the scapholunate and lunotriquetral ligaments and triangular

fibrocartilage disk: Initial experience and correlation with arthrography and magnetic resonance arthrography. J Ultrasound Med. 2008, 27: 179-91.

220. Tang JB. Re: Levels of experience of surgeons in clinical studies. The Journal of hand surgery, European volume. 2009, 34: 137-8.

221. Tang JB, Ryu J, Kish V. The triangular fibrocartilage complex: An important component of the pulley for the ulnar wrist extensor. The Journal of hand surgery. 1998, 23: 986-91.

222. Tashman S, Anderst W. In-vivo measurement of dynamic joint motion using high speed biplane radiography and ct: Application to canine acl deficiency. J Biomech Eng-T Asme. 2003, 125: 238-45.

223. Tay SC, Berger RA, Tomita K, Tan ET, Amrami KK, An KN. In vivo three-dimensional displacement of the distal radioulnar joint during resisted forearm rotation. J Hand Surg-Am. 2007, 32a: 450-8.

224. Tay SC, Tomita K, Berger RA. The "ulnar fovea sign" for defining ulnar wrist pain: An analysis of sensitivity and specificity. The Journal of hand surgery. 2007, 32: 438-44.

225. Tay SC, van Riet R, Kazunari T, Amrami KK, An KN, Berger RA. In-vivo kinematic analysis of forearm rotation using helical axis analysis. Clin Biomech. 2010, 25: 655-9.

226. Tay SC, van Riet R, Kazunari T et al. A method for in-vivo kinematic analysis of the forearm. J Biomech. 2008, 41: 56-62.

227. Ten Brinke B, Beumer A, Koenraadt KLM, Eygendaal D, Kraan GA, Mathijssen NMC. The accuracy and precision of radiostereometric analysis in upper limb arthroplasty. Acta orthopaedica. 2017, 88: 320-5.

228. Therapists ASoH. Clinical assessment recommendations. American Society of Hand Therapists. 1992, 2nd edition: 41-5, 56-70.

229. Thillemann JK, De Raedt S, Hansen TB, Munk B, Stilling M. Distal radioulnar joint stabilization with open foveal reinsertion versus tendon graft reconstruction: An experimental study using radiostereometry. Journal of experimental orthopaedics. 2021a, 8: 10.

230. Thillemann JK, De Raedt S, Jorgensen PB, Romer L, Hansen TB, Stilling M. Distal radioulnar joint stability measured with radiostereometry during the piano key test. The Journal of hand surgery, European volume. 2020: 1753193420934689.

231. Thillemann JK, De Raedt S, S. Petersen, E. T. Puhakka, K. B. Hansen, T. B. Stilling, M. Kinematics of the distal radioulnar joint before and after open reinsertion of the foveal triangular fibrocartilage complex in comparison to normal joints. Acta orthopaedica. 2022.

232. Thillemann JT, De Raedt S, Petersen ET, Puhakka KB, Hansen TB, Stilling M. Normal values of distal radioulnar joint kinematics during a dynamic press test. J Wrist Surg. 2021b. e-publication December 2021. DOI: 10.1055/s-0041-1740486

233. Tolat AR, Stanley JK, Trail IA. A cadaveric study of the anatomy and stability of the distal radioulnar joint in the coronal and transverse planes. J Hand Surg Br. 1996, 21: 587-94.

234. Tomaino MM. The importance of the pronated grip x-ray view in evaluating ulnar variance. The Journal of hand surgery. 2000, 25: 352-7.

235. Trumble TE, Gilbert M, Vedder N. Isolated tears of the triangular fibrocartilage: Management by early arthroscopic repair. The Journal of hand surgery. 1997, 22: 57-65.

236. Tsai PC, Paksima N. The distal radioulnar joint. Bull NYU Hosp Jt Dis. 2009, 67: 90-6.

237. Tse WL, Lau SW, Wong WY et al. Arthroscopic reconstruction of triangular fibrocartilage complex (tfcc) with tendon graft for chronic druj instability. Injury. 2013, 44: 386-90.

238. Uvehammer J, Karrholm J. Inducible displacements of cemented tibial components during weight-bearing and knee extension observations during dynamic radiostereometry related to joint positions and 2 years history of migration in 16 tkr. Journal of orthopaedic research : official publication of the Orthopaedic Research Society. 2001, 19: 1168-77.

239. Valstar ER, Gill R, Ryd L, Flivik G, Borlin N, Karrholm J. Guidelines for standardization of radiostereometry (rsa) of implants. Acta orthopaedica. 2005, 76: 563-72.

240. Valstar ER, Nelissen RGHH, Reiber JHC, Rozing PM. The use of roentgen stereophotogrammetry to study micromotion of orthopaedic implants. Isprs J Photogramm. 2002, 56: 376-89.

241. Vezeridis PS, Yoshioka H, Han R, Blazar P. Ulnar-sided wrist pain. Part i: Anatomy and physical examination. Skeletal Radiol. 2010, 39: 733-45.

242. Walenkamp MM, de Muinck Keizer RJ, Goslings JC, Vos LM, Rosenwasser MP, Schep NW. The minimum clinically important difference of the patient-rated wrist evaluation score for patients with distal radius fractures. Clin Orthop Relat Res. 2015, 473: 3235-41.

243. Watanabe A, Souza F, Vezeridis PS, Blazar P, Yoshioka H. Ulnar-sided wrist pain. Ii. Clinical imaging and treatment. Skeletal Radiol. 2010, 39: 837-57.

244. Wechsler RJ, Wehbe MA, Rifkin MD, Edeiken J, Branch HM. Computed tomography diagnosis of distal radioulnar subluxation. Skeletal Radiol. 1987, 16: 1-5.

245. Wells GA, Russell AS, Haraoui B, Bissonnette R, Ware CF. Validity of quality of life measurement tools--from generic to disease-specific. J Rheumatol Suppl. 2011, 88: 2-6.

246. Whipple TL, Geissler WB. Arthroscopic management of wrist triangular fibrocartilage complex injuries in the athlete. Orthopedics. 1993, 16: 1061-7.

247. Wijffels M, Ring D. The influence of non-union of the ulnar styloid on pain, wrist function and instability after distal radius fracture. J Hand Microsurg. 2011, 3: 11-4.

248. Wijffels M, Stomp W, Krijnen P, Reijnierse M, Schipper I. Computed tomography for the detection of distal radioulnar joint instability: Normal variation and reliability of four ct scoring systems in 46 patients. Skeletal Radiol. 2016, 45: 1487-93.

249. Wijffels MM, Keizer J, Buijze GA et al. Ulnar styloid process nonunion and outcome in patients with a distal radius fracture: A meta-analysis of comparative clinical trials. Injury. 2014, 45: 1889-95.

250. Xu J, Tang JB. In vivo changes in lengths of the ligaments stabilizing the distal radioulnar joint. The Journal of hand surgery. 2009, 34: 40-5.

251. Yeh KT, Shih JT. Arthroscopic triangular fibrocartilage complex reconstruction with free tendon graft for chronic distal radioulnar joint instability. J Orthop Surg Res. 2021, 16: 678.

252. Yoshii Y, Yuine H, Tung WL, Ishii T. Quantitative assessment of distal radioulnar joint stability with pressure-monitor ultrasonography. J Orthop Surg Res. 2019, 14: 195.

253. You BM, Siy P, Anderst W, Tashman S. In vivo measurement of 3-d skeletal kinematics from sequences of biplane radiographs: Application to knee kinematics. IEEE Trans Med Imaging. 2001, 20: 514-25.

254. Zanetti M, Bram J, Hodler J. Triangular fibrocartilage and intercarpal ligaments of the wrist: Does mr arthrography improve standard mri? J Magn Reson Imaging. 1997, 7: 590-4.

255. Zhang W, Hou P, Wang C, Wu T, Ho PC, Sun L. Arthroscopic one-tunnel transosseous reconstruction of chronic triangular fibrocartilage complex foveal tears: Outcomes in 12 patients. The Journal of hand surgery, European volume. 2021: 17531934211056854.

256. Zlatkin MB, Rosner J. Mr imaging of ligaments and triangular fibrocartilage complex of the wrist. Radiol Clin North Am. 2006, 44: 595-623, ix.

257. Aasheim T, Finsen V. The dash and the quickdash instruments. Normative values in the general population in norway. The Journal of hand surgery, European volume. 2014, 39: 140-4.

# 12 Appendices

# 12

# Appendices

## 12.1 List of Appendices

**Appendix I**

Quick Disabilities of the Arm, Shoulder and Hand (QDASH) questionnaire
(Danish version)

**Appendix II**

Patient-Rated Wrist Evaluation (PRWE) questionnaire
(Danish version)

**Appendix III**

MRI settings

# APPENDIX I

DISABILITIES OF THE ARM, SHOULDER AND HAND
(HANDICAPS I ARM, SKULDER OG HÅND)

# *Quick* DASH

**VEJLEDNING**

I dette spørgeskema stiller vi dig spørgsmål om dine symptomer og din evne til at udføre visse aktiviteter.

Vær venlig at svare på hvert eneste spørgsmål ved at sætte en cirkel om det tal, der passer bedst til din tilstand i den forløbne uge.

Hvis du ikke har haft lejlighed til at udføre en bestemt aktivitet i den forløbne uge, beder vi dig angive det svar, du mener ville dække bedst.

Det er uden betydning, hvilken hånd eller arm du anvender til at udføre aktiviteten; dit svar skal afspejle din evne til at udføre selve handlingen, uanset hvordan du gør det.

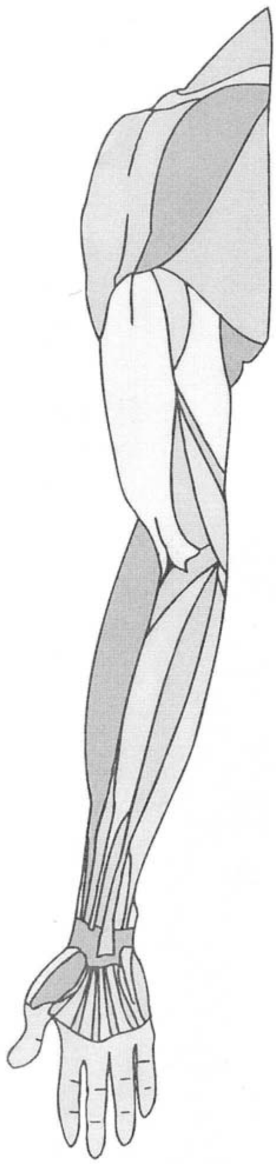

# *Quick* DASH

**Vurder venligst, hvordan din evne til at udføre følgende handlinger har været i den forløbne uge ved at sætte en cirkel om tallet under det svar, der passer bedst.**

| | IKKE VANSKELIGT | LIDT VANSKELIGT | NOGET VANSKELIGT | MEGET VANSKELIGT | UMULIGT |
|---|---|---|---|---|---|
| 1. Åbne et (marmelade)glas med stramt låg. | 1 | 2 | 3 | 4 | 5 |
| 2. Udføre tungt husarbejde(fx vaske vægge, vaske gulve). | 1 | 2 | 3 | 4 | 5 |
| 3. Bære en indkøbspose eller en mappe. | 1 | 2 | 3 | 4 | 5 |
| 4. Vaske dig selv på ryggen. | 1 | 2 | 3 | 4 | 5 |
| 5. Bruge en kniv til at skære mad ud. | 1 | 2 | 3 | 4 | 5 |
| 6. Fritidsaktiviteter, som sender en vis kraft eller stød gennem din arm, skulder eller hånd (fx golf, slag med hammer, tennis, osv.). | 1 | 2 | 3 | 4 | 5 |

| | SLET IKKE | LIDT | EN DEL | TEMMELIG MEGET | VIRKELIG MEGET |
|---|---|---|---|---|---|
| 7. Hvor *vanskeligt* har det været for dig i den forløbne uge, at omgås familie, venner, naboer og grupper pga din arm, skulder eller hånd? | 1 | 2 | 3 | 4 | 5 |

| | SLET IKKE HÆMMET | LIDT HÆMMET | EN DEL HÆMMET | MEGET HÆMMET | UDE AF STAND TIL |
|---|---|---|---|---|---|
| 8. Har du i den forløbne uge været hæmmet i at udføre dit arbejde eller andre gøremål pga. din arm, skulder eller hånd? | 1 | 2 | 3 | 4 | 5 |

| **Vær venlig at angive sværhedsgraden af følgende symptomer i den forløbne uge. (sæt cirkel om tallet)** | INGEN | LIDT | EN DEL | SVÆR | EKSTREM |
|---|---|---|---|---|---|
| 9. Smerte i din arm, skulder eller hånd når du laver noget bestemt. | 1 | 2 | 3 | 4 | 5 |
| 10. Prikken i din arm, skulder eller hånd. | 1 | 2 | 3 | 4 | 5 |

| | IKKE VANSKELIGT | LIDT VANSKELIGT | NOGET VANSKELIGT | MEGET VANSKELIGT | SÅ VANSKELIGT AT DET FORHINDRER MIG I AT SOVE |
|---|---|---|---|---|---|
| 11. Hvor vanskeligt har det i den forløbne uge været for dig, at sove pga. smerter i din arm, skulder eller hånd? (sæt cirkel om tallet) | 1 | 2 | 3 | 4 | 5 |

*Quick***DASH HANDICAP-/SYMPTOMSCORING**= [(summen af n svar)/n – 1] x 25, hvor n er lig med antallet af afgivne svar. **En *Quick*DASH-scoring må <u>ikke</u> udregnes, hvis der er mere end 1 ubesvaret spørgsmål.**

# *Quick* DASH

## ARBEJDSMODUL (VALGFRIT)

De følgende spørgsmål drejer sig om påvirkningen af din arbejdsevne pga. din arm, skulder eller hånd (inklusive husarbejde, hvis det er din hovedbeskæftigelse).

Angiv venligst hvad dit arbejde består i:_______________________________________________

□ Jeg arbejder ikke. (Du kan springe dette afsnit over.)

Sæt venligst en cirkel om det tal, der bedst beskriver din fysiske formåen i den forløbne uge. Havde du vanskeligt ved at:

| | IKKE VANSKELIGT | LIDT VANSKELIGT | NOGET VANSKELIGT | MEGET VANSKELIGT | UMULIGT |
|---|---|---|---|---|---|
| 1. Bruge din sædvanlige fremgangsmåde i dit arbejde? | **1** | **2** | **3** | **4** | **5** |
| 2. Udføre dit sædvanlige arbejde pga. smerter i din arm, skulder eller hånd? | **1** | **2** | **3** | **4** | **5** |
| 3. Udføre dit arbejde så godt, som du gerne ville? | **1** | **2** | **3** | **4** | **5** |
| 4. Udføre dit arbejde på den tid du plejer? | **1** | **2** | **3** | **4** | **5** |

## MODUL FOR SPORTSFOLK OG UDØVENDE KUNSTNERE (VALGFRIT)

De følgende spørgsmål drejer sig om, hvor stor en betydning dit arm-, skulder eller håndproblem har, når du spiller dit instrument, udøver din idræt eller begge dele. Hvis du dyrker mere end en sporstgren eller spiller mere end et instrument (eller begge dele), så svar venligst på grundlag af den aktivitet, som er vigtigst for dig.

Angiv venligst den sportsgren eller det instrument, som er vigtigst for dig:_______________________________

□ Jeg dyrker ikke nogen sportsgren eller spiller noget instrument. (Du kan springe dette afsnit over)

Sæt venligst en cirkel om det tal, der bedst beskriver din fysiske formåen i den forløbne uge. Havde du vanskeligt ved at:

| | IKKE VANSKELIGT | LIDT VANSKELIGT | NOGET VANSKELIGT | MEGET VANSKELIGT | UMULIGT |
|---|---|---|---|---|---|
| 1. Bruge din sædvanlige fremgangsmåde når du spiller dit instrument eller dyrker din idræt? | **1** | **2** | **3** | **4** | **5** |
| 2. Spille dit instrument eller dyrke din idræt pga. smerter i din arm, skulder eller hånd? | **1** | **2** | **3** | **4** | **5** |
| 3. Spille dit instrument eller dyrke din idræt så godt som du gerne ville? | **1** | **2** | **3** | **4** | **5** |
| 4. Bruge den tid du plejer på at øve dig eller spille dit instrument / træne eller dyrke din idræt? | **1** | **2** | **3** | **4** | **5** |

**SCORING AF DE VALGFRI MODULER:** Beregn summen af de afgivne svarværdier, divider med 4 (antallet af spørgsmål); træk 1 fra; gang med 25.

Scoring af et valgfrit modul må ikke udregnes, hvis der mangler besvarelser.

# APPENDIX II

## *Spørgeskema om smerter og bevægelser i håndled*

## *(The Patient-Rated Wrist Evaluation (PRWE)©)*

Svarene på spørgsmålene vil hjælpe os til at forstå, hvor ondt du har haft og hvor meget besvær du har haft i den sidste uge i det håndled, som du har problemer med.
Tænk på dine problemer med håndleddet i løbet af den sidste uge. Besvar venligst alle spørgsmålene. Hvis du ikke—i den sidste uge—har udført det, der spørges om, skal du forestille dig den smerte eller det besvær, du ville have haft.
Hvis du aldrig tidligere har gjort det, der spørges om, skal du ikke besvare spørgsmålet. Sæt en ring om det tal, som bedst beskriver smerten eller problemet. 0 beskriver, at du ikke har haft smerte eller problemer, og 10 beskriver, at du har haft den værste smerte eller størst mulige problem, eller at du ikke har kunnet gøre det, der bliver spurgt om.

| **1. Hvor ondt har du haft, når du har haft mest ondt - i den sidste uge** | |
|---|---|
| Når du har holdt håndleddet i ro | 0 1 2 3 4 5 6 7 8 9 10<br>Ingen smerte Værste smerte |
| Når du har gjort den samme bevægelse mange gange lige efter hinanden | 0 1 2 3 4 5 6 7 8 9 10<br>Ingen smerte Værste smerte |
| Når du har løftet noget tungt (f.eks. en kasse øl eller vand eller et lille barn) | 0 1 2 3 4 5 6 7 8 9 10<br>Ingen smerte Værste smerte |
| Når smerten har været værst | 0 1 2 3 4 5 6 7 8 9 10<br>Ingen smerte Værste smerte |
| Hvor ofte har du ondt? 0 1 2 3 4 5 6 7 8 9 10<br>Aldrig Hele tiden | |

| **2. Bevægelser** | |
|---|---|
| A. Særlige bevægelser | |
| **Hvor meget besvær har du i den sidste uge haft, når du skulle:** | |
| - dreje en nøgle i en lås med den syge hånd | 0 1 2 3 4 5 6 7 8 9 10<br>Intet besvær Kunne ikke gøre det |
| - skære med en kniv med den syge hånd | 0 1 2 3 4 5 6 7 8 9 10<br>Intet besvær Kunne ikke gøre det |
| - knappe en skjorte eller bluse | 0 1 2 3 4 5 6 7 8 9 10<br>Intet besvær Kunne ikke gøre det |
| - bruge den syge hånd til at skubbe fra, når du skulle rejse dig fra en stol | 0 1 2 3 4 5 6 7 8 9 10<br>Intet besvær Kunne ikke gøre det |
| - bære noget i den syge hånd, som vejer 5 kilo (f.eks. en pose med 5 liter mælk) | 0 1 2 3 4 5 6 7 8 9 10<br>Intet besvær Kunne ikke gøre det |
| - bruge toiletpapir med den syge hånd | 0 1 2 3 4 5 6 7 8 9 10<br>Intet besvær Kunne ikke gøre det |

| B. Daglige gøremål | |
|---|---|
| **Hvor meget besvær har du haft i den sidste uge med det, du gjorde, før du fik problemer med håndleddet:** | |
| Klæde dig på og/eller tage bad | 0 1 2 3 4 5 6 7 8 9 10<br>Intet besvær Kunne ikke gøre det |
| Gøre rent eller andet husarbejde | 0 1 2 3 4 5 6 7 8 9 10<br>Intet besvær Kunne ikke gøre det |
| Være på arbejde eller gøre det du plejer til daglig | 0 1 2 3 4 5 6 7 8 9 10<br>Intet besvær Kunne ikke gøre det |
| Gøre det, du plejer I din fritid | 0 1 2 3 4 5 6 7 8 9 10<br>Intet besvær Kunne ikke gøre det |
| Du er velkommen til at skrive noget her, som du synes er vigtigt: | |

# APPENDIX III

| Appendix III. Magnetic Resonance Imaging (MRI) scanners and frequently used settings | | | |
|---|---|---|---|
| *MRI scanner* | *Sequence* | *TR/TE (ms)* | *Thickness/increment (mm)* |
| *Achieva* | | | |
| Philips Medical Systems | T1 cor | 525/14 | 2/2.2 |
| (1.5T) | T1 ax | 525/14 | 3/3.3 |
| (Holstebro Hospital) | PD FS 3D with recon | 1500/33 | 0.7/0.36 |
| | T2 me3d cor | 33/18 | 0.75/0.75 |
| *Optima* | | | |
| GE healthcare (1.5T) | T1 cor | 700/11 | 2/2.2 |
| (Aarhus University Hospital) | T1 ax | 700/9 | 3/3.3 |
| | PD FS cor | 1800/27 | 2/2.2 |
| | 3DGEt2* with recon | 25/13 | 0.5/0.5 |
| *Skyra* | | | |
| Siemens (1.5T) | T1 cor, ax | 550/15 | 2/2.42 |
| (Aarhus University Hospital) | PD FS cor, sag, ax | 3700/30 | 2.2/2.42 |
| | T2me2d | 780/28 | 1.5/1.95 |

*PD: Proton density, FS: Fat saturation; TR: Repetition Time, TE: Echo time*
*Recon: Reconstructions in 3 planes (coronal, sagittal, axial)*

# 13 Co-authorship declarations

# 13

# Co-authorship declarations

## Declaration of co-authorship concerning article for PhD dissertations

Full name of the PhD student: Janni Kjærgaard Thillemann

This declaration concerns the following article/manuscript:

| | |
|---|---|
| Title: | Distal radioulnar joint stability measured with radiostereometry during the piano key test |
| Authors: | Janni Kjærgaard Thillemann, Sepp De Raedt, Peter Bo Jørgensen, Lone Rømer, Torben Bæk Hansen and Maiken Stilling |

The article/manuscript is: Published ☒ Accepted ☐ Submitted ☐ In preperation ☐

If published, state full reference:
Thillemann JK, De Raedt S, Jorgensen PB, Romer L, Hansen TB, Stilling M. Distal radioulnar joint stability measured with radiostereometry during the piano key test. J Hand Surg Eur Vol. 2020 Nov;45(9):923-930. doi: 10.1177/1753193420934689.Epub 2020 Jun 28.

If accepted or submitted, state journal:

Has the article/manuscript previously been used in other PhD or doctoral dissertations?

No ☒ Yes ☐ If yes, give details:

**Your contribution**

Please rate (A-F) your contribution to the elements of this article/manuscript, **and** elaborate on your rating in the free text section below.

A. Has essentially done all the work (>90%)
B. Has done most of the work (67-90 %)
C. Has contributed considerably (34-66 %)
D. Has contributed (10-33 %)
E. No or little contribution (<10%)
F. N/A

| Category of contribution | Extent (A-F) |
|---|---|
| The conception or design of the work: | C |
| *Free text description of PhD student's contribution* ***(mandatory)*** The AutoRSA analysis was developed before the beginning of the PhD project. The conception and design of the study was done by the student and the supervisors. | |
| The acquisition, analysis, or interpretation of data: | B |
| *Free text description of PhD student's contribution* ***(mandatory)*** Acquisition of data, AutoRSA analysis was done by the student and the co-authors. Interpretation of the data and data analysis was done by the student. | |
| Drafting the manuscript: | A |
| *Free text description of PhD student's contribution* ***(mandatory)*** The student drafted the manuscript with guidance from the supervisors. | |
| Submission process including revisions: | B |

| *Free text description of PhD student's contribution* ***(mandatory)*** |
| --- |
| The student did the submission process. Revisions with guidance from the supervisors. |

**Signatures of first- and last author, and main supervisor**

| Date | Name | Signature |
| --- | --- | --- |
| 19.12.2021 | Janni Kjærgaard Thillemann | |
| 19.12.2021 | Maiken Stilling | Maiken Stilling |
| | | |

Date: 19.12.2021

Signature of the PhD student

AARHUS UNIVERSITY

# Declaration of co-authorship concerning article for PhD dissertations

Full name of the PhD student: Janni Kjærgaard Thillemann

This declaration concerns the following article/manuscript:

| | |
|---|---|
| Title: | Distal radioulnar joint stabilization with open foveal reinsertion versus tendon graft reconstruction: an experimental study using radiostereometry |
| Authors: | Janni Kjærgaard Thillemann, Sepp De Raedt, Torben Bæk Hansen, Bo Munk and Maiken Stilling |

The article/manuscript is: Published ☒ Accepted ☐ Submitted ☐ In preperation ☐

If published, state full reference:
Thillemann JK, De Raedt S, Hansen TB, Munk B, Stilling M. Distal radioulnar joint stabilization with open foveal reinsertion versus tendon graft reconstruction: An experimental study using radiostereometry. Journal of experimental orthopaedics. 2021, 8: 10.

If accepted or submitted, state journal:

Has the article/manuscript previously been used in other PhD or doctoral dissertations?

No ☒ Yes ☐ If yes, give details:

**Your contribution**

Please rate (A-F) your contribution to the elements of this article/manuscript, **and** elaborate on your rating in the free text section below.

A. Has essentially done all the work (>90%)
B. Has done most of the work (67-90 %)
C. Has contributed considerably (34-66 %)
D. Has contributed (10-33 %)
E. No or little contribution (<10%)
F. N/A

| Category of contribution | Extent (A-F) |
|---|---|
| The conception or design of the work: | B |
| *Free text description of PhD student's contribution* ***(mandatory)*** The AutoRSA analysis was developed before the beginning of the PhD project. The conception and design of the study was done by the student and the supervisors. Interventions before data aquisision was performed by the student and main supervisor. | |
| The acquisition, analysis, or interpretation of data: | B |
| *Free text description of PhD student's contribution* ***(mandatory)*** Acquisition of data, AutoRSA analysis was done by the student and the co-authors. Interpretation of the data and data analysis was done by the student. | |
| Drafting the manuscript: | A |
| *Free text description of PhD student's contribution* ***(mandatory)*** The student drafted the manuscript with guidance from the supervisors. | |

| Submission process including revisions: | B |
|---|---|
| *Free text description of PhD student's contribution* ***(mandatory)***<br>The student did the submission process. Revisions with guidance from the supervisors. | |

**Signatures of first- and last author, and main supervisor**

| Date | Name | Signature |
|---|---|---|
| 19.12.2021 | Janni Kjærgaard Thillemann | |
| 19.12.2021 | Maiken Stilling | Maiken Stilling |
| | | |

Date: 19.12.2021

Signature of the PhD student

# Declaration of co-authorship concerning <u>article for PhD dissertations</u>

Full name of the PhD student: Janni Kjærgaard Thillemann

This declaration concerns the following article/manuscript:

| | |
|---|---|
| Title: | Normal values of Distal Radioulnar Joint kinematics during a dynamic press-test |
| Authors: | Janni Kjærgaard Thillemann, Sepp De Raedt, Emil Toft Petersen, Katriina Bøcker Puhakka, Torben Bæk Hansen and Maiken Stilling |

The article/manuscript is: Published ☐ Accepted ☒ Submitted ☐ In preperation ☐

If published, state full reference:

If accepted or submitted, state journal: Journal of Wrist Surgery

Has the article/manuscript previously been used in other PhD or doctoral dissertations?

No ☒ Yes ☐ If yes, give details:

**Your contribution**

Please rate (A-F) your contribution to the elements of this article/manuscript, **and** elaborate on your rating in the free text section below.

A. Has essentially done all the work (>90%)
B. Has done most of the work (67-90 %)
C. Has contributed considerably (34-66 %)
D. Has contributed (10-33 %)
E. No or little contribution (<10%)
F. N/A

| Category of contribution | Extent (A-F) |
|---|---|
| The conception or design of the work: | B |
| *Free text description of PhD student's contribution* ***(mandatory)***<br>The AutoRSA analysis was developed before the beginning of the PhD project. The conception and design of the study was done by the student and the supervisors. | |
| The acquisition, analysis, or interpretation of data: | B |
| *Free text description of PhD student's contribution* ***(mandatory)***<br>Acquisition of data was done by the student. AutoRSA analysis and statistical prarmetric mapping was done by the student and the co-authors. Interpretation of the data and remaining data analysis was done by the student. | |
| Drafting the manuscript: | A |
| *Free text description of PhD student's contribution* ***(mandatory)***<br>The student drafted the manuscript with guidance from the main supervisor. | |
| Submission process including revisions: | A |

| *Free text description of PhD student's contribution* ***(mandatory)*** |
|---|
| Manuscript revisions were performed with guidance from the supervisors. The student submitted the manuscript. |

**Signatures of first- and last author, and main supervisor**

| Date | Name | Signature |
|---|---|---|
| 19.12.2021 | Janni Kjærgaard Thillemann | |
| 19.12.2021 | Maiken Stilling | Maiken Stilling |
| | | |

Date: 19.12.2021

Signature of the PhD student

# Declaration of co-authorship concerning article for PhD dissertations

Full name of the PhD student: Janni Kjærgaard Thillemann

This declaration concerns the following article/manuscript:

| | |
|---|---|
| Title: | Kinematics of the Distal Radioulnar Joint before and after open reinsertion of the foveal Triangular Fibrocartilage Complex in comparison to normal joints |
| Authors: | Janni Kjærgaard Thillemann, Sepp De Raedt, Emil Toft Petersen, Katriina Bøcker Puhakka, Torben Bæk Hansen and Maiken Stilling |

The article/manuscript is: Published ☐ Accepted ☐ Submitted ☒ In preperation ☐

If published, state full reference:

If accepted or submitted, state journal: Journal of Bone and Joint Surgery

Has the article/manuscript previously been used in other PhD or doctoral dissertations?

No ☒ Yes ☐ If yes, give details:

**Your contribution**

Please rate (A-F) your contribution to the elements of this article/manuscript, **and** elaborate on your rating in the free text section below.

A. Has essentially done all the work (>90%)
B. Has done most of the work (67-90 %)
C. Has contributed considerably (34-66 %)
D. Has contributed (10-33 %)
E. No or little contribution (<10%)
F. N/A

| Category of contribution | Extent (A-F) |
|---|---|
| The conception or design of the work: | B |
| *Free text description of PhD student's contribution* ***(mandatory)*** The AutoRSA analysis was developed before the beginning of the PhD project. The conception and design of the study was done by the student and the supervisors. | |
| The acquisition, analysis, or interpretation of data: | B |
| *Free text description of PhD student's contribution* ***(mandatory)*** Acquisition of data was done by the student. AutoRSA analysis and statistical prarmetric mapping was done by the student and the co-authors. Interpretation of the data and remaining data analysis was done by the student. | |
| Drafting the manuscript: | A |
| *Free text description of PhD student's contribution* ***(mandatory)*** The student drafted the manuscript with guidance from the main supervisor. | |
| Submission process including revisions: | A |

AARHUS UNIVERSITY

| |
|---|
| *Free text description of PhD student's contribution* ***(mandatory)***<br>Manuscript revisions were performed with guidance from the supervisors. The student submitted the manuscript. |

**Signatures of first- and last author, and main supervisor**

| Date | Name | Signature |
|---|---|---|
| 19.12.2021 | Janni Kjærgaard Thillemann | |
| 19.12.2021 | Maiken Stilling | Maiken Stilling |
| | | |

Date: 19.12.2021

_______________________________________________
Signature of the PhD student

# 14 List of papers

# 14

# Papers

## 14.1 List of Papers

**Paper I:**

Distal radioulnar joint stability measured with radiostereometry during the piano key test. Thillemann JK, de Raedt S, Jorgensen PB, Romer L, Hansen TB, Stilling M.
*Journal of Hand Surgery European Volume. 2020 Nov;45(9):923-930.*
*DOI: 10.1177/1753193420934689.*

**Paper II:**

Distal radioulnar joint stabilization with open foveal reinsertion versus tendon graft reconstruction: an experimental study using radiostereometry.
Thillemann JK, de Raedt S, Hansen TB, Munk B, Stilling M.
*Journal of Experimental Orthopaedics. 2021, 8: 10. DOI: 10.1186/s40634-021-00329-y*

**Paper III:**

Normal values of Distal Radioulnar Joint kinematics during a dynamic press-test.
Thillemann JT, de Raedt S, Petersen ET, Puhakka KB, Hansen TB, Stilling M.
*Journal of Wrist Surgery, e-publication December 2021.* DOI: 10.1055/s-0041-1740486

**Paper IV:** Kinematics of the Distal Radioulnar Joint before and after open reinsertion of the foveal Triangular Fibrocartilage Complex in comparison to normal joints. Thillemann JT, de Raedt S, Petersen ET, Puhakka KB, Hansen TB, Stilling M. *Manuscript submitted to Acta Orthopaedica, December 2021.*

PAPER I

*Full Length Article*

JHS(E)

Journal of Hand Surgery
(European Volume)
0(0) 1–8

DOI: 10.1177/1753193420934689
journals.sagepub.com/home/jhs
SAGE

# Distal radioulnar joint stability measured with radiostereometry during the piano key test

**Janni Kjærgaard Thillemann[1,2,3], Sepp De Raedt[4], Peter Bo Jørgensen[3], Lone Rømer[5], Torben Bæk Hansen[1,3] and Maiken Stilling[2,3]**

**Abstract**

Distal radioulnar joint instability is difficult to grade by clinical examination and interobserver reliability is low. This study used a new and precise radiostereometry method for measurement of distal radioulnar joint translation. Eight human donor arms were positioned in a custom-made fixture and a standardized piano key test was done with pressure on the ulnar head. Examination was done before and after dividing the styloid and foveal insertions of the triangular fibrocartilage complex. In the intact wrists, the piano key test induced a mean 1.36 mm translation of the ulnar head, which increased statistically significantly to 1.96 mm after a lesion of the styloid ligament insertion and to 2.3 mm after combined lesions of the styloid and foveal ligament insertions. This experimental cadaver study demonstrates a radiological method for precise quantification of distal radioulnar joint stability after different grades of triangular fibrocartilage complex injury.

**Keywords**

Distal radioulnar joint, instability, kinematics, radiostereometry, triangular fibrocartilage complex

Date received: 30th March 2020; accepted: 25th May 2020

## Introduction

A triangular fibrocartilage complex (TFCC) lesion is frequently associated with a fall on the outstretched hand and may occur with or without a simultaneous distal radial fracture. A traumatic TFCC injury may lead to altered kinematics and instability in the distal radioulnar joint (DRUJ) with increased anteroposterior translation and the risk of ulnar head subluxation in the sigmoid notch (Hagert, 1992). DRUJ instability can subsequently lead to impaired hand function, wrist pain, decreased forearm rotation strength and reduced range of motion. Treatment is recommended in patients presenting with subjective symptoms and a clinically unstable DRUJ (Gofton et al., 2004). However, the correct diagnosis can be missed since the clinical assessment and the grading of increased translation are difficult and observer dependent (Nagata et al., 2013).

The complex anatomy and biomechanics of the DRUJ allow joint motion in three planes (Tolat et al., 1996): rotation around the radioulnar axis, longitudinal pistoning in the length axis, and anteroposterior DRUJ translation (af Ekenstam, 1992). The articulating joint surfaces are asymmetrically shaped and account for only 20% of the joint stability (Stuart et al., 2000). Therefore, Szabo (2006) described the DRUJ as 'inherently unstable', as the joint relies on the TFCC as the main soft tissue stabilizer (af Ekenstam and Hagert, 1985; Stuart et al., 2000).

[1]Department of Orthopaedics, University Clinic of Hand, Hip and Knee Surgery, Holstebro, Denmark
[2]Department of Orthopaedic Surgery, Aarhus University, Aarhus, Denmark
[3]Department of Clinical Medicine, Aarhus University, Incuba Skejby, Denmark
[4]NRT X-Ray A/S, Hasselager, Denmark
[5]Department of Radiology, Aarhus University Hospital, Aarhus, Denmark

**Corresponding Author:**
Janni K. Thillemann, Department of Orthopaedics, Hospital Unit West, University Clinic of Hand, Hip and Knee Surgery, Lægaardsvej 12, 7500 Holstebro, Denmark.
Email: teamjanni@gmail.com

An external rig for objective measurement of linear anteroposterior DRUJ translations has been described (Pickering et al., 2016).

Currently, wrist arthroscopy remains the reference standard for diagnosing and assessing TFCC ligament lesions and deciding on treatment (Atzei, 2009; Pederzini et al., 1992). Overall, two types of TFCC lesions are of clinical importance: lesions of the distal component (dc-TFCC), which inserts at the ulnar styloid, and lesions to the proximal component (pc-TFCC), which inserts in the ulnar fovea. In cadavers, a variable degree of instability after TFCC lesions has been shown, and the pc-TFCC contributes more to DRUJ stability than the dc-TFCC (Nakamura and Makita, 2000). Arthroscopic examination can differentiate these using the trampoline test (dc-TFCC) (Hermansdorfer and Kleinman, 1991) and the hook test (pc-TFCC) (Atzei, 2009).

There is as yet no reference standard imaging method for diagnosing DRUJ instability (Lees, 2013). Magnetic resonance imaging (MRI) with specific protocols can visualize lesions in the TFCC with a sensitivity of up to 92% and specificity of up to 89% (Andersson et al., 2015; Zlatkin and Rosner, 2006), but it does not demonstrate the degree of instability. Computed tomography (CT) with the forearm in a supinated and pronated position can detect subluxation in the DRUJ (Nakamura et al., 1996), but in cases with minor functional instability, static imaging of the unloaded joint will not display the significance of the instability (Tay et al., 2007).

Radiostereometric analysis (RSA) is a precise calibrated radiographic method that has previously been used to assess stability and kinematics in the knee and hip joints (Hansen et al., 2018; Nielsen et al., 2018), but has not been used in the wrist or DRUJ. The purposes of this cadaver study was to introduce a new RSA method (AutoRSA) for the examination of DRUJ translation with forearm pronation and the measurement of DRUJ translation produced by the piano key test (PKT) (Glowacki and Shin, 1999) in the intact DRUJ, and after dc-TFCC and combined dc-TFCC/pc-TFCC lesions.

## Methods

### *Donor specimens and preparation*

This experimental study used freshly frozen (not embalmed) human donor arms, including the hand, forearm, elbow and part of the humerus, which were thawed for 48 hours at 5°C. There were eight donor specimens from seven men and one woman with a mean age of 78 years (range 72–90) that met the following inclusion criteria: normal fluoroscopy of the wrist, forearm and elbow, with no signs of previous fracture or malunion and a normal hook test at arthroscopic assessment. Central TFCC tears of Palmer type 1 A/2 (Palmer, 1989) were accepted. All soft tissue and DRUJ stabilizers were kept intact to mimic the in-vivo kinematics as closely as possible. The study was approved by The Central Denmark Region Committees on Health Research Ethics (Casenr. 1-10-72-6-16 issued on 24 February 2016).

### *Arthroscopic TFCC examination and production of ligament lesion*

Wrist arthroscopy for verification of an intact TFCC was done before the study set out and was repeated after each intervention to confirm the ligament lesion. The stability of the pc-TFCC was assessed by the hook test in all three phases of the study. With instrumentation through the 6-R portal, the stability of the pc-TFCC was tested by pulling the ulnar edge of the TFCC. The hook test was regarded as positive when the probe could lift the TFCC from its foveal insertion in a distal and radial direction (Atzei, 2009).

An increase in TFCC trampoline laxity in the intact cadavers cannot be ruled out, so the trampoline test was not used to assess the status after the dc-TFCC lesion. In the ligament lesion intervention, we aimed to spare other TFCC stabilizing structures and soft tissues. The posterior DRUJ capsule was opened transversely by a 1 cm incision proximal to the TFCC and under fluoroscopic visualization. First, the dc-TFCC was cut at the ulnar styloid insertion and later the pc-TFCC was detached from the ulnar fovea insertion.

### *Bone models*

Before intervention, CT scans of the human donor forearms were done with a Philips Brilliance 64 scanner (Philips Medical Systems, Best, The Netherlands) (120 kV, 100 mAs) and image reconstruction was made with a 0.9 mm slice thickness, a 0.45 mm slice increment and an in-plane pixel size of $0.27 \times 0.27$ mm. Subject specific bone models of the radius and the ulna were generated from the CT images. First, the bones were segmented from the CT image using an automated graph-cut segmentation method (Hansen et al., 2018). Next, bone surface models of the radius and the ulna were created and simplified to approximately 10,000 triangles. Last, bone volume models with the greyscale information from the CT scan were extracted. All image processing was done with custom implemented software based on The Insight Segmentation and The Visualization Toolkit (Kitware, New York, USA).

## *Test set-up*

A custom-made radiolucent motorized fixture was designed to simulate in-vivo forearm rotation and the PKT examination in a standardized setting (Figure 1). The fixture allowed for positioning of the forearm in neutral rotation or pronation. The hand was fixed to a plate in neutral wrist extension and neutral wrist deviation while allowing the PKT to be done with a 7 kg load on the ulnar head by the use of a fixture lever. A 7 kg load corresponds to the thumb force we could manually apply to the ulnar head during a clinical PKT.

## *Static RSA recordings*

Specimens were recorded with the digital Adora RSA system (NRT X-Ray, Hasselager, Denmark). Two digital Canon CXDI-50RF image detectors were slotted beneath the uniplanar carbon calibration box (Carbon box 19, Medis Specials, Leiden, The Netherlands). Images were obtained with the X-ray tubes in a 20°–20° tube position, the source to images distance (SID) was 150 cm and the source to skin distance (SSD) was 100 cm. Exposure settings for static RSA recordings were 60 kV, 2.5mAs and the resolution was $2208 \times 2688$ pixels ($0.16 \times 0.16$ mm/pixel). All specimens were recorded with synchronized static RSA before and after the dc-TFCC and combined dc-TFCC/pc-TFCC lesions. Two clinical tests were carried out. A forearm pronation test, in which the specimens were were positioned with neutral forearm rotation and neutral wrist extension. The first RSA recording was made in this position and a second RSA recording was obtained after 90° of forearm pronation. In the PKT the specimens were positioned with a pronated forearm and neutral wrist extension. The first RSA recording was made in this position without load and a second RSA recording was obtained with a 7 kg load on the ulnar head using a fixture lever (Figure 1).

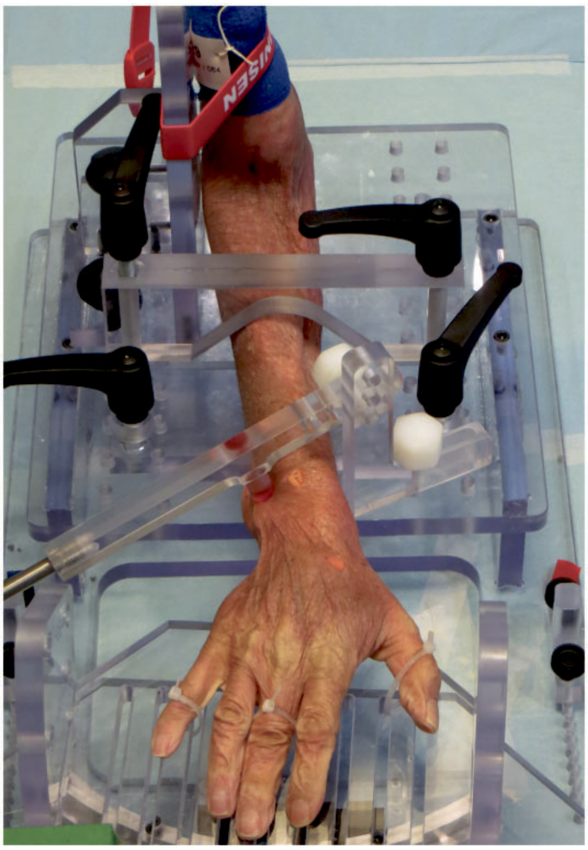

**Figure 1.** Transparent and radiolucent fixture for standardized examination of the pronated forearm in the piano key test.

## *Analysis of static stereoradiographs*

Model-based RSA software (MBRSA) (RSAcore, Leiden, The Netherlands) was used for calibrating the RSA images and initializing the ulna and radius bone surface models (Kaptein et al., 2004). The bone edges of the radius and ulna were detected automatically using MBRSA on the stereoradiographs, and the pertinent bone edges were selected manually. The CT-based bone surface models were imported into the MBRSA program; after initial positioning, the best position of the bones was automatically estimated by minimizing the error of the bone model projections versus the manually detected bone edges on the radiographs. This was used as an initial position in the final analysis of the stereoradiograph with non-commercial AutoRSA software. The CT-based bone volume models were used to simulate digital reconstructed radiographs (DRR), and the AutoRSA software calculated the optimal three-dimensional position and orientation of the bone model by repeated comparison between the simulated DRR and the RSA images until no further improvements could be made (Figure 2). Masks were automatically produced from the initial position by projecting the CT bone-volume model on the RSA images and focusing the registration on the bone area.

The AutoRSA method was recently validated against the reference standard, marker-based RSA, on the femur and pelvis. The validation demonstrated precision less than 0.162 mm for all translations and below 0.71° for rotations (Hansen et al., 2018).

## *Coordinate system*

Standardized anatomical coordinate systems defined by the three orthogonal axes ($x$, $y$, $z$) were determined

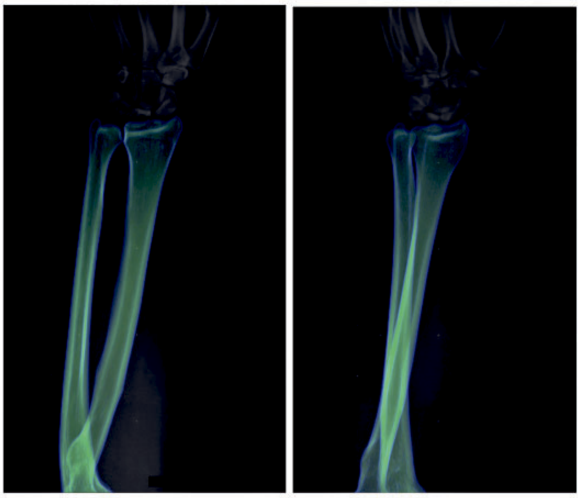

**Figure 2.** Digital reconstructed radiographs (green) simulated from computerized tomography-based bone models and matched to the radius and ulna on the stereoradiographs.

for the radius and ulna as described by McDonald et al. (2012).

The anatomical coordinate system of each bone was created using three defined anatomical landmarks on each three-dimensional CT bone-surface model. The radius landmarks were the proximal rotation centre of the radial head ($C_{prox}$), the tip of the radial styloid and the centre of the DRUJ surface. The landmarks for the ulna were the centre of the ulnar head ($C_{dist}$), the tip of the distal ulnar styloid and the centre of the greater sigmoid notch. The centre points were computed from the best fitted sphere of three points picked on the radial and ulnar head surfaces. The landmarks of each bone model represent exactly the same bone model points in examinations before and after the ligament lesion. The landmarks therefore do not have any effect on the precision.

### Kinematics and outcome variables

The single radioulnar joint axis (RUJ axis) extending from $C_{prox}$ in the radial head to $C_{dist}$ ulnar head, as described by Hagert (1992), was used to calculate ulnar head centre movements. The orthogonal projection of the RUJ axis on the radial sigmoid notch line, connecting the midpoint of the anterior rim and the midpoint of the posterior rim of the radius sigmoid notch, determined the DRUJ position. A ratio was calculated based on the DRUJ position and the length of the radial sigmoid notch line. The DRUJ translation was calculated as the change in the DRUJ position in millimetres (Figure 3).

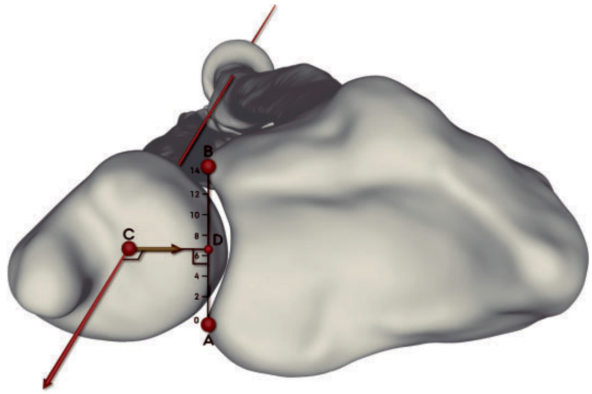


**Figure 3.** The distal radioulnar joint (DRUJ) position (D) was defined by the orthogonal projection (yellow arrow) from the radioulnar joint axis (red line) perpendicular to the line (AB) connecting the anterior (A) and posterior (B) rim points of the sigmoid notch. The DRUJ translation was calculated from the change in DRUJ position on this sigmoid notch line. The position ratio was calculated as AD/AB.

### Statistical analysis

QQ plots and histograms were used to test continuous data for Gaussian distribution. All data were normally distributed with equal variances and are reported as means and 95% confidence intervals (95% CI). A paired *t*-test was used to test changes in the DRUJ position before and after forearm pronation and the PKT. Mixed-model analysis was used to test repeated measurements of DRUJ translation before and after intervention by lesion of the dc-TFCC and the pc-TFCC. The significance level was set at $p < 0.05$.

The sample size calculation in this experimental cadaver study was based on a study by Omokawa et al. (2017) that used a magnetic tracking system to measure anterior–posterior DRUJ translation using the ballottement test. The translation in the DRUJ was 7 mm (SD 3) in intact wrists, and 14 mm (SD 4) after the TFCC lesion. With a power of 0.80 and alpha of 0.05, an estimated sample size of seven patients for two-sample comparison of paired-means with positive correlation was obtained.

## Results

### The intact TFCC

The mean anterior–posterior sigmoid notch length was 13.8 mm (95% CI: 12.5 to 15.2; range 11.0 to 15.6) measured from the midpoint of the anterior sigmoid notch rim to the midpoint of the posterior sigmoid notch rim of the radius.

In intact joints with neutral forearm rotation, the centre of the ulnar head (RUJ axis) was positioned at a mean of 7.4 mm (95% CI: 6.6 to 8.2) from the anterior rim on the radius sigmoid notch line (DRUJ position). Considering the natural variation of joint size, this corresponds to a DRUJ position ratio of 0.54 (95% CI: 0.48 to 0.59).

Pronation of the forearm resulted in a posterior-directed translation of the ulnar head RUJ axis with respect to the sigmoid notch line, which significantly increased the mean DRUJ position ratio ($p = 0.0001$) (Table 1).

The PKT induced an anteriorly directed position change of the ulnar head in the DRUJ (Figure 4). The DRUJ translation corresponded to a significant change in the DRUJ position ratio ($p = 0.02$) (Table 1).

### *TFCC lesion*

The DRUJ position in the pronated forearm was similar after dividing the dc-TFCC and pc-TCCC, compared with the intact situation ($p > 0.07$).

With the PKT, DRUJ translation increased significantly after the TFCC lesions in comparison with the intact TFCC ($p < 0.04$). The DRUJ translation after the dc-TFCC lesion, corresponded to a significant change in the DRUJ position ratio ($p = 0.02$) (Table 1). The combined dc-TFCC/pc-TFCC lesion further increased the DRUJ translation (Table 1; Figure 4).

## Discussion

We introduced a new RSA method (AutoRSA) to examine the change of the ulnar head position with respect to the radius sigmoid notch during forearm pronation in both intact cadaver wrists, and after dc-TFCC and combined dc-TFCC/pc-TFCC lesions. Further, we measured the DRUJ translation with the loaded PKT in the intact DRUJ and measured the effect of dc-TFCC and combined dc-TFCC/pc-TFCC lesions on DRUJ translation.

With increasing forearm pronation, the intact DRUJ stabilizes due to the shallow concavity of the bony sigmoid notch (af Ekenstam, 1992; af Ekenstam and Hagert, 1985) and the stabilizing effect of the dorsal fibres of the dc-TFCC, but mainly due to the taut volar part of the pc-TFCC that prevents posterior ulnar head subluxation relative to the radius (Hagert, 1994; Kleinman, 2007; Xu and Tang, 2009). In our unloaded set-up, at 80° forearm pronation, an isolated lesion of the dc-TFCC and dc-TFCC/pc-TFCC did not displace the ulnar head further posteriorly in the sigmoid notch. A sonographic study of the position of the ulnar head with respect to the radius in 30° forearm pronation reported similar findings in healthy wrists and wrists with arthroscopically verified TFCC injuries (Hess et al., 2012).

Numerous CT-based methods have used the ulnar head position relative to the radius for assessment of DRUJ instability by detecting subluxation in unloaded supination and pronation of the forearm, namely the radioulnar ratio (RUR), radioulnar line, subluxation ratio, epicentre method and the Mino criteria (Mino et al., 1983; Wechsler et al., 1987). These CT-based studies have used single, two-dimensional, axial slices for measurements, but the degree of forearm rotation was not reported (Lo et al., 2001; Mino et al., 1983; Park and Kim, 2008; Wechsler et al., 1987). An increase in pronation may cause a more posterior contact point between the radial sigmoid notch and the ulnar head, and vice versa in supination. Thus, variation in rotation may influence the measured ulnar head subluxation (Chen and Tang, 2013; Gammon et al., 2018; King et al., 1986; Linscheid, 1992; Pirela-Cruz et al., 1991).

Lo et al. (2001) found high intra- and interobserver reliabilities with the RUR method, which is based on a calculated position ratio of the ulnar head centre with respect to the sigmoid notch. In healthy individuals,

**Table 1.** Kinematic measures with pronated forearm and piano key test. Values are displayed as means (95% CI).

| Forearm position/test | Intact | dc-TFCC lesion | dc-TFCC/pc-TFCC lesion |
|---|---|---|---|
| *Pronated forearm* | | | |
| Degrees of pronation (°) | 80 (76 to 85) | 83 (79 to 87) | 81 (75 to 88) |
| DRUJ position ratio | 0.72 (0.65 to 0.78) | 0.71 (0.65 to 0.76) | 0.67 (0.58 to 0.76) |
| *Piano key test* | | | |
| DRUJ position ratio | 0.61 (0.55 to 0.67) | 0.56 (0.49 to 0.63)[a] | 0.50 (0.41 to 0.60)[a] |
| DRUJ translation (mm) | 1.36 (0.17 to 2.55) | 1.96 (1.05 to 2.86)[a] | 2.30 (1.41 to 3.20)[a] |

DRUJ: distal radioulnar joint; dc-TFCC: distal component of the triangular fibrocartilage complex; pc-TCCC: proximal component of the triangular fibrocartilage complex.
[a]Statistically significant difference compared with the intact DRUJ.

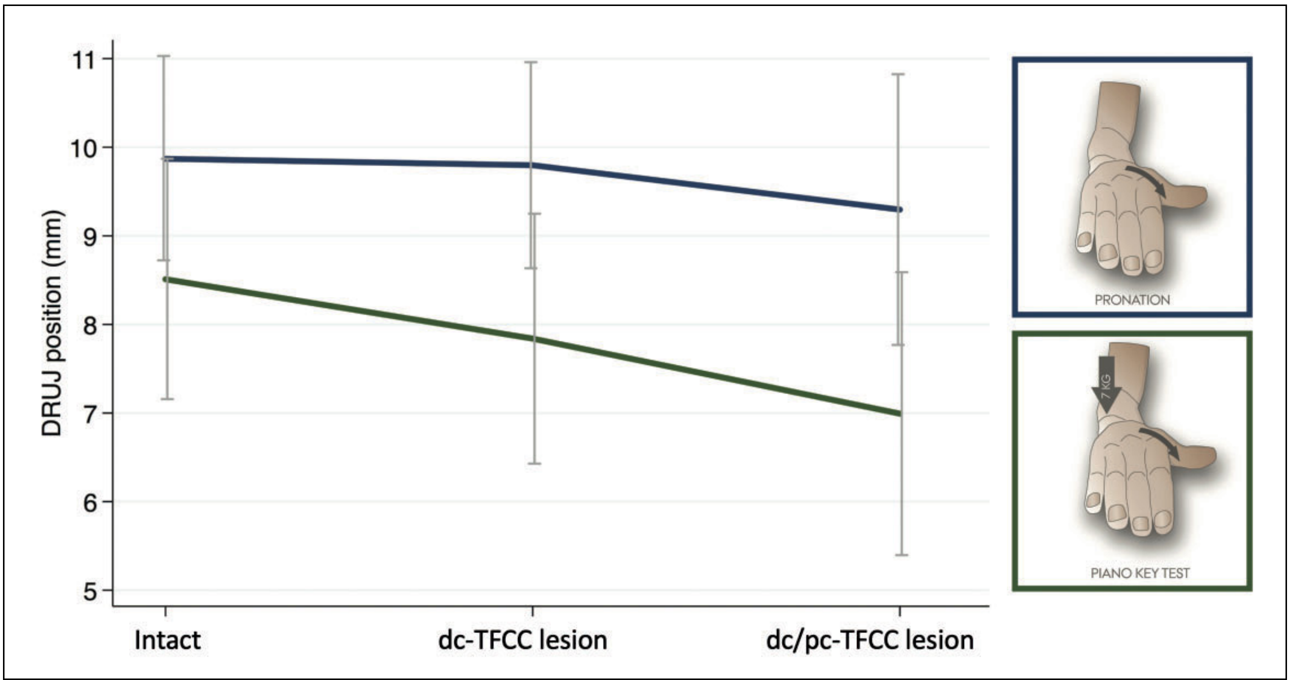


**Figure 4.** The distal radioulnar joint (DRUJ) position in pronation (blue) and after the piano key test (green), measured from the anterior rim of the sigmoid notch (mm), with the intact triangular fibrocartilage complex (TFCC), after lesion of the distal component (dc-TFCC) and after combined lesions of the distal and proximal components (dc/pc-TFCC) of the TFCC. The DRUJ translation is the distance between the two lines. The points indicate the means and the whiskers the 95% confidence intervals.

the mean RUR was 0.50 (SD 0.04) with neutral forearm rotation; pronation translated the ulnar head posteriorly to a mean RUR of 0.60 (SD 0.05) (Lo et al., 2001). The DRUJ position ratio reported in our study was based on landmarks resembling the RUR method but in three dimensions. We found a mean DRUJ position ratio of 0.54 in neutral forearm rotation, which increased to 0.72 after pronation. The diversity between studies of the pronated DRUJ position could be the effect of differences in degree of pronation.

Translation in the DRUJ with an intact TFCC has been studied in cadavers, and in-vivo using magnetic tracking devices, externally mounted rigs and ultrasound (Iida et al., 2014; Omokawa et al., 2017; Onishi et al., 2017). Omowaka et al. (2017) reported a bi-directional DRUJ translation of 6 mm (SD 5) in intact cadavers tested with the ballottement test on a pronated forearm. Pickering et al. (2016) developed an externally mounted device suitable for clinical use. Using the ballottement test on a pronated forearm, the bi-directional DRUJ translation was 4.2 mm (SD 0.06) in healthy controls. Hess et al. (2012) reported a uni-directional DRUJ translation of 2.5 mm (SD 1.03) in a sonographic study on 40 healthy wrists when doing a press test.

The DRUJ translations reported in intact cadaver wrists differ. Removal of the joint capsule and soft tissue components allows precise tracking devices to be attached to bone but is likely to increase joint laxity. However, soft tissue movement may affect DRUJ translations obtained with externally mounted devices by decreasing precision and overestimation of the true DRUJ translation. The combination of the use of RSA and anatomical kinematic axes and landmarks reduced the likelihood of overestimations due to soft tissue components and simultaneously recorded the actual degree of DRUJ rotation.

TFCC lesions have a broad spectrum of severity, leading to different degrees of DRUJ instability. Minor DRUJ instability does not necessarily lead to ulnar head subluxation and detection of TFCC lesions by current imaging techniques is not sensitive and cannot clearly detect functional DRUJ instability (Ng et al., 2017). Measures of DRUJ translation during loaded exercises may have more value in grading functional DRUJ instability. Using sonography on patients, Hess et al. (2012) found an absolute difference of 1 mm in anteriorly directed DRUJ translation between a wrist with a TFCC lesion and the contralateral wrist with an intact TFCC during a standardized press test examination. The 1 mm difference was proposed as a clinically relevant diagnostic cut-off (Hess et al., 2012). We measured an increase in anteriorly directed DRUJ translation of 0.94 mm after the dc-TFCC/pc-TFCC lesion, which supports the proposal of Hess at al. (2012).

To our knowledge, only one other biomechanical study has measured uni-directional DRUJ translation with the PKT, but it reported no measurable differences before and after sectioning the TFCC in 11 cadaver arms (Moriya et al., 2009). One explanation for this may be that the PKT was applied manually in full pronation. Extreme pronation may limit the DRUJ translation in spite of a TFCC lesion because of the constraining effect of the intact interosseous membrane (Stuart et al., 2000) and the bony support from the posterior sigmoid notch (af Ekenstam, 1992).

The limitations of this study include the experimental design and the study of cadaver specimens. Ex-vivo ligament laxity may differ from in-vivo, and the aged cadavers used in the study may have other wrist disorders. Further, the TFCC lesions may not resemble in-vivo traumatic TFCC injuries. We aimed to reduce the effect of these limitations by prestudy fluoroscopy and CT scans to exclude specimens with visible pathology that could influence DRUJ kinematics and stability (e.g. a malunion of the distal radius). In addition, prestudy arthroscopy was done to exclude specimens with Palmer type 1B/C/D TFCC lesions and to confirm the pc-TFCC lesions before testing.

This experimental cadaver study demonstrates a new radiostereometry method for precise quantification of DRUJ instability in different grades of TFCC injury. A valid and precise tool to measure DRUJ instability is required in the clinical setting. The AutoRSA-based method is likely to be applicable during dynamic loaded tests to assess DRUJ translation and DRUJ kinematics in patients, pre- and postoperatively. In-vivo investigations of its feasibility and validity is recommended to establish the normal values for DRUJ stability.

**Acknowledgements** We would like to thank Lars Lindgren, from the Department of Radiology, Aarhus University Hospital, for his valued help with the RSA recordings.

**Declaration of conflicting interests** The authors declare no potential conflicts of interest with respect to the research, authorship, and/or publication of this article.

**Funding** The authors disclosed receipt of the following financial support for the research, authorship, and/or publication of this article: the study was performed under the Innovation Fund Grant 69-2013-1, 'Transforming radiological technology for assessment of implant fixation: from research tool to clinical application', and grants from The Danish Rheumatism Association, Health Research Fund of Central Denmark Region, and Aase og Ejnar Danielsens Fund.

**Ethical approval** Ethical approval for this study was obtained from the Central Denmark Region Committee on Health Research Ethics (Casenr. 1-10-72-6-16 issued on February 24th, 2016).

## References

af Ekenstam F. Anatomy of the distal radioulnar joint. Clin Orthop Relat Res. 1992, 275: 14–8.

af Ekenstam F, Hagert CG. Anatomical studies on the geometry and stability of the distal radio ulnar joint. Scand J Plast Reconstr Surg. 1985, 19: 17–25.

Andersson JK, Andernord D, Karlsson J, Friden J. Efficacy of magnetic resonance imaging and clinical tests in diagnostics of wrist ligament injuries: a systematic review. Arthroscopy. 2015, 31: 2014–20 e2.

Atzei A. New trends in arthroscopic management of Type 1-b TFCC injuries with DRUJ instability. J Hand Surg Eur. 2009, 34: 582–91.

Chen YR, Tang JB. In vivo gliding and contact characteristics of the sigmoid notch and the ulna in forearm rotation. J Hand Surg Am. 2013, 38: 1513–9.

Gammon B, Lalone E, Nishiwaki M, Willing R, Johnson J, King GJW. Arthrokinematics of the distal radioulnar joint measured using intercartilage distance in an in vitro model. J Hand Surg Am. 2018, 43: 283 e1–e9.

Glowacki KA, Shin LA. Stabilization of the unstable distal ulna: the Linscheid–Hui procedure. Tech Hand Up Extrem Surg. 1999, 3: 229–36.

Gofton WT, Gordon KD, Dunning CE, Johnson JA, King GJ. Soft-tissue stabilizers of the distal radioulnar joint: an invitro kinematic study. J Hand Surg Am. 2004, 29: 423–31.

Hagert CG. The distal radioulnar joint in relation to the whole forearm. Clin Orthop Relat Res. 1992, 275: 56–64.

Hagert CG. Distal radius fracture and the distal radioulnar joint – anatomical considerations. Handchir Mikrochir Plast Chir. 1994, 26: 22–6.

Hansen L, De Raedt S, Jorgensen PB, Mygind-Klavsen B, Kaptein B, Stilling M. Marker free model-based radiostereometric analysis for evaluation of hip joint kinematics: a validation study. Bone Joint Res. 2018, 7: 379–87.

Hermansdorfer JD, Kleinman WB. Management of chronic peripheral tears of the triangular fibrocartilage complex. J Hand Surg Am. 1991, 16: 340–6.

Hess F, Farshad M, Sutter R, Nagy L, Schweizer A. A novel technique for detecting instability of the distal radioulnar joint in complete triangular fibrocartilage complex lesions. J Wrist Surg. 2012, 1: 153–8.

Iida A, Omokawa S, Moritomo H et al. Effect of wrist position on distal radioulnar joint stability: a biomechanical study. J Orthop Res. 2014, 32: 1247–51.

Kaptein BL, Valstar ER, Stoel BC, Rozing PM, Reiber JHC. Evaluation of three pose estimation algorithms for model-based roentgen stereophotogrammetric analysis. Prod IMechE Part H: J Engng Med. 2004, 218: 231–8.

King GJ, McMurtry RY, Rubenstein JD, Gertzbein SD. Kinematics of the distal radioulnar joint. J Hand Surg Am. 1986, 11: 798–804.

Kleinman WB. Stability of the distal radioulna joint: biomechanics, pathophysiology, physical diagnosis, and restoration of function what we have learned in 25 years. J Hand Surg Am. 2007, 32: 1086–106.

Lees VC. Functional anatomy of the distal radioulnar joint in health and disease. Ann R Coll Surg Engl. 2013, 95: 163–70.

Linscheid RL. Biomechanics of the distal radioulnar joint. Clin Orthop Relat Res. 1992, 275: 46–55.

Lo IK, MacDermid JC, Bennett JD, Bogoch E, King GJ. The radioulnar ratio: a new method of quantifying distal radioulnar joint subluxation. J Hand Surg Am. 2001, 26: 236–43.

McDonald CP, Moutzouros V, Bey MJ. Measuring dynamic in-vivo elbow kinematics: description of technique and estimation of accuracy. J Biomech Eng. 2012, 134: 124502.

Mino DE, Palmer AK, Levinsohn EM. The role of radiography and computerized tomography in the diagnosis of subluxation and dislocation of the distal radioulnar joint. J Hand Surg Am. 1983, 8: 23–31.

Moriya T, Aoki M, Iba K, Ozasa Y, Wada T, Yamashita T. Effect of triangular ligament tears on distal radioulnar joint instability and evaluation of three clinical tests: a biomechanical study. J Hand Surg Eur. 2009, 34: 219–23.

Nakamura R, Horii E, Imaeda T, Nakao E. Criteria for diagnosing distal radioulnar joint subluxation by computed tomography. Skeletal Radiol. 1996, 25: 649–53.

Nakamura T, Makita A. The proximal ligamentous component of the triangular fibrocartilage complex. J Hand Surg Br. 2000, 25: 479–86.

Ng AWH, Griffith JF, Fung CSY et al. Mr imaging of the traumatic triangular fibrocartilaginous complex tear. Quant Imaging Med Surg. 2017, 7: 443–60.

Nielsen ET, Stentz-Olesen K, de Raedt S et al. Influence of the anterolateral ligament on knee laxity: a biomechanical cadaveric study measuring knee kinematics in 6 degrees of freedom using dynamic radiostereometric analysis. Orthop J Sports Med. Epub ahead of print 6 August 2018. DOI: 10.1177/2325967118789699.

Omokawa S, Iida A, Kawamura K et al. A biomechanical perspective on distal radioulnar joint instability. J Wrist Surg. 2017, 6: 88–96.

Onishi T, Omokawa S, Iida A et al. Biomechanical study of distal radioulnar joint ballottement test. J Orthp Res. 2017, 35: 1123–7.

Palmer AK. Triangular fibrocartilage complex lesions: a classification. Hand Surg Am. 1989, 14: 594–606.

Park MJ, Kim JP. Reliability and normal values of various computed tomography methods for quantifying distal radioulnar joint translation. J Bone Joint Surg Am. 2008, 90: 145–53.

Pederzini L, Luchetti R, Soragni O et al. Evaluation of the triangular fibrocartilage complex tears by arthroscopy, arthrography, and magnetic resonance imaging. Arthroscopy. 1992, 8: 191–7.

Pickering GT, Nagata H, Giddins GEB. In-vivo three-dimensional measurement of distal radioulnar joint translation in normal and clinically unstable populations. J Hand Surg Eur. 2016, 41: 521–6.

Pirela-Cruz MA, Goll SR, Klug M, Windler D. Stress computed tomography analysis of the distal radioulnar joint: a diagnostic tool for determining translational motion. J Hand Surg Am. 1991, 16: 75–82.

Stuart PR, Berger RA, Linscheid RL, An KN. The dorsopalmar stability of the distal radioulnar joint. J Hand Surg Am. 2000, 25: 689–99.

Szabo RM. Distal radioulnar joint instability. J Bone Joint Surg Am. 2006, 88: 884–94.

Tay SC, Berger RA, Tomita K, Tan ET, Amrami KK, An KN. In vivo three-dimensional displacement of the distal radioulnar joint during resisted forearm rotation. J Hand Surg Am. 2007, 32: 450–8.

Tolat AR, Stanley JK, Trail IA. A cadaveric study of the anatomy and stability of the distal radioulnar joint in the coronal and transverse planes. J Hand Surg Br. 1996, 21: 587–94.

Wechsler RJ, Wehbe MA, Rifkin MD, Edeiken J, Branch HM. Computed tomography diagnosis of distal radioulnar subluxation. Skeletal Radiol. 1987, 16: 1–5.

Xu J, Tang JB. In vivo changes in lengths of the ligaments stabilizing the distal radioulnar joint. J Hand Surg Am. 2009, 34: 40–5.

Zlatkin MB, Rosner J. MR imaging of ligaments and triangular fibrocartilage complex of the wrist. Radiol Clin North Am. 2006, 44: 595–623.

# PAPER II

Thillemann *et al. J EXP ORTOP* (2021) 8:10
https://doi.org/10.1186/s40634-021-00329-y

Journal of
Experimental Orthopaedics

ORIGINAL PAPER

Open Access

# Distal radioulnar joint stabilization with open foveal reinsertion versus tendon graft reconstruction: an experimental study using radiostereometry

Janni Kjærgaard Thillemann[1,2*], Sepp De Raedt[3], Torben Bæk Hansen[1,2], Bo Munk[4] and Maiken Stilling[2,4]


## Abstract

**Purpose:** Symptomatic instability of the distal radioulnar joint (DRUJ) caused by lesion of the Triangular Fibrocartilage Complex (TFCC) can be treated with a number of surgical techniques. Clinical examination of DRUJ translation is subjective and limited by inter-observer variability.

The aim of this study was to compare the stabilizing effect on DRUJ translation with two different surgical methods using the Piano-key test and a new precise low-dose, non-invasive radiostereometric imaging method (AutoRSA).

**Methods:** In a randomized experimental study we evaluated the DRUJ translation in ten human cadaver arms (8 males, mean age 78 years) after cutting the proximal and distal TFCC insertions, and after open surgical TFCC reinsertion ($n=5$) or TFCC reconstruction using a palmaris longus tendon graft ad modum Adams ($n=5$).

The cadaver arms were mounted in a custom-made fixture for a standardized Piano-key test. Radiostereometric images were recorded and AutoRSA software was used for image analyses. Standardised anatomical axes and coordinate systems of the forearm computer tomography bone models were applied to estimate DRUJ translation after TFCC lesions and after surgical repair.

**Results:** The DRUJ translation after cutting the proximal and distal TFCC insertions was 2.48 mm (95% CI 1.61; 3.36). Foveal TFCC reinsertion reduced DRUJ translation by 1.78 mm (95% CI 0.82; 2.74, $p=0.007$), while TFCC reconstruction reduced DRUJ translation by 1.01 mm (95% CI -1.58; 3.60, $p=0.17$).

**Conclusion:** In conclusion, foveal TFCC reinsertion significantly decreased DRUJ translation while the stabilizing effect of Adams TFCC reconstruction was heterogeneous. This supports the clinical recommendation of TFCC reinsertion in patients suffering from symptomatic DRUJ instability due to acute fovea TFCC lesions.


**Keywords:** Distal radioulnar joint, Instability, Radiostereometry, Reconstruction, Surgery, Triangular fibrocartilage complex

*Correspondence: teamjanni@gmail.com
[1] University Clinic for Hand, Hip and Knee Surgery, Hospital Unit West, Lægaardvej 12, 7500 Holstebro, Denmark
Full list of author information is available at the end of the article

## Background

Symptomatic instability of the distal radioulnar joint (DRUJ) can result from lesion of the DRUJ stabilizing Triangular Fibrocartilage Complex (TFCC). Nakamura et al. described that the ulnar-sided TFCC insertion consist of both a distal component (dc) at the ulnar styloid and a proximal component (pc) at the ulnar fovea [22]. The pc-TFCC lesion is associated with a higher degree of DRUJ instability than the dc-TFCC lesion [32].

A treatmenet algorithm for ulnar-sided TFCC injuries has been proposed, in which treatment depend on both the completeness of the lesion (dc-TFCC or/and pc-TFCC) as well as the condition of the TCFF (repairable or non-repairable) [8]. Complete repairable combined dc- and pc-TFCC (class 2) can be surgically treated by open or arthroscopic foveal TFCC reinsertion. Contrary, delayed diagnosis of complete TFCC tears may result in a chronic (>6 months) [7] non-repairable TFCC tear (class 4) with degenerative retracted edges and poor healing potential [6, 7, 23]. These injuries require surgical TFCC reconstruction with a tendon graft [2, 7]. It is unknown if these surgical methods perform equivalently in terms of regaining primary DRUJ stability.

Investigations of the stabilizing effect of different surgical methods should preferably be performed in cadaver studies prior to clinical introduction. A non-invasive method for automated radiostereometric analysis (AutoRSA) was recently shown to provide precise quantification of DRUJ translation during the Piano-key test in cadavers [30].

The aim of this experimental study in human cadaver arms was to compare the effect of; open surgery with foveal reinsertion of the TFCC, or ligament reconstruction of the TFCC with palmaris longus graft ad modum Adams on the primary stability of the DRUJ.

## Methods

### Study design and specimens

We conducted a parallel group randomized controlled trial on human donorarms. The primary outcome in this experimental cadaver study was translation in the DRUJ during the Piano-key test. Ten freshly frozen human donorarms including hand, forearm, elbow and part of the humerus were used (Department of Biomedicine, Aarhus University). They were thawed for 48 h at 5 °C before use in the study.

The specimens (eight men, mean age 78 years (range 63–90)) were evaluated at baseline and met the inclusion criteria: no signs of previous fracture or malunion as evaluated by fluoroscopy of the wrist, forearm and elbow. The Central Denmark Region Committees on Health Research Ethics approved the study (Casenr. 1–10-72–6-16 issued on February 24th, 2016).

### Experimental setup

A radiolucent motorized fixture was used [30]. It allowed for a 7 kg load to be applied on the ulnar head by use of a fixture lever to imitate the clinical Piano-key test examination in a standardized setting [11]. An quivalent force was described not to give "obvious disruption of the soft tissues" in an experimental study [29]. In the test set-up the humerus was fixed in a 90 degrees vertical position, the forearm was pronated, and the hand was fixed to a horizontal plate, in zero degrees wrist extension and wrist deviation [30].

### Test protocol

Ligament lesion of the TFCC was performed using fluoroscopic visualization. The dorsal DRUJ capsule was opened transversely proximal to the TFCC, the dc-TFCC was released from the insertion on the ulnar styloid and the pc-TFCC was cut from the insertion in the ulnar fovea. Additional soft tissue and the remaining TFCC stabilizers of the DRUJ, including the interosseous membrane, were preserved.

Clinical examination of all specimens before and after intervention (Piano-key test and Ballottement test) was performed by two hand surgeons and consensus was obtained. DRUJ instability was evaluated as translation with the Ballottement test and categorized as proposed by Atzei et al.: less than 5 mm, between 5–10 mm (mild instability) or above 10 mm (severe instability) [9].

Wrist artrhroscopy was performed to confirm dc- and pc-TFCC lesion in terms of a positive trampoline test [15] and a positive Hook test [6].

For evaluation of DRUJ translation, the specimens were positioned in the custom-made fixture and recorded with synchronized static stereoradiographs before and after applying the Piano-Key test. The test was done twice on the specimens: first, after inflicted dc- and pc-TFCC lesion, and second, after surgical intervention.

### Intervention

The specimens were randomly assigned to one of two treatment groups. The open foveal TFCC reinsertion group was treated by open surgery: The skin was incized dorsal over the DRUJ and the DRUJ capsule was exposed through the $5^{th}$ extensor compartment, leaving the most distal part of the extensor retinaculum intact. A L-shaped capsular opening was performed by extending the opening to the radial side of the extensor carpi ulnaris tendon sheat on the proximal aspect of the dorsal radioulnar ligment, preserving the radial insertion. Any DRUJ synovitis was removed, the fovea was identifyed and controlled by fluroscopy before drilling and inserting a 2–0 Mitec Mini QUICKANCHOR® (DePuy Mitek, Raynham, MA, USA). The pc-TFCC was reinserted by a matress suture through the TFCC from proximal to distal and the Mitec suture was tied with 5 knots while the assistant compressed the DRUJ in neutral forearm rotation. Finaly, the dorsal capsule and the skin was closed with 3–0 vicryl sutures.

The Adams TFCC reconstruction group was reconstructed with a palmaris longus graft as described by Adams [1]. The DRUJ capsule was exposed through the 5$^{th}$ extensor compartment and an L-shaped capsular flap. Placement of the radius tunnel was guided by fluroscopy: a k-wire was placed for over-drilling of a 4 mm tunnel proximal to the lunate fossa and radial to the articular surface of the sigmoid notch. Likewise, a k-wire guided oblique ulnar tunnel was drilled from the lateral ulnar neck and emerging in the ulnar fovea. The palmaris graft was harvested and passed from the dorsal to the volar aspect of the wrist through a volar incision extending 3 cm promimal from the proximal wrist crease. The volar aspect of the radial tunnel was exposed and the graft was retracted with a straight tendon grasper. The volar limb of the graft was passed through the DRUJ capsule proximal to the TFCC remnants and both tendon limbs were passed through the ulnar tunnel. Finaly, the volar tendon limb was passed volarly around the ulnar neck, close to the bone, and tied dorsally with the first half of a surgeons knot while the assistant compressed the DRUJ in neutral forearm rotation. The tendon knot was secured with three 3–0 fiberwire mattress sutures. In addition a second tendon knot was tied and secured with further three mattress sutures. Finaly, the dorsal capsule and the skin was closed with 3–0 vicryl sutures.

### Randomization

The specimens were numbered and subsequently randomized by sequential drawing of ten sealed opaque envelopes, prepared with an equal 1:1 ratio distribution of intervention labels, that randomly assigned the specimens to two intervention groups: open surgery with foveal TFCC reinsertion [15]; or Adams TFCC reconstruction, with palmaris longus graft [1].

### Static radiostereometry setup

A digital radiostereometric system (AdoraRSA, NRT X-Ray, Hasselager, Denmark) was used to record static examinations of the specimens. Images were obtained with two digital image detectors (Canon CXDI-50RF) slotted beneath the uniplanar carbon calibration box (Carbon box 19, Medis Specials, Leiden, The Netherlands) and exposed with two x-ray tubes (20°-20° tube position on the vertical plane) (Fig. 1). Exposure settings for static stereoradiographs were 60 kV, 2.5 mAs, 2208 × 2688 pixels resolution (0.16 × 0.16 mm/pixel). The Source Skin Distance (SSD) was 100 cm and the Source to Images Distance (SID) was 150 cm.

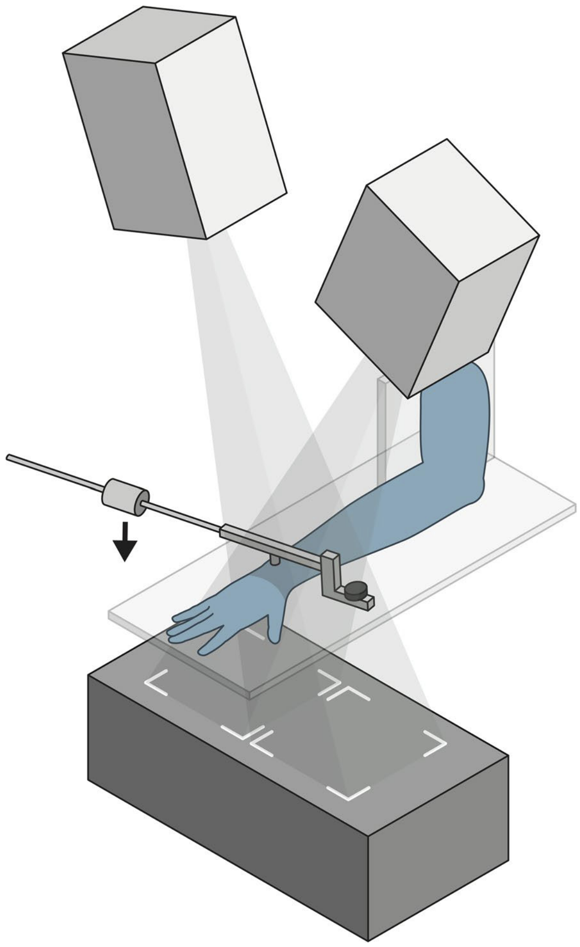

**Fig. 1** Digital radiostereometric system setup. The x-ray tubes are positioned with a 20°-20° tilt on the vertical plane. Static wrist examinations were recorded with two digital image detectors (Canon CXDI-50RF) beneath a horizontal positioned uniplanar carbon calibration box. The Piano-key test is indicated by the arrow and appyed by a lever (7 kg)

### Analysis of radiographs

Analysis of the static stereoradiographs depend on bone models and kinematic axis. The bone models were generated form computer tomography (CT) scans (Philips Brilliance 64, 120 kV, 100 mAs) of the intact human donor forearms. CT images were reconstructed (0.9 mm slice thickness, 0.45 mm slice increment and 0.27 × 0.27 mm in-plane pixel size) and The Insight Segmentation and The Visualization Toolkit softwares (Kitware, New York, USA) were used for image processing of subject specific bone models (radius and ulna). First, an automated graph-cut method was used for bone segmentation. Second, bone volume models with greyscale information were extracted. Surface bone models were created and finaly simplified to consist of 10.000 triangles [14].

Analysis of the stereoradiographs defined the three-dimensional position and orientation of the ulna and radius bone. Model-based radiostereometric analysis software (MBRSA 4.11, RSAcore, Leiden) was used for image calibration. Further, the Model-based RSA software automatically detected the bone edges of the ulna and radius on the stereoradiographs and the relevant edges were selected manually [18] (Fig. 2). The CT based surface bone models were imported in the program and the best pose of the bones was automatically estimated by minimizing the error of the surface bone model projections versus the manually detected bone edges on the stereoradiographs. The final pose was used as an initial bone position in the subsequent analysis of the stereoradiograph with non-commercial AutoRSA software.

The CT based volume bone models were used to simulate digital reconstructed radiographs (DRR), and the AutoRSA software calculated the optimal pose of the models by repeated comparison between the simulated DRR and the stereoradiographic images until no further improvements could be made (Fig. 3). The bone registration area was focused on the stereoradiograph with an automatically produced mask projected from the CT bone volume model.

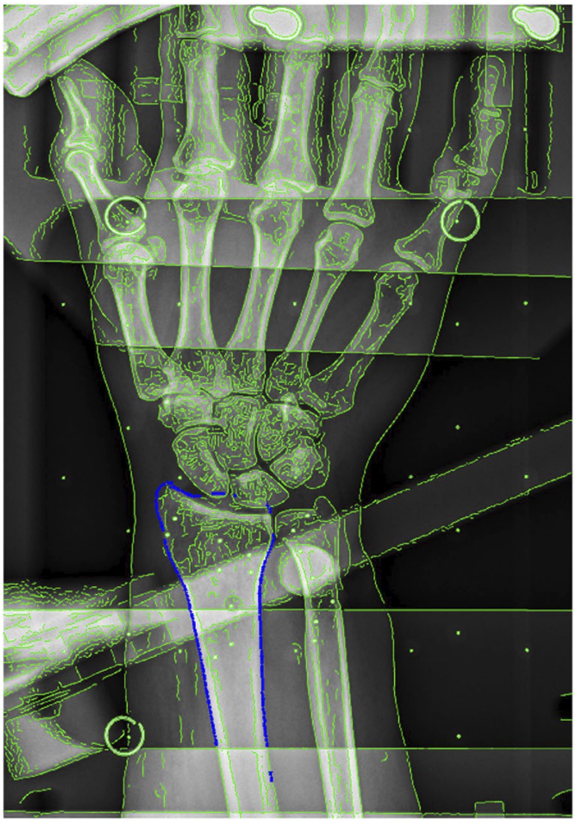

**Fig. 2** Model-based radiostereometric analysis (MBRSA). MBRSA software automatically detected the ulna and radius bone edges (green) and relevant edges (blue) was manually selected on the stereoradiographs

We have previously examined the precision of the AutoRSA software, as compared to marker-based radiostereometric analysis (reference standard), for dynamic examinations of the radius and ulna. The precision of AutoRSA (95% Limits of agreement) was below 0.12 mm for translation of the radius, below 0.18 mm for translation of the ulna, and less than 0.98 degrees in rotations for both the radius and ulna.

### Coordinate system and kinematic axis

The position of the radius and ulna in the calibration box coordinate system was transformed to a standardized anatomical coordinate system for each bone. Three orthogonal axes (x,y,z), were each defined from three anatomical landmarks [20] on the 3D CT of each bone surface model. The radius landmarks were; the proximal rotation center of the radial head ($C_{prox}$), the radial styloid tip, and the distal radioulnar joint surface center. On the ulna the landmarks were; the ulnar head center ($C_{dist}$), the distal ulnar styloid tip, and greater sigmoid notch center. The best fitted sphere of 3 points picked on the radial and ulnar head surfaces was used to compute the center points.

A single radioulnar joint axis (RUJ axis) extending from the radial head centre to the ulnar head centre as described by Hagert et al. was used to calculated kinematics [20]. Further, the radius sigmoid notch line, a connecting line from the midpoint of the volar to dorsal rim of the radius sigmoid notch, was definedThe orthogonal projection of the RUL axis on the radius sigmoid notch line determined the DRUJ position. The DRUJ position ratio was calculated as the relation of the DRUJ position and the individual sigmoid notch length, to take the difference of individual bone-sizes into account. The DRUJ translation was the change of DRUJ position in millimeters (Figs. 4 and 5).

Forearm rotation was calculated as; the angle between the line from the radial styloid tip to the midpoint on the sigmoid notch line, and the line from the ulnar head center and to the distal ulnar styloid tip (Fig. 4).

### Sample size

The sample size calculation was based on a study by Pickering et al. who used an externally mounted rig to measure DRUJ translation on pronated forearms in normal and clinically unstable populations [5]. The DRUJ translation on the pronated forearm was 4.2 mm (SD 0.5) in healthy controls compared to 7.0 mm (SD 0.5) in the clinically unstable patient group. With a power of 0.90 and alfa of 0.05 a sample size of three patients per group for a two-sample comparison of means was estimated.

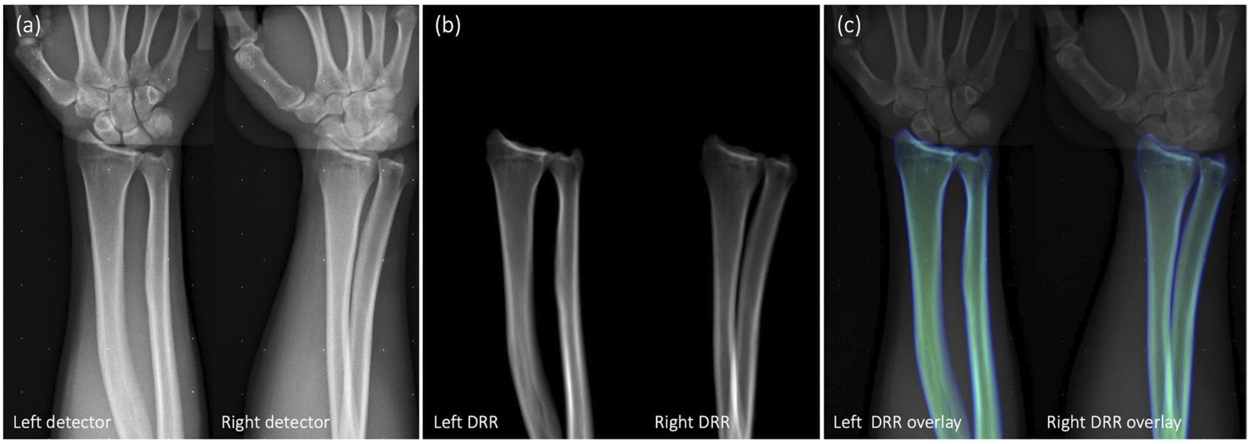


**Fig. 3** AutoRSA analysis of radiostereometric images. Comparison of (**a**) radiostereometric images and (**b**) CT based digital reconstructed radiographs (DRR), was performed with a mathematical algorithm in the AutoRSA software until no further improvements could be made. The optimal overlay (**c**) was calculated by the AutoRSA software

A sample size of five patients per group was selected to allow for incomplete data collection/imaging errors.

### Statistical analysis

Categorical data was reported as numbers and were compared between groups using the chi-squared test. Normality of continous data was evaluated by instpection of frequenzy and probability plots (quantile–quantile plots). The student's paired t-test was used to compare forearm rotation, DRUJ position and DRUJ translation before and after intervention within groups. Comparison between the independent groups were performed with the non-paired t-test. The level of significance was set at $p < 0.05$ and data was reported as means and 95% confidence intervals (95% CI).

## Results

### Preoperative group comparison

The two groups had comparable preoperative characteristics including age, sex, right/left hand, clinical instability evaluation with the Ballottement test and arthroscopic evaluation (Table 1).

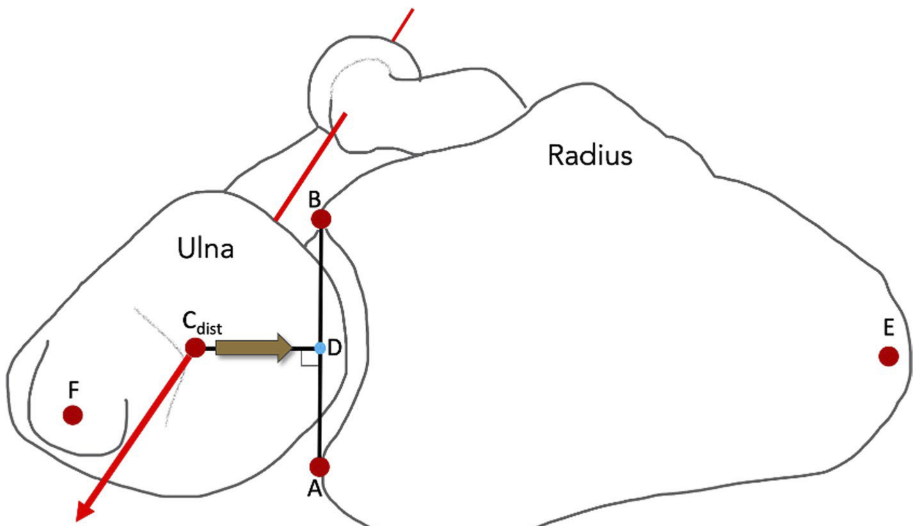


**Fig. 4** Kinematic axis and anatomical landmarks. The distal radioulnar (DRUJ) position (D) was defined as the orthogonal projection (yellow arrow) from the radioulnar axis (red line) perpendicular to the radius sigmoid notch line (AB) connecting the anterior (A) and posterior (B) rim points. The DRUJ translation was calculated as the change of DRUJ position (D) on the sigmoid notch line (AB) in millimeters. The DRUJ postion ratio was calculated as AD/AB. Forearm rotation was calculated as; the angle between the line from the radial styloid tip (E) to the midpoint on the sigmoid notch line (AB), and the line from the ulnar head center ($C_{dist}$) to the distal ulnar styloid tip (F)

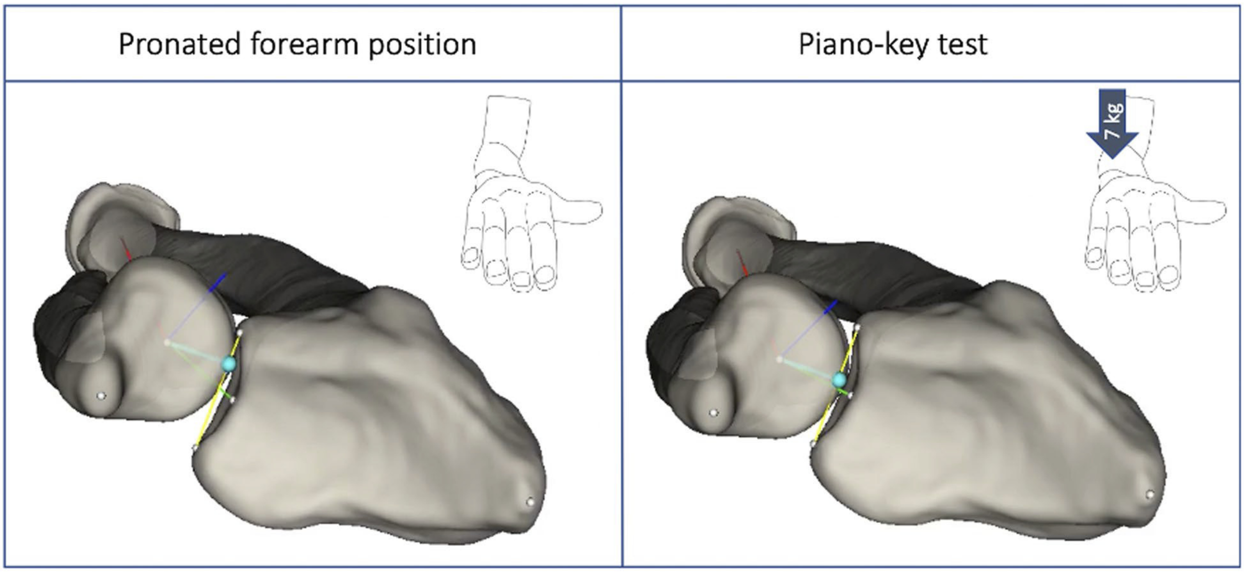


**Fig. 5** Bone model position after AutoRSA analysis of a cadaver arm before and after the Piano-key test

## Clinical examination

After combined TFCC lesion, a consensus evaluation between two hand surgeons categorized all 10 cadaver arms with > 5 mm translation in the DRUJ during the Ballottement test on neutral forearm rotation.

Both the foveal TFCC reinsertion and the Adams TFCC reconstruction stabilized the DRUJ, as the Ballottement test on neutral forearm rotation, was categorized to translate less than 5 mm in all 10 cadaver arms, after surgical treatment (Table 1).

**Table 1 Specimen characteristica**

| | Foveal reinsertion | Adams reconstruction | *p* |
|---|---|---|---|
| **Number** | 5 | 5 | |
| **Age in years** (mean, range) | 77 (72–90) | 79 (63–90) | 0.98 |
| **Sex** (men/women) | 5/0 | 3/2 | 0.11 |
| **Side** (right/left) | 4/1 | 1/4 | 0.06 |
| **Ballottement test** [a] | | | |
| ***Neutral position*** | 0/2/3 | 0/4/1 | 0.29 |
| ***Supination*** | 3/2/0 | 4/1/0 | 0.49 |
| ***Pronation*** | 0/5/0 | 0/5/0 | 1.0 |
| **Trampoline test (-/+)** | 0/5 | 0/5 | 1.0 |
| **Hook test (-/+)** | 0/5 | 0/5 | 1.0 |

Summarized characteristica and pre-operative clinical- and arthroscopic findings of cadaver wrists with combined dc- and pc-TFCC lesion

[a] Numbers evaluated with less than 5 mm, between 5–10 mm (mild instability) or above 10 mm DRUJ translation (severe)

## Atrhroscopic evaluation

The preoperative arthroscopic evaluation revealed a positive Trampoline test and Hook test in all ten cadaver arms after ligament lesion including the dc- and pc-TFCC (Table 1).

## Preoperative radiostereometric evaluation

The DRUJ position ratio in pronated forearms ($n = 10$) with inflicted dc- and pc-TFCC lesion was mean 0.68 (95% CI 0.61; 0.75). The Piano-key test induced a dorsovolar DRUJ translation of mean 18% (95% CI 12; 25) of the sigmoid notch length, cooresponding to 2.45 mm (95% CI 1.68; 3.22).

A comparison of the foveal TFCC reinsertion and Adams TFCC reconstruction groups with inflicted dc- and pc-TFCC showed no difference in DRUJ position ratio before apying the Piano-key test ($p = 0.21$). In both groups the Piano-key test induced a statistically significant volarly directed translation of the ulnar head in the sigmoid notch ($p < 0.01$) (Fig. 5). The resulting DRUJ position was mean 0.51 (95% CI 0.45;0.57) and mean 0.48 (05% CI 0.28;0.68), respectively ($p = 0.72$) (Table 2, Fig. 6).

The preoperative DRUJ translation induced by the Piano-key test was mean 1.86 mm (95% CI 0.84; 2.89) in the foveal TFCC reinsertion group and mean 3.05 mm (95% CI 1.78; 4.32) in the Adams TFCC reconstruction group ($p = 0.08$) (Fig. 7).

With lesion of the dc- and pc-TFCC, the maximum passive forearm pronation in the test fixture was mean 81 degrees (95% CI 68; 93) in the FR group and mean

**Table 2 Specimens distal radioulnar joint pronation and position ratio**

| *Group* | **With dc/pc-TFCC lesion** | | | **After surgical treatment** | | |
|---|---|---|---|---|---|---|
| | ***Foveal TFCC reinsertion*** | ***Adams TFCC reconstruction*** | ***p*** | ***Foveal TFCC reinsertion*** | ***Adams TFCC reconstruction*** | ***p*** |
| Number | 5 | 5 | | 5 | 5 | |
| **Pronated forearm** | | | | | | |
| Degrees pronation (°) | 81 (68–93) | 82 (72–91) | 0.87 | 58 (44–73) | 68 (49–88) | 0.31 |
| DRUJ position ratio | 0.63 (0.52–0.75) | 0.72 (0.60–0.84) | 0.21 | 0.60 (0.57–0.63) | 0.77 (0.65–0.89) | 0.005 |
| **Piano- key test** | | | | | | |
| Degrees pronation (°) | 68 (61–76) | 59 (53–65) | 0.02 | 60 (44–76) | 60 (45–69) | 0.68 |
| DRUJ position ratio | 0.51 (0.45–0.57) | 0.48 (0.28–0.68) | 0.72 | 0.60 (0.57–0.63) | 0.61 (0.41–0.81) | 0.87 |

Degrees of forearm pronation and DRUJ position ratio before and after the Piano-key test in cadaverarms with combined dc- and pc-TFCC lesion and after surgical repair with foveal TFCC reinsertion or Adams TFCC reconstruction. Data are presented as means and (95% CI)

*DRUJ* Distal radioulnar joint, *dc* distal component, *pc* proximal component, *TFCC* triangular fibrocartilage complex

82 degrees (95% CI 72; 91) in the Adams TFCC reconstruction group ($p = 0.87$) (Table 2).

**Postoperative radiostereometric evaluation**

Surgical treatment did not shift the DRUJ position ratio of the pronated arm significantly in either group ($p > 0.30$). The Piano-key test shifted the ulnar head to a similar DRUJ position ratio of mean 0.60 (95% CI 0.57; 0.63) in the foveal TFCC reinsertion group and to mean 0.61 (95% CI 0.41; 0.81) in the Adams TFCC reconstruction group ($p = 0.87$) (Table 2, Fig. 6).

Surgical treatment reduced the DRUJ translation by mean 1.78 mm (95% CI 0.82; 2.74) in the foveal TFCC reinsertion group ($p = 0.007$), and by mean 1.01 mm (95% CI -1.58; 3.60) in the Adams TFCC reconstruction group ($p = 0.17$) (Fig. 7). The stabilizing effect of the two surgical methods was similar ($p = 0.31$), but with greater variation in the Adams TFCC reconstruction group.

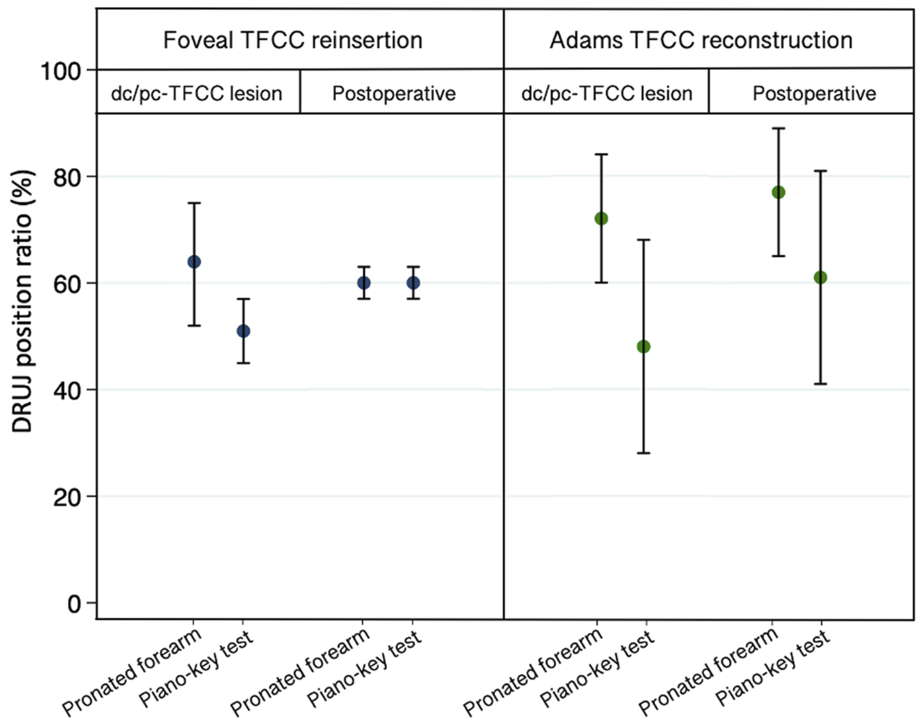


**Fig. 6** DRUJ position ratio (%) in the foveal TFCC reinsertion group ($n = 5$) and the Adams reconstruction group ($n = 5$), on pronated forearm and during the Piano-key test, with combined distal- and proximal component TFCC lesion and after surgical treatment. (DRUJ: Distal radioulnar joint, dc: distal component, pc: proximal component, TFCC: triangular fibrocartilage complex; dc-TFCC: distal component TFCC; pc: proximal component TFCC)

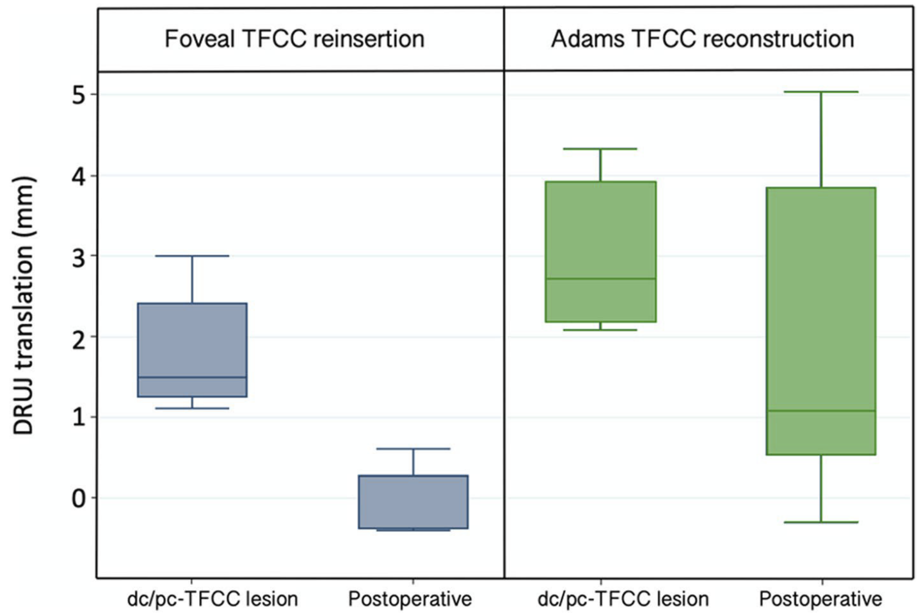


**Fig. 7** Box plot of DRUJ translation (mm) induced by the Piano-key test in the foveal TFCC reinsertion group ($n = 5$) and the Adams reconstruction group ($n = 5$), with combined dc/pc-TFCC lesion and after surgical treatment. (DRUJ: Distal radioulnar joint, dc: distal component, pc: proximal component, TFCC: triangular fibrocartilage complex)

The final DRUJ translation induced by the Piano-key test after surgery, was mean 0.08 mm (95% CI -0.48; 0.64) in the foveal TFCC reinsertion group and mean 2.04 mm (95% CI -0.81; 4.89) in the Adams TFCC reconstruction group ($p = 0.10$) (Fig. 7).

Surgery reduced the passive pronation with mean 23 degrees (95% CI -3; 46) in the foveal TFCC reinsertion group ($p = 0.07$) and with mean 14 degrees (95% CI -5; 32) in the Adams TFCC reconstruction group ($p = 0.12$) (Table 2). The decrease in pronation was similar in the two groups ($p = 0.46$).

## Discussion

In the present study, we found a mean DRUJ translation after Adams TFCC reconstruction of mean 2.03 mm (95% CI -0.81; 4.89).

Objective measuring tools useful for clinical assesment of DRUJ stability in surgically treated patients are few, and to our knowledge, Hess et al. is the only other research group who have developed, validated and used an objective measuring tool, for assessment of DRUJ stability in surgically treated patients [16]. They treated 11 patients with open TFCC reconstruction similar to the Adams [1] method, but with a modification of the graft fixation, and used ultrasonography to evaluate the DRUJ translation of the operated wrist in comparison with the contralateral healthy wrist. After TFCC reconstruction the uni-directional sonography measured DRUJ translation was mean 3.5 mm (range 1.1–6.2) [16]. Yet, a marked variation in stabilization effect was seen as the DRUJ translation was decreased in three patients, another three had DRUJ translation comparable to the contralateral healthy wrist, and the remaining five patiens were still more lax than on the contralateral side. This is in accordance with the present study as we observed high variability of the stabilizing effect of the Adams ligament reconstruction and no significant improvement of the DRUJ translation.

Contrary, open foveal TFCC reinsertion stabilized the DRUJ significantly and homogenuously with a mean DRUJ translation of 0.08 mm (95% CI -0.48; 0.64). However, the method tended to reduce the DRUJ translation to nearly zero. In a previous study on uninjured cadaver wrists with normal arthroscopic Hook test and trampoline test, examined with a similar radiostereometry setup, we found a DRUJ translation of mean 1.36 mm (95% CI 0.17;2.55) [30]. It is unknow if overtightening of the radioulnar ligaments during TFCC surgery will obstruct the rehabilitation of supination and pronation motions or result in pain. Hess et al. reported poor patient reported outcomes (PRWE) and persisting wrist pain in one patient with decreased DRUJ translation compared to the contralateral side, but the forearm rotation was acceptable [16].

### Clinical evaluation of DRUJ stability

In this study, clinical examination of DRUJ instability was assesed with the ballottement test.

We did not have a contralateral arm to compare to, as recommended by Nakamura et al. [23]. Therefore, we categorized the DRUJ instability grade as proposed by Atzei et al. [9]. The postoperative DRUJ translation was graded to be less than 5 mm in all cadaver arms with no difference between the foveal TFCC reinsertion and Adams TFCC reconstruction groups. Thus, the difference of surgical methods on the effect of DRUJ stability was only detectable with radiostereometry.

In patients, abnormal translation with a 'soft' resistance can be felt in the clinically unstable DRUJ [7]. However, muscular stabilizers of the DRUJ can lead to a false negative examination in DRUJ unstable patients [6]. Clinical wrist examination has previously been described as subjective, highly observer dependent, and of limited diagnostic value to detect TFCC lesions [27]. This may contribute to the problem of delayed diagnosis of DRUJ instability after wrist fractures and/or sprains [4], as well as to challenge a reliable objective evaluation of DRUJ stability in the postoperative phase. Despite this fact, surgeons most frequently use clinical examination for postoperative evaluation of DRUJ stability in clinical studies [2, 21, 23], whereas precise and validated objective examination tools are rarely used.

### Other methods for evaluation of DRUJ stability

In-vivo methods for diagnosing DRUJ instability are available. Computer tomography (CT) of static forearm supination and pronation have been used to detect DRUJ instability in terms of subluxation, but the reliability of these static methods vary and do not asses the DRUJ translation [25]. Pickering et al. developd and used an externally mounted rig for examination of 50 patients with TFCC lesions, and found a bi-directional translation of 7.0 mm (SD 0.5) in pronated forearms [26]. Hess et al. used ultrasonography for preoperative examination of in 17 patients with TFCC lesions, and measured a uni-directional DRUJ translation of mean 5.1 mm (range 2.4–7.1) [17].

With devices only applicable for ex-vivo use the bi-directional DRUJ translation in pronated forarms was repored to range from 2.9–12.4 mm [19, 24, 28].

In the present study the uni-directional DRUJ translation was 2.45 mm (95% CI 1.68; 3.22) in cadaverarms with combined distal component and proximal component TFCC lesion. This is less than previous reports, which may be explained by differences in bi/uni-directional measures, soft tissue movement being included in the rig measures, and the degree of pronation during examination.

A clinical applicable method including measures of bone and joint kinematics only, is preferable and increase realiability in small joints.

### DRUJ position ratio

The native DRUJ was previously described to be stabilized in pronation by the bony sigmoid notch concavity [3] and moreover, by the proximal component of the TCFF which insert in the fovea [12, 22, 29]. In a previous radiostereometric study on intact cadaverarms, the DRUJ position ratio was 0.61 (95% CI 55;67) when applying the Piano-key test, which is comparable to the final DRUJ position ration obtained after surgery in both the foveal TFCC reinsertion and Adams TFCC reconstruction groups in the present study [30].

### Limitations

This experimental study was performed on an aged cadaver population and has natural limitations. Postmortem ligament laxity and tensile strength as well as the type of TFCC lesion that can be applied ex-vivo do probably not completely resemble the conditions of in-vivo traumatic TFCC lesions and the resulting pre-operative group instability varied despite randomization.

Efforts were made to standardize the test set-up by performing fluoroscopy assisted ligament lesion, and all specimens had similar clinical assessment and arthroscopic verification of a positive Hook test was performed before RSA examination (Table 1). Despite this, the sample size may not have been sufficiently large to ensure high preoperative similarity or sufficiently large to detect significant differences in stability gained by the surgical procedure (type 2 error).

We performed pre-study fluoroscopy and CT scans of the used specimens and excluded any with visible fracture deformity, which could influence the DRUJ kinematics. In addition, arthroscopy was used to confirm and classify TFCC lesions like in the clinical situation. The original method of TFCC reconstruction, described by Adams et al. was used [1]. The final palmaris graft closure depend on knots and suturing of the graft. The tecnique has been modified by other authors to replace tendon knots with an intereference screw to secure the tendon graft in the ulna bone, which may produce more reliable DRUJ stability [16, 31].

This study is experimental and can only account for the stability of the surgical techniques directly after surgery. In patients, the effects of adhesions, scar tissue generation and developed laxity during rehabilitation, may affect DRUJ stability after longer-term clinical follow-up.

## Conclusions

This study demonstrates the feasibility of radiostereometric imaging and AutoRSA analysis in an experimental setup, a non-invasive CT bone model-based method, for precise quantification of DRUJ translation before and after surgical treatment.

Dynamic radiostereometry and AutoRSA analysis is an innovative method that has been proven feasible for studies of kinematics of other joints [10, 13]. In a clinical perspective, a valid imaging and analysis method for examination of DRUJ translation in patients is demanded. The AutoRSA method is likely applicable in patients during dynamic loaded tests for evaluation of DRUJ translation in a diagnostic assessment and after surgical treatments. Investigations of feasibility and validity in patients and establishment of normal values for DRUJ stability are warranted.

In conclusion, the open foveal TFCC reinsertion to the ulnar fovea provided a significant decrease in DRUJ translation with foveal TFCC reinsertion, whereas the stabilizing effect of the Adams TFCC reconstruction had greater variation and demonstrated no significant improvement of the DRUJ translation.

This supports the current clinical recommendation of TFCC reinsertion in patients suffering from symptomatic DRUJ instability due to acute fovea TFCC lesions and emphazice the importance of timely diagnosis and treatment. On the contrary, this also reinforce the recommendation that TFCC reconstruction should be spared for treatment of chronic lesions, where the remnant of the TFCC is absent or too weak to be repaired.

However, the clinical relevance of the observed difference has to be studied in a clinical setup with focus on the stabilizing effect on patient reported outcome.

### Abbreviations

DRUJ: Distal radioulnar joint; TFCC: Triangular Fibrocartilage Complex; pc: Proximal component; dc: Distal component; CT: Computer tomography; AutoRSA: Automated radiostereometric analysis; SSD: Source Skin Distance; SID: Source to Images Distance; DRR: Digital reconstructed radiographs; $C_{prox}$: Proximal rotation center point of the radial head; $C_{dist}$: Ulnar head center point; RUJ: Radioulnar joint; PRWE: Patient-Rated Wrist Evaluation.

### Acknowledgements

We would like to thank radiographer Lars Lindgren, from the Department of Radiology, Aarhus University Hospital, for his valuable help with the radiostereometric recordings.

### Authors' contributions

JKT, SDR, TBH and MS carried out the design of the study. JKT, BM and MS participated in data acquisition. JKT, SDR and MS participated in analysis and interpretation of data. SDR and MS developed the AutoRSA software used in the work. JKT drafted the manuscript. TBH, SDR, BM and MS participated with critical revision of the manuscript. All authors read and approved the final manuscript.

### Funding

This study was supported by the Innovation Fund Grant 69–2013-1, "Transforming radiological technology for assessment of implant fixation: from research tool to clinical application", The Danish Rheumatism Association and the Health Research Fund of Central Denmark Region and Health Research Fund of Central Denmark Region, Aarhus University.

### Availability of data and materials

The datasets used and/or analysed during the current study are available from the corresponding author on reasonable request.

### Ethics approval and consent to participate

The study was approved by The Central Denmark Region Committees on Health Research Ethics.

### Consent for publication

Not applicable.

### Competing interests

The authors declare that they have no competing interests.

### Author details

[1] University Clinic for Hand, Hip and Knee Surgery, Hospital Unit West, Lægaardvej 12, 7500 Holstebro, Denmark. [2] Department of Clinical Medicine, Aarhus University, Palle Juul-Jensens Boulevard 165, 8200 Aarhus N, Denmark. [3] NRT X-RAY A/S, Birkegårdsvej 16, 8361 Hasselager, Denmark. [4] Department of Orthopaedic Surgery, Aarhus University, Palle Juul-Jensens Boulevard 165, J-501, 8200 Aarhus N, Denmark.

Received: 14 December 2020 Accepted: 19 January 2021
Published online: 04 February 2021

### References

1. Adams BD (2000) Anatomic reconstruction of the distal radioulnar ligaments for DRUJ instability. Tech Hand UpExtremSurg 4(3):154–160
2. Adams BD, Berger RA (2002) An anatomic reconstruction of the distal radioulnar ligaments for posttraumatic distal radioulnar joint instability. J Hand Surg Am 27(2):243–251
3. afEkenstam F (1992) Anatomy of the distal radioulnar joint. Clin Orthop Relat Res 275:14–18
4. Andersson JK, Lindau T, Karlsson J, Friden J (2014) Distal radio-ulnar joint instability in children and adolescents after wrist trauma. J Hand Surg Eur 39(6):653–661. https://doi.org/10.1177/1753193413518707
5. Andersson JK, Andernord D, Karlsson J, Friden J (2015) Efficacy of magnetic resonance imaging and clinical tests in diagnostics of wrist ligament injuries: a systematic review. Arthroscopy 31(10):2014–20.e2. https://doi.org/10.1016/j.arthro.2015.04.090
6. Atzei A (2009) New trends in arthroscopic management of type 1-B TFCC injuries with DRUJ instability. J Hand Surg Eur 34(5):582–591. https://doi.org/10.1177/1753193409100120
7. Atzei A, Luchetti R (2011) Foveal TFCC tear classification and treatment. Hand Clin 27(3):263–272. https://doi.org/10.1016/j.hcl.2011.05.014
8. Atzei A, Luchetti R, Garagnani L (2017) Classification of ulnar triangular fibrocartilage complex tears. A treatment algorithm for Palmer type IB tears. J Hand Surg Eur 42(4):405–14. https://doi.org/10.1177/1753193416687479
9. Atzei A, Rizzo A, Luchetti R, Fairplay T (2008) Arthroscopic foveal repair of triangular fibrocartilage complex peripheral lesion with distal radioulnar joint instability. Tech Hand Up Extrem Surg 12(4):226–235. https://doi.org/10.1097/BTH.0b013e3181901b1
10. Christensen R, Petersen ET, Jurgens-Lahnstein J, Rytter S, Lindgren L, De Raedt S et al (2020) Assessment of knee kinematics with dynamic radiostereometry: validation of an automated model-based method of analysis using bone models. J Orthop Res. https://doi.org/10.1002/jor.24875
11. Cooney WP 3rd, Dobyns JH, Linscheid RL (1980) Complications of Colles' fractures. J Bone Joint Surg Am 62(4):613–619
12. Hagert E, Hagert CG (2010) Understanding stability of the distal radioulnar joint through an understanding of its anatomy. Hand Clin 26(4):459–466. https://doi.org/10.1016/j.hcl.2010.05.002
13. Hansen L, de Raedt S, Jorgensen PB, Mygind-Klavsen B, Kaptein B, Stilling M (2017) Dynamic radiostereometric analysis for evaluation of hip joint pathomechanics. J Exp Orthop 4(1):20. https://doi.org/10.1186/s40634-017-0096-2

14. Hansen L, De Raedt S, Jorgensen PB, Mygind-Klavsen B, Kaptein B, Stilling M (2018) Marker free model-based radiostereometric analysis for evaluation of hip joint kinematics: a validation study. Bone Joint Res 7(6):379–387. https://doi.org/10.1302/2046-3758.76.BJR-2017-0268.R1
15. Hermansdorfer JD, Kleinman WB (1991) Management of chronic peripheral tears of the triangular fibrocartilage complex. J Hand Surg Am 16(2):340–346
16. Hess F, Sutter R, Nagy L, Schweizer A (2016) Stability and clinical outcome after reconstruction of complete triangular fibrocartilage disruption. J Wrist Surg 5(2):124–130. https://doi.org/10.1055/s-0036-1571282
17. Hess F, Farshad M, Sutter R, Nagy L, Schweizer A (2012) A novel technique for detecting instability of the distal radioulnar joint in complete triangular fibrocartilage complex lesions. J Wrist Surg 1(2):153–158. https://doi.org/10.1055/s-0032-1312046
18. Kaptein BL, Valstar ER, Stoel BC, Rozing PM, Reiber JHC (2004) Evaluation of three pose estimation algorithms for model-based Roentgen stereophotogrammetric analysis. Proc Inst Mech Eng H 218(4):231–238. https://doi.org/10.1243/0954411041561036
19. Kihara H, Short WH, Werner FW, Fortino MD, Palmer AK (1995) The stabilizing mechanism of the distal radioulnar joint during pronation and supination. J Hand Surg Am 20(6):930–936. https://doi.org/10.1016/S0363-5023(05)80139-X
20. McDonald CP, Moutzouros V, Bey MJ (2012) Measuring dynamic in-vivo elbow kinematics: description of technique and estimation of accuracy. J Biomech Eng 134(12):124502. https://doi.org/10.1115/1.4007951
21. Moritomo H, Masatomi T, Murase T, Miyake J, Okada K, Yoshikawa H (2010) Open repair of foveal avulsion of the triangular fibrocartilage complex and comparison by types of injury mechanism. J Hand Surg Am 35(12):1955–1963. https://doi.org/10.1016/j.jhsa.2010.07.031
22. Nakamura T, Yabe Y, Horiuchi Y (1996) Functional anatomy of the triangular fibrocartilage complex. J Hand Surg Br 21(5):581–586. https://doi.org/10.1016/S0266-7681(96)80135-5
23. Nakamura T, Sato K, Okazaki M, Toyama Y, Ikegami H (2011) Repair of foveal detachment of the triangular fibrocartilage complex: open and arthroscopic transosseous techniques. Hand Clin 27(3):281–290. https://doi.org/10.1016/j.hcl.2011.05.002
24. Onishi T, Omokawa S, Iida A, Nakanishi Y, Kira T, Moritomo H et al (2017) Biomechanical study of distal radioulnar joint ballottement test. J Orthop Res 35(5):1123–1127. https://doi.org/10.1002/jor.23355
25. Park MJ, Kim JP (2008) Reliability and normal values of various computed tomography methods for quantifying distal radioulnar joint translation. J Bone Joint Surg Am 90(1):145–153. https://doi.org/10.2106/JBJS.F.01603
26. Pickering GT, Nagata H, Giddins GEB (2016) In-vivo three-dimensional measurement of distal radioulnar joint translation in normal and clinically unstable populations. J Hand Surg Eur 41(5):521–526. https://doi.org/10.1177/1753193415618110
27. Prosser R, Harvey L, Lastayo P, Hargreaves I, Scougall P, Herbert RD (2011) Provocative wrist tests and MRI are of limited diagnostic value for suspected wrist ligament injuries: a cross-sectional study. J Physiother 57(4):247–253. https://doi.org/10.1016/S1836-9553(11)70055-8
28. Riggenbach MD, Conrad BP, Wright TW, Dell PC (2013) Distal oblique bundle reconstruction and distal radioulnar joint instability. J Wrist Surg 2(4):330–336. https://doi.org/10.1055/s-0033-1358546
29. Stuart PR, Berger RA, Linscheid RL, An KN (2000) The dorsopalmar stability of the distal radioulnar joint. J Hand Surg Am 25(4):689–699. https://doi.org/10.1053/jhsu.2000.9418
30. Thillemann JK, De Raedt S, Jorgensen PB, Romer L, Hansen TB, Stilling M (2020) Distal radioulnar joint stability measured with radiostereometry during the piano key test. J Hand Surg Eur 45(9):923–930. https://doi.org/10.1177/1753193420934689
31. Tse WL, Lau SW, Wong WY, Cheng HS, Chow CS, Ho PC et al (2013) Arthroscopic reconstruction of triangular fibrocartilage complex (TFCC) with tendon graft for chronic DRUJ instability. Injury 44(3):386–390. https://doi.org/10.1016/j.injury.2013.01.009
32. Wysocki RW, Richard MJ, Crowe MM, Leversedge FJ, Ruch DS (2012) Arthroscopic treatment of peripheral triangular fibrocartilage complex tears with the deep fibers intact. J Hand Surg Am 37(3):509–516. https://doi.org/10.1016/j.jhsa.2011.12.023

## Publisher's Note

Springer Nature remains neutral with regard to jurisdictional claims in published maps and institutional affiliations.

PAPER III

Published online: 2021-12-27



# Normal Values of Distal Radioulnar Joint Kinematics during a Dynamic Press Test

Janni Kjærgaard Thillemann, MD[1,2,3] Sepp De Raedt, MSc, PhD[3,4] Emil Toft Petersen, MSc[1,2,3]
Katriina Bøcker Puhakka, MD, PhD[5,6] Torben Bæk Hansen, MD, PhD[1,2] Maiken Stilling, MD, PhD[2,3,7]

[1] Department of Orthopaedics, University Clinic for Hand, Hip and Knee Surgery, Hospital Unit West, Holstebro, Denmark
[2] Department of Clinical Medicine, Aarhus University, Aarhus N, Denmark
[3] AutoRSA Research Group, Orthopaedic Research Unit, Aarhus University Hospital, Aarhus N, Denmark
[4] NRT X-RAY A/S, Hasselager, Denmark
[5] Department of Radiology, Aarhus University Hospital, Aarhus N, Denmark
[6] Department of Radiology, Regional Hospital Horsens, Horsens, Denmark
[7] Department of Orthopaedic Surgery, Aarhus University, Aarhus N, Denmark

**Address for correspondence** Janni Kjærgaard Thillemann, MD, University Clinic for Hand, Hip and Knee Surgery, Hospital Unit West, Lægaardvej 12, Holstebro 7500, Denmark (e-mail: teamjanni@gmail.com).

J Wrist Surg

## Abstract

**Background** Measurement of in vivo distal radioulnar joint (DRUJ) pathomechanics during simple activities can represent the disability experienced by patients and may be useful in diagnostics of DRUJ instability. A first step is to describe the physiological normal limits for DRUJ kinematics in a reproducible and precise test setup, which was the aim of this study.

**Methods** DRUJ kinematics were evaluated in 33 participants with dynamic radiostereometry (RSA) while performing a standardized press test examination. AutoRSA software was used for image analyses. Computed tomography (CT) forearm bone models were generated, and standardized anatomical axes were applied to estimate kinematic outcomes including, DRUJ translation, DRUJ position ratio, and changes in ulnar variance. Repeatability of dynamic RSA press test double examinations was evaluated to estimate the precision and intraclass correlation coefficient (ICC) test–retest agreement.

**Results** The maximum force during the press test was 6.0 kg (95% confidence interval [CI]: 5.1–6.9), which resulted in 4.7 mm (95% CI: 4.2–5.1) DRUJ translation, DRUJ position ratio of 0.40 (95% CI: 0.33–0.44), and increase in ulnar variance of 1.1 mm (95% CI: 1.0–1.2). The mean maximum DRUJ translation leveled off after a 5 kg force application. The DRUJ translation ICC coefficient was 0.93 within a prediction interval of $\pm$ 0.53mm.

**Conclusions** This clinical study demonstrates the normal values of DRUJ kinematics and reports excellent agreement and high precision of the press tests examination using an automated noninvasive dynamic RSA imaging method based on patient-specific CT bone models. The next step is the application of the method in patients with arthroscopic verified triangular fibrocartilage complex injuries.

**Level of Evidence** This is a Level IV, case series study.

**Keywords**
- radioulnar ligaments
- distal radioulnar joint
- normal values
- radiostereometry
- joint kinematics



**received**
June 2, 2021
**accepted**
November 9, 2021


Thieme Medical Publishers, Inc., 333 Seventh Avenue, 18th Floor, New York, NY 10001, USA

**DOI** https://doi.org/10.1055/s-0041-1740486.
**ISSN** 2163-3916.

Clinical examination of distal radioulnar joint (DRUJ) instability is subjective, relies on passive testing of increased radioulnar translation, and remains challenged by poor reproducibility.[1–3] The diagnosis is often missed both in patients with low-grade DRUJ instability and in patients with high-grade DRUJ instability due to pain or strong muscular joint stabilizers.[4]

Methods based on computed tomography (CT) have been suggested for the evaluation of DRUJ instability, but their reliability is limited.[3,5,6] The CT-based methods investigate DRUJ subluxation on axial reconstructions of the forearm in passive supinated and pronated positions.[7] However, static imaging may not reveal the full range of DRUJ instability, which patients can provoke during loaded hand activities and active movement.

Evaluation of DRUJ instability based on ultrasonography (US) was introduced by Hess et al and has shown promising results.[8] Transverse US relies on the timing of snapshots of the ulnar head prominence relative to the distal radius during active patient-induced ulnar head translation.

Previously, we introduced static radiostereometry (RSA) in an experimental setting for the examination of DRUJ translation before and after triangular fibrocartilage complex (TFCC) injury.[9] Radiostereometry may also be applied dynamically (dRSA) as a stereo-image of active joint motions and loaded exercises and is a precise noninvasive calibrated radiographic method that allows for the registration of CT-based bone models and evaluation of joint kinematics.[10] Previously, dRSA has not been applied for the evaluation of DRUJ kinematics in vivo.

The purpose of this study was to determine physiological normal values and variations of DRUJ translation, the position of the ulnar head with respect to the sigmoid notch (SN), and changes in ulnar variance in individuals with asymptomatic uninjured forearms, using dRSA imaging of a participant-applied press test exercise. Furthermore, we evaluated DRUJ translation by US and estimated the reliability of both methods.

## Patients and Methods

### Study Design and Participants

Thirty-three consecutive participants, 14 men and 19 women were recruited between February 2017 and February 2020 for a prospective cohort study on normative DRUJ kinematics using dRSA imaging.

Study criteria were an age between 18 and 50 years, no ulnar-sided wrist pain, and no previous surgery or sequelae after upper limb injuries. Only one healthy forearm from each participant was included. Informed consent was obtained from the participants. The study was approved by the Danish Data Protection Agency (Journal no. 2012–58–006; issued May 2016) and the Central Denmark Region Committees on Health Research Ethics (Journal no.1–10–72–146–16; issued August 2016).

### Patient Demographics and Clinical Examination

Patient characteristics included sex, age, hand dominance, and side of the investigated forearm. Clinical examination was performed by the first author. Grip strength was measured using the DHD-1 digital Jamar Hand Dynamometer (SAEHAN Corporation, Gyeongsangnam-do, South Korea) and reported as an average of three measures. The wrist and forearm motion was measured as an angle using a goniometer. Stability of the DRUJ was evaluated clinically with the ballottement test, and the DRUJ instability grade was categorized as less than 5 mm, between 5 and 10 mm, or above 10 mm, as proposed by Atzei et al.[11]

### Bone Models and Bone-Specific Coordinate Systems

Patients eligible for study participation were referred for a dRSA examination during a standardized press test. Bone models for analysis of dRSA images were obtained from CT image series of the whole forearm on all patients (Philips Brilliance 64, Philips Medical Systems, Best, the Netherlands). All scans were acquired with 120 kV, and 100 mAs settings and images were reconstructed with 0.9 mm slice thickness, 0.45 mm slice increment, and 0.27 mm in-plane pixel size. Individualized three-dimensional (3D) bone volume and surface models of the radius and ulna were created from the CT images by automated graph cut segmentation (►**Fig. 1A–D**).

Bone-specific orthogonal axes (x, y, z) for each individual 3D CT bone surface model were defined from three anatomical landmarks (►**Fig. 1E–F**).[9,12] The anatomical landmarks were also used to define the radioulnar joint (RUJ) axis (►**Fig. 1G**) and to estimate kinematic outcomes (►**Fig. 1H**).

### Kinematic Outcomes

The RUJ axis of forearm rotation was defined as extending through the radial head center to the ulnar head center (►**Fig. 1G**).[13] The SN line was defined by connecting the midpoint of the volar and dorsal radius SN rims. This SN length was measured (►**Fig. 1H**). The RUJ axis and the SN line were used to estimate the kinematic outcomes.[9]

The primary outcome was DRUJ translation at the maximum force applied during the dRSA-evaluated press test motion cycle. Secondary outcomes were US-examined DRUJ translation and maximum force, DRUJ position ratio, and change in ulnar variance within the RSA-evaluated press test motion cycle (►**Fig. 1H**).

### Press Test Setup

The participants were positioned in a standardized setting to perform a press test examination on a custom-made unidirectional weight platform with a radiolucent plate mounted for force application. Instructions were to apply force by the hypothenar region gradually to their maximum and release the force gradually until no force was applied (one press test motion cycle). Thus, a visually confirmed volar translation of the ulnar head was induced and recorded during the press test by dRSA (►**Fig. 2**). Double examinations were conducted for reliability.

A custom-made software was designed for a small single-board computer (Raspberry Pi) to timestamp and relate the force (measured in kg) applied on the weight platform and the simultaneously recorded dRSA images.

 

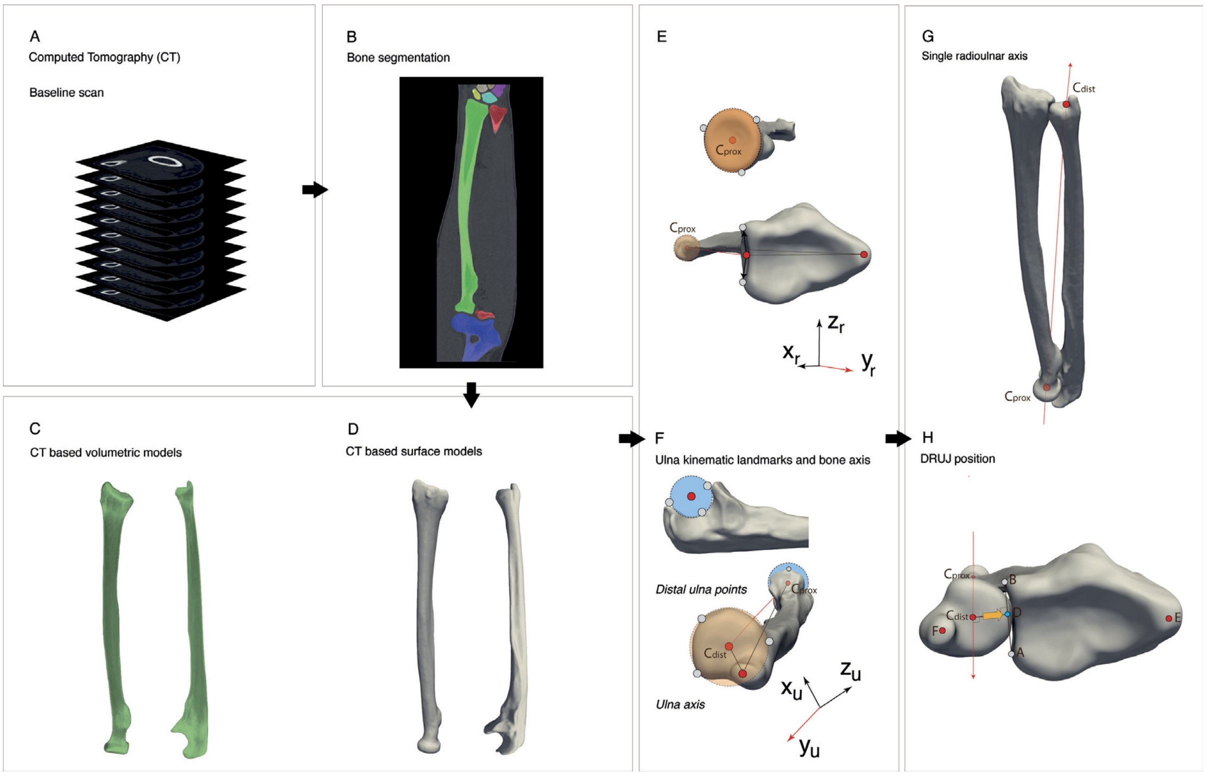


**Fig. 1** Computer tomography (CT)-generated bone models, kinematic landmarks, and bone axes. (**A**) Grayscale information was extracted from CT scans. (**B**) Graph cut segmentation was used to generate (**C**) three-dimensional bone volume models and (**D**) simplified 3D bone surface models of ~10,000 triangles. Custom-implemented software based on the Insight Segmentation Toolkit and the Visualization Toolkit (Kitware, NY) was used for all image processing as described by Hansen et al.[15] (**E–F**) Bony landmarks were used to define bone axes (x, y, z). The radius landmarks were the proximal rotation center of the radial head ($C_{prox}$), the radial styloid tip, and the center of the distal radioulnar joint (RUJ) surface. The ulnar landmarks were the ulnar head center ($C_{dist}$), the distal ulnar styloid tip, and the greater sigmoid notch (SN) center. The best-fitted sphere of three points picked on the center of the articulating surfaces of the radial and ulnar heads was used to compute the center points. (**G**) The RUJ axis was the axis of forearm rotation extending through the radial head center to the ulnar head center. (**H**) The SN line connects the midpoint of the volar (landmark A) and dorsal (landmark B) radius SN rims. The position of the ulnar head rotational center on the SN line (DRUJ position) was estimated by projection of the RUJ axis orthogonally on the SN line and measured in millimeters from the volar SN rim. Considering the individual differences in bone sizes and SN line lengths, the DRUJ position ratio was calculated (DRUJ position ratio = DRUJ position/SN line length). Translation in the DRUJ was calculated as the change of DRUJ position in millimeters. The change in ulnar variance was calculated as the change of (Cdist) along the RUJ axis with respect to the SN line midpoint.

## Dynamic RSA Setup and Recordings

The digital Adora RSA system (NRT X-Ray, Hasselager, Denmark) was used to record the dRSA images at a frequency of 10 images per second (10 Hz) during the press test application (►**Fig. 3A**). The dRSA exposures used were 60 kV and 630 mA settings and a 2.0 milliseconds exposure time for acquiring a resolution of 2208 × 2688 pixels resolution (0.16 mm × 0.16 mm image area per pixel). Images were exported as multiframe DICOM files.

Image calibration was performed on an averaged image of all image frames in the dRSA image series. This reduced image noise from the moving arm and ensured a clear view of fiducial and controls markers from the calibration box.

## Analysis of Dynamic RSA

Model-based RSA software (MBRSA 4.11, RSAcore, Leiden, the Netherlands) was used for calibration of the averaged calibration image.[14]

An automated custom software system (AutoRSA, Orthopedic Research Unit, Aarhus, Denmark) was used for analysis of the dRSA image series. AutoRSA utilizes digital reconstructed radiographs (DRRs) for 3D to 2D image registration. A DRR is a projection of the 3D CT bone models (►**Fig. 3B**) on an 2D image plane, thus a virtual radiograph.

Prior to the automated image registration process, a manual initialization was performed for the first dRSA image. This process included first a manual positioning of the bone models until the 2D DRR projection-overlay approximately fit the first dRSA image (►**Fig. 3C**). Second, mathematical optimization algorithms were used to obtain the best match between DRR and the actual dRSA image—defining the 3D position and orientation (i.e., pose) of the ulna and radius bone in the calibration box coordinate system (►**Fig. 3D**). Prior to each image registration, extrapolation of the previous poses initialized the approximately pose of the bone models.[10,15,16] The final pose of the bones in the calibration box coordinate system was transformed to the standardized bone-specific coordinate systems (►**Fig. 1E–F**).

## Data Management

The data logging of the force (kg) applied to the weight-platform was merged with the outcome measures from the

 


**Fig. 2** Dynamic radiostereometry (dRSA) setup during press test examination on a weight platform. The participants were positioned with ∼60 degrees shoulder flexion, with adducted upper arm, the elbow flexed, and the pronated forearm positioned in the horizontal plane resting with the hand flat on a weight-platform that logged the applied force (measured in kg). The instructions were to gradually apply maximum force through the hypothenar region of the palm resulting in a visually confirmed volar translation of the ulnar head before the force was gradually released. The dRSA test setup consisted of two ceiling-mounted X-ray tubes with a 20 to 20 degrees tube position on the vertical plane and two digital image detectors (Canon CXDI-50RF) slotted beneath a uniplanar carbon box (Carbon box 24, Medis Specials, Leiden, the Netherlands). The source-to-skin distance was 100 cm and the source-to-images distance was 150 cm. The image frequency of the dRSA recordings was 10 Hz.

analyzed dRSA examinations. The participants' individual delay in applying force on the weight platform was handled using a customized software application to automatically identify the start and end points of the first and second motion cycles. The motion cycle with the highest force application was chosen for data analysis (►**Fig. 4**). The maximum force applied in each cycle was defined as the 50% mark of the motion cycle and was used to normalize the motion cycle in a downstroke and release phase via linear interpolation of the force and the kinematic outcomes.

The maximum force ($P_{max}$) and corresponding kinematic outcome values (PO) from the two motion cycles were used for the examination of reliability (►**Fig. 4**).

### Ultrasonography Examinations

A US-based DRUJ stability examination was performed as described by Hess et al.[8] The participants were placed in a

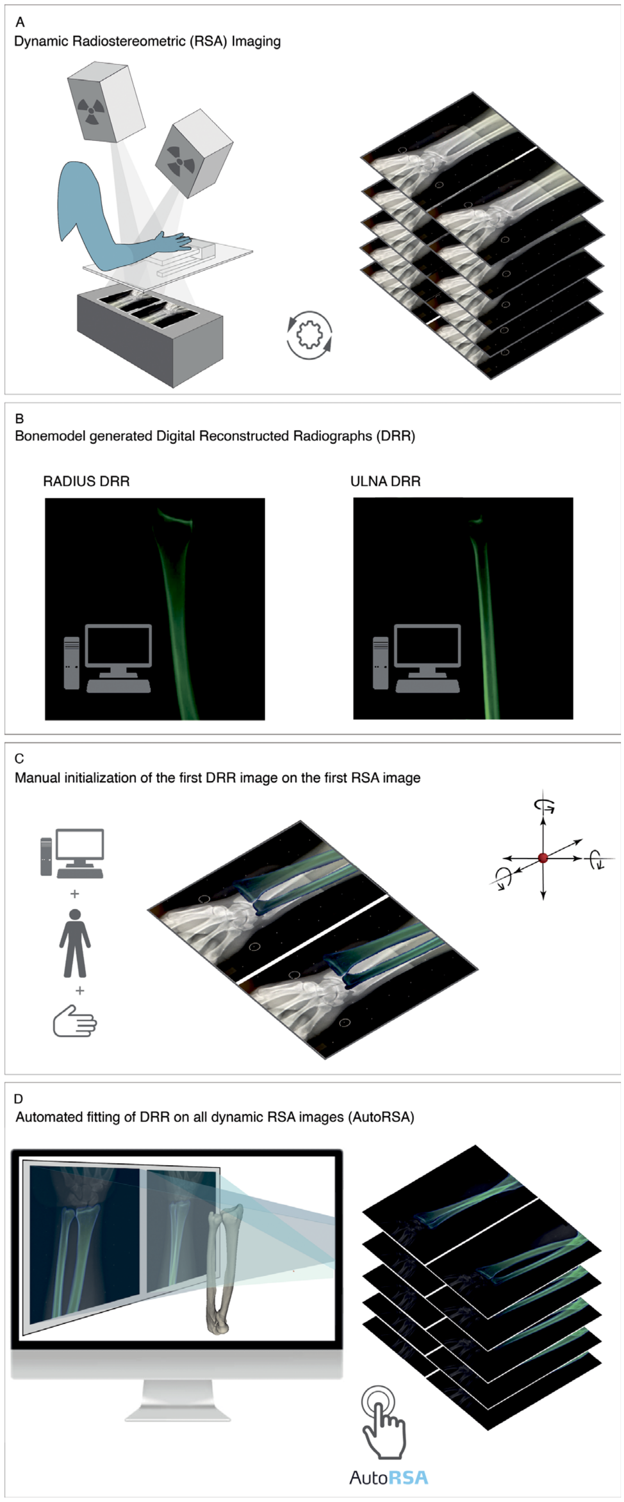


**Fig. 3** Analysis of dynamic radiostereometry (dRSA) recordings. (**A**) The participants performed the press test on a weight platform during dRSA with images recorded at 10 Hz. (**B**) Digital reconstructed radiographs (DRR) were generated from computed tomography-based bone surface and volume models. (**C**) Primary manual orientation and positioning of the bone models were required to initialize the DRR image to approximately fit the initial dRSA image. (**D**) The subsequent dRSA images and DRRs were analyzed automatically using AutoRSA software, as the software sets initialization of the next DRR image by extrapolation from the previous movement.

 

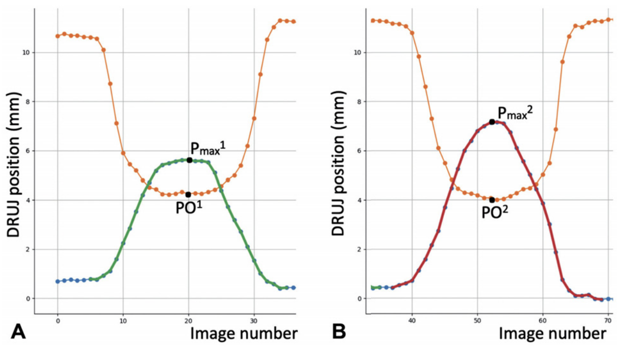


**Fig. 4** Definition of the motion cycle generated from press test force data and synchronized dynamic radiostereometry outcomes. The first (**A**) and second (**B**) press test motion cycle were determined from the participant-applied force on the weight platform (kg). The cycle start point was defined as the point just before the press data exceeded a threshold value of 0.1 kg relative to the press value corresponding to the course start point, and vice versa the end point was defined in the same manner by tracking from the end of press data (green and red cycles). The cycle with the highest maximum force ($P_{max}{}^{2} > P_{max}{}^{1}$) was used for data management (red cycle) of the corresponding outcome (orange) throughout the selected cycle. The maximum force ($P_{max}$) was used to define the corresponding maximum force outcome value (PO) (i.e., the distal radioulnar joint [DRUJ] position).

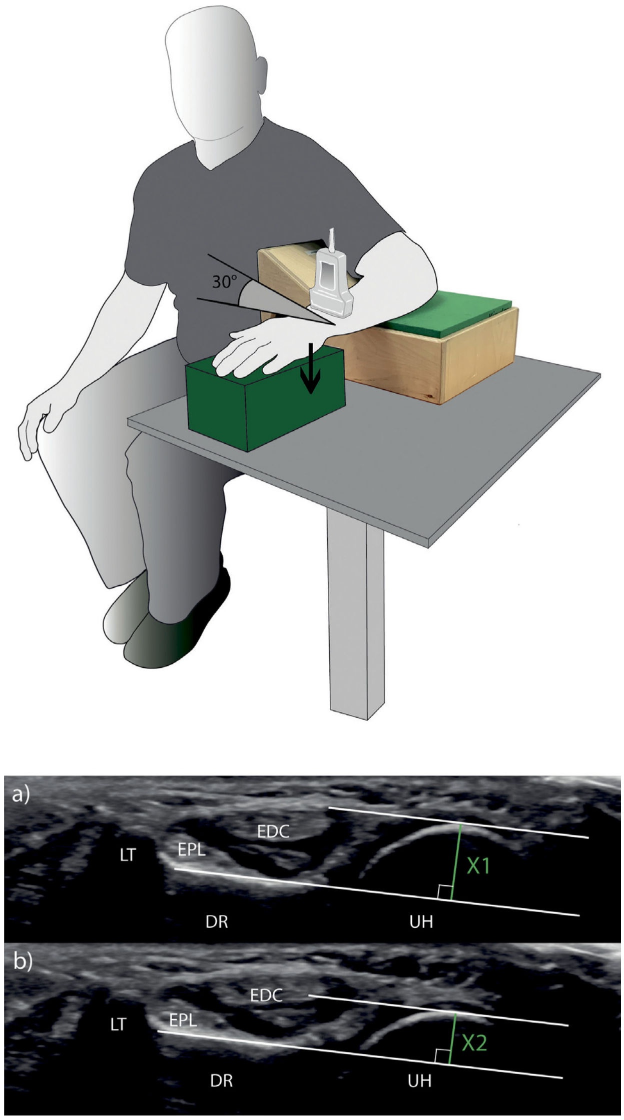


**Fig. 5** Examinations of distal radioulnar joint (DRUJ) stability by ultrasonography. The participant was placed on a chair with their arm on a positioner abducting the upper arm 60 degrees from the vertical plane and ensuring standardized measures with ~30 degrees forearm pronation. Measures were made by placing the transducer dorsal over the DRUJ, perpendicular to the ulna longitudinal axis, displaying the dorsal surface of the distal radius (DR) and the center of the ulnar head (UH) at the level of the Lister's tubercle (LT). The most dorsal bromination of the ulnar head was displayed and chosen for static measurement of the perpendicular distance to an extended line from the floor of the 4th extensor compartment at the DR at rest ($X_1$), and after maximum force of the palm and the hypothenar region was applied to a leveled box, inducing a palmar shift of the ulnar head, the perpendicular distance was measured again ($X_2$). The DRUJ translation quotient ($Q = [X_1 - X_2] / X_1$) and the DRUJ translation ($T = X_1 - X_2$) were calculated. EDC, extensor digitorum communis; EPL, extensor pollicis longus.

standardized position to measure DRUJ translation ($T = X_1 - X_2$) and calculate the DRUJ translation quotient ($Q = [X_1 – X_2] / X_1$) (►**Fig. 5**). The US examination was repeated after ~4 weeks (range: 3–6) enabling evaluation of test–retest reliability.

### Statistical Analysis

Descriptive analyses of patient demographics were performed. Continuous data estimated from clinical examination, dRSA analysis, and US evaluations were checked for normality by evaluation of frequency and probability plots. Parametric data were reported as means with 95% confidence intervals (95% CI). The Student's independent *t*-test (equal variance) was used to compare kinematic RSA outcomes, for men and women at the beginning of the cycle (at 0% of the motion cycle) and at maximum force (at 50% of the motion cycle). Categorical data were reported as numbers and were compared between groups using the chi-squared test.

Repeatability of force and kinematic outcomes from the dRSA press test were evaluated to approximate the precision. The systematic bias was reported as the absolute mean difference with standard deviations (SD) and prediction intervals ($SD \times 1.96$). Interrater agreement of dRSA press test and US double examination outcomes was calculated as intraclass correlation coefficients (ICC) based on an assumption of a single rater, absolute-agreement, two-way mixed effects model (ICC [2,1])). The rater consistency was reported with 95% CIs.

The level of significance was set at $p < 0.05$. All analyses were computed using Stata 16.0 software (StataCorp LP, TX).

## Results

### Patient Demographics

The included participants had a mean age of 31 years (range: 19–50). Demographic data including sex, side of the investigated forearm, and hand dominance are described in ►**Table 1**.

 

**Table 1** Demographics of the participants investigated

| Characteristics | Asymptomatic forearms |
|---|---|
| Sex (men/women) | 14/19 |
| Mean age at time of inclusion (range) | 31 (19–50) |
| Investigated healthy hand (dominant hands %) | 58 |
| Dominant hand (right %) | 94 |

### Clinical Examination

The forearms were mainly the participant's dominant side (19 out of 33), and all DRUJs were evaluated as stabile using the ballottement test in neutral, supinated, and pronated forearm positions (►**Table 2**). The grip strength was 32.8 kg (95% CI: 30.1–35.5) for women and 53.4 kg (95% CI: 48.7–58.1) for men. Wrist motion and forearm rotation are reported in ►**Table 2**.

### DRUJ Kinematics

The dynamic outcomes of normal DRUJ kinematics during the press test examination, including 95% CIs and prediction intervals ($1.96 \times SD$) are shown in ►**Fig. 6**, with the downstroke phase displayed as 0 to 50% of the motion cycle and the release phase as 51 to 100% of the motion cycle.

At the maximum force (50% of the motion cycle), a mean of 6.0 kg (95% CI: 5.1–6.9) was applied onto the weight platform, which induced a DRUJ translation of mean 4.7 mm (95% CI: 4.2–5.5) (►**Table 3**).

The SN length was significantly different in men and women ($p = 0.005$) (►**Table 3**). Taking the SN length into account, the calculated DRUJ position ratio was not significantly different between genders before force application ($p = 0.23$). The press test moved the center of the ulnar head below the SN center at the maximum force in both men and women to a common mean DRUJ position ratio of 0.40 (95% CI: 0.33–0.44) (►**Table 3**).

Twenty-four of the 33 patients pressed 5 kg or more (►**Table 3**), and a clear flooring effect of the press test-induced DRUJ position ratio was seen after 5 kg of force application (►**Fig. 7**).

The ulnar variance increased mean 1.1 mm (95% CI: 1.0–1.2) during the press test (►**Table 3**).

### Reliability of the Press Test

There was no systematic bias of the applied maximum force in the first and second tests. The absolute mean difference of the maximum force was 0.80 kg, and the biological variation of the group resulted in a prediction interval of the applied force of $\pm$ 1.35 kg. This maximum force difference generated a mean difference of 0.39 mm absolute DRUJ translation, a mean difference of 0.02 in the DRUJ position ratio, and a mean difference of 0.10 mm in ulnar variance (►**Table 4**).

ICC rater consistency of the test–retest maximum force, DRUJ translation, DRUJ position ratio, and ulnar variance at maximum force was excellent ($r > 0.90$), with a lower limit 95% CI indicating good or excellent consistency ($r > 0.80$).

**Table 2** Clinical results in participants with asymptomatic forearms

| Examination | Asymptomatic arms |
|---|---|
| Number of participants | 33 |
| Grip strength total (kg)<br>Women ($n = 19$)<br>Men ($n = 14$) | 41.5 (37.2–45.9)<br>32.8 (30.1–35.5)<br>53.4 (48.7–58.1) |
| Wrist motion (degrees)<br>Flexion<br>Extension<br>Radial deviation<br>Ulnar deviation | <br>79 (75–82)<br>74 (71–77)<br>23 (20–25)<br>36 (34–38) |
| Forearm rotation (degrees)<br>Supination<br>Pronation | <br>84 (82–87)<br>81 (78–84) |
| Clinical evaluation of DRUJ stability:<br>Ballottement test ($n$)<br>Neutral forearm rotation<br>Pronated forearm rotation<br>Supinated forearm rotation | <br><br>33/0/0[a]<br>33/0/0[a]<br>33/0/0[a] |

Abbreviation: DRUJ, distal radioulnar joint.
Note: Numbers are reported as means with 95% confidence intervals and standard deviation (SD).
[a]Definition of Ballottement test stability evaluation: Stable or slight instability ( < 5 mm)/mild instability (5–10mm)/severe instability (>10 mm). Displayed as number of patients ($n$).

### Sonography Test Retest Reliability

Specificity of US measurements was 82%, since 6 of the 33 asymptomatic forearms in the first US examination were above the DRUJ translation quotient cutoff value ($Q = 0.80$) proposed by Hess et al.[8] The US-measured DRUJ translation quotient (Q) had a mean of 0.59 (95% CI: 0.44–0.74) and 0.56 (95% CI: 0.45–0.68) ($p = 0.59$), and the DRUJ translation (T) had a mean of 2.3 mm (95% CI: 1.7–2.8) and 2.4 mm (95% CI: 1.8–2.9) at the first and second examinations, respectively ($p = 0.58$). The ICC (2,1) rater consistency of the test–retest sonography-examined DRUJ translation indicated moderate reliability ($r = 0.74$, 95% CI: 0.53–0.87).

## Discussion

### DRUJ Translation and DRUJ Position Ratio

In the present study, the patient-induced DRUJ translation during the dRSA press test had a mean of 4.7 mm (SD: 1.3) in asymptomatic stable joints; the DRUJ position ratio with pronated unloaded forearm had a mean of 0.75, (SD: 0.10), and at maximum force a mean of 0.40 (SD: 0.11). In a previous static radiostereometry study evaluating ex vivo DRUJ kinematics during a passive piano key test in uninjured cadaver forearms, a limited DRUJ translation of 1.36 mm was detected.[9] This translation measure was unidirectional, and ex vivo examination of DRUJ kinematics may not directly resemble in vivo measures.

In the US-based study by Hess et al, a DRUJ translation of mean 2.5 mm (SD: 1.03) was reported when the applied force exceeded 5 kg.[8] This was similar to our reported US DRUJ translation of 2.3 mm (SD: 1.5) using the same press test.

 

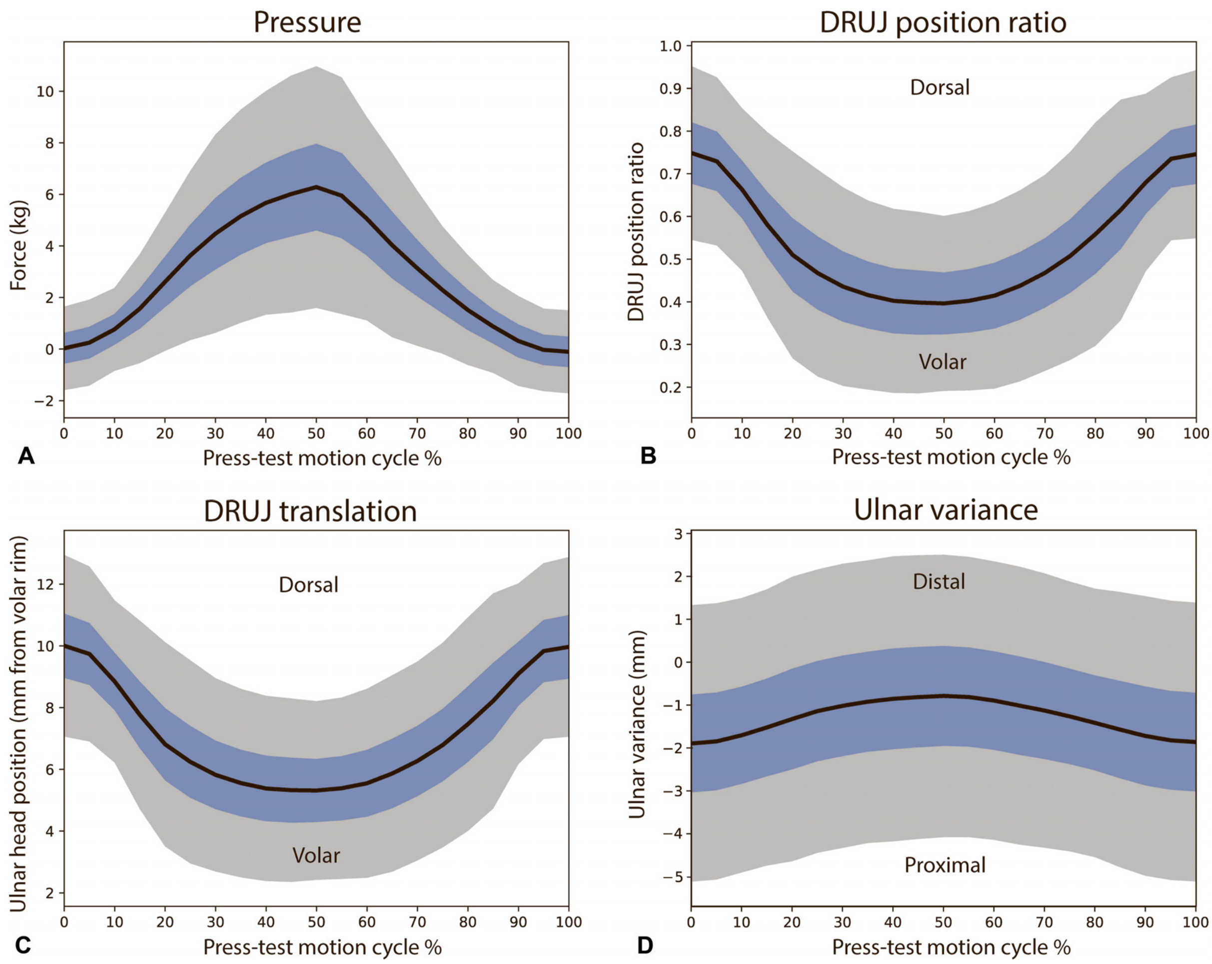


**Fig. 6** Kinematic outcomes during the press test motion cycle (0–100%) recorded by dynamic radiostereometry (dRSA). Graphs of the means with 95% confidence intervals (CIs; blue area) and prediction interval (gray area; 1.96 × standard deviation). (**A**) Force applied during the press test, (**B**) the corresponding distal radioulnar joint (DRUJ) position ratio, (**C**) the resulting DRUJ translation, and (**D**) ulnar variance.

**Table 3** dRSA outcome measures of the DRUJ in asymptomatic forearms

| Outcome in asymptomatic forearms | Total | Men | Women | *p*-Value[a] |
|---|---|---|---|---|
| Number of forearms | 33 | 14 | 19 | |
| Sigmoid notch length (mm) | 13.4 (13.0–13.8) SD: 1.2 | 14.1 (13.3–14.8) SD: 1.3 | 12.9 (12.4–13.4) SD: 0.9 | 0.005 |
| *At 0% of the motion cycle* | | | | |
| Forearm pronation (degrees) | 62 (58–66) SD: 11 | 57 (53–61) SD: 7 | 65 (59–71) SD: 12 | 0.03 |
| DRUJ position ratio | 0.75 (0.71–0.78) SD: 0.10 | 0.72 (0.65–0.79) SD: 0.12 | 0.77 (0.73–0.81) SD: 0.08 | 0.23 |
| *At 50% of the motion cycle* | | | | |
| Maximum force (kg) | 6.0 (5.1–6.9) SD: 2.4 | 6.3 (4.7–7.9) SD: 2.8 | 5.8 (4.8–6.8) SD: 2.1 | 0.55 |
| Forearm pronation (degrees) | 53 (48–57) SD: 13 | 48 (42–54) SD: 10 | 56 (50–63) SD: 13 | 0.08 |
| DRUJ translation (mm) | 4.7 (4.2–5.1) SD: 1.3 | 4.3 (3.5–5.0) SD: 1.3 | 4.9 (4.4–5.5) SD: 1.2 | 0.15 |
| DRUJ position ratio | 0.40 (0.33–0.44) SD: 0.11 | 0.42 (0.37–0.47) SD: 0.09 | 0.38 (0.33–0.44) SD: 0.11 | 0.32 |
| Increase in ulnar variance along the RUJ axis (mm) | 1.1 (1.0–1.2) SD: 0.4 | 1.1 (0.8–1.3) SD: 0.5 | 1.1 (0.9–1.3) SD: 0.4 | 0.94 |

Abbreviations: dRSA, dynamic radiostereometry; DRUJ, distal radioulnar joint; RUJ, radioulnar joint.
[a]Independent *t*-test comparing men and women. Numbers are reported as means with 95% confidence intervals and standard deviation (SD).

 

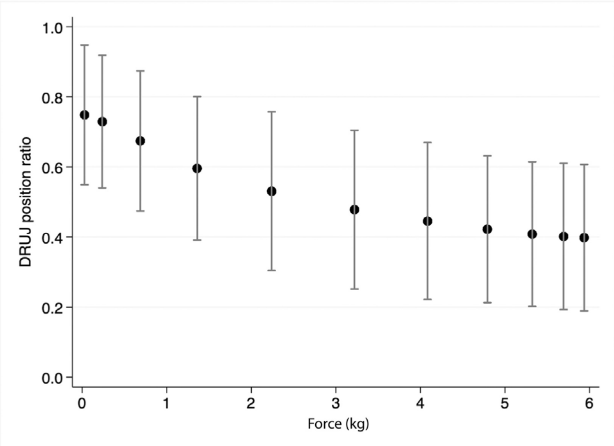


**Fig. 7** Relationship between press test force (kg) and the distal radioulnar joint (DRUJ) position ratio recorded by dynamic radiostereometry (dRSA). The mean DRUJ position ratio with 95% confidence intervals displays a floor effect with increased force during the press test.

Thus, the unidirectional DRUJ translation of 4.7 mm (SD: 1.3) detected during our dRSA press test was higher compared with US-based measures, whereas the variation was similar. The correlation between the US measured translation and the RSA measured DRUJ translation at maximum force was poor ($r = 0.137$; 95% CI: -0.228 to 0.469). This may be an effect of the dynamic detection, which ensures registration of the full range of DRUJ translation, whereas US-based still pictures may not be taken exactly at minimum and maximum force applications. Furthermore, in the present study, the forearm pronation had a mean of 53 degrees (95% CI: 48–57) when the maximum force was applied, whereas US-based method was performed with the forearm in a standardized position at ~30 degrees pronation.

The DRUJ is not a constricted joint due to the different radiuses of the articular surfaces of the ulnar head and the SN. This allows for a sliding contact point during forearm rotation, which is most pronounced in an interval from 0 to 60 degrees pronation where the ulnar head glides dorsally in the SN.[17] Thus, unidirectional examinations of DRUJ translations that initiate from a more pronated forearm position may contribute to the higher translation measures. In contrast, the radioulnar ligaments are known to yield a stabilizing effect of the ulnar head in the SN as they tighten increasingly with pronation,[18] and from 60 to 90 degrees pronation, the dorsal sliding of the ulnar head is limited.[17]

Gender differences in DRUJ translation were seen, but the mean values detected in women (5.11 mm) were not significantly higher than in men (4.42 mm). The SN length has been estimated as a mean of 15 mm in cadaver specimens.[19] We report a similar SN length of 13.4 mm, but also significant anatomical variation between men and women, with a larger SN length in men. Thus, estimates of DRUJ translation should preferably be normalized by considering the individual anatomical variation of the SN length.

## Ulnar Variance

Ulnar variance plays a role in the dynamic process of ulnocarpal abutment, but TFCC pathology with DRUJ instability has also been related to increased ulnar variance. In asymptomatic forearms, static tests with a strong grip or heavy axial load the ulnar variance increased up to 1.95 mm (SD: 0.74).[20–22] This change in ulnar variance may not be directly comparable with the increase in ulnar variance of mean 1.1 mm (SD: 0.4) during the dynamic press test, as this was induced by a volar-directed force application by the hand despite the forearm supinated slightly during the press test. Nevertheless, these types of loading increased the ulnar variance.

## Test Reliability

The applied force peaked (50% of the motion cycle) at a mean of 6.0 kg, whereas the DRUJ translation and the DRUJ position ratio flattened out at 40 to 60% of the motion cycle (►**Fig. 6**).

This floor effect of the measured DRUJ position started at forces lower than the maximum force and may explain the high precision and excellent ICC agreement ($r > 0.93$) of the press test kinematic outcomes.

Likewise, the press test sonography study by Hess et al concluded that maximum DRUJ translation was present at 5 kg force, as higher forces (measured from 0 to 10 kg at 2.5 kg intervals) did not further increase DRUJ translation.[8] This was supported by the current study, as we detected a flooring effect of the DRUJ position ratio when a force of 5 kg or more was applied. A clear force threshold creates the option of a simpler static RSA test setup comparing DRUJ kinematics between an unloaded and a minimum 5 kg-loaded press test setup. Such a setup can be created in any radiology department with a mobile X-ray tube in addition to the standard tube.

The US-based method benefits from device availability and easy application in clinical practice, but measures and reliability are highly subjective. In the present study, the ICC rater consistency of the test–retest US-examined DRUJ translation had moderate reliability for one hand surgeon with moderate US experience ($r = 0.75$ [ 95% CI: 0.54–0.87]). In comparison, Hess et al reported high interobserver agreement of sonographic measurements (Pearson correlation $r = 0.83$). Despite the fact that the participants forearms being pain free, uninjured, and evaluated as completely stable by clinical examination using the ballottement test, the US specificity was 82%, similar to the specificity reported by Hess et al.[8] Thus, to reduce the false positive rate, this emphasizes the importance of comparison with the patients uninjured DRUJ.

## Limitations

DRUJ translation in normal joints with an intact TFCC can be seen with broad variability ranging from hypermobility to highly stable joints and an inability to relax the DRUJ-supporting muscular stabilizers during testing. Likewise, force application varies and especially women did not exceed a 5 kg force application during the press test. Thus, this may affect the normal values and variations reported in the study.

 

**Table 4** Repeatability of the press test and synchronized kinematic outcomes recorded by dRSA double examinations

| Value | Maximum force (kg) | DRUJ translation at max force (mm) | DRUJ position ratio at max force | Ulnar variance (mm) |
|---|---|---|---|---|
| Double examinations | 33 | 33 | 33 | 33 |
| Mean difference (SD) | 0.80 (0.69) | 0.39 (0.27) | 0.02 (0.02) | 0.10 (0.09) |
| Prediction interval (SD × 1.96) | 1.35 | 0.53 | 0.04 | 0.18 |
| ICC (95% CI) | 0.87 (0.76–0.94) | 0.93 (0.86–0.96) | 0.95 (0.91–0.98) | 0.996 (0.99–1.00) |

Abbreviations: CI, confidence interval; dRSA, dynamic radiostereometry; DRUJ, distal radioulnar joint, ICC, intraclass coefficient; SD, standard deviation.
Notes: The systematic biases are reported as absolute mean differences with standard deviations (SD) and prediction intervals (SD × 1.96). ICC (2,1) calculated as two-way mixed effects, absolute agreement to evaluate rater consistency between first and second examinations.

## Conclusions

In conclusion, this study demonstrates excellent agreement between repeated press test examinations using an observer-independent noninvasive dRSA imaging method based on patient-individual CT-based bone models and AutoRSA in clinical practice.

The DRUJ position ratio in asymptomatic participants leveled off at 5 kg force; hence, the complicated dRSA setup may be replaced by a simplified unloaded and loaded static RSA test setup, which should be applicable in any institution.

Press test examination and AutoRSA analysis in patients with confirmed TFCC injuries have not yet been evaluated, but is likely applicable, and previous cadaver studies have shown promising results concerning detection of differences in DRUJ translations using RSA.[9,23] Evaluation of kinematic differences between uninjured and injured forearms remains to be examined in vivo.

### Note

The institutions at Which the work was performed were Department of Orthopaedics, University Clinic for Hand, Hip and Knee Surgery, Hospital Unit West, Lægaardvej 12, 7500 Holstebro, Denmark and Department of Orthopaedic Surgery, Aarhus University, Palle Juul-Jensens Boulevard 165, 8200 Aarhus N, Denmark

### Ethical Approval

The Danish Data Protection Agency (Journal no.2012–58–006; issued May 2016) and The Central Denmark Region Committees on Health Research Ethics (Journal no.1–10–72–146–16; issued August 2016) approved the study. Informed consent was obtained from the participating subjects.

### Funding

This research has received grants from Health Research Fund of Central Denmark Region, Aarhus University, The Danish Rheumatism Association and Innovation Fund Denmark (Grant 69-2013-1). All funding sources did not play a role in the study investigation.

### Conflict of Interest

None declared.

### Acknowledgments

The authors thank radiographer Lars Lindgren from the Department of Radiology, Aarhus University Hospital, and Michael Frosted Mathiasen, from the Department of Radiology, Hospital Unit Vest, for their valuable help with the radiostereometric recordings.

## References

1 Nagata H, Hosny S, Giddins GE. In-vivo measurement of distal radio-ulnar joint translation. Hand Surg 2013;18(01):15–20
2 Pickering GT, Nagata H, Giddins GEB. In-vivo three-dimensional measurement of distal radioulnar joint translation in normal and clinically unstable populations. J Hand Surg Eur Vol 2016;41(05):521–526
3 Wijffels M, Stomp W, Krijnen P, Reijnierse M, Schipper I. Computed tomography for the detection of distal radioulnar joint instability: normal variation and reliability of four CT scoring systems in 46 patients. Skeletal Radiol 2016;45(11):1487–1493
4 Schnetzke M, Porschke F, Hoppe K, Studier-Fischer S, Gruetzner PA, Guehring T. Outcome of early and late diagnosed Essex-Lopresti Injury. J Bone Joint Surg Am 2017;99(12):1043–1050
5 Park MJ, Kim JP. Reliability and normal values of various computed tomography methods for quantifying distal radioulnar joint translation. J Bone Joint Surg Am 2008;90(01):145–153
6 Lo IK, MacDermid JC, Bennett JD, Bogoch E, King GJ. The radioulnar ratio: a new method of quantifying distal radioulnar joint subluxation. J Hand Surg Am 2001;26(02):236–243
7 King GJ, McMurtry RY, Rubenstein JD, Gertzbein SD. Kinematics of the distal radioulnar joint. J Hand Surg Am 1986;11(06):798–804
8 Hess F, Farshad M, Sutter R, Nagy L, Schweizer A. A novel technique for detecting instability of the distal radioulnar joint in complete triangular fibrocartilage complex lesions. J Wrist Surg 2012;1(02):153–158
9 Thillemann JK, De Raedt S, Jørgensen PB, Rømer L, Hansen TB, Stilling M. Distal radioulnar joint stability measured with radiostereometry during the piano key test. J Hand Surg Eur Vol 2020;45(09):923–930
10 Christensen R, Petersen ET, Jürgens-Lahnstein J, et al. Assessment of knee kinematics with dynamic radiostereometry: validation of an automated model-based method of analysis using bone models. J Orthop Res 2021;39(03):597–608
11 Atzei A, Rizzo A, Luchetti R, Fairplay T. Arthroscopic foveal repair of triangular fibrocartilage complex peripheral lesion with distal radioulnar joint instability. Tech Hand Up Extrem Surg 2008;12(04):226–235

 

12 McDonald CP, Moutzouros V, Bey MJ. Measuring dynamic in-vivo elbow kinematics: description of technique and estimation of accuracy. J Biomech Eng 2012;134(12):124502
13 Hagert CG. The distal radioulnar joint in relation to the whole forearm. Clin Orthop Relat Res 1992;(275):56–64
14 Kaptein BL, Valstar ER, Stoel BC, Rozing PM, Reiber JHC. Evaluation of three pose estimation algorithms for model-based roentgen stereophotogrammetric analysis. Proc Inst Mech Eng H 2004;218 (4, H4):231–238
15 Hansen L, De Raedt S, Jørgensen PB, Mygind-Klavsen B, Kaptein B, Stilling M. Marker free model-based radiostereometric analysis for evaluation of hip joint kinematics: A validation study. Bone Joint Res 2018;7(06):379–387
16 Hemmingsen CK, Thillemann TM, Elmengaard B, et al. Elbow biomechanics, radiocapitellar joint pressure, and interosseous membrane strain before and after radial head arthroplasty. J Orthop Res 2020;38(03):510–522
17 Chen YR, Tang JB. In vivo gliding and contact characteristics of the sigmoid notch and the ulna in forearm rotation. J Hand Surg Am 2013;38(08):1513–1519
18 Xu J, Tang JB. In vivo changes in lengths of the ligaments stabilizing the distal radioulnar joint. J Hand Surg Am 2009;34 (01):40–45
19 af Ekenstam F, Hagert CG. Anatomical studies on the geometry and stability of the distal radio ulnar joint. Scand J Plast Reconstr Surg 1985;19(01):17–25
20 Hojo J, Omokawa S, Iida A, Ono H, Moritomo H, Tanaka Y. Three-dimensional kinematic analysis of the distal radioulnar joint in the axial-loaded extended wrist position. J Hand Surg Am 2019; 44(04):336.e1–336.e6, e336
21 Ozer K, Zhu AF, Siljander B, Lawton JN, Waljee JF. The Effect of Axial Loading on Ulnar Variance. J Wrist Surg 2018;7(03): 247–252
22 Friedman SL, Palmer AK, Short WH, Levinsohn EM, Halperin LS. The change in ulnar variance with grip. J Hand Surg Am 1993;18 (04):713–716
23 Thillemann JK, De Raedt S, Hansen TB, Munk B, Stilling M. Distal radioulnar joint stabilization with open foveal reinsertion versus tendon graft reconstruction: an experimental study using radio-stereometry. J Exp Orthop 2021;8(01):10

 

PAPER IV

# Kinematics of the distal radioulnar joint before and after open reinsertion of the foveal triangular fibrocartilage complex in comparison to normal joints

**Author names**

Janni K Thillemann[a,b,c], Sepp De Raedt[c,d], Emil T Petersen[a,b,c] Katriina B Puhakka[e,f], Torben B Hansen[a,b] and Maiken Stilling[b,c,g]

**Author affiliations**

[a] Department of Orthopaedics, University Clinic for Hand, Hip and Knee Surgery, Hospital Unit West, Lægaardvej 12, 7500 Holstebro, Denmark.

[b] Department of Clinical Medicine, Aarhus University, Palle Juul-Jensens Boulevard 99, 8200 Aarhus N, Denmark.

[c] AutoRSA Research Group, Orthopaedic Research Unit, Aarhus University Hospital, Palle Juul-Jensens Boulevard 165, 8200 Aarhus N, Denmark.

[d] NRT X-RAY A/S, Birkegårdsvej 16, 8361 Hasselager, Denmark.

[e] Department of Radiology, Aarhus University Hospital, Palle Juul-Jensens Boulevard 165, 8200 Aarhus N, Denmark.

[f] Department of Radiology, Regional Hospital Horsens, Sundvej 30, 8700 Horsens, Denmark

[g] Department of Orthopaedic Surgery, Aarhus University, Palle Juul-Jensens Boulevard 165, 8200 Aarhus N, Denmark.

**Corresponding author/main affiliation address**

Janni Kjærgaard Thillemann, University Clinic for Hand, Hip and Knee Surgery, Hospital Unit West, Lægårdvej 12, 7500 Holstebro, Denmark

Phone: +45 28137303

E-mail: teamjanni@gmail.com

**Funding**

This research has received grants from Innovation Fund Denmark (grant nr. 69-2013-1), The Health Research Fund of Central Denmark Region, Aarhus University Fellowship, The Aase and Ejnar Danielsen's Foundation and The Danish Rheumatism Association.

**ABSTRACT**

**Background and purpose –** Foveal triangular fibrocartilage complex (TFCC) lesion may cause distal radioulnar joint (DRUJ) instability. Dynamic radiostereometry (dRSA) has been validated for objective measurement of DRUJ. We evaluated the stabilizing effect of open foveal TFCC reinsertion surgery in patients, by use of dRSA.

**Patients and methods –** In a prospective cohort study, 21 patients (11 men) at mean age 34 years (range 22-50) with arthroscopically confirmed foveal TFCC lesion were evaluated preoperatively, and 6 and 12 months after open foveal TFCC reinsertion with QDASH, PRWE, pain on NRS, and dRSA during a press test motion cycle, including a force-loaded downstroke and release phase.

**Results –** Preoperatively, the force-loaded part (>2.3kg (CI 1.6–3.0)) of the press test motion cycle (from 15-75%) revealed increased volar position of the ulnar head in the sigmoid notch (DRUJ position ratio) and increased distance in DRUJs with foveal TFCC lesion compared to the patients' contralateral non-injured DRUJ (p<0.05). 6 months postoperatively, the DRUJ position was generally normalized and remained normalized at 12 months. However, the DRUJ distance remained higher on the injured side 6 and 12 months after surgery. 12 months postoperatively, patients reported less pain during activities, improved QDASH and PRWE scores (p<0.007).

**Interpretation –** DRUJs with foveal TFCC lesion revealed more instability during an active press test using paired comparison with the contralateral non-injured DRUJ. Open foveal TFCC reinsertion had a stabilizing effect on DRUJ kinematics towards normalization, 6 and 12 months after surgery.

**Level of Evidence**

Level II, Prospective cohort study.

## INTRODUCTION

The triangular fibrocartilaginous complex (TFCC) is the main stabilizer of the distal radioulnar joint (DRUJ) and lesions may lead to DRUJ instability and ulnar wrist pain during activities. Wrist arthroscopy with a positive Hook test, or DRUJ arthroscopy with direct visualization of a foveal TFCC lesion, have been the diagnostic gold standard for many years (1,2) as clinical examination of DRUJ stability (Ballottement test) is observer depend end and lacks validity across observers (3). Imaging modalities such as computer tomography (CT) has poor agreement to clinical examination (4) and magnetic resonance imaging (MRI) has limited sensitivity and specificity for visualizing TFCC lesions (5-8). We recently validated a non-invasive highly precise dynamic radiostereometry (dRSA) imaging method for objective measurement of DRUJ kinematics and instability in vivo (9). Foveal TFCC lesions can be treated surgically by open or arthroscopic reinsertion with similar results evaluated clinically by a radioulnar stress test (i.e., the Ballottement test) (10,11).

In a prospective cohort study, we aimed to evaluate the paired DRUJ kinematic patterns in patients with arthroscopically verified foveal TFCC lesion on one side to their contralateral non-injured side, and the DRUJ stabilizing effect of open foveal TFCC reinsertion with 12-month follow-up.

## PATIENTS AND METHODS

Between February 2017 and April 2020, 21 eligible patients were recruited prospectively to the study at Regional Hospital West and Aarhus University Hospital.

The inclusion criteria were age >18 years, ulnar sided wrist pain related to a history of trauma, clinical impression of DRUJ instability with Ballottement test (12), radiological signs of TFCC injury (DRUJ gapping on radiographs or TFCC injury on MRI), and arthroscopic confirmation of a foveal TFCC lesion as evaluated by the Hook test (13). In addition, it was mandatory for intra-subject comparison that the included patients had a contralateral asymptomatic side without any history of pain, wrist or forearm trauma, or previous surgery. The exclusion criteria were pre-existing rheumatoid conditions, wrist or DRUJ osteoarthritis, MRI verified ulnocarpal impaction with ulnar variance >2 mm, arthroscopically verified intercarpal ligament injury, presence of osteosynthesis material (metal artefacts on bone models), malunion in case of previous distal radius fracture, previous forearm or elbow fracture, and inability to communicate in Danish. At baseline patient characteristics including sex, age, hand dominance, side of the injured wrist and injury mechanism were collected.

**Sample size**

In a cadaver study, DRUJ translation measured with RSA was 1.36 mm (SD 1.42) with intact TFCC and (2.3mm (SD 1.07) after lesion of the peripheral TFCC insertions at the styloid and in the fovea (14). Based on two-sample comparison of paired-means, power of 0.90, and alpha of 0.05, a sample size of 12 patients was estimated. Inclusion of 20 patients in the study period was selected to allow for incomplete data collection, follow-up, and imaging errors.

**Clinical Examination and Patient-Reported Outcome Measures**

At baseline, 6-month, and 12-month follow-up, data from clinical examinations and PROMs were recorded by the surgeon (JKT). Stability of the DRUJ was categorized the amount of DRUJ translation examined by the Ballottement test grades DRUJ instability as slight (<5mm), mild (5-10mm) or severe (>10mm) (15). Grip strength was measured by the DHD-1 digital Hand Dynamometer (SAEHAN Corporation, Gyeongsangnam-do, South Korea) and active range of motion (AROM) was measured with a goniometer. PROMs included Quick Disabilities of the Arm, Shoulder and Hand (QDASH) (range 0 to 100, 0 represents no disability)(16) and Patient-Rated Wrist Evaluation (PRWE) (range 0 to 100, 0 represents no disability and pain)(17). Pain was rated on numeric rating scale (NRS) at rest and during defined activities (range 0–10, 0 indicate no pain).

## CT and MRI imaging

All 21 patients were investigated preoperatively with conventional wrist radiographs of the injured wrist. Bilateral CT scans of the forearm were used to generate individualized 3D bone volume-models and surface-models of the radius and ulna by segmentation (Kitware, New York, USA)(18). The 3D bone models were used for simulation of 2D digital reconstructed radiographs (DRR) and analysis of dRSA recordings. This enables in-vivo estimation of joint kinematics using anatomical landmarks and axes (Fig. 1)(9). Preoperative MRI of the patient's symptomatic wrist was performed for evaluation of 1) foveal TFCC tear (positive), 2) no tear detected but abnormal 'signal' with peripheral edema (uncertain), and 3) other competing injuries by an experienced consultant radiologist (KBP). MR sequences and scanner details are available (Supplementary Table I).

## Press test setup and dynamic RSA

A custom-made weight platform recorded the applied force (kg) during a standardized press test performed by the patients, as related dRSA images were recorded digitally at an image rate of 10Hz (Adora RSA system, NRT X-Ray, Hasselager, Denmark) (Fig. 2) (9). Preoperative, bilateral press test double examinations were conducted to test the dRSA repeatability. At 6-months and 12-month follow-up, dRSA imaging of the press test was repeated on the injured side. An averaged calibration image from all dRSA images was compiled by custom made software and Model-based RSA software was used for calibration (MBRSA 4.11, RSAcore, Leiden, Netherlands). The DRR was manually initialized to approximately fit the initial image of the dRSA recording prior to automated radiostereometric analysis (AutoRSA software, Orthopaedic Research Unit, Aarhus, Denmark) (19). The AutoRSA software was used to estimate the 3D bone position and orientation in the calibration box coordinate system, which was later transformed into individual anatomical coordinate systems of the radius and ulna from anatomical landmarks defined on the individual 3D bone surface-models (9).

### Arthroscopic evaluation and TFCC surgery

Stability of the foveal TFCC insertion was assessed by Hook test through a 6-R portal(13). Open foveal TFCC reinsertion was performed with exposure of the DRUJ through a dorsal skin incision via the 5th extensor compartment. Through an L-shaped capsular opening proximal to the dorsal radioulnar ligament DRUJ synovitis was removed in the ulnar fovea and a 2–0 suture anchor inserted (Mitek Mini Quickanchor, DePuy Syntes, Raynham, MA, USA). The distal side of the TFCC was approached through a 1cm transverse incision in the wrist capsule. The TFCC was reinserted to the ulnar fovea with a mattress suture (5 knots) while compressing the DRUJ positioned in neutral forearm rotation. The dorsal capsule was closed with 3–0 absorbable braided sutures before closure of the skin. An above elbow back-slap cast was applied.

### Rehabilitation program and follow-up

An above elbow cast was worn for a total of 6 weeks. Thereafter, a removable wrist splint was used for another 4 weeks during a protocolled staged 3-month rehabilitation program supervised by an occupational therapist. The aim was normalization of the upper extremity AROM and strength. 8 weeks postoperatively the treatment involved also proprioceptive and neuromuscular wrist exercises. 10 weeks postoperatively, increasing loads were allowed and neuromuscular wrist strengthening increased, and splinting was only recommended during risk activities. 6 months after surgery, unlimited use was allowed if tolerated.

### Kinematic outcomes and data management

Bony landmarks were used to estimate the kinematic outcomes and to define the individual radioulnar joint (RUJ) axis of forearm rotation. The kinematic outcomes were DRUJ translation (primary outcome), DRUJ position ratio, DRUJ distance, and change in ulnar variance (pistoning) (Fig. 1.) (9).

The press test examination with the highest applied force during a motion cycle was chosen for data analysis. Customized software was used to handle individual differences in timing of force application. Each motion cycle was split in a downstroke and a release phase at the point of maximum force, defined as the 50% mark of the motion cycle. Linear interpolation was used to construct new data points (percentage of the motion cycle with 5% increment) from the known RSA image numbers and to estimate new time-normalized force data and related kinematic outcome data(9).

**Statistical analysis**

Descriptive analysis of patient demographics was performed. Continuous data were cheeked for normality by evaluation probability plots and reported as appropriate as means and 95% confidence intervals (CI) (parametric data) or medians with interquartile range (IQR) (non-parametric data). Preoperative data was compared by paired two-tailed student's t-test or Wilcoxon signed-rank test as appropriate. Categorical data were reported as numbers and compared by the chi-squared test. Repeated data and repeated press test motion cycle outcome data were analyzed using KWALLIS test (non-parametric) or multivariate repeated measurements ANOVA statistics as appropriate.

Repeatability of dynamic RSA press test double examinations was estimated and reported as absolute mean difference with standard deviations (SD) and prediction intervals (SDx1.96). The US and dRSA double examinations were used to determine the Intraclass Correlation Coefficients (ICC) based on an assumption of a single rater (inter-rater agreement), absolute-agreement, and two-way mixed-effects model (ICC 2,1). Stata 16 (StataCorp, College Station, TX, USA) was used for statistical analysis. The statistical significance was set at $p<0.05$.

### Ethics, registration, funding, and potential conflict of interests

The study was conducted in accordance the Helsinki guidelines and approved by the Central Denmark Region Committees on Health Research Ethics (j.no.1–10–72–146–16, August 2016). Funding sources had no influence on data interpretation and presentation. The authors have no conflicts of interest.

## RESULTS

Demographics of the patient cohort is presented in Table I.

### Clinical examination

On the TFCC-injured side, the preoperative AROM was reduced ($p<0.04$) and the grip strength was mean 5.7kg (CI 1.8–9.6) less ($p=0.006$) in comparison with the contralateral non-injured side.

12 months after surgery, grip strength recovered to the preoperative level ($p=0.9$) but did not reach the level of the contralateral non-injured side ($p=0.002$) (Table II). Clinical examination of DRUJ stability evaluated by the Ballottement test had improved after surgical treatment ($p<0.01$) (Table II).

### Patient-reported outcomes

At 12-month follow-up, the QDASH score improved 14 points (CI 7–21) ($p=0.000$) and the total PRWE improved 21 points (CI 13–28) ($p=0.000$) (Table III). There was a reduction in patient reported pain during activities after surgical treatment ($p<0.007$) (Fig. 3).

### Magnetic resonance imaging

The sensitivity of diagnosing a foveal TFCC lesion by MRI was 33% and increased to 71% when peripheral edema detected around the foveal TFCC insertion was included and regarded as a sign of foveal TFCC lesion.

**Dynamic DRUJ Kinematics**

Table IV display the press test maximum force and the related kinematic outcomes measured by dRSA.

The precision of DRUJ kinematics at maximum force was comparable for the TFCC-injured side and the contralateral non-injured side ($p$>0.29) and with prediction intervals of <0.62 mm. The ICC rater consistency was excellent ($r$>0.90) (Supplementary table II). Throughout the entire press test motion cycle, the mean differences in force application, by the TFCC-injured side and the contralateral non-injured side, was less than 0.9 kg at all follow-up times ($p$>0.28) (Fig. 4).

The preoperative DRUJ translation during the downstroke phase was mean 5.3mm (CI 4.4–6.1) in in DRUJs with TFCC lesion and mean 4.4mm (CI 3.9–5.0) in the contralateral non-injured DRUJ ($p$=0.09). The preoperative DRUJ position ratio in DRUJs with TFCC injury, was significantly smaller (more volar position) compared to the contralateral non-injured DRUJ ($p$<0.05) in the most force-loaded phase (mean force >2.3kg (CI 1.6–3.0)) of downstroke and release (15% to 75% of the motion cycle) (Fig. 5a). At maximum force, the DRUJ position ratio was 10 percent points (CI 1–19) more volar in the DRUJs with foveal TFCC injury, compared to the contralateral non-injured DRUJSs ($p$=0.02) (Table IV) (Figure 5 and Video 1).

At 6-month follow-up, no statistically significant difference in DRUJ position ratio throughout the press test motion cycle was present when comparing the TFCC-injured DRUJs and the contralateral non-injured DRUJs ($p$>0.06), except at 55% of the motion cycle when the release phase was initiated. The kinematic pattern after TFCC reinsertion normalized towards the kinematic pattern of the contralateral non-injured DRUJs and was unchanged 12-month after surgery ($p$>0.44) (Fig. 6a).

The DRUJ distance decreased as the press test motion cycle was initiated (0 to 15% of the press test motion cycle), regardless of the presence of a TFCC injury. Thereafter, the DRUJ distance reduced further in the contralateral non-injured DRUJs as the mean DRUJ position of the ulnar head was centered in the sigmoid notch and the DRUJ position ratio remained above a level of 0.4 until the force was released (Fig. 6b).

Contrary, the DRUJ distance in wrists with foveal TFCC lesion was higher until 75% of the press test motion cycle, where the ulnar head was below the DRUJ position ratio level of 0.4 (Fig. 6b). At maximum force, the preoperative difference in DRUJ distance between the TFCC-injured side and the contralateral non-injured DRUJ was 1.5mm (CI 0.6–2.4) ($p$=0.002) (Table IV). Surgical treatment did not change the pattern of the DRUJ distance at 6-month or 12-month follow-up (Fig. 6b) ($p>0.21$).

**DISCUSSION**

The most important findings were that assessment of DRUJ kinematics by dRSA during press test revealed a pattern of increased DRUJ translation with foveal TFCC lesion compared to the patient's non-injured side, and a pattern towards normalization after open foveal TFCC reinsertion.

We used a highly precise method that only evaluate the translation of the bone whereas other ex vivo (20-22) and in vivo clinical studies (23) have utilized measurement methods that were biased by soft tissue movements and resulted in greater translation measures. Therefore, direct comparisons between studies cannot be made.

Individual variation in distal radius size and sigmoid notch length is an important factor for comparison of DRUJ translation, and we previously recommended to evaluate DRUJ instability using the DRUJ position ratio (9). At maximum press test force, we found a DRUJ position ratio a difference between non-injured and foveal TFCC-injured DRUJs of 10 percent point of the total sigmoid notch length. Thus, foveal TFCC-injured DRUJs were positioned at a more volar in the SN at a mean 0.29 DRUJ position ratio. Surprisingly, in pronation the DRUJ position ratio did not indicate dorsal ulnar head prominence in DRUJs with foveal TFCC injury compared with the non-injured DRUJs, when examined without load, despite the fact that dorsal prominence of the ulnar head, in clinical practice has been associated with DRUJ instability on lateral radiographs (24) and axial CT scans (25,26).

The DRUJ stability is highly dependent on the TFCC as the major DRUJ stabilizer (27), as the joint is inherently unstable due to bony and articular incongruency between the smaller ulnar head and the greater sigmoid notch concavity (28,29). Under loaded conditions, the DRUJ stability especially depend on the proximal TFCC fibers inserting in the ulnar fovea (30-32). The DRUJ stabilizers allow for complex joint motions including forearm rotation, longitudinal pistoning, and anteroposterior translation (33,34), but gapping is not expected in the stable DRUJ as the TFCC, provide a compressive force perpendicular to the articular surface (35). In unstable DRUJs, gross joint gapping can be detected on plain posteroanterior radiographs or by clenched fist radiographs (36). However, submillimeter differences between non-injured and injured arms with foveal TFCC lesion may not be visible. We reported increased DRUJ distance during the press test in DRUJs with foveal TFCC lesion. Moreover, this may reflect gliding of the ulnar head onto the volar rim of the radius sigmoid notch, as the DRUJ position ratio decrease below a 0.4 level, rather than increased distance between the articulating surfaces of the DRUJ. Future studies, on in vivo DRUJ distance (proximity mapping) may be useful (37,38) for mapping the contact point during movement and for estimating the DRUJ distance of the closest articulating surfaces.

In general, studies on surgical effect of foveal TFCC reinsertion is evaluated by clinical examination of stability (39). Frequently, the Ballottement test is used for this clinical DRUH stability assessment, but suffers from subjectivity and has poor (3) to moderate inter-observer agreement (40). Further, positive Ballottement test is correlated to DRUJ instability but the sensitivity of diagnosing foveal TFCC injuries in comparison with arthroscopic findings was only moderate (sensitivity 59%) (41). Thus, clinical examination of surgical outcomes of DRUJ stability is a biased and an uncertain outcome measure.

To our knowledge, the present study is the only clinical publication that present dynamic kinematic patterns of the DRUJ before and after TFCC stabilizing surgery compared to the normal values on the non-injured DRUJ. We found a statistically significant difference during the loaded phase of the press test motion cycle of non-injured DRUJs compared to DRUJs with foveal TFCC injury. Open foveal reinsertion improved the PROMs at 12-month follow-up and had a normalizing effect on the DRUJ position ratio kinematics, but the stability level of the non-injured contralateral arms was not reached.

Arthroscopic foveal TFCC reinsertion is used increasingly, and numerous techniques has been proposed to achieve a good strong footprint and an anatomical TFCC reinsertion (15,42-45). However, the stabilizing effect on DRUJ kinematics after open and arthroscopic foveal TFCC reinsertion has not yet been compared. Rather, similar clinically evaluated stability and frequency of surgical failure (DRUJ re-instability) has been shown repeatedly (10,11,46). The only randomized study to compare osseous foveal TFCC repair techniques by open vs arthroscopic techniques presented similar improvement of clinical outcomes and recurrence of DRUJ instability (evaluated by the Ballottement test), but with significant differences in PROMs including pain and DASH score, favoring arthroscopic treatment (11).

**Strengths and Limitations**

Dynamic RSA was validated as a precise non-invasive dynamic imaging method that has the advantage of excluding examination bias from the clinician. Further, dRSA captures the kinematic endpoints if recorded by a sufficiently high image frequency (Hz). The press test may not be the ideal examination to display kinematics in unstable DRUJs i.e., if the patient is unable to present his/her maximum instability due to reflective muscle contraction upon loading.

The DRUJ distance was evaluated as the projected perpendicular distance from the ulnar fovea and RUL axis to the sigmoid notch line. Thus, the gapping between joint surfaces of the DRUJ is not portrayed by this study.

In conclusion, dynamic RSA of DRUJ kinematics showed increased DRUJ translation after foveal TFCC lesion compared to non-injured DRUJs, and a DRUJ stabilization towards normal values 6 months and 12 months after open foveal TFCC reinsertion. In support hereof, pain during loaded activity, QDASH and PRWE also improved until 12 months follow-up and to the level of the minimal clinically important difference (MCID). Dynamic RSA for assessment of DRUJ translation before and after other open and arthroscopic TFCC reinsertion and reconstruction techniques may help to identify the most effective treatments.

**TABLES**

**Table I.** Demographics of patients with foveal TFCC injury

| | *Patient cohort* |
|---|---|
| Number | 21 |
| Sex (Male/Female) | 11/10 |
| Mean age at inclusion in years (range) | 34 (22–50) |
| Smoker | 4/17 |
| Dominant hand (Right/Left) | 20/1 |
| Injured hand (Right/Left) | 9/12 |
| Trauma mechanism (fall/rotation/other) | 15/3/3 |
| Time since injury in month (median (IQR)) | 9 (6–58) |

TFCC: Triangular Fibrocartilage Complex, IQR: Interquartile Range

**Table II.** Clinical evaluation of DRUJ stability in the non-injured DRUJ and the DRUJ with foveal TFCC lesion, before and after surgical treatment.

| | *Non-injured* | *TFCC lesion* | | | $p^1$ | $p^2$ |
|---|---|---|---|---|---|---|
| | *Preoperative (n=21)* | *Preoperative (n=21)* | *6-month FU (n=19)* | *12-month FU (n=19)* | | |
| Number of patients (n) | 21 | 21 | 19 | 19 | | |
| Women | 10 | 10 | 8 | 8 | | |
| Men | 11 | 11 | 11 | 11 | | |
| Grip strength total (kg) | 45.0 (39.0–51.0) | 39.3 (32.0–46.6) | 36.1 (29.9–42.4) | 39.5 (31.7–47.3) | 0.006 | 0.04** |
| Women | 33.1 (28.5–37.6) | 25.1 (20.0–30.3) | 23.0 (17.2–28.8) | 25.0 (17.1–32.9) | 0.002 | 0.30 |
| Men | 55.8 (51.8–59.9) | 52.1 (46.0–58.3) | 47.6 (44.1–51.1) | 52.5 (46.0–58.9) | 0.26 | 0.048** |
| Wrist AROM (°) | | | | | | |
| - flexion | 78 (73–82) | 70 (65–76) | 67 (62–72) | 68 (62–73) | 0.001 | 0.59 |
| - extension | 74 (70–78) | 67 (61–73) | 68 (64–72) | 66 (61–71) | 0.004 | 0.63 |
| - radial deviation | 22 (19–25) | 20 (17–24) | 18 (16–20) | 19 (17–22) | 0.01 | 0.13 |
| - ulnar deviation | 37 (34–40) | 33 (29–37) | 28 (25–30) | 32 (28–37) | 0.01 | 0.02* |
| Forearm rotation (°) | | | | | | |
| - supination | 84 (81–87) | 78 (75–82) | 76 (72–80) | 74 (70–78) | 0.001 | 0.17 |
| - pronation | 81 (77–85) | 79 (74–83) | 77 (73–81) | 79 (75–83) | 0.04 | 0.49 |
| Clinical evaluation of DRUJ stability | | | | | | |
| Ballottement test [a] | 21/0/0 | 0/15/6 | 13/6/0 | 13/6/0 | 0.00 | <0.01 |

Numbers are displayed as means with 95% confidence intervals (CI).
DRUJ: Distal Radioulnar Joint, AROM: active range of motion.
[a] Slight instability (<5 mm)/mild instability (5-10mm)/severe instability (>10 mm)
[1] Preoperative comparison between the healthy arm and the foveal TFCC injury arm using either a t-test, Wilcoxon sing-rank or a chi-square test.
[2] Comparison of the foveal TFCC injury arm over time, from preoperative, 6 month and 12-month follow-up with mixed model analysis of repeated measures or chi-square test.
* Statistically significant difference between preoperative and 6-month follow-up (FU) in the DRUJs with foveal TFCC lesion.
** Statistically significant difference between 6-month and 12-month follow-up (FU) in the DRUJs with foveal TFCC lesion.

**Table III.** Patient reported outcomes relating to the TFCC-injured wrist before and after surgical treatment.

| | *Preoperative (n=21)* | *6-month (n=19)* | *12-month (n=19)* | *p-value* |
|---|---|---|---|---|
| Pain on NRS at (median (IQR)) [2] | | | | |
| - At rest | 0 (0–3) | 0 (0–0) | 0 (0–0) | 0.16 |
| - Unloaded forearm rotation | 1 (0–5) | 0 (0–0) | 0 (0–1) | 0.007* |
| - Resisted forearm rotation | 5 (3–8) | 1 (0–3) | 1 (0–2) | <0.001* |
| - Lifting >5 kg | 5 (4–6) | 1 (0–3) | 2 (0–4) | <0.001* |
| QDASH preop [1] | 39 (31–47) | 29 (22–36) | 25 (16–34) | 0.000* |
| Pain PRWE[1] | 29 (25–33) | 17 (14–20) | 18 (13–23) | 0.000* |
| Function PRWE [1] | 20 (15–24) | 12 (8–15) | 10 (6–14) | 0.000* |
| Total PRWE [1] | 49 (41–57) | 29 (23–35) | 28 (19–37) | 0.000* |

Numbers are displayed as means with 95% confidence intervals (CI) unless others are displayed.
[1] Comparison over time with ANOVA repeated measures.
[2] KWALLIS test non-parametric repeated measures (paired)
* Statistically significant difference between 6-month and 12-month outcomes compared to the preoperative outcome of the foveal TFCC-injured wrist.
** Statistically significant difference between 6-month and 12-month follow-up (FU) in the foveal TFCC injury arm.

**Table IV.** Kinematic outcomes at maximum force and during the downstroke phase of the press test in the patient's non-injured DRUJ and TFCC-injured DRUJ before and after surgical treatment.

| | *Non-injured* | *TFCC lesion* | | | p [1] | p [2] |
|---|---|---|---|---|---|---|
| | *Preoperative* (n=21) | *Preoperative* (n=21) | *6-month* (n=19) | *12-month* (n=19) | | |
| Sigmoid notch size (mm) | 13.4 (12.9–14.0) | 13.7 (13.0–14.4) | - | - | 0.57 | |
| *At 0 % of the motion cycle* | | | | | | |
| Forearm pronation (º) | 61 (56–67) | 59 (54–65) | 60 (55–65) | 59 (54–64) | 0.61 | 0.46 |
| DRUJ position ratio | 0.72 (0.68–0.76) | 0.68 (0.61–0.75) | 0.69 (0.62–0.75) | 0.70 (0.63–0.77) | 0.28 | 0.53 |
| DRUJ distance (mm) | 9.9 (9.4–10.4) | 10.6 (10.0–11.1) | 10.6 (10.0–11.1) | 10.7 (10.1–11.2) | 0.07 | 0.22 |
| *At 50 % of the motion cycle* | | | | | | |
| Forearm pronation (º) | 52 (47–58) | 50 (44–57) | 54 (49–59) | 53 (48–59) | 0.64 | 0.23 |
| Maximum force in kg | 6.7 (5.6–7.7) | 6.9 (5.7–8.1) | 7.4 (6.2–8.6) | 7.5 (6.0–9.1) | 0.71 | 0.65 |
| DRUJ position ratio | 0.39 (0.34–0.44) | 0.29 (0.21–0.37) | 0.32 (0.24–0.39) | 0.31 (0.22–0.40) | **0.02** | 0.53 |
| DRUJ distance (mm) | 9.1 (8.5–9.7) | 10.6 (9.9–11.4) | 10.5 (9.9–11.2) | 10.5 (9.7–11.2) | **0.002** | 0.21 |
| *From 0% to 50 % of the motion cycle* | | | | | | |
| DRUJ translation (mm) | 4.4 (3.9–5.0) | 5.3 (4.4–6.1) | 5.1 (4.3–5.8) | 5.3 (4.5–6.1) | 0.09 | 0.65 |
| Increase in ulnar variance (mm) | 1.14 (0.95–1.32) | 0.96 (0.75–1.07) | 0.94 (0.74–1.13) | 1.03 (0.85–1.2) | 0.14 | 0.31 |
| Pain on NRS during RSA press test (median (IQR)) | 0 (0–0) | 1 (0–4) | 0 (0–1) | 0 (0–0) | **0.000** | **0.0001** |

Numbers are displayed as means with 95% confidence intervals (CI) or medians with inter quartile ranges (IQR).
[1] Paired t-test or Wilcoxon signed-rank test as appropriate. Preoperative comparison of non-injured DRUJs and DRUJs with foveal TFCC lesion. [2] *Mixed or* Kruskal Wallis test as appropriate. Comparison of DRUJs with foveal TFCC lesion over time.
FU: Follow-up, DRUJ: distal radioulnar joint, TFCC: triangular fibrocartilage complex, IQR: inter quartile range.

**Supplementary table I.** Magnetic Resonance Scanners units of 1.5T or 3.0T with a hand coil were used in the study

| | Sequence | TR/TE (ms) | Thickness/increment (mm) |
|---|---|---|---|
| Holstebro Hospital Achieva, Philips Medical Systems (1.5T) | T1 cor | 525/14 | 2/2.2 |
| | T1 ax | 525/14 | 3/3.3 |
| | PD FS 3D with recon | 1500/33 | 0.7/0.36 |
| | T2 me3d cor | 33/18 | 0.75/0.75 |
| Aarhus University Hospital Optima, GE healthcare (1.5T) | T1 cor | 700/11 | 2/2.2 |
| | T1 ax | 700/9 | 3/3.3 |
| | PD FS cor | 1800/27 | 2/2.2 |
| | 3DGEt2* with recon | 25/13 | 0.5/0.5 |
| Aarhus University Hospital Skyra, Siemens (3.0T) | T1 cor, ax | 550/15 | 2/2.42 |
| | PD FS cor, sag, ax | 3700/30 | 2.2/2.42 |
| | T2me2d | 780/28 | 1.5/1.95 |

PD: Proton density, FS: Fat saturation; TR: Repetition Time, TE: Echo time
Recon: Reconstructions in 3 planes (coronal, sagittal, axial)

**Supplementary table II.** Repeatability of press test RSA double-examination maximum force outcomes and synchronized kinematic outcomes reported as absolute mean differences with standard deviation and prediction intervals.

| | *Systematic bias* (mean difference) | *P*[1] | *Precision* (SD) | *Prediction interval* (SD x 1.96) | *ICC*[2] |
|---|---|---|---|---|---|
| Maximum force (kg) | | | | | |
| - Non-injured | 0.74 (0.43–1.06) | 0.80 | 0.69 | 1.35 | 0.89 (0.75–0.95) |
| - Foveal TFCC injury | 0.80 (0.48–1.12) | | 0.70 | 1.38 | 0.93 (0.80–0.97) |
| DRUJ translation (mm) | | | | | |
| - Non-injured | 0.32 (0.25–0.38) | 0.86 | 0.14 | 0.28 | 0.96 (0.91–0.98) |
| - Foveal TFCC injury | 0.30 (0.16–0.44) | | 0.31 | 0.62 | 0.97 (0.94–0.99) |
| DRUJ position ratio | | | | | |
| - Non-injured DRUJ | 0.02 (0.01–0.03) | 0.82 | 0.014 | 0.03 | 0.97 (0.93–0.99) |
| - Foveal TFCC injury | 0.02 (0.01–0.04) | | 0.030 | 0.06 | 0.98 (0.94–0.99) |
| Ulnar variance (mm) | | | | | |
| - Non-injured DRUJ | 0.09 (0.06–0.13) | 0.29 | 0.07 | 0.14 | 0.95 (0.88–0.98) |
| - Foveal TFCC injury | 0.12 (0.08–0.16) | | 0.09 | 0.18 | 0.91 (0.79–0.96) |
| DRUJ distance (mm) | | | | | |
| - Non-injured DRUJ | 0.30 (0.18–0.43) | 0.31 | 0.28 | 0.55 | 0.84 (0.52–0.94) |
| - Foveal TFCC injury | 0.23 (0.15–0.31) | | 0.18 | 0.35 | 0.97 (0.93–0.99) |

[1] Paired t-test

[2] Intraclass Coefficient: ICC (2,1) rater consistency between first and second examination was calculated as two-way mixed effects, absolute agreement displayed with 95% confidence intervals (CI).

**FIGURE LEGENDS**

***Fig. 1.*** *Bony landmarks, bone axis and kinematic outcome measures on CT based bone models.*

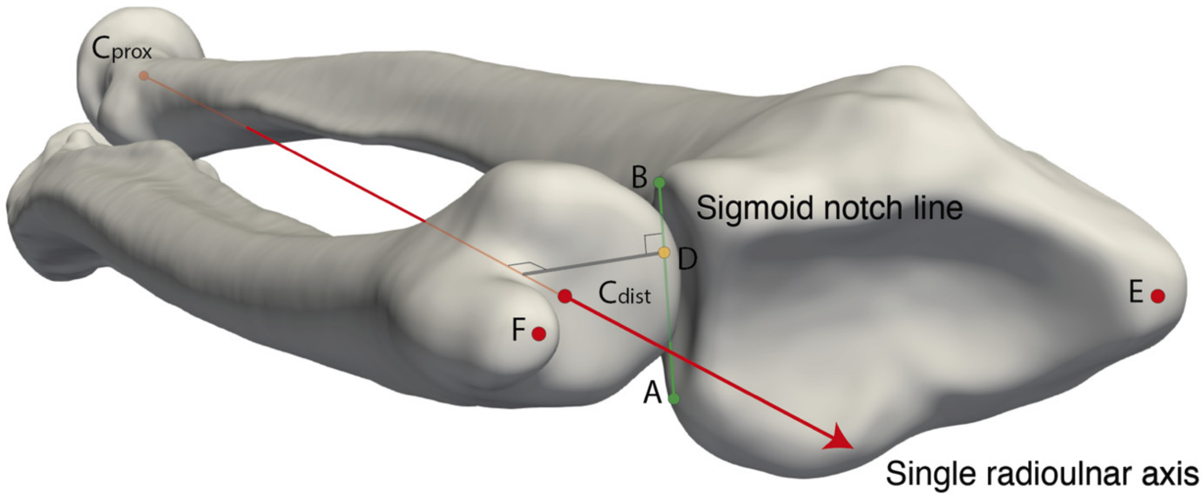


The sigmoid notch (SN) line connects the midpoint of the volar (landmark A) and dorsal (landmark B) radius sigmoid notch rims. The axis of rotation in the forearm was defined as the radioulnar joint axis (RUJ axis) extending thorough the radial head center ($C_{prox}$) to the ulnar head center ($C_{dist}$) (47). The forearm rotation was defined as the angle between a plane formed from the radial head centre ($C_{prox}$), the ulnar head center ($C_{dist}$) to the ulnar styloid (F) and the plane formed from the $C_{prox}$, the radial styloid (E), and the midpoint of the sigmoid notch line.

The position of the ulnar head center in the sigmoid notch (DRUJ position=yellow ball) was estimated by orthogonal projection of the RUJ axis on the sigmoid notch line and measured in mm from the volar sigmoid notch rim. Considering the individual differences of bone-sizes and sigmoid notch length, the DRUJ position ratio was calculated (DRUJ position ratio=DRUJ position/SN length). Translation in the DRUJ was calculated as the change of DRUJ position in millimeters. Change of ulnar variance was calculated as movement of $C_{dist}$ along the RUJ axis with respect to the SN line midpoint and, finally, DRUJ distance was estimated as the orthogonal projected distance (grey line) from the RUJ axis to the SN line (AB).

***Figure 2****. Dynamic radiostereometric setup during press test application.*

The patients were positioned with shoulder adduction, elbow flexion and the approximately 90$^{o}$ pronated forearm resting in the horizontal plane with the hand flat on a custom-made weight platform logging the force (kg) gradually applied by the patients to their maximum, and released gradually, to no force, to induce dorso-volar directed translation of the ulnar head.

A custom-made Raspberry Pi was used to timestamp dynamic radiostereometric image recordings (dRSA) (10 Hz), and further to record and relate the dRSA images and the force applied on the weight platform.

The press test was performed during by two ceiling mounted x-ray tubes with 20°-20° tube position on the vertical plane, projecting on two digital image detectors (Canon CXDI-50RF) slotted beneath a uniplanar carbon box (Carbon box 24, Medis Specials, Leiden, The Netherlands).

The Source to Image Distance (SID) was 150 cm and the Source to Skin Distance (SSD) was 100 cm. The exposures were 60kV, 630 mA and 2.0 ms exposure time for acquiring a resolution of 2208 x 2688 pixels resolution (0.16 x 0.16 mm/pixel). Images were exported as multi-frame DICOM files.

***Figure 3.*** *Patient reported pain on Numeric Rating Scale in patients with foveal TFCC injury.* Boxplots of the patient reported pain at rest, during lifting more than 5 kg, with loaded- and unloaded forearm rotation, from the preoperatively throughout the 6-month and 12-month follow-up. Boxplot display median pain, with inter quartile ranges (IQR), whiskers (1.5 x IQR) and outliers.

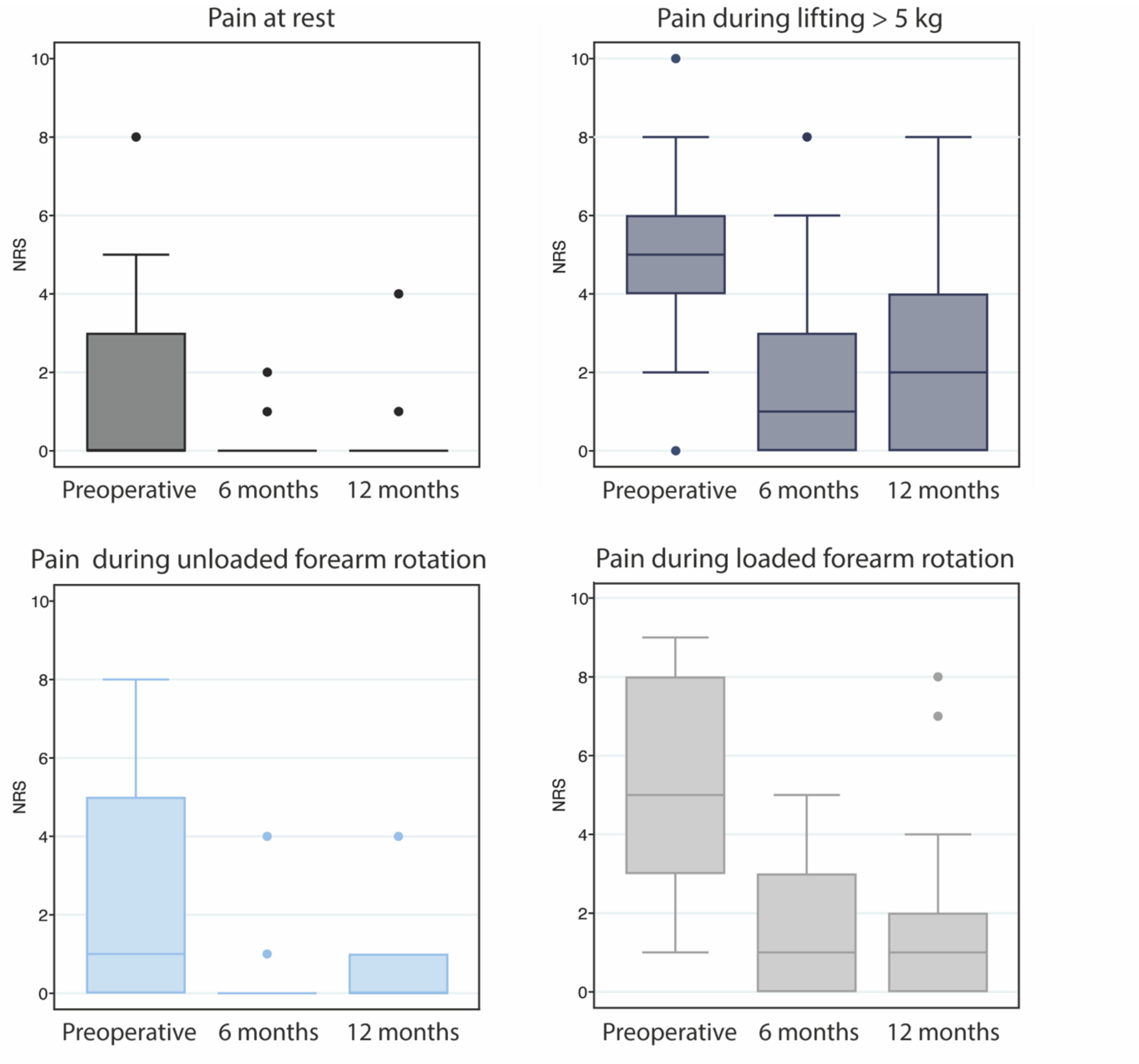


500

***Figure 4.*** *Dynamic pressure force during the press test motion cycle downstroke (0%-50%) and release (51%-100%) phase.*

The applied force of the contralateral non-injured arms (black) and arms with foveal TFCC injury (red) is displayed as means with 95% confidence intervals, preoperatively (solid line), at 6-month, and at 12-month follow-up (dashed lines).

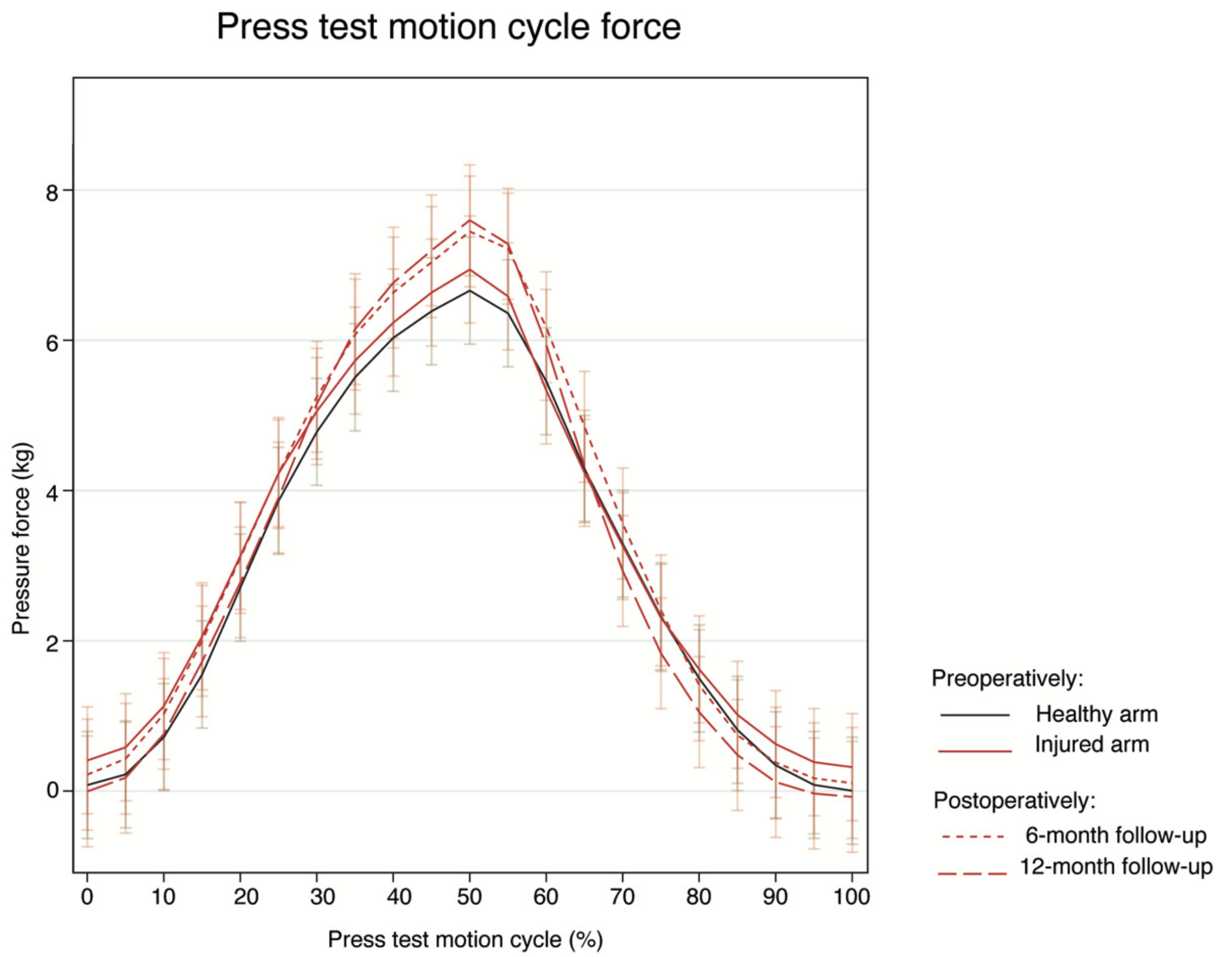

**Figure.** ***6.*** *Example of DRUJ kinematics during the press test.*

The applied force result in volar ulnar head translation and DRUJ gapping on the (left) DRUJ with foveal TFCC injury compared to the (right) non-injured DRUJ.

(a) Maximal force after downstroke on the weight platform and (b) after release.

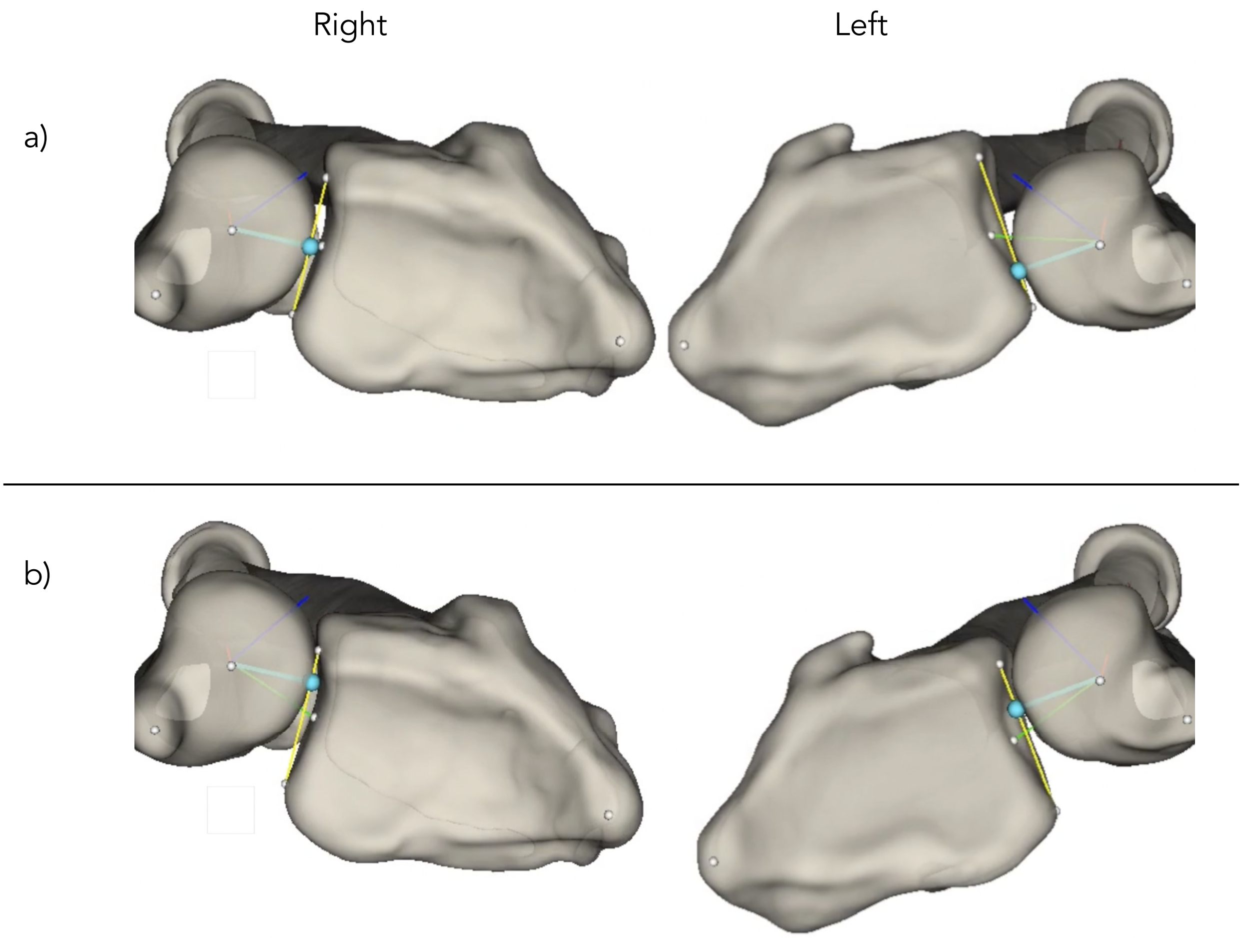

**Figure.** ***6.*** *Dynamic kinematic outcomes during the press test*

Preoperative (solid line) and postoperative (dashed lines) comparison of the mean distal radioulnar joint position ratio (a) and mean distal radioulnar joint distance (DRUJ) (mm) (b) of patient DRUJs with foveal TFCC lesion (red) and the contralateral non-injured DRUJ (black), with 95% confidence intervals. Mixed model statistics was used to define intervals of the press test motion cycle with significant differences (displayed as light grey areas). The DRUJ position ratio resembles the position of the ulnar head center in the sigmoid notch (0 indicate the most volar position and 1 indicate the most dorsal position). The DRUJ distance increased as the DRUJ position ratio was below a 0.4 level (green line).

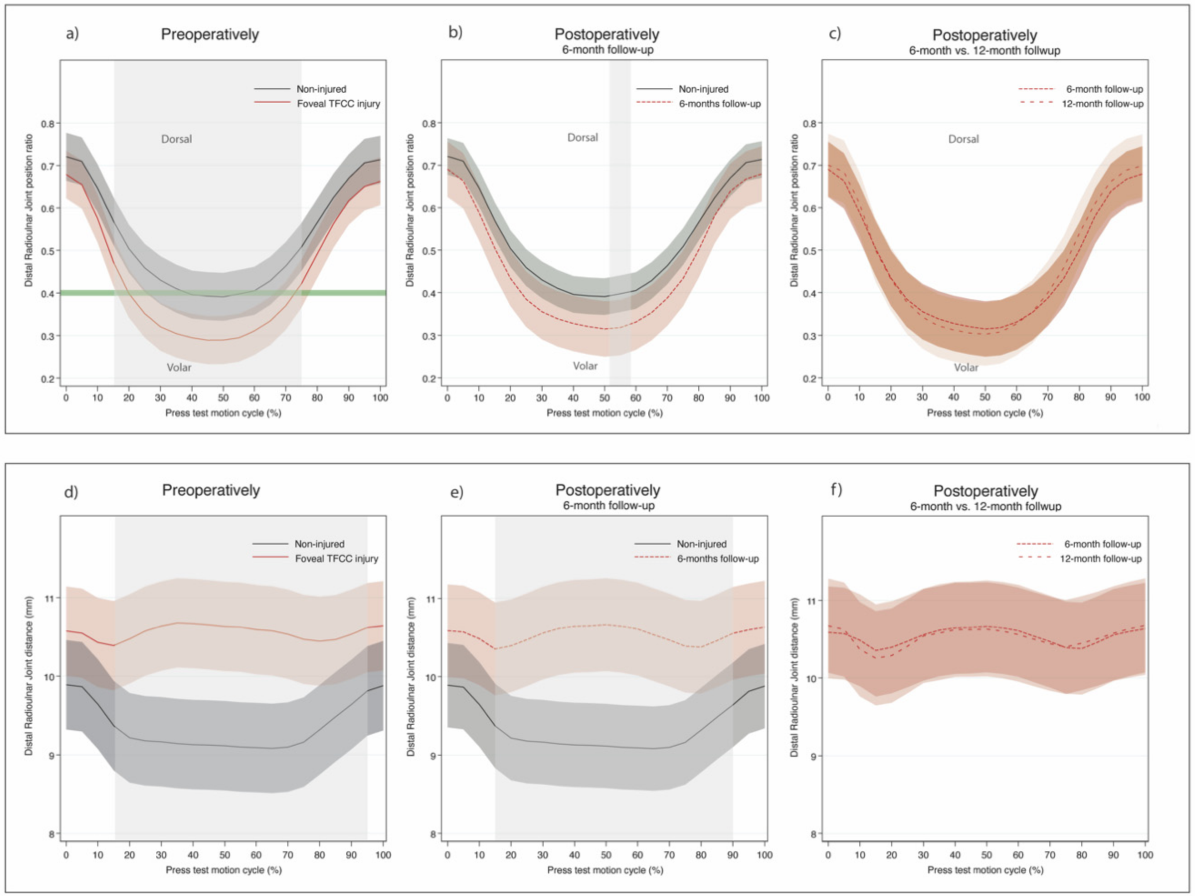

## AUTHOR CONTRIBUTIONS

JKT, SDR, TBH and MS carried out the design of the study. JKT and MS Participated in data acquisition. JKT, KBP, ETP, SDR and MS participated in analysis and interpretation of data. SDR and MS developed the AutoRSA software used in the work. JKT drafted the manuscript. SDR, KBP, ETP, TBH, and MS participated with critical revision of the manuscript. All authors read and approved the final manuscript.

## ACKNOWLEDGEMENTS

We thank radiographer Lars Lindgren from the Department of Radiology, Aarhus University Hospital, and Michael Frosted Mathiasen, from the Department of Radiology, Hospital Unit West, for their valuable help with the radiostereometric recordings.

**VIDEO**

***Video I.*** Presentation of press test dRSA examination comparing a patient's non-injured (right) distal radioulnar joint (DRUJ) and the contralateral DRUJ with foveal TFCC lesion.

*REFERENCE LIST*

1. Pederzini L, Luchetti R, Soragni O, Alfarano M, Montagna G, Cerofolini E, et al. Evaluation of the triangular fibrocartilage complex tears by arthroscopy, arthrography, and magnetic resonance imaging. Arthroscopy 1992; 8: 191-197.

2. Atzei A, Luchetti R, Garagnani L. Classification of ulnar triangular fibrocartilage complex tears. A treatment algorithm for Palmer type IB tears. The Journal of hand surgery, European volume 2017; 42: 405-414.

3. Jupiter JB. Commentary: the effect of ulnar styloid fractures on patient-rated outcomes after volar locking plating of distal radius fractures. The Journal of hand surgery 2009; 34: 1603-1604.
4. Kim JP, Park MJ. Assessment of distal radioulnar joint instability after distal radius fracture: comparison of computed tomography and clinical examination results. The Journal of hand surgery 2008; 33: 1486-1492.

5. Boer BC, Vestering M, van Raak SM, van Kooten EO, Huis In 't Veld R, Vochteloo AJH. MR arthrography is slightly more accurate than conventional MRI in detecting TFCC lesions of the wrist. Eur J Orthop Surg Traumatol 2018; 28: 1549-1553.

6. Andersson JK, Andernord D, Karlsson J, Friden J. Efficacy of Magnetic Resonance Imaging and Clinical Tests in Diagnostics of Wrist Ligament Injuries: A Systematic Review. Arthroscopy 2015; 31: 2014-2020 e2012.

7. Zlatkin MB, Rosner J. MR imaging of ligaments and triangular fibrocartilage complex of the wrist. Radiol Clin North Am 2006; 44: 595-623, ix.

8. Lee YH, Choi YR, Kim S, Song HT, Suh JS. Intrinsic ligament and triangular fibrocartilage complex (TFCC) tears of the wrist: comparison of isovolumetric 3D-THRIVE sequence MR arthrography and conventional MR image at 3 T. Magn Reson Imaging 2013; 31: 221-226.

9. Thillemann JT, De Raedt S, Petersen ET, Puhakka KB, Hansen TB, Stilling M. Normal Values of Distal Radioulnar Joint Kinematics during a Dynamic Press Test. J Wrist Surg 2021b.

10. Andersson JK, Ahlen M, Andernord D. Open versus arthroscopic repair of the triangular fibrocartilage complex: a systematic review. Journal of experimental orthopaedics 2018; 5: 6.

11. Luchetti R, Atzei A, Cozzolino R, Fairplay T, Badur N. Comparison between open and arthroscopic-assisted foveal triangular fibrocartilage complex repair for post-traumatic distal radio-ulnar joint instability. The Journal of hand surgery, European volume 2014; 39: 845-855.

12. Kleinman WB. Stability of the distal radioulna joint: biomechanics, pathophysiology, physical diagnosis, and restoration of function what we have learned in 25 years. The Journal of hand surgery 2007; 32: 1086-1106.

13. Atzei A. New trends in arthroscopic management of type 1-B TFCC injuries with DRUJ instability. The Journal of hand surgery, European volume 2009; 34: 582-591.

14. Thillemann JK, De Raedt S, Jorgensen PB, Romer L, Hansen TB, Stilling M. Distal radioulnar joint stability measured with radiostereometry during the piano key test. The Journal of hand surgery, European volume 2020; 10.1177/1753193420934689: 1753193420934689.

15. Atzei A, Rizzo A, Luchetti R, Fairplay T. Arthroscopic foveal repair of triangular fibrocartilage complex peripheral lesion with distal radioulnar joint instability. Techniques in hand & upper extremity surgery 2008; 12: 226-235.

16. Hudak PL, Amadio PC, Bombardier C. Development of an upper extremity outcome measure: the DASH (disabilities of the arm, shoulder and hand) [corrected]. The Upper Extremity Collaborative Group (UECG). American journal of industrial medicine 1996; 29: 602-608.

17. MacDermid JC, Turgeon T, Richards RS, Beadle M, Roth JH. Patient rating of wrist pain and disability: a reliable and valid measurement tool. J Orthop Trauma 1998; 12: 577-586.

18. Hansen L, De Raedt S, Jorgensen PB, Mygind-Klavsen B, Kaptein B, Stilling M. Marker free model-based radiostereometric analysis for evaluation of hip joint kinematics: A validation study. Bone & joint research 2018; 7: 379-387.

19. Christensen R, Petersen ET, Jurgens-Lahnstein J, Rytter S, Lindgren L, De Raedt S, et al. Assessment of knee kinematics with dynamic radiostereometry: Validation of an automated model-based method of analysis using bone models. Journal of orthopaedic research : official publication of the Orthopaedic Research Society 2020; 10.1002/jor.24875.

20. Omokawa S, Iida A, Kawamura K, Nakanishi Y, Shimizu T, Kira T, et al. A Biomechanical Perspective on Distal Radioulnar Joint Instability. J Wrist Surg 2017; 6: 88-96.

21. Onishi T, Omokawa S, Iida A, Nakanishi Y, Kira T, Moritomo H, et al. Biomechanical study of distal radioulnar joint ballottement test. Journal of orthopaedic research : official publication of the Orthopaedic Research Society 2017; 35: 1123-1127.

22. Iida A, Omokawa S, Moritomo H, Omori S, Kataoka T, Aoki M, et al. Effect of wrist position on distal radioulnar joint stability: a biomechanical study. Journal of orthopaedic research : official publication of the Orthopaedic Research Society 2014; 32: 1247-1251.

23. Pickering GT, Nagata H, Giddins GEB. In-vivo three-dimensional measurement of distal radioulnar joint translation in normal and clinically unstable populations. J Hand Surg-Eur Vol 2016; 41: 521-526.

24. Nakamura R, Horii E, Imaeda T, Tsunoda K, Nakao E. Distal radioulnar joint subluxation and dislocation diagnosed by standard roentgenography. Skeletal Radiol 1995; 24: 91-94.

25. Park MJ, Kim JP. Reliability and normal values of various computed tomography methods for quantifying distal radioulnar joint translation. J Bone Joint Surg Am 2008; 90: 145-153.

26. Lo IK, MacDermid JC, Bennett JD, Bogoch E, King GJ. The radioulnar ratio: a new method of quantifying distal radioulnar joint subluxation. The Journal of hand surgery 2001; 26: 236-243.

27. Palmer AK, Werner FW. The triangular fibrocartilage complex of the wrist--anatomy and function. The Journal of hand surgery 1981; 6: 153-162.

28. Stuart PR, Berger RA, Linscheid RL, An KN. The dorsopalmar stability of the distal radioulnar joint. The Journal of hand surgery 2000; 25: 689-699.

29. Szabo RM. Distal radioulnar joint instability. J Bone Joint Surg Am 2006; 88: 884-894.

30. Haugstvedt JR, Berger RA, Nakamura T, Neale P, Berglund L, An KN. Relative contributions of the ulnar attachments of the triangular fibrocartilage complex to the dynamic stability of the distal radioulnar joint. The Journal of hand surgery 2006; 31: 445-451.

31. Xu J, Tang JB. In vivo changes in lengths of the ligaments stabilizing the distal radioulnar joint. The Journal of hand surgery 2009; 34: 40-45.

32. Hagert CG. Distal radius fracture and the distal radioulnar joint--anatomical considerations. Handchir Mikrochir Plast Chir 1994; 26: 22-26.

33. Tolat AR, Stanley JK, Trail IA. A cadaveric study of the anatomy and stability of the distal radioulnar joint in the coronal and transverse planes. J Hand Surg Br 1996; 21: 587-594.

34. af Ekenstam F. Anatomy of the distal radioulnar joint. Clin Orthop Relat Res 1992: 14-18.

35. Hagert E, Hagert CG. Understanding stability of the distal radioulnar joint through an understanding of its anatomy. Hand Clin 2010; 26: 459-466.

36. Iida A, Omokawa S, Akahane M, Kawamura K, Takayama K, Tanaka Y. Distal radioulnar joint stress radiography for detecting radioulnar ligament injury. The Journal of hand surgery 2012; 37: 968-974.

37. Anderst WJ, Tashman S. A method to estimate in vivo dynamic articular surface interaction. J Biomech 2003; 36: 1291-1299.

38. Nielsen ET, Stentz-Olesen K, de Raedt S, Jorgensen PB, Sorensen OG, Kaptein B, et al. Influence of the Anterolateral Ligament on Knee Laxity: A Biomechanical Cadaveric Study Measuring Knee Kinematics in 6 Degrees of Freedom Using Dynamic Radiostereometric Analysis. Orthop J Sports Med 2018; 6: 2325967118789699.

39. Robba V, Fowler A, Karantana A, Grindlay D, Lindau T. Open Versus Arthroscopic Repair of 1B Ulnar-Sided Triangular Fibrocartilage Complex Tears: A Systematic Review. Hand (N Y) 2020; 15: 456-464.

40. Lindau T, Runnquist K, Aspenberg P. Patients with laxity of the distal radioulnar joint after distal radial fractures have impaired function, but no loss of strength. Acta Orthop Scand 2002; 73: 151-156.

41. Lindau T, Adlercreutz C, Aspenberg P. Peripheral tears of the triangular fibrocartilage complex cause distal radioulnar joint instability after distal radial fractures. The Journal of hand surgery 2000; 25: 464-468.

42. Iwasaki N, Minami A. Arthroscopically assisted reattachment of avulsed triangular fibrocartilage complex to the fovea of the ulnar head. The Journal of hand surgery 2009; 34: 1323-1326.

43. Nakamura T, Sato K, Okazaki M, Toyama Y, Ikegami H. Repair of foveal detachment of the triangular fibrocartilage complex: open and arthroscopic transosseous techniques. Hand Clin 2011; 27: 281-290.

44. Shinohara T, Tatebe M, Okui N, Yamamoto M, Kurimoto S, Hirata H. Arthroscopically assisted repair of triangular fibrocartilage complex foveal tears. The Journal of hand surgery 2013; 38: 271-277.

45. Kermarrec G, Cohen G, Upex P, Fontes D. Arthroscopic Foveal Reattachment of the Triangular Fibro Cartilaginous Complex. J Wrist Surg 2020; 9: 256-262.

46. Anderson ML, Larson AN, Moran SL, Cooney WP, Amrami KK, Berger RA. Clinical comparison of arthroscopic versus open repair of triangular fibrocartilage complex tears. The Journal of hand surgery 2008; 33: 675-682.

47. Hagert CG. The distal radioulnar joint in relation to the whole forearm. Clin Orthop Relat Res 1992: 56-64.